Aus dem Institut für Humangenetik

Theoretische Medizin und Biowissenschaften

der Medizinischen Fakultät

der Universität des Saarlandes, Homburg/Saar

Expressions- und Replikationsanalyse in differenzierenden menschlichen Stammzellen

(Expression and replication analysis in differentiating human stem cells)

Dissertation zur Erlangung des Grades eines Doktors der Naturwissenschaften

der Medizinischen Fakultät

der UNIVERSITÄT DES SAARLANDES

2023

vorgelegt von Marie Minet

geb. am: 04.04.1992 in Angers (Frankreich)

Table of content

Tables and figures list

Figure 7.12: Heatmaps of the normalized expression levels of miRNAs known to be important in embryonic stem cells and found to be deregulated in the hMSC adipogenesis, chondrogenesis, osteogenesis, hNSC, and HSkM differentiation assays.

Figure 7.13: Heatmaps of the scaled and normalized expression levels of miRNAs known to be important in embryonic stem cells and found to be deregulated in the hMSC adipogenesis, chondrogenesis, osteogenesis, hNSC, and HSkM differentiation assays.

Abbreviation list

Abbreviation	Meaning
°C	degree Celsius
µg	microgram
µl	microliter
µm	micrometer
µM	micromolar
ABCC3	ATP binding cassette subfamily C member 3
ADAMTS9	ADAM metallopeptidase with thrombospondin type 1 motif 9
ADIPOQ	adiponectin, C1Q and collagen domain containing
AKT1	serine/threonine kinase 1
AKT2	serine/threonine kinase 2
alpha-MHC	myosin heavy chain 6
AMPD2	adenylate deaminase 2
APC	anaphase-promoting complex
ATM	Ataxia telangiectasia mutated
ATP	adenosine triphosphate
ATR	Ataxia telangiectasia and Rad3-related protein
BAT	brown adipose tissue
beta-MHC	myosin heavy chain 7
BFB	breakage-fusion-bridge
bFGF	basic fibroblast growth factor
bHLH	basic helix–loop–helix
BMP	bone morphogenetic protein
BMP2	bone morphogenetic protein 2
BMP4	bone morphogenetic protein 4
BMPR1A	bone morphogenetic protein receptor type 1A
BrdU	bromodeoxyuridine
C/EBPA	CCAAT-enhancer-binding protein alpha
Ca	calcium
CCN5	cellular communication network factor 5
CD105	ENG, endoglin
CD11b	ITGAM, integrin alpha M
CD13	ANPEP, alanyl aminopeptidase
CD14	CD14 molecule
CD19	CD19 molecule
CD235a	GYPA, glycophorin A
CD29	ITGB1, integrin subunit beta 1
CD31	PECAM1, platelet and endothelial cell adhesion molecule 1
CD34	CD34 molecule
CD36	CD36 molecule
CD44	CD44 molecule
CD45	PTPRC, protein tyrosine phosphatase receptor type C
CD73	NT5E, 5'-nucleotidase ecto
CD79a	CD79a molecule
CD90	THY1, Thy-1 cell surface antigen

CDC20	cell division cycle 20
CDC45	cell division cycle 45
CDC6	cell division cycle 6
CDC7	cell division cycle 7
CDH1	cadherin 1
CDK	cyclin-dependent kinase
CDK1	cyclin-dependent kinase 1
CDK2	cyclin-dependent t kinase 2
CDK3	cyclin-dependent kinase 3
CDK4	cyclin-dependent kinase 4
CDK7	cyclin-dependent kinase 7
cDNA	complementary DNA
CDT1	chromatin licensing and DNA replication factor 1
CDT2	DTL, denticleless E3 ubiquitin protein ligase homolog
CFD	adipsin
CHEK2	CHK2, checkpoint kinase 2
CldU	5-chloro-2'-deoxyuridine
cm^2	square centimeter
c-MYC	MYC proto-oncogene, BHLH transcription factor
CNGB1	cyclic nucleotide gated channel subunit beta 1
CNV	copy number variation
CO_2	carbon dioxide
cRNA	complementary RNA
CST	CTC1-STN1-TEN1
CTC1	CST telomere replication complex component 1
CTNNB1	beta-catenin, catenin beta 1
CUL4	cullin 4
CXCL12	C-X-C motif chemokine ligand 12
DAPI	4′,6-diamidino-2-phenylindole
DCX	doublecortin
DDB1	damage specific DNA binding protein 1
ddH_2O	double-distilled water
DFB4	DumbBell Former
DGCR8	DiGeorge Syndrome Critical Region 8
DKK1	Dickkopf-related protein 1
DKK2	Dickkopf-related protein 2
DKK3	Dickkopf-related protein 3
DKK4	Dickkopf-related protein 4
DM	double minute
DMEM	Dulbecco's Modified Eagle Medium
DNA	desoxyribonucleic acid
DNA2	DNA replication helicase/nuclease 2
DONSON	downstream neighbor of SON
DPBS	Dulbecco's phosphate-buffered saline
DRCR	double rolling-circle replication
DSB	double-strand break
eccDNA	extrachromosomal circular DNA

ECM	extracellular matrix
EDTA	ethylenediaminetetraacetic acid
EdU	5-ethynyl-2′-deoxyuridine
EFNA2	ephrin A2
EGF	epidermal growth factor
ERK	MAPK1, mitogen-activated protein kinase 1
ESC	embryonal stem cell
ESP	EDTA-N-lauroylsarcosine sodium salt - proteinase K buffer
et al.	et alii; and colleagues
FAM20A	FAM20A Golgi associated secretory pathway pseudokinase
FC	fold change
FCS	fetal calf serum
FEN1	Flap endonuclease 1
FOSB	FosB proto-oncogene, AP-1 transcription factor subunit
FoSTeS	replication fork stalling and template switching
FOXA2	Forkhead box A2
FOXO1A	Forkhead box O1A
FOXO3A	Forkhead box O3A
FRMD4A	FERM domain containing 4A
g	gram
G1 phase	gap or growth 1 phase
G2 phase	gap or growth 2 phase
GALC	galatosylceramidase
GAT	gonadal adipose tissue
GEO	Gene Expression Omnibus
GFAP	glial fibrillar acidic protein
GINS	GINS protein complex, *go-ichi-ni-san*
GLI1	GLI family zinc finger 1
GLI2	GLI family zinc finger 2
GLI3	GLI family zinc finger 3
GMNN	geminin
GO	Gene Ontology
GSK3	glycogen synthase kinase 3
h	hour
H3K79me2	dimethylation of lysine 79 on histone H3 protein subunit
H4	histone 4
HBO1	histone acetyltransferase binding to ORC1
HH	hedgehog
HIVEP2	HIVEP zinc finger 2
HLA	human leukocyte antigen
HLA-DR	human leukocyte antigen - DR isotype
hMSC	human mesenchymal stem cell
hNSC	human neural stem cell
HSC70	heat shock cognate 71
HSkM	human skeletal myoblast
HSP90	heat shock protein 90
HSR	homogeneously staining region
HUS1	HUS1 checkpoint clamp component

i.e.	id est, that is
IdU	2'-deoxy-5-iodouridine
IER3	immediate early response 3
IGF1	insulin like growth factor 1
IGF1R	insulin like growth factor 1 receptor
IGFBP2	insulin like growth factor binding protein 2
IGFBP4	insulin like growth factor binding protein 4
IgG	immunoglobulin
iPSC	induced pluripotent stem cell
JUN	Jun proto-oncogene, AP-1 transcription factor subunit
kb	kilobase
KCl	potassium chloride
KEGG	Kyoto encyclopedia of genes and genomes
KH_2PO_4	monopotassium phosphate
l	liter
LAD	lamin-associated domain
LEP	leptin
LIG1	DNA ligase 1
LMP	low melting point
LPL	lipoprotein lipase
LSM4	LSM4 homolog, U6 small nuclear RNA and mRNA degradation associated
M	molar
M phase	mitotic phase
MAP2	microtubule-associated protein 2
MAPK1	mitogen-activated protein kinase 1
MAT	marrow adipose tissue
Mb	megabase
MCM10	minichromosome maintenance 10
MCM2-7	minichromosome maintenance protein complex
MDM2	MDM2 proto-oncogene
MES	2-ethanesulfonic acid buffer
Mg	magnesium
miEAA	miRNA enrichment analysis and annotation
mirDIP	microRNA Data Integration Portal
miRNA	microRNA
ml	milliliter
mM	millimolar
mm	millimeter
MMP1	matrix metallopeptidase 1
MMP13	matrix metallopeptidase 13
MRE	miRNA response element
mRNA	messenger RNA
MSC	mesenchymal stem cell
MSigDB	Molecular Signatures Database
MYF5	myogenic factor 5
MYF6	myogenic factor 6
MYH7B	myosin heavy chain 7B

MYOD1	myogenic differentiation 1
MYOG	myogenin
n	number
NA	not applicable
Na_2HPO_4	disodium phosphate
NaCl	sodium chloride
NADPH	reduced nicotinamide adenine dinucleotide phosphate
NAHR	non-allelic homologous recombination
NANOG	Nanog homeobox
ncRNA	non-coding RNA
NEF	neurofilament
ng	nanogram
nm	nanometer
nM	nanomolar
NOG	noggin
NOX1	NADPH oxidase 1
NPTX1	neuronal pentraxin 1
NSC	neural stem cells
OCT4	POU5F1, POU Class 5 Homeobox 1
OLIG1	oligodendrocyte transcription factor 1
OLIG2	oligodendrocyte transcription factor 2
ORA	over-representation analysis
ORC	origin recognition complex
ORC1	origin recognition complex subunit 1
ORC2	origin recognition complex subunit 2
ORC3	origin recognition complex subunit 3
ORC4	origin recognition complex subunit 4
ORC5	origin recognition complex subunit 5
ORC6	origin recognition complex subunit 6
P	penicillin
p63	tumor protein p63
PAX6	paired box 6
PAX7	paired box 7
PBS	phosphate-buffered saline
PCNA	proliferating cell nuclear antigen
PCSK9	proprotein convertase subtilisin/kexin type 9
pH	potential of hydrogen
PODXL	podocalyxin like
PPARA	peroxisome proliferator activated receptor alpha
PPARD	peroxisome proliferator activated receptor delta
PPARG	peroxisome proliferator activated receptor gamma
PTCH1	patched 1
PTK2B	protein tyrosine kinase 2 beta
p-value	probability value
RAD1	RAD1 checkpoint DNA exonuclease
RAD17	RAD17 checkpoint clamp loader component
RAD53	RAD53 checkpoint kinase 2

RAD9	RAD9 checkpoint clamp component
RC	replication complex
RFC	replication factor C
RISC	RNA-induced silencing complex
RNA	ribonucleic acid
RNAi	RNA interference
ROI	region of interest
RRIGA	re-replication-induced gene amplification
rRNA	ribosomal RNA
RUNX2	RUNX family transcription factor 2
RUVC	recombination UV C
RXRA	retinoid X receptor alpha
S	streptomycin
S phase	replication phase
s.d.	standard deviation
S100B	S100 calcium-binding protein B
SCAT	subcutaneous adipose tissue
SCF	Skp, Cullin, F-box containing complex
siRNA	small interfering RNA
SKP2	S-phase kinase-associated protein 1
SLC39A3	ZIP3, zinc transporter
SLD2	synthetically lethal with Dpb11-1 2
SLD3	synthetically lethal with Dpb11-1 3
SMAD	mothers against DPP homolog
SMAD1	SMAD family member 1
SMAD5	SMAD family member 5
SMAD6	SMAD family member 6
SMAD9	SMAD family member 9
SNV	single-nucleotide variation
SOX	SRY-box transcription factor
SOX13	SRY-box transcription factor 13
SOX2	SRY-box transcription factor 2
SOX5	SRY-box transcription factor 5
SOX9	SRY-box transcription factor 9
SPTB	spectrin beta, erythrocytic
SRC	SRC proto-oncogene
STN1	STN1 subunit of CST complex
TAZ	Tafazzin, phospholipid-lysophospholipid transacylase
TE	Tris EDTA solution
TEN1	TEN1 subunit of CST complex
TFPI2	tissue factor pathway inhibitor 2
TGF-beta	transforming growth factor beta
TNS3	tensin 3
TOPBP1	DNA topoisomerase 2-binding protein 1
tRNA	transfer RNA
TUBB3	βIII-tubulin
U	unit
UTR	untranslated region

vs.	versus
WNT	wingless-type MMTV integration site family
WNT1	Wnt Family Member 1
WNT10B	Wnt Family Member 10B
WNT3A	Wnt Family Member 3A

1. Summary

Gene amplifications, or additional copies of a specific gene or genomic region, are known to occur in cancer cells and to be linked to worse prognosis, probably by aiding them to resist chemotherapeutic agents. In the last few years, they have also been described in human stem cells. However, the mechanism(s) by which they arise have not been yet elucidated, although different models, including re-replication, have been proposed. Re-replication refers to a replication error characterized by the licensing and subsequent firing of an origin of replication after its initial activation. Previous profiling studies usually used stem cells that were differentiating for at least one or a few days, leaving a significant gap in understanding the molecular events occurring during the crucial early hours of differentiation. This thesis investigates the possibility of re-replication happening during the early differentiation of human stem cells, as well as their microRNA (miRNA) and messenger RNA (mRNA) profiles since miRNAs, small non-coding RNAs, are known to play a role in stem cell differentiation.

To address this research objective, time-resolved approaches were used to capture dynamic changes throughout the differentiation process, in five distinct differentiation assays: spontaneous differentiation of human neural stem cells and human skeletal myoblasts, as well as human mesenchymal stem cells undergoing adipogenesis, chondrogenesis, and osteogenesis. The first aspect of this thesis involved the analysis of miRNA and mRNA expression profiles using microarray technology, followed by bioinformatic analysis to elucidate their functional implications. In the second part, molecular combing in conjunction with thymidine analog incorporation was used to investigate the occurrence of re-replication events in human mesenchymal stem cells undergoing chondrogenesis and in human skeletal myoblasts.

This work yielded three key results: Firstly, it revealed the involvement of the hsa-miR-29 family during early stem cell differentiation. Secondly, it highlighted the correlations and pathway significance of miRNAs and genes in early stem cell differentiation. Lastly, it uncovered the occurrence of re-replication events in differentiating human skeletal myoblasts and human mesenchymal stem cells undergoing chondrogenesis. The hsa-miR-29 family, consisting of four miRNAs, was consistently among the top 10 downregulated miRNAs across all differentiation assays and predominantly clustered together. The targets of these miRNAs were enriched in specific clusters, many of which showed increased expression. In particular, pathways related to cell cycle and differentiation were enriched across all differentiation assays. Strong correlations were observed between specific miRNA clusters and gene clusters in each differentiation assay,

with the centroid lines of these clusters often displaying mirroring patterns. Members of the hsa-miR-29 family have already been described to influence certain differentiation processes, although their exact role and mechanism of regulation are still unclear.

In spontaneously differentiating skeletal myoblasts, re-replication events were observed between the 2 h and 6 h time points while no such events were observed before or after, indicating a defined timeframe for re-replication. No re-replication events were observed in proliferating human skeletal myoblasts. Re-replication events were also observed in differentiating and proliferating human mesenchymal stem cells undergoing chondrogenesis at all three time points studied (0 h, 4 h, 6 h).

Re-replication may be more common than previously thought in healthy human stem cells, particularly during differentiation, which may raise concerns about genome stability in induced pluripotent stem cells and other stem cells used for stem cell therapies. This highlights the need to elucidate the mechanisms of gene amplification formation.

These findings elucidate novel miRNA-mediated regulation and occurrences of re-replication during initial stem cell differentiation, raising important questions about their roles in cell fate determination and genome stability. Further unraveling the interplay between re-replication and stem cell differentiation will be essential for developing safe and effective stem cell therapies.

Zusammenfassung

Es ist bekannt, dass Genamplifikationen, d.h. zusätzliche Kopien eines bestimmten Gens oder einer Genomregion, in Krebszellen vorkommen und mit einer schlechteren Prognose assoziiert sind, wahrscheinlich weil sie die Resistenz gegen Chemotherapeutika fördern. In den letzten Jahren wurden sie auch in menschlichen Stammzellen beschrieben. Der Mechanismus oder die Mechanismen, durch die sie entstehen, sind jedoch noch nicht geklärt, obwohl verschiedene Modelle vorgeschlagen wurden, einschließlich der Re-Replikation. Unter Re-Replikation versteht man einen Replikationsfehler, der durch die Lizenzierung und nachfolgende Aktivierung eines Replikationsursprungs nach seiner initialen Aktivierung gekennzeichnet ist. Bisherige Studien zur Erstellung von Zellprofilen haben in der Regel Stammzellen verwendet, die schon einen Tag oder einige Tage lang differenziert wurden, so dass eine erhebliche Lücke im Verständnis der molekularen Ereignisse in den entscheidenden frühen Stunden der Differenzierung besteht. In dieser Arbeit wird untersucht, ob während der frühen Differenzierung menschlicher Stammzellen eine Re-Replikation stattfindet, und es werden die Profile von microRNAs (miRNAs) und der messengerRNAs (mRNAs) untersucht, da miRNAs, kleine nicht-kodierende RNAs, bekanntermaßen eine Rolle bei der Differenzierung von Stammzellen spielen.

Um dieses Forschungsziel zu erreichen, wurden zeitaufgelöste Ansätze verwendet, um dynamische Veränderungen während des Differenzierungsprozesses in fünf Differenzierungsexperimenten zu erfassen: spontane Differenzierung von menschlichen neuralen Stammzellen und menschlichen Skelettmyoblasten sowie von menschlichen mesenchymalen Stammzellen, die Adipogenese, Chondrogenese und Osteogenese durchlaufen. Der erste Teil der Arbeit befasste sich mit der Analyse von miRNA- und mRNA-Expressionsprofilen mittels Microarray-Technologie, gefolgt von einer bioinformatischen Analyse, zur Klärung ihrer funktionellen Auswirkungen. Im zweiten Teil wurde die molekulare Kombination in Verbindung mit dem Einbau von Thymidin-Analoga verwendet, um das Auftreten von Re-Replikationsereignissen zu untersuchen.

Diese Arbeit lieferte drei Schlüsselergebnisse: die Beteiligung der hsa-miR-29-Familie und die Korrelation zwischen miRNAs und Genen in der frühen Stammzelldifferenzierung sowie das Auftreten von Replikationsereignissen in differenzierenden menschlichen Skelettmyoblasten und menschlichen mesenchymalen Stammzellen, die eine Chondrogenese durchlaufen. Die hsa-miR-29-Familie, bestehend aus vier miRNAs, befand sich bei allen Differenzierungsexperimenten konsistent unter den 10 am stärksten herunterregulierten miRNAs und war überwiegend in Clustern organisiert. Die Targets

dieser miRNAs waren in spezifischen Clustern angereichert, von denen viele eine erhöhte Expression aufwiesen. Insbesondere die mit dem Zellzyklus und der Differenzierung in Verbindung stehenden Wege waren über allen Differenzierungsexperimenten angereichert. Es wurden starke Korrelationen zwischen spezifischen miRNA-Clustern und Genclustern in jedem Differenzierungsexperiment beobachtet, wobei die Schwerpunktlinien dieser Cluster oft spiegelbildliche Muster aufwiesen. Es wurde bereits beschrieben, dass Mitglieder der hsa-miR-29-Familie bestimmte Differenzierungsprozesse beeinflussen, obwohl ihre genaue Rolle und der Regulationsmechanismus noch unklar sind.

In spontan differenzierenden Skelettmyoblasten wurden Re-Replikationsereignisse zwischen den Zeitpunkten 2 h und 6 h beobachtet, während davor und danach keine derartigen Ereignisse auftraten, was auf einen spezifischen Zeitrahmen für die Re-Replikation hinweist. In proliferierenden menschlichen Skelettmyoblasten wurden keine Re-Replikationsereignisse beobachtet. Re-Replikationsereignisse wurden auch in differenzierenden und proliferierenden menschlichen mesenchymalen Stammzellen, die eine Chondrogenese durchlaufen, zu allen drei untersuchten Zeitpunkten (0 h, 4 h, 6 h) beobachtet.

Re-Replikation könnte in gesunden menschlichen Stammzellen häufiger auftreten als bisher angenommen, insbesondere während der Differenzierung, was Bedenken hinsichtlich der Genomstabilität in induzierten pluripotenten Stammzellen und anderen Stammzellen, die für Stammzelltherapien verwendet werden, aufwerfen könnte. Dies unterstreicht die Notwendigkeit, die Mechanismen der Entstehung von Genamplifikationen zu erforschen.

Diese Ergebnisse liefern Einblicke in die neuartige miRNA-vermittelte Regulation und das Auftreten von Replikation während der anfänglichen Stammzelldifferenzierung und werfen wichtige Fragen zu ihrer Rolle bei der Bestimmung des Zellschicksals und der Genomstabilität auf. Die weitere Entschlüsselung des Zusammenspiels zwischen Replikation und Stammzelldifferenzierung wird für die Entwicklung sicherer und wirksamer Stammzelltherapien von entscheidender Bedeutung sein.

2. Introduction

2.1.   History of gene amplification

Amplifications are defined as an increase in copy number at a specific and limited genomic region, the amplicon. If this region contains genes, it is called a gene amplification.

They were first observed in plants in the 1940s-1950s (maize, *Zea mays* [376,378]) and a few years later in insects (*Rhynchosciara angelae/Americana* [47], *Drosophila melanogaster* [458], [434,435], and *Sciara coprophila* [90]). There they appeared to play a role in larval development and in salivary glands, which was confirmed in the 1980s [419,420,502,503]. A similar developmental role of gene amplifications has been described in oocytes of annelids, mollusks, and amphibians (*Necturus maculosus*, *Siredon mexicanum*, *Xenopus laevi*, *Urechis caupo* (echiuroid worm), *Spisula solidissima* (surf clam) [52], *Triturus cristatus* [353], *Ambystoma mexicanum* [59], and *Xenopus laevi* [388]).

By the 1970s, gene amplifications were known in two forms: genomic homogeneously staining regions (HSRs), and double minutes (DMs), which are double-stranded, extrachromosomal, paired circular DNA fragments [36,263,490]. Soon thereafter, the theory was proposed that these two forms are the two sides of the same coin and that DMs can integrate the genome by recombination to become HSRs, while HSRs can be derived from the genome to form extrachromosomal DMs [22,49,61]. Around the same time, George and Powers demonstrated that DMs and HSRs contain gene amplifications [174]. Episomes, genetic elements that combine aspects of plasmids and viral genomes, can be precursors for DMs [61].

Simultaneously, a hypothesis about the function of gene amplification in cultured mammalian cells emerged. Indeed, numerous studies reported amplification in rodent cells cultured *in vitro* and the fact that these cells became resistant to drugs [7,36,263,466,467,562]. Since the degree of drug resistance was correlated with the number of amplifications [7,466], it was soon theorized that gene amplifications were responsible for drug resistance in these cells [228,467]. Observations of tumor cells that became resistant to chemotherapeutic agents [4,22,49,141,142,399,470,471], or radiotherapy [143] confirmed the hypothesis that gene amplifications can be used by cells to overexpress genes essential to their survival.

One supporting factor for this hypothesis is the preferential occurrence of gene amplifications in non-random regions of the genome. Since the 1990s, numerous studies have reported the occurrence of gene amplifications at specific loci, both in cultured cells and in cancerous cells [8,141–144,146,150,371,399,444,462,463,470]. Several of these regions contain proto-oncogenes, like for example *CDK4* and *MDM2*, both in the q13-q15 regions of the human chromosome 12, which are frequently found amplified in tumors [142,145,444].

In the last decade, gene amplifications have been discovered in mouse and human stem cells, both *in vitro* [8,147,148,150] and *in vivo* [199,382].

In vitro analyses of myoblasts and neural stem cells showed that several of the amplified genes correspond to those that are also amplified in tumors [8,141,142,144,147,150]. Moreover, the amplification pattern within specific time windows during the differentiation of specific stem cell populations suggested that amplification occurs in an orderly organized sequence during the differentiation of these cells [151].

In vivo, trophoblasts and trophoblast giant cells, which are naturally occurring placental cells, have been shown to exhibit polyploidy and other copy number variations [89,198,550]. Gene amplification patterns have also been identified in mouse neural stem cells and embryos [148,149]. As in insects and amphibians, gene amplifications seemed to play a developmental role: amplification loci contained different placental gene families, although the mechanism through which these amplifications arose appeared different than the one in *Drosophila* [199]).

2.2.   Regulation of gene expression by microRNAs

Gene expression is regulated by many factors other than gene copy number, such as epigenetic marks, transcription factors, and non-coding RNAs (ncRNAs). Most ncRNA classes are involved in gene expression processes: transfer RNAs (tRNAs), ribosomal RNAs (rRNAs), microRNAs (miRNAs), etc. [81,96,116,315,327,414]. Non-coding RNAs, unlike messenger RNAs (mRNAs), are not translated into proteins.

The microRNAs class regulates gene expression via the phenomenon of RNA interference (RNAi), by forming an RNA-induced silencing complex (RISC) with an Argonaute protein [28]. They target mRNAs via so-called miRNA response elements (MREs), which are usually located in the 3'-UTR (untranslated region) of the mRNA [319,469,505], but sometimes also in the 5'-UTR or even the open reading frame [405,469,637]. Nucleotides 2 to 8 of the miRNA are referred to as the seed region, and they play a central role in the recognition and binding of MREs [28]. Both MREs and seed regions are evolutionarily highly conserved [1,28,318,319,469,505]. After recognition of the MRE by the RISC, the mRNA is degraded via decapping mechanisms [28], which is the usual outcome in metazoans [127,193], or its translation is repressed [255,555].

Perfect complementarity of the seed and corresponding MREs is not required for the miRNA to recognize and bind its target mRNA, although it does influence the strength of the gene expression repression [28,50,188]. This is one of the reasons why one miRNA can target numerous mRNAs and one mRNA can be targeted by more than one miRNA. This repression network is thought to encompass most, if not all, of the human transcriptome [156,319].

The biogenesis of miRNAs follows several possible pathways, focusing here on the canonical pathway in metazoans. miRNA genes can be found alone or in clusters [454], either in introns or exons of gene-coding proteins or in intergenic regions [155,457]. The main RNA polymerase responsible for miRNA gene transcription is RNA polymerase II, resulting in long-capped and polyadenylated RNA molecules that form at least one hairpin structure, called pri-miRNAs. The hairpin(s) are then cleaved by the microprocessor complex, which consists of the endonuclease Drosha and its cofactor DGCR8 (DiGeorge Syndrome Critical Region 8). The consequent 60- to 70-nucleotide-long hairpin, referred to as pre-miRNA, is exported to the cytoplasm by Exportin 5 and RanGTP [44,311,603]. There, it is cleaved by the endonuclease Dicer at the base of the loop, resulting in a miRNA duplex [33,189,226]. One of the two miRNAs is loaded onto an Argonaute protein (one of four in humans; [28,518]), aided by the chaperones HSC70 (heat shock cognate 71) and HSP90 (heat shock protein 90; [238]) to form the RISC, whereas the other strand is frequently degraded [267,381].

2.3. Stem cells

Stem cells are unspecialized cells that occur in both developing and adult organisms and are capable of self-renewal. They were first described by Ernst Haeckel in the late 19th century [445] and, thanks to telomere regeneration, can theoretically divide indefinitely, something more specialized cells cannot do [534]. They are also capable of differentiating into multiple cell types, with totipotent stem cells being able to become each type of cell found in an organism [369]. However, most stem cells available to researchers are multipotent at best [451], such as embryonic stem cells (ESCs), which can give rise to any cell type of the three germ layers (endoderm, mesoderm, ectoderm), as well as germ cells.

Stem cells are often characterized according to their origin (embryonic or adult, tissue of origin) or their differentiation capabilities (e.g., "neural progenitor cells" for example). ESCs are derived from cells isolated from blastocyst stage embryos, they were first isolated from murine embryos by Evans and Kaufman in 1981 [132], and in 1998 from human embryos by Thomson and colleagues [534]. Adult or somatic stem cells are less pluripotent than embryonic stem cells since they are generally bound to a specific tissue and, therefore, more specialized. Some types of adult stem cells also have a more limited division potential than ESCs [105]. Induced pluripotent stem cells (iPSCs) are adult stem cells that have been genetically reprogrammed into a more ESC-like state. The technique for their production was first published by Takahashi and Yamanaka (the Yamanaka factors; [522,523]), but since then many other reprogramming cocktails have been developed. These include, for example, the so-called Thomson factors [608] or lentiviral expression of miRNAs [12,392].

2.3.1. Stem cell differentiation

Stem cell differentiation often begins with a fate commitment phase that is determined by a variety of factors, from extracellular chemical signals to the physical properties of the substrate, or internal signaling pathways [72].

2.3.1.1. Differentiation of mesenchymal stem cells

Human mesenchymal stem cells (hMSCs) are adult stem cells, well known in the stem cell community for their ability to differentiate into numerous cell types, including but not limited to adipocytes, chondrocytes, and osteoblasts [51,403]. They are defined by specific

surface markers: CD73, CD90, CD105 (> 95 % positive cells), CD13, CD29, CD44 (> 80 % positive cells), and CD11B, CD14, CD19, CD31, CD34, CD45, CD7A, CD235A/GYPA, HLA-DR (< 2 % positive cells), according to the International Society for Cellular Therapy [120].

Possible fates for mesenchymal stem cells include differentiation into adipocytes, chondrocytes, neurons, and osteocytes.

Chondrogenesis in hMSCs is usually characterized by three phases: first cell attachment, then differentiation of chondroprogenitor cells into proliferating then pre-hypertrophic chondrocytes, and finally Wnt signaling inhibition and hypertrophy [230,398]. Specific sets of genes are associated with each phase, such as the Wnt, Notch, and IGF1 signaling pathways for the differentiation induction phase [398]. Collagen and other genes related to the extracellular matrix also show changes in their expression levels during chondrogenesis [232,370,494]. Transcription factors involved in chondrogenesis comprise members of the SOX family (including SOX9, the major chondrogenic factor, and SOX13), FOXO1A, FOXO3A, and FOXA2, the FOS/JUN complex, the TGFB signaling pathway, and retinoic acid receptors [2,219,227,266,398,493,546].

The differentiation of hMSCs into adipocytes consists of two phases: a determination or commitment phase, followed by terminal differentiation of the preadipocytes [402]. To become osteoblasts, hMSCs first undergo a commitment phase in which they become osteoprogenitor cells, then differentiate into pre-osteoblasts that mature into osteoblasts or osteocytes [406].

It has been shown that the commitment of hMSCs to adipogenesis inhibits osteogenesis and vice versa [32,72,243,453]. This so-called adipogenesis-osteogenesis balance can be observed in expression levels even before commitment, which occurs between 2 and 5 days after induction of differentiation [465]. Although Robert and colleagues did not see differences in the expression of genes involved in osteogenesis in the first 24 hours after induction of differentiation, they did observe differences for genes associated with adipogenesis [452]. The two most important transcription factors for the adipogenesis-osteogenesis balance are PPARG (peroxisome proliferator-activated receptor gamma) and RUNX2 (RUNX family transcription factor 2), which control adipogenesis and osteogenesis, respectively [245]. Most signaling pathways involved in either differentiation direction, such as Wnt, hedgehog (HH), BMPs, IGF1 (insulin-like growth factor 1), and

many other pathways, affect the expression or activity of PPARG and/or RUNX2 [94,152,243,244,283,307,421,520]. Thus, the HH signaling pathway, which is involved in osteogenesis, decreases the expression of PPARG itself and also that of CD36 (cluster of differentiation 36) and C/EBPA (CCAAT-enhancer-binding protein alpha), both of which play a role in adipogenesis [152,245,558]. Rescue experiments in mice showed that *PPARG* knock-out inhibits adipogenesis and can not be rescued [380,616] and that lack of RUNX2 is fatal shortly after birth as there is no ossification [421], although this phenotype can be partially rescued [621]. Some miRNAs also play a role in the balance between adipogenesis and osteogenesis, such as hsa-miR-204 which targets, among others, *RUNX2* [205]. While this adipogenesis-osteogenesis balance appears to be quite binary, some signaling pathways have been shown to play a role in both differentiation directions, like the BMPs and IGF1 pathways [123,245,259].

2.3.1.2. Differentiation of skeletal stem cells

Myogenic progenitor cells are skeletal muscle precursors that first differentiate into myoblasts, then myotubes, and finally myofibers [279,521]. In an adult, healthy organism, they are quiescent and are activated only to repair damage to muscle fibers or to prolong their growth [78,191]. Myogenesis is governed by many myogenic regulatory factors of the basic helix–loop–helix (bHLH) family, such as MYOD1 (myogenic differentiation 1), MYF5 (myogenic factor 5), MYOG (myogenin), and MYF6 (myogenic factor 6; [211]).

2.3.1.3. Differentiation of neural stem cells

Neural stem cells (NSCs) can give rise to neurons but also glial cells such as astrocytes or oligodendrocytes. In the adult organism, the immediate environment of neural stem cells limits their differentiation potential to one of a few cell types [545].

According to the literature, OLIG1 (oligodendrocyte transcription factor 1), a member of the bHLH family, inhibits all fates except the neuronal one [639], leading to the expression of neuronal markers such as βIII-tubulin (TUBB3), doublecortin (DCX), microtubule-associated protein 2 (MAP2), and neurofilament proteins (NEFs; [53,299,496]). In the event a neuronal differentiation is not initiated, NSCs can differentiate into oligodendrocytes through expression of OLIG2 (oligodendrocyte transcription factor 2; [639]) and eventually express markers such as galatosylceramidase (GALC), OLIG1, OLIG2, and surface markers O1 and O4 [27,540]. If neither *OLIG1* nor *OLIG2* was expressed, NSCs differentiate by default into glial cells such as astrocytes [279,639],

which express surface marker CD44, S100 calcium-binding protein B (S100B), and glial fibrillar acidic protein (GFAP; [121,443,499]). In cell culture, this is the most common fate.

2.3.2.   Role of miRNAs in stem cells

Stem cell differentiation requires swift and massive changes in gene expression to switch phenotypes. One of the most rapid means of altering gene expression is miRNAs due to their post-transcriptional regulatory role. These have been shown to play a very important role in stem cell differentiation as well as in maintaining stemness [604].

Many miRNAs are upregulated during the chondrogenesis of human cells [187,373,599,625]. Among them are three miRNAs targeting *MMP13* (matrix metallopeptidase 13): hsa-miR-127-5p [424], hsa-miR-27b [324], and hsa-miR-320c [197]. The chicken homolog of hsa-miR-9 (gga-miR-9) also targets *MMP13* and promotes chondrogenesis [331]. Additionally, hsa-miR-320c has been shown to target *RUNX2* [196,646], as does hsa-miR-455-3p [73,625]. The chondrogenic miRNA hsa-miR-335-5p is regulated by multiple feedback loops, including one involving downregulation of the expression of hsa-miR-29a and hsa-miR-29b [338], two chondrogenesis-inhibiting miRNAs [192,594].

Numerous miRNAs known to repress chondrogenesis target *SOX9* or *SOX5*: miR-101 [92], hsa-miR-1247 [368], hsa-miR-145 [367,595], hsa-miR-194 [589], hsa-miR-30a [615], miR-30b [559], hsa-miR-3677-3p [361], and hsa-miR-495 [310]. TGFB signaling is also frequently targeted by chondrogenesis-inhibiting miRNAs such as the miR-17/92 family [331], hsa-miR-337 [579,634], and by hsa-miR-193b-3p, which exerts a dual role during chondrogenic differentiation [213,385]. Like some other miRNAs, hsa-miR-193b-3p promotes the latter steps of chondrogenesis (hypertrophy) but suppresses early differentiation [213,331,385,512].

The two members of the miR-27 family, miR-27a and miR-27b, are known to be involved in the repression of adipogenesis by inhibiting the expression of *PPARG*, *C/EBPA*, and *LPL* (lipoprotein lipase; [217,248,261,277,335,585]. *PPARG* is also targeted by hsa-miR-130 [303] and miR-301 [325]. Other miRNAs such as hsa-miR-138 [131,598], miR-155 [341,563], miR-31 [515,530], and miR-335 [404,537] target adipogenic factors and thus have anti-adipogenic effects.

The miRNAs let-7a and -b have been shown to promote adipogenesis and are upregulated during adipogenic differentiation [257,515], as are other miRNAs such as hsa-miR-143 [130,257,586], miR-15a and b [122,257], hsa-miR-26b [479,495], hsa-miR-30 [479,611], and others. hsa-miR-143 has been found to be essential for adipogenesis [130], and its expression level correlates with markers of adipocyte differentiation [525]. At least three adipogenic miRNAs are known to target members of the TGFB signaling pathway: miR-20a [638], hsa-miR-21 [258,278,342], and miR-210 [439]. Some of the miRNAs known to promote adipogenesis have been shown to target osteogenic factors: hsa-miR-148a [479,586], hsa-miR-204-5p [205,221], and miR-30e [565].

Conversely, some miRNAs promoting osteogenesis target adipogenic factors such as *SMAD1* (SMAD family member 1), *DKK1* (Dickkopf-related protein 1), or *DKK2*: hsa-miR-146a [112,587], miR-217 [93,474,622], hsa-miR-218 [168,200,620,622], hsa-miR-26a [80,90, 247,393], miR-335-5p [617,630], miR-433-3p [529], and miR-9 [343]. One of the best-known miRNAs associated with osteogenesis, miR-21, plays a dual role depending on the context: either promotion of osteogenesis or bone resorption [215,326,342,488,568].

As expected, a large proportion of miRNAs involved in the repression of osteogenesis target the major osteogenic factor, *RUNX2*: miR-133a-5p [619,622], miR-204 [221,250,622], miR-205 [622], hsa-miR-23a [474,622], miR-30b [474,581], hsa-miR-30c [581,622], and many others [134,229,474,581,622].

For the differentiation of skeletal myoblasts or satellite cells, i.e., muscle cell progenitors, a group of miRNAs called myomiRs is critical. This group includes hsa-miR-1, hsa-miR-133a, hsa-miR-133b, hsa-miR-206, hsa-miR-208a, miR-486, and miR-499, which are all muscle-specific or enriched miRNAs [211,394]. Other miRNAs involved in myogenesis involve miR-221, miR-222 [60], miR-322, miR-424, miR-503 [171], miR-196 [212], miR-125b [172], miR-203 [351], and miR-431 [306]. Some of these miRNAs have a highly similar sequence, for example, miR-1 and miR-206 only have four non-identical nucleotides, all outside the seed region. Other pairs comprise mir-221/miR-222, miR-208/miR-499, and miR-322/-424/-503 [171]. Having identical seed regions, the two miRNAs of a pair probably have common targets.

The mir-1 and miR-206 pair share many similarities other than their sequences. Both are upregulated in mice, rats, dogs, and human patients after muscle injury, although their

expression levels are transiently reduced just after the injury [184,246,374,375,516,609]. This decrease has been linked to the anti-proliferation effect by *PAX7* targeting of both miRNAs [57,71,110] and is also observed in the early muscle regeneration phase in mice, dogs, and human [71,172,184,609]. Satellite cells have been shown to actively proliferate during this phase [202]. Both miR-1 and miR-206 have been reported to be essential for the differentiation of satellite cells into skeletal myoblasts and muscle fibers [71,539], and miR-1 is required for the differentiation of ESCs into cardiomyocytes [526].

In addition to miR-1 and miR-206, *PAX7* was also shown to be targeted by miR-486 [71,110], triggering a positive feedback loop via upregulation of *MYOD1* [110,487].

The myomiRs miR-133 has also been shown to play an important role in the differentiation of ESCs into cardiomyocytes [285,526] but appears to be involved in promoting proliferation in skeletal myoblasts [70,74,448,539]. Like miR-1 and miR-206, it has been reported to be upregulated during the muscle regeneration process [246,374,609]. According to miRBase release 22.1 [286], hsa-miR-206 and hsa-miR-133b are located in the same cluster on chromosome 6, and hsa-miR-1-2 and hsa-miR-133a-1 share a cluster on chromosome 18.

The genes of the myomiRs miR-208a, miR-208b, and miR-499 are all located in introns of myosin genes (*alpha-MHC*, *beta-MHC*, and *MYH7B*, respectively; [547]). These miRNAs are involved in the terminal differentiation of myotubes into myofibers [160,234,547].

The best-known miRNAs influencing neurogenesis are miR-124 and miR-9, both of which promote the differentiation of neural stem cells into neurons (124 [77,359,552,605]; 9 [103,317,481,626]). In rat PC12 cells, miR-124 plays a role in neuron guidance [76], and it is specifically expressed in the murine and human central nervous system [106,298], with increased expression during brain development [289,476,489] and during adult neuroblast differentiation [77]. Similarly, hsa-miR-9 is enriched in the brain, and its expression is increased during embryonic brain development [101,103,289,489].

Other miRNAs involved in neurogenesis include miR-132, which promotes dendritic growth [356,553,572], hsa-let-7-a, -b, -c, and -e, which promote neuronal differentiation [313,345,363, 483] and whose expression is increased during neuronal differentiation [476], hsa-miR-128 [54,289,489], and hsa-miR-137, which regulates proliferation, differentiation, and dendritic morphology of adult neural stem cells [484,492,513,519], and inhibits synaptogenesis [509].

Differentiation of NSCs into glial cells such as oligodendrocytes is also regulated by miRNAs: miR-138, miR-219, and miR-338 among others [125,129,334,408,535].

2.4. The DNA replication process

In order to divide, cells must first replicate their genome. For them, it is of utmost importance that the DNA replication process encompasses the entire genome, but also that it takes place only once per cell cycle. To ensure this, the replication process is highly regulated, sometimes even by seemingly redundant mechanisms. The DNA replication process consists of the licensing of replication origins, the activation of the loaded helicase that unwinds the double strand, allowing the formation of replisomes, and the migration of replication forks that eventually converge with others to terminate the replication by disassembling the replisomes [170].

This work focuses on the replication of eukaryotic genomic DNA, but not the replication of mitochondrial DNA (reviewed in [91,136,645]).

Jacob and colleagues proposed the replicon model in 1963, in which each replicon is defined by an initiator acting in *trans* and a replicator sequence in *cis* [242]. This replicator sequence is now referred to as the origin of replication and is present in all organisms, albeit in different forms and expressions [48,271,440,554]. A replicon can be defined as the length of chromatin replicated from a single origin; thus, its size depends on the number of origins, the speed of the replication process, etc.

2.4.1. Origins of replication

While most bacteria have only one origin of replication in their genome, eukaryotic genomes have many more. Originally, it was assumed that they would need that many to complete replication in a reasonable time frame. However, eukaryotic genomes have been shown to possess at least 4 to 10 times more origins than expected for this reason only [34,58,108,169,231].

Redundancy of origins is thought to be the eukaryotic response to the problem of replication stress, in contrast to prokaryotes for which replication fork restart is of paramount importance. Eukaryotic genomes, therefore, have constitutive origins that are fired in all replication cycles in all cells, flexible origins whose activation depends on the cell type, and dormant origins that are activated only in the event of replication fork stalling or other manifestations of replication stress in their vicinity [3,11,87,241,578]. Moiseeva and Bakkenist estimated in 2019 that only about 50,000 of about 500,000 licensed origins replicate in the human genome [393]. A 2016 study by Smith and colleagues profiled the origins of replication in eight human cell lines, including some cancer cell lines. They found that the origin pool distribution was highly comparable for non-cancer and cancer cell lines of similar lineages [491]. However, it should be noted that the pools of constitutive, flexible, and dormant origins are not identical in all cell types of an individual [104].

According to Löb and colleagues, this model implies that dormant replication origins must be prevented from firing by replication forks, a passive suppression that occurs at a distance of about 7 to 120 kb [344]. This mechanism has been termed "origin interference". A well-known example is oriGNAI3, a replication origin located in the *AMPD2* (adenylate deaminase 2) gene in Chinese hamster cells. As Anglana and colleagues demonstrated in 2013, the firing of oriGNAI3 correlates with the silencing of neighboring origins, and in the case of activation of other origins of replication in the same region, the efficiency of initiation of oriGNAI3 is reduced [11].

There also appears to be a mechanism controlling the speed of replication forks. It has been shown to correlate with the replicon length, i.e., with the distance between fired origins: the closer these were situated, the slower the fork moved [84].

Replication origins are not distributed evenly across metazoan genomes. While the resolution of older studies only permitted the identification of "initiation zones" [107], the method of molecular combing allowed researchers to investigate at a new resolution [56,207].

Molecular combing is a method for producing naked DNA fibers using the receding air-water interphase of a DNA solution. Silanized glass coverslips are immersed into the solution and then slowly and steadily lifted, allowing the bound fibers to unwind and unravel without breaking. This method results in parallel fibers stretched uniformly at approximately the same factor (2 kb/μm), in the range of hundreds of kb to a few Mb [30,83,268].

Some regions of the chromatin replicate constitutively early in the S phase, while others are constitutively replicated late in the S phase; these regions, composed of multiple replicons, are called replication-timing domains (see Figure 2.1) [3]. These domains are highly linked to the 3D organization of the chromatin and the nuclear architecture [459]: late-replicating domains and lamin-associated domains (LADs) colocalize at the nuclear periphery [431,592]. Moreover, late-replicating origins are associated with repressive chromatin marks, and early-replicating origins are associated with active euchromatin marks. Replication-timing domains were also shown to be conserved between cells in a population [117] and between homologous chromosomes [524].
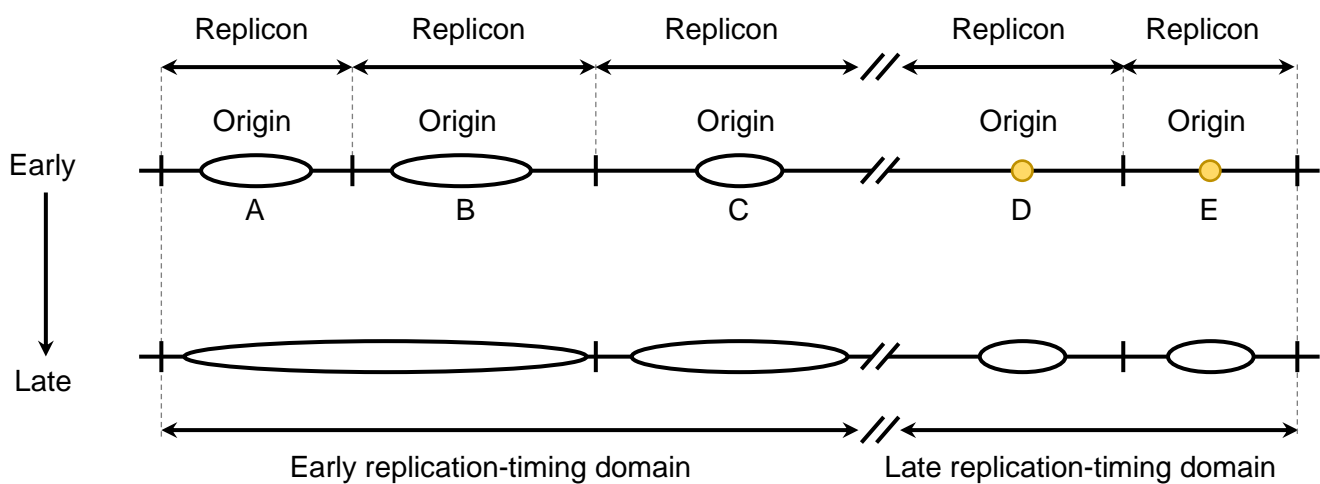
Figure 2.1: Replication timing domains. Schematic of a portion of a eukaryotic genome, in which replication origins A, B, C, D, and E each define a replicon. Origins A, B, and C start replication early in the S phase, either concomitantly or in rapid succession, and form together an early replication-timing domain. Origins D and E are activated later and form a late replication-timing domain. Figure modified from [3].

Due to the differences in the chromosomal environment between early- and late-replicating origins and regions, it was suggested early on that replication timing was not defined genetically [40,348]. According to these observations, it was rather pre-determined at the chromosomal domains level, while remaining stochastic at the single-origin level [297]: each region is defined by a small number of replication origins, from which one will be activated per replication cycle ("flexible replication model"; [63]). This theory was further corroborated by two *in silico* models [178,344] that integrated chromatin structures, and, among others, the flexible replicon model, respectively, and that yielded results highly similar to the experimental data. Other complementary findings came from Das and colleagues, who showed that some components of the replisome can be loaded in multiple

exemplars at a single origin and that this overloading is associated with early replication timing [97]. Together with similar findings for other replication factors [360,528,538], these results led to a model of the mechanism of replication timing based on limiting quantities of replication factors. The prevailing hypothesis proposes that early and late-replicating regions are influenced by the availability of replication factors, such as DFB4, the fungal CDK substrates SLD2 and SLD3, and their binding partner DPB11/TOPBP1 ((DNA topoisomerase 2-binding protein 1), which limit the number of origins fired and replicated simultaneously [288,360,425,580]. Furthermore, the density of origins may also contribute to replication timing. Indeed, early-replicating regions tend to be richer in replication origins than late-replicating regions [63,391].

Since replication origins in prokaryotes and yeast are associated with a particular nucleotide sequence, researchers looked for a similar sequence in metazoans. Over the years, however, they could not find such a consensus sequence, whether by mapping approximately 52.000 binding sites of one of the components of the origin recognition complex (ORC) against the human genome [391] or by genome-wide analysis of nascent strands in *Drosophila melanogaster* and mouse (*Mus musculus*) cell lines [63] or in human cell lines [34].

2.4.2. The replication process

At the end of the M (mitosis) phase and the beginning of G1, the genome slowly assumes its conformation in the nucleus, and the origins of replication are licensed [79]. This licensing occurs through the docking of the pre-RC (replication complex) to the origins.

First, the ORC (origin recognition complex), which consists of the proteins ORC1, ORC2, ORC3, ORC4, ORC5, and ORC6, binds to the DNA via nucleoplasmin [41]. Analysis of the ORC structure showed that this hexameric protein complex forms a ring around the DNA strands [39]. The binding of the ORC complex then allows the loading of the hexameric DNA helicases MCM2-7, which is dependent on CDT1 (chromatin licensing and DNA replication factor 1) and CDC6 (cell division cycle 6) [41,446]. This whole complex is referred to as the pre-replication complex (pre-RC; [436]). HBO1 (histone acetyltransferase binding to ORC1), the coactivator of CDT1, is also required for licensing [390].

The pre-RC stays at the origin throughout the remainder of the G1 (growth) phase, and MCMs helicases are activated during the S phase (DNA synthesis) by CDK2 and CDC7-mediated phosphorylation events and by recruitment of CDC45 and GINS via MCM10 and the CDC7-DFB4-complex. CDT1 also plays a role in MCM2-7 activation by interacting with DBF4 (DumbBell Former), thereby contributing to CDC45 recruitment and directly stimulating helicase activity [436]. The entire replicative complex, including the MCMs helicases, is removed after replication of the replicon is complete to prevent the re-firing of the origin [41].

The DNA is unwound by the ATPases MCM2 and MCM7 [109,166], first at the origin of replication, then using the energy released by nucleotide hydrolysis to migrate on the DNA [508].

The DNA polymerase alpha-primase complex is recruited to freshly unwound DNA to synthesize an RNA primer of about 10 ribonucleotides and extend it with about 20 deoxynucleotides [349]. Replication factor C (RFC) recognizes this RNA-DNA primer, thereby displacing DNA polymerase alpha and recruiting PCNA (proliferating cell nuclear antigen), which clamps onto the DNA and supports the processivity of DNA polymerase delta [17,355]. In addition to synthesizing the daughter strand of DNA, the replisome also detects and corrects errors, so that the overall accuracy of the replication process is about one mistake per 10^9 nucleotides [293].

Although the two replication forks originating from a single origin of replication generally move at the same velocity [84], the replication process is different for the two DNA strands. Because the DNA helix is anti-parallel and the DNA polymerases are only able to synthesize new DNA in the 5' to 3' direction, one strand called "lagging strand", must be synthesized in small pieces called Okazaki fragments [461]. The ribonucleotides of the primer are replaced with deoxynucleotides by DNA polymerase delta and Flap endonuclease 1 (FEN1) or endonuclease DNA2, and the fragments are ligated by DNA ligase 1 (LIG1; [18,23,180,576,632]).

To avoid telomere defects, the CST complex (CTC1-STN1-TEN1) associates with telomeres and recruits DNA polymerase alpha to the leading strand or C-strand [270,449,507].

The replication termination process is usually broken down into four steps, although their order and requirement or not for a specific sequence are not yet clear: fork convergence, synthesis completion or gap filling, replisome disassembly, and decatenation [109].

2.4.3.   Regulation of replication & replication stress

Because DNA replication is such an important biological process, it is tightly regulated.

One of the major sources of replication stress is fork arrest, in which replication fork progression stalls or is stopped altogether. Several events can cause fork arrest, including transcription of highly expressed genes, DNA damage, or tightly bound protein complexes [19,538,543,544]. Some DNA regions such as telomeres also act as "natural replication barriers" [507].

To mitigate the impact of fork arrest, dormant origins of replication located in the vicinity are often activated, possibly via STN1, one of the subunits of the CST complex [42,507,602].

Other proteins such as DONSON (downstream neighbor of SON) may play a role by protecting the stalled replication fork [133,316,447].

Replication stress also activates the S phase replication checkpoint, which stops replication origins from firing throughout the genome [239,574,602,635]. Several proteins such as the ATM (Ataxia telangiectasia mutated) and ATR (Ataxia telangiectasia and Rad3-related protein) kinases, some of the pre-RC proteins, DBF4, RAD1, RAD9, RAD17, and HUS1 act as sensors of DNA damage or replication stress [135,239,365]. All these pathways activate the effector kinase CHEK2 (checkpoint kinase 2), also known as CHK2 or RAD53 [423,482]. It has been suggested that DNA replication progresses normally below a certain threshold of CHEK2 activation, possibly supported by the firing of dormant origins of replication, and is halted only when replication stress exceeds this threshold [460,482]. This intra-S phase dose-dependent process of checkpoint activation might be suppressed in embryonic nuclei, in which replication timing and initiation rules are different from those in adult nuclei [40,223,483].

Cyclin-dependent kinases (CDKs) play more than one role during DNA replication and more generally in the S phase. CDK2 and CDK3 are necessary and sufficient for the transition from G1 to the S phase [79]. CDK2 is also required for the activation of the origins of replication [288,358]. In addition, CDK1 and possibly CDK2 are involved in inhibiting the re-activation of replication origins, limiting DNA replication to one copy per cell cycle [29,119,203,354]. This is achieved by blocking the binding of the ORC complex to DNA downstream of G1 [88,128,139,236,321,591], nuclear exclusion of MCM2-7, and downregulation of CDC6 activity [514].

Other regulatory pathways result in the degradation of CDC6, MCM2-7, or ORC subunits [126,195,322,384,464].

However, CDT1 appears to be the most commonly targeted factor to prevent origin re-firing, i.e., re-replication. In mammalian cells, at least three mechanisms targeting CDT1 are active: degradation of CDT1 via the CUL4-DDB1^{CDT2} pathway, via the SCF^{SKP2} pathway, and sequestration by geminin (GMNN) [16,17,541]. The interplay between these pathways appears to be cell-type dependent [17,290,346,354,412,643].

Proteolysis of CDT1 via the CUL4-DDB1^{CDT2} pathway relies on the binding of chromatin-bound PCNA (proliferating cell nuclear antigen) to CDT1 [16,17], which induces its ubiquitylation. This pathway is also activated in the event of DNA damage [208,216,251,413,441].

The SCF^{SKP2}-dependent degradation of CDT1 is triggered by CDK2 [17] and can be inhibited by GMNN, at least during the M phase, to allow proper licensing [542].

Sequestration of CDT1 by GMNN prevents it to bind and recruit MCM2-7 but does not block the interaction of CDT1 with replication origins [85,138,177,302,352]. This process appears to be associated with H4 acetylation by HBO1 [390] and to be CDK-independent [25,320,511]. GMNN expression begins in late G1 and gradually increases during the S phase until it reaches its maximum in the early G2 phase [41,379,577]. In early anaphase, geminin is degraded along with other targets of APCCDC20 and APCCDH1 [379,442]. This destruction liberates CDT1, which can play its licensing role in G1. It has been suggested that the sequestration of CDT1 by GMNN protects it from degradation by the SCF^{SKP2} pathway but not from the CUL4-DDB1^{CDT2}-dependent proteolysis [15].

2.5. Models for gene amplification

Although the roles of gene amplifications are now well understood, the mechanism(s) by which they arise still puzzles researchers. Nowadays, four models have been proposed as explanations: the breakage-fusion-bridge (BFB) model, the re-replication model, the (DRCR) model, and the replication fork stalling and template switching (FoSTeS) models [371], all of which rely on specific mechanisms of DNA replication. It is important to note that these models are not mutually exclusive, and gene amplifications may potentially arise through a combination of these mechanisms depending on the cellular context and conditions.

2.5.1. The BFB model

The breakage-fusion-bridge model was first proposed by McClintock in 1941 after observations of gene amplifications in maize [376,377]. A few decades later, drug selection experiments in mammalian cells provided the first experimental evidence for this model [86]. This mechanism could also be observed in human osteosarcoma cell lines [475].

To form a BFB cycle, a double-strand break (DSB) must occur on a chromosome, causing it to lose a telomere. After replication, two sister chromatids are formed, each with only one telomere. They fuse, leading to a dicentric chromosome that breaks during the following anaphase, creating two chromosomes without telomeres so that the cycle repeats during the next division. The resulting gene amplifications consist of inverted repeats. Certain loci, such as fragile sites, are susceptible to DSBs and thus to BFB-driven gene amplification [4,206,294].

2.5.2. The DRCR model

Futcher and colleagues proposed the double rolling-circle replication model in 1986 [162], in which a replication fork is arrested, resulting in DSBs at the forks. The broken strands recombine with each other to form a circle. Break-induced replication then occurs, amplifying the genomic region within the circle into repeats. DRCR can also arise from a BFB cycle, in which case inverted repeats are created.

Experimental evidence for this model was provided in 2005 and 2011 in *Saccharomyces cerevisiae* and Chinese hamster cells [570,571].

2.5.3. The FoSTeS model

The replication fork stalling and template switching model was suggested in 2006 by Slack and colleagues [486], and it has been supported by studies in human patients [304,613].

This model also starts with an arrested replication fork, but here the lagging strand anneals to the lagging strand of the sister chromatid, forming a microhomology junction. The consequent Holliday junction is resolved by the RUVC protein, resulting in recombined products, one of which contains the two copies of the region upstream of the microhomology junction.

2.5.4. The re-replication model

Re-replication is a possible error of replication where an origin of replication is licensed and fired again after it has been activated the first time [541]. Dormant origins may also be fired after their genomic region has already been replicated [98,531]. This results in some genomic regions being amplified and is thus distinct from endoreplication (also called endoreduplication), in which the entire genome is duplicated [17,372].

Re-replication was first proposed as a model ("onionskin model") for gene amplification in the 1980s when studies of oogenesis in *Drosophila melanogaster* revealed that gene amplification was required for normal egg development [468,502,503,506,557]. More recent studies refer to RRIGA, or re-replication-induced gene amplification, and link this mechanism to mediation via NAHR (non-allelic homologous recombination; [140,185,372]).

Prevention of re-replication is achieved by prevention of re-licensing, targeting CDT1 and CDC6 [41,541] or specific histone modifications such as H3K79me2 [3,158]. Experimental depletion of geminin or overexpression of CDT1 and/or CDC6 results in re-replication, although overexpression of CDC6 alone produces lower levels of re-replication [124,541,549]. Under these conditions, re-replication occurs very early, within 1 to 4 hours of entry in the S phase, and mainly at the early origins of replication, at least in mammalian cells [159,549]. One study reported that re-replication following geminin depletion in *Drosophila melanogaster* occurs preferentially in late-replicating regions [118].

2.5.4.1. Consequences of re-replication

Since re-replication usually occurs relatively soon after the initial firing of the origin of replication, multiple replication forks could follow each other and possibly collide and collapse. This is one of the proposed explanations for the amount of DNA double-strand breaks observed after re-replication induction [5,98,643,644]. The consequences of such DNA damage include stimulation of the NAHR mechanism, which was argued to mediate RRIGA [140,185]. Another outcome is the activation of the replication checkpoint by ATM and ATR [17,41,98,541], resulting in cell cycle arrest and eventual apoptosis. However, there appears to be a threshold of tolerable DNA damage below which the checkpoint is not activated [460,482], and some studies show that checkpoint activation leads to the repair of DNA and a reduction in re-replicated regions [296,549].

2.5.4.2. Links with cancer

Deregulation of replication is as expected linked to diseases, including inherited disorders such as microcephaly-micromelia syndrome [133,316,447]. However, it is mainly studied in the context of cancers and tumorigenesis [43,164,623]. CDT1 overexpression is common in several human cancers [14,260,588], as is CDC6 overexpression [3,210,260,339,541]. These are associated with a worse prognosis [357]. As expected, several factors of the replication or regulation of replication machineries have been suggested as potential targets for anti-cancer therapies, such as CDT1 [42,400], and geminin [548].

2.6. Motivation & goals

Gene amplifications are present in both stem cells and cancer cells, and it has been shown that the number of amplifications of oncogenes is a good prognostic tool in certain cancers: breast, colon, ovarian cancer, neuroblastomas, small-cell lung cancer [471]. Data from the Pan-Cancer Analysis of Whole Genomes Consortium of the International Cancer Genome Consortium and The Cancer Genome Atlas, among others, confirmed the association between gene amplification and cancer [329].

Understanding the mechanisms by which they arise and whether the mechanisms are similar in stem cells may therefore provide new ideas to specifically target cancer cells and/or diminish their chemo- and radioresistance in the future, which would alleviate the burden of current cancer therapies.

Moreover, more fundamental research on human stem cells is needed in the hope of using them in future therapeutic approaches. Better knowledge and understanding of the mechanisms involved during differentiation and reprogramming will lead to more safety for patients and new questions for researchers.

In the current literature, healthy differentiating human stem cells are characterized after one or a few days, but the first hours after induction of differentiation are poorly understood [9,291,350,429,453,551,564]. This work focuses on two questions pertaining to the characterization of healthy human stem cells in the first hours of differentiation:

1. Time-resolved transcriptional and miRNA profiles of differentiating hMSCs, hNSCs, and HSkMs were prepared using micro-arrays and analyzed with bioinformatic tools. This allowed to investigate a) clusters of RNA expression, b) pathways enriched after induction of differentiation, c) correlations between miRNA and mRNA levels of expression, and d) a miRNA family seemingly involved in differentiation in all cell types studied. These results will be presented in part 4.1.

2. Gene amplifications have been detected in differentiating stem cells [8,147,148,150,151,199,382], yet the precise mechanism underlying their formation remains elusive. The second part of this thesis aims to delve into this matter and explore the possibility that re-replication could be one of the driving forces behind these amplifications. To this end, hMSCs undergoing chondrogenesis and HSkMs were examined to determine a) whether re-replication occurs in these cells, and b) if so, in which time frame. The methods required to study this phenomenon had to be established and will be discussed in part 4.2. of this work.

3. Materials and methods

3.1. Materials

3.1.1. Chemicals and reagents

The following table lists all the chemicals and reagents used in this work and their respective sources.

Table 3.1: Overview of all chemicals and reagents used in the present work.

Chemical / Reagent	Manufacturer	Headquarters
1X DPBS with Ca & Mg	Gibco	Waltham, MA, USA
1X PBS	Gibco	Waltham, MA, USA
Accutase®	Sigma Aldrich	St. Louis, MO, USA
Agarase	Thermo Fisher Scientific Inc.	Waltham, MA, USA
Antibody against BrdU (mouse)	Becton Dickinson and Company (BD)	Franklin Lakes, NJ, USA
Antibody against CldU (rat)	Abcam	Cambridge, UK
Antibody against mouse IgG (goat), Alexa 594	Life Technologies	Carlsbad, CA, USA
Antibody against rat IgG (donkey), Alexa 488	Invitrogen	Waltham, MA, USA
Antibody against rat IgG (goat), Alexa 350	Invitrogen	Waltham, MA, USA
BSA (bovine serum albumin)	Sigma Aldrich	St. Louis, MO, USA
Click-iT™ EdU Cell Proliferation Kit for Imaging, Alexa Fluor™ 594 dye	Invitrogen	Waltham, MA, USA
ddH$_2$O	In-house facility (see 3.1.5)	-
EDTA (ethylenediaminetetraacetic acid)	Carl Roth GmbH & Co. KG	Karlsruhe, Germany
Ethanol absolute anhydrous	Th. Geyer GmbH & Co. KG	Renningen, Germany
Normal goat serum	Thermo Fisher Scientific Inc.	Waltham, MA, USA
KCl (potassium chloride)	Carl Roth GmbH & Co. KG	Karlsruhe, Germany
KH$_2$PO$_4$ (monopotassium phosphate)	Carl Roth GmbH & Co. KG	Karlsruhe, Germany
LMP agarose	Carl Roth GmbH & Co. KG	Karlsruhe, Germany
miRNeasy® Mini Kit	Qiagen	Hilden, Germany
Na$_2$HPO$_4$ (disodium phosphate)	Sigma Aldrich	St. Louis, MO, USA
NaCl (sodium chloride)	Carl Roth GmbH & Co. KG	Karlsruhe, Germany
N-lauroylsarcosine sodium salt	ICN Biomedicals Inc.	Costa Mesa, CA, USA

Nuclease free water	Thermo Fisher Scientific Inc.	Waltham, MA, USA		
Proteinase K, recombinant	Roche Holding	Basel, Switzerland		
Trichloromethane (chloroform)	Carl Roth GmbH & Co. KG	Karlsruhe, Germany		
Tris (tris(hydroxymethyl)aminomethane)	Carl Roth GmbH & Co. KG	Karlsruhe, Germany		
YOYO™-1 Iodide	Thermo Fisher Scientific Inc.	Waltham, MA, USA		

3.1.2. Buffer and solution recipes

The following table lists all the buffers and solutions used in this work, along with their components and their quantities.

Table 3.2: Overview of all buffers and solutions used in the present work, and of their respective recipes.
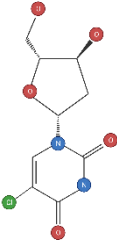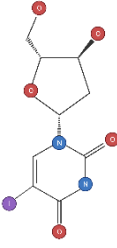
Solution	Quantity	Components	Quantity	Concentration
1X PBS	1 l	Na_2HPO_4	1.78 g	-
		KH_2PO_4	0.24 g	-
		NaCl	8 g	-
		KCl	0.2 g	-
100X CldU	10 ml	CldU	0.06566 g	-
		ddH_2O	10 ml	-
100X IdU	10 ml	IdU	0.010623 g	-
		ddH_2O	10 ml	-
Antifade + YOYO™-1	2 ml	Antifade	2 ml	-
		YOYO™-1	0.2 µl	1 mM
0.5 M MES pH 6.5	100 ml	MES	1.95 g	-
		ddH_2O	100 ml	-
ESP	9 ml	EDTA	9 ml	0.5 M
		N-lauroylsarcosine sodium salt	0.1 g	-
		Proteinase K	100 µl	5 mg/ml
TE	1 l	Tris	10 ml	1 M
		EDTA	2 ml	0.5 M
StemPro® MSC SFM CTS™ complete medium	50 ml	StemPro® MSC SFM CTS™ Basal Medium	42 ml	-
		Xeno-Free Supplement	7.5 ml	-
		GlutaMAX™-I	500 µl	100X
		Penicillin-Streptomycin	250 µl	10 000 U/ml (P), 10 000 µg/ml (S)

StemPro® Adipocyte Differentiation Complete Medium	50 ml	StemPro® Adipocyte Differentiation Basal Medium	45 ml	-
		StemPro® Adipocyte Supplement	5 ml	-
		Penicillin-Streptomycin	250 µl	10 000 U/ml (P), 10 000 µg/ml (S)
StemPro® Osteocyte Differentiation Complete Medium	50 ml	StemPro® Osteocyte/Chondrocyte Differentiation Basal Medium	45 ml	-
		StemPro® Osteocyte Supplement	5 ml	-
		Penicillin-Streptomycin	250 µl	10 000 U/ml (P), 10 000 µg/ml (S)
StemPro® complete NSC culture medium	50 ml	KnockOut™ DMEM™/F-12	48.5 ml	-
		StemPro™ Neural Supplement	1 ml	-
		bFGF	50 µl	20 µg/ml
		EGF	50 µl	20 µg/ml
		GlutaMAX™-I	500 µl	100X
		Ascorbic acid	50 µl	200 mM
		Heparin	50 µl	6 000 U/ml
		Penicillin-Streptomycin	250 µl	10 000 U/ml (P), 10 000 µg/ml (S)
StemPro® NSC differentiation medium	50 ml	KnockOut™ DMEM™/F-12	48.5 ml	-
		StemPro™ Neural Supplement	1 ml	-
		GlutaMAX™-I	500 µl	100X
		Ascorbic acid	50 µl	200 mM
		Heparin	50 µl	6 000 U/ml
		Penicillin-Streptomycin	250 µl	10 000 U/ml (P), 10 000 µg/ml (S)

3.1.3. Thymidine analogs

Thymidine analogs were used in the incorporation assays. They were added to the culture medium of differentiating cells (see 3.1.5). The following table lists all thymidine analogs used in the present work, along with their respective systematic name, structure, and source.

Table 3.3: Overview of all thymidine analogs used in the present work. Structures were generated using BioRender.com.

Analog	Systematic name	Structure	Supplier	Headquarters
CldU	5-chloro-2'-deoxyuridine		Sigma Aldrich	St. Louis, MO, USA
EdU	5-ethynyl-2′-deoxyuridine		Invitrogen	Waltham, MA, USA
IdU	2'-deoxy-5-iodouridine		Sigma Aldrich	St. Louis, MO, USA

3.1.4. Stem cells

The following tables list all the stem cells used in the present work, with their biological origin and supplier, as well as all culture media used in this thesis.

Table 3.4: Overview of all stem cells used in the present work.

Abbreviation	Full name	Biological origin	Supplier	Headquarters
hMSC	human mesenchymal stem cell	Bone marrow	Thermo Fisher Scientific (StemPro) (adipogenesis & osteogenesis); Promo Cell (chondrogenesis)	Waltham, MA, USA; Heidelberg, Germany
hNSC	human neural stem cell	Cryopreserved fetal cells	Thermo Fisher Scientific (StemPro)	Waltham, MA, USA
HSkM-S	human skeletal myoblasts	Human donors	Thermo Fisher Scientific	Waltham, MA, USA

Table 3.5: Overview of all cell culture media and supplements used in the present work.

Cell culture medium or supplement	Manufacturer	Headquarters
L-Ascorbic acid	Sigma Aldrich	St. Louis, MO, USA
CELL Start™ CTS™	Thermo Fisher Scientific Inc.	Waltham, MA, USA
DMEM (Dulbecco's Modified Eagle Medium)	Gibco	Waltham, MA, USA
Donor Horse Serum, EU origin, 0.2 µm sterile filtered	PAN-Biotech GmbH	Aidenbach, Germany
Geltrex™	Thermo Fisher Scientific Inc.	Waltham, MA, USA
GlutaMAX™-I	Gibco	Waltham, MA, USA
Heparin	Sigma Aldrich	St. Louis, MO, USA
Mesenchymal Stem Cell Chondrogenic Differentiation Medium	Promo Cell	Heidelberg, Germany

MSC Growth Medium 2	Promo Cell	Heidelberg, Germany
Penicillin-Streptomycin	Gibco	Waltham, MA, USA
StemPro® Adipocyte Differentiation Basal Medium	Thermo Fisher Scientific Inc.	Waltham, MA, USA
StemPro® Adipocyte Supplement	Thermo Fisher Scientific Inc.	Waltham, MA, USA
StemPro® MSC SFM CTS™ Basal Medium	Thermo Fisher Scientific Inc.	Waltham, MA, USA
StemPro® MSC SFM XenoFree Supplement	Thermo Fisher Scientific Inc.	Waltham, MA, USA
StemPro® NSC SFM™	Thermo Fisher Scientific Inc.	Waltham, MA, USA
StemPro® Osteocyte Supplement	Thermo Fisher Scientific Inc.	Waltham, MA, USA
StemPro® Osteocyte/Chondrocyte Differentiation Basal Medium	Thermo Fisher Scientific Inc.	Waltham, MA, USA

3.1.5.   Laboratory equipment

The following table lists all laboratory equipment used in this work.

Table 3.6: Overview of all laboratory equipment used in the present work.

Equipment type	Equipment	Manufacturer	Headquarters
Camera	DSC-S70 camera	Sony	Tokyo, Japan
Cell culture	Galaxy 170S CO_2 incubator	Eppendorf AG	Hamburg, Germany
Cell culture	MSC Advantage 1.2 cell culture hood	Thermo Fisher Scientific Inc.	Waltham, MA, USA
Centrifuge	5417R centrifuge	Eppendorf AG	Hamburg, Germany
Centrifuge	5810R centrifuge	Eppendorf AG	Hamburg, Germany
Centrifuge	Rotofix 32	Andreas Hettich GmbH & Co. KG	Tuttligen, Germany
Heating equipment	Bead bath™	LabArmor	Plano, TX, USA
Heating equipment	Dry block incubator	Boekel Scientific	Feasterville, PA, USA
Heating equipment	Hot plate	Medax GmbH & Co. KG	Neumünster, Germany
Heating equipment	Memmert™ Natural Convection Standard Incubator	Memmert GmbH + Co. KG	Schwabach, Germany

Heating equipment	peqSTAR 2x thermocycler	PEQLAB Biotechnologie GmbH	Erlangen, Germany
Heating equipment	W 6 water bath	Rheotest Medingen GmbH	Ottendorf-Okrilla, Germany
Magnetic stirrer	Magnetic stirrer	Hanna Instruments	Woonsocket, RI, USA
Microarray	Agilent G2545A	Agilent Technologies	Santa Clara, CA, USA
Microarray	SureScan Microarray Scanner	Agilent Technologies	Santa Clara, CA, USA
Microscope	Axiovert 25 bright field microscope	Carl Zeiss	Oberkochen, Germany
Microscope	Luna™ fl Dual Fluorescence Cell Counter	logos biosystems	Gyeonggi-do, South Korea
Microscope	Olympus AX70 fluorescence microscope	Olympus	Tokyo, Japan
Microscope	Zeiss Mikroskop Axio Imager KMAT	Carl Zeiss	Oberkochen, Germany
Molecular combing	FiberComb® Molecular Combing System	Genomic Vision	Bagneux, France
Shaker	CMV-1 overhead rotator	Fröbel Labortechnik GmbH	Lindau, Germany
Shaker	IKA™KS125 Basic® Laboratory Shaker	IKA-Werke	Staufen im Breisgau, Germany
Shaker	VF2 vortex mixer	IKA-Werke	Staufen im Breisgau, Germany
Spectrophotometer	NanoDrop™ 2000c	Thermo Fisher Scientific Inc.	Waltham, MA, USA
Water & ice facility	Flake ice maker F 75 L Flake-Line	WESSAMAT Eismaschinenfabrik GmbH	Kaiserslautern, Germany
Water & ice facility	Ultrapure water system ELGA PURELAB Chorus, PURELAB flex Dispenser	ELGA LabWater/Veolia Water Technologies Deutschland GmbH	Celle, Germany

3.1.6. Other materials

The following table lists other materials used in this work.

Table 3.7: Overview of other materials used in the present work.

Material	Manufacturer	Headquarters
accu-jet® pro pipette controller	Brand Scientific GmbH	Wertheim, Germany
Agilent Human SurePrint G3 Gene Expression (V3, G4851C)	Agilent Technologies	Santa Clara, CA, USA
Bemis™ Parafilm™ M Laboratory Wrapping Film	Bemis	Neenah, WI, USA
Cell culture flasks (25 cm²)	Greiner Bio-One International GmbH	Kremsmünster, Austria
CellStar® sterile tubes (15 ml, 50 ml)	Greiner Bio-One International GmbH	Kremsmünster, Austria
CombiCoverslips™ Vinylsilane Coated Coverslips 22x22 mm, engraved	Genomic Vision	Bagneux, France
Coverslips 24x60 mm	Carl Roth GmbH & Co. KG	Karlsruhe, Germany
Disposable DNA reservoirs	Genomic Vision	Bagneux, France
Disposable plug molds (90 µl)	Bio-Rad Laboratories Inc.	Hercules, CA, USA
Disposable wipes KIMTECH®	Kimberly Clark Professional	Roswell, GA, USA
Drying block	Schleicher & Schuell	Dassel, Germany
Eppendorf Research plus pipettes (0.1-2.5 µl, 0.5-10 µl, 2-20 µl, 20-200 µl, 100-1 000 µl)	Eppendorf AG	Hamburg, Germany
Eppendorf Safe-lock microcentrifuge tubes (1.5 ml, 2.0 ml)	Eppendorf AG	Hamburg, Germany
Human SurePrint G3 Unrestricted miRNA 8x60K Array-Chips (Release 21.0, G4872A)	Agilent Technologies	Santa Clara, CA, USA
Hybridization Gasket Slide Kit - 8 microarrays per slide format	Agilent Technologies	Santa Clara, CA, USA
Immersol®	Carl Zeiss	Oberkochen, Germany
Multiwell cell culture plate (6-well, 24-well)	Greiner Bio-One International GmbH	Kremsmünster, Austria
Pipette tips eTIPS Motion (50 µl, 300 µl, 1 000 µl)	Eppendorf AG	Hamburg, Germany
Pipette tips Multiguard Barrier Tips (10 µl, 20 µl, 200 µl, 1 000 µl)	Sorenson Bioscience, Inc.	Salt Lake City, UT, USA
ProLong™ Gold Antifade Mountant	Thermo Fisher Scientific Inc.	Waltham, MA, USA

RNase-free microcentrifuge tubes (1.5 ml, from the miRNeasy Mini Kit)	Qiagen	Hilden, Germany
Rotiprotect® Nitril Evo gloves	Carl Roth GmbH & Co. KG	Karlsruhe, Germany
Rotiprotect® Nitril light gloves	Carl Roth GmbH & Co. KG	Karlsruhe, Germany
Serological pipettes (sterile, 5 ml, 10 ml, 25 ml)	Greiner Bio-One International GmbH	Kremsmünster, Austria
Super Stay Gel Nail Color	Maybelline	New York City, NY, USA
VWR® Microscope Slides, Ground Edges Frosted	VWR International	Radnor, PA, USA

3.1.7. Software, and *in silico* tools

The following table lists all of the software and *in silico* tools used for the present work, their developers, and the websites where they can be found (as of May 2023).

Table 3.8: Overview of all software and *in silico* tools used in the present work, and of their respective developers or websites.

Software or tool	Developer or website
Agilent Feature Extraction Software	Agilent Technologies
BioRender	biorender.com
CalculatorSoup Random Number Generator	calculatorsoup.com/calculators/statistics/random-number-generator.php
cellSens Dimension 1.8.1	Olympus
FiberStudio	Genomic Vision
GeneTrail 2.0 / 3.2	genetrail.bioinf.uni-sb.de
Inkscape	inkscape.org
Microsoft Office Excel	Microsoft Corporation
Microsoft Office PowerPoint	Microsoft Corporation
Microsoft Office Word	Microsoft Corporation
miEAA 2.0	ccb-compute2.cs.uni-saarland.de/mieaa2
miRBase releases 21 and 22	mirbase.org
R (programming language)	r-project.org
Venny 2.1.0	bioinfogp.cnb.csic.es/tools/venny
Wilcoxon Signed-Rank Test Calculator	socscistatistics.com/tests/signedranks/default2.aspx
Zeiss ZEN	Zeiss
Zotero	zotero.org

All figures were created using Inkscape, BioRender, the R programming language, Microsoft Office Excel, or PowerPoint. The program Microsoft Office Excel was used to sort and manage lists and to perform simple arithmetic operations.

Data from the Tabula Muris Senis dataset were obtained through the Gene Expression Omnibus (GEO) under the accession number GSE132042.

3.2. Methods

3.2.1. Human stem cell culture

All cells were incubated at 37 °C and 5 % CO_2.

Human mesenchymal stem cells (hMSCs) were cultured in StemPro® MSC SFM CTS™ complete medium (for adipogenesis and osteogenesis assays) or in MSC Growth Medium 2 (for chondrogenesis assays) supplemented with 0.5 % antibiotics (penicillin-streptomycin) until passage 3, at which time they were seeded at a density of 1×10^4 cells/cm² for the adipogenesis and chondrogenesis assays, and at 5×10^3 cells/cm² for the osteogenesis assay. The adipogenesis and osteogenesis flasks were coated with CELL Start™ CTS™ for 1 hour before cell addition.

Human skeletal myoblasts (HSkM) spontaneously begin differentiation within 48 hours of thawing, according to the manufacturer. They were differentiated in Dulbecco's modified Eagle medium (DMEM) supplemented with 2 % horse serum and 0.5 % antibiotics (penicillin-streptomycin). For proliferation control, HSkMs were cultured in DMEM supplemented with 10 % fetal calf serum (FCS).

Human neural stem cells (hNSCs) were obtained from Thermo Fisher Scientific (Gibco™ StemPro®) at passage 4 and cultured in suspension in StemPro® complete NSC culture medium supplemented with 0.5 % antibiotics (penicillin-streptomycin). This differentiation process does not induce a unique cell fate.

3.2.2. RNA isolation

Total RNA was isolated using the miRNeasy Mini Kit (Qiagen) at 0 h, 3 h, 6 h, 9 h, 12 h, 24 h, and 48 h after differentiation induction.

The miRNeasy Mini Kit method is based on the QIAzol Lysis Reagent, which simultaneously lyses the tissues or cells, inhibits RNases, and avoids DNA or protein contamination. After a lysis step with the QIAzol Lysis Reagent, chloroform is added to the sample, which is then centrifuged to separate the different phases. The upper, aqueous phase, containing the RNA molecules, is extracted, and mixed with ethanol. After a binding step on a silica-based membrane, a DNase digestion step, and a washing step, all RNA molecules longer than 18 nucleotides are eluted from the column and can be used in various experimental methods, including microarray-based high-throughput expression profiling, as described in the next section.

3.2.3. Microarray high-throughput expression analysis

Expression profiles of mRNAs and miRNAs were obtained using high-throughput microarray-based expression analysis methods from Agilent Technologies: One-Color Microarray-Based Gene Expression Analysis and miRNA Microarray System respectively.

Briefly, for the One-Color Microarray-Based Gene Expression Analysis, 100 ng of total RNA is converted into cDNA by reverse transcriptase. The cDNA is then transcribed into cRNA, labeled, amplified, and purified. 600 ng of cRNA is loaded onto hybridization chambers and hybridized overnight (17 h). The next day, the microarray chips are washed and scanned with the SureScan Microarray Scanner to obtain raw data.

For the miRNA Microarray System, 100 ng of total RNA is labeled directly with Cyanine 3-pCp. Then 100 ng are loaded onto hybridization chambers and hybridized overnight (20 h). The next day, the microarray chips are washed and scanned with the SureScan Microarray Scanner to obtain raw data.

The expression values of the microarray high-throughput mRNA and miRNA expression profiles were extracted from the raw data using Agilent Feature Extraction Software and further processed using the R programming language.

3.2.4. Differentiation assay

Differentiation of hMSCs was induced 2 days after passage 3 by changing the culture medium to a differentiation medium: StemPro® Adipocyte Differentiation Complete Medium, Mesenchymal Stem Cell Chondrogenic Differentiation Medium, and StemPro® Osteocyte Differentiation Complete Medium for the adipogenesis, chondrogenesis, and osteogenesis assays, respectively. Differentiation assays of the HSkM cells were started immediately after thawing. Differentiation of hNSCs was induced by switching to a differentiation medium, consisting of StemPro® complete NSC culture medium without bFGF and EGF. The flasks were previously coated with Geltrex™ to allow the cells to adhere.

Cells for the microarray high-throughput expression profiling experiments were harvested at predetermined time points (0 h, 3 h, 6 h, 9 h, 12 h, 24 h, 48 h) using Accutase® and further processed for RNA isolation. Cells for the incorporation assays were further treated during the differentiation process, as described in the next section.

3.2.5.   Treatment with thymidine analogs

Cell differentiation was induced by switching to one of the differentiation culture media, as described in the previous section. Cells were allowed to differentiate undisturbed for predetermined periods (0 h, 1 h, 2 h, 3 h, 4 h, 5 h, 6 h, 7 h). Then, for the first pulse, the first thymidine analog (EdU for in-house experiments, CldU for the Genomic Vision experiments) was added to the differentiation culture medium at a final concentration of 200 µM and 250 µM, respectively. Cells were further incubated for 1.5 hours, then washed briefly with pre-warmed 1X PBS (at 37 °C), and given fresh differentiation culture medium for 15 minutes. For the second pulse, the second thymidine analog (CldU for in-house experiments, IdU for the Genomic Vision experiments) was administered for 45 minutes at a final concentration of 250 µM and 30 µM, respectively. Finally, the cells were harvested using Accutase® and further processed for DNA fiber preparation, as explained in the next section.

Figure 3.1 shows a schematic of the procedure in the case of 4 h of differentiation time before pulse labeling.
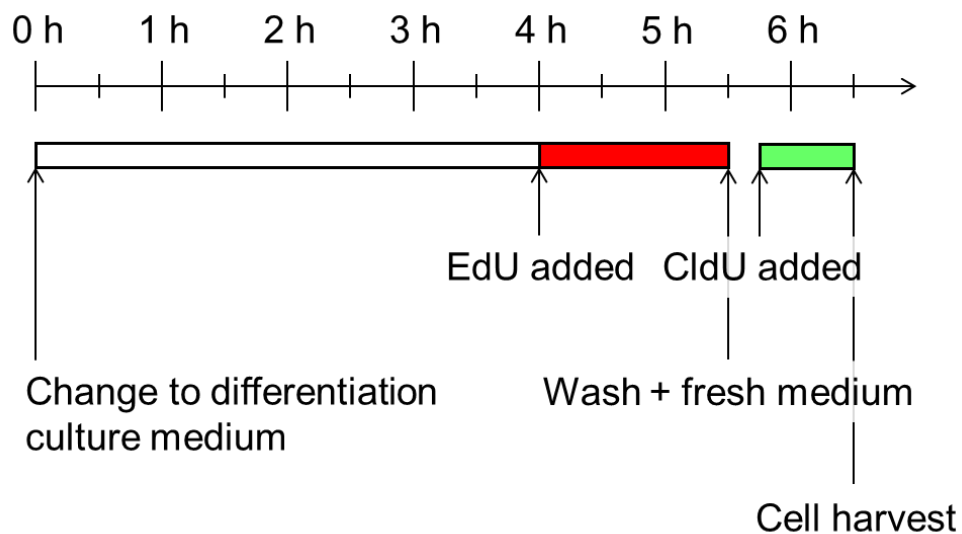
Figure 3.1: Schematic of thymidine analog treatment for cells differentiated for 4 h prior to pulse labeling.

3.2.6. DNA fiber preparation for molecular combing
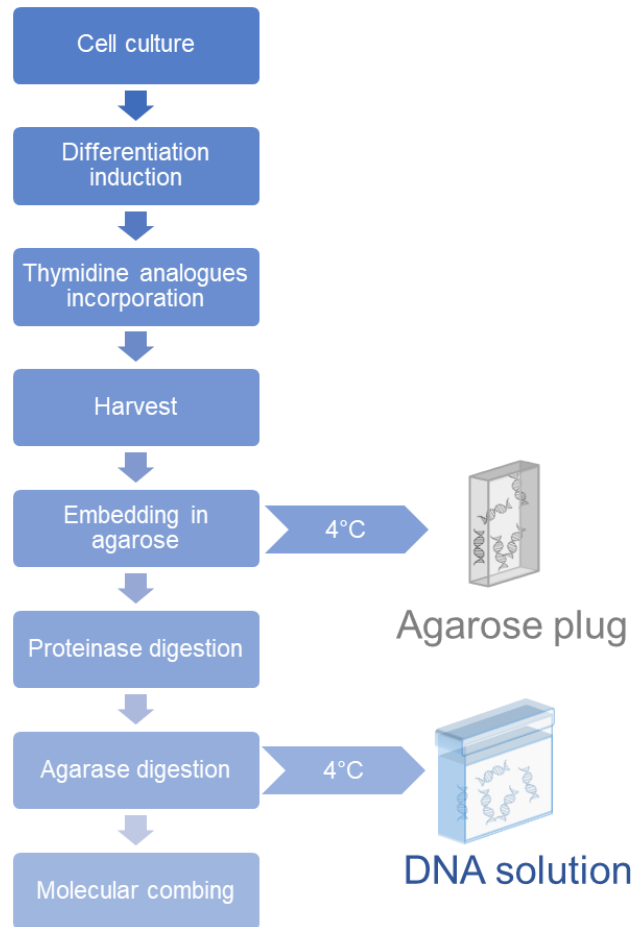
Figure 3.2: Schematic of the process of obtaining combed DNA fibers, from cell culture to molecular combing.

Figure 3.2 shows the process of preparing combed DNA fibers from cell culture. Harvested cells were resuspended in 45 µl of 1X cold PBS. An equal volume of melted low melting point (LMP) agarose was added to the cell suspension. After brief homogenization, this solution was transferred to a 90 µl mold and allowed to solidify on ice. The agarose plug was then extracted and immersed in 250 µl of ESP buffer pre-warmed at 50 °C containing Proteinase K. After overnight digestion, the plug was washed three times in 1X TE buffer on an overhead rotator. At this point, the plug could be further processed or stored at 4 °C in 1X TE for up to one year. Further processing of the plugs consisted of melting a plug in 0.1 M MES buffer pH 6.5 for 20 minutes, subsequently transferring the tube containing the melted agarose and DNA fibers to a bead bath – to prevent any movement – and adding agarase to the mixture. After overnight digestion, the DNA-containing solution was

carefully transferred to a combing reservoir obtained from the FiberPrep® Kit. This solution could then be stored at 4 °C for a few days, or used directly for molecular combing, as explained in the next section.

For the plugs sent to the company Genomic Vision for combing and staining, the procedure described was followed up to the washing steps after the overnight Proteinase K digestion.

3.2.7. Molecular combing

After cooling (if used immediately) or warming (if stored) to room temperature, the final DNA suspension in the FiberComb reservoirs was gently placed in the FiberComb Molecular Combing Device, along with one to two silanized coverslips (Genomic Vision, Bagneux, France). The coverslips were then mechanically inserted into the DNA suspension according to the default parameters provided by the manufacturer and pulled out at a slow, constant rate. The resulting combed DNA fibers adhere to the silanized surface at a constant rate of 2 kb/µm. To fix the DNA fibers to the coverslips, these were incubated at 65 °C for two hours. With this method, both sides of the silanized coverslips were coated with DNA fibers. After fixation, the coverslips can either be stained directly or stored at -20 °C.

3.2.8. YOYO™-1 staining

YOYO™-1 iodide is a dimeric cyanine dye that intercalates into nucleic acid with a preference for double-stranded DNA. YOYO™-1 emits light at 509 nm, which corresponds to green light. Because YOYO™-1 is brighter than other intercalating nucleic acid dyes such as DAPI, it is more suitable for studying combed DNA fibers. For this thesis, two staining protocols were performed.

To quickly assess the quality of combed fibers, a test coverslip was incubated at 100 °C for 3 minutes and then mounted on a microscope slide with one drop of ProLong™ Gold Antifade mounting medium containing YOYO™-1 (2 µl for 2 ml mounting medium).

For more homogenous DNA staining, 1 µl of YOYO™-1 was added to 415.6 µl of 1X PBS for a final concentration of 24 nM. After staining the thymidine analogs (see next section), the coverslip was placed on 200 µl of the YOYO™-1 solution and incubated for 20 minutes at room temperature in the dark. It was then washed three times for 5 minutes each with 1X PBS, again at room temperature in the dark. It was then immersed in solutions containing 70 %, 90 %, and 100 % absolute ethanol for 1 minute each, and allowed to dry.

Finally, the stained coverslip was mounted on a microscope slide with one drop of ProLong™ Gold Antifade mounting medium.

3.2.9. Staining of thymidine analogs

Because the DNA fibers fixed to the coverslip contained thymidine analogs, they were light-sensitive. Therefore, all staining and washing steps were performed in the dark.

3.2.9.1. Staining of EdU

The Click-iT™ EdU Cell Proliferation Kit for Imaging (Alexa Fluor™ 594) from Invitrogen™ was used to stain the EdU analog.

The coverslip was first immersed in 1X PBS for a few minutes to rehydrate. It was then covered with 3 % BSA in 1X PBS. 250 µl of Click-iT™ solution was prepared according to the manufacturer's instructions using Click-iT™ reaction buffer and reaction buffer additive diluted to 1X with ddH$_2$O, and the mixture was placed on top of the coverslip. After 30 minutes of incubation at room temperature in a humid chamber, as much of the solution as possible was removed, and the coverslip was washed with 3 % BSA in 1X PBS and further processed with CldU staining, as explained in the next section. Alternatively, for the preliminary EdU incorporation assay, the coverslip was washed three times for 5 minutes each in 1X PBS, dried in an ethanol series, and mounted with a drop of ProLongTM Gold Antifade mounting medium.

3.2.9.2. Staining of CldU

CldU was stained by indirect immunofluorescence using a rat IgG2a-isotype monoclonal antibody (Abcam 6326) and an Alexa Fluor™ 350-conjugated goat anti-rat IgG (H+L) secondary antibody (Invitrogen™ A-21093).

For immunofluorescence staining, the coverslip was first incubated with 50 µl of blocking solution consisting of 10 % goat serum in 1X PBS. After incubation for 30 minutes at 37 °C in a humid chamber, the coverslip was transferred to 25 µl of primary antibody solution containing 2 µl of the primary antibody diluted in the blocking solution (1:50) and incubated for 1 hour at 37 °C in a humid chamber. It was then washed three times for 5 minutes in 1X PBS, and placed on the secondary antibody solution consisting of 3.5 µl of a secondary antibody and 21.5 µl of blocking solution (1:75). After incubation for 30 minutes at room

temperature in a humid chamber, the coverslip was again washed three times for 5 minutes in 1X PBS and stained with YOYO^{TM}-1 as explained in section 8.

3.2.10. Confocal fluorescence microscopy

Confocal fluorescence microscopy images were obtained either in-house or through the Genomic Vision company.

Coverslips for in-house experiments were individually documented and analyzed using the Olympus AX70 fluorescence microscope and the cellSens Dimension 1.8.1 program (Olympus) or the Zeiss Mikroskop Axio Imager KMAT and the Zeiss ZEN program (Zeiss).

Agarose plugs containing DNA were sent to Genomic Vision to be combed, scanned, and processed using their proprietary reagents and scanning facility (EasyComb Plus Service DNA Replication). Once images were acquired, they could be viewed and analyzed remotely using their proprietary FiberStudio® tool (Genomic Vision).

3.2.11. Bioinformatic-based methods

3.2.11.1. Processing of microarray raw data

Microarray expression values were determined by processing the raw data obtained with Agilent Feature Extraction software as described in Leidinger *et al.* 2014 [314]. Briefly, all average background-corrected signals were summed for each miRNA. For mRNA microarrays, the median of the background-corrected signals of probes belonging to the same transcript was extracted. Using quantile normalization (as implemented in the R package preprocessCore, version 1.46.0), the resulting values were normalized separately for each cell differentiation assay and shifted with a pseudo-count so that the lowest value was equal to 1. A log2 transformation was then applied. For miRNAs, the identifiers were converted from miRBase version 21 to 22 using miEAA 2.0 [272].

The resulting expression matrices were then filtered such that a miRNA or mRNA was retained only if it was detected in at least one time point and the highest expression value was at least 1.5 times greater than the largest undetected measurement value.

3.2.11.2. Clustering

Expression trajectories of mRNAs and miRNAs with a fold-change of at least 1.5 between the highest and the lowest measurement value during differentiation profiling were clustered using fuzzy c-means clustering, as implemented in the R package Mfuzz, version 2.54.0 [292]. The approach proposed by Schwämmle and Jensen [473] was used to estimate the fuziffier parameter, and the number of clusters was manually determined based on the elbow of the minimum cluster centroid distance plot (see Figure 4.5).

For each miRNA cluster, over-representation enrichment analysis was performed using miEAA 2.0, and for each mRNA with Gene Trail 3.2.

3.2.11.3. Generation of random cluster pairs and trios

Control pairs of clusters were randomly generated as follows: five numbers were randomly chosen from 1 to 10 (unsorted, using the CalculatorSoup random number generator). The first number indicated the type of microarray considered: 1 to 5 for miRNAs, and 6 to 10 for genes. The next two numbers indicated the differentiation assay: 1 or 2 for hMSC adipogenesis, 3 or 4 for hMSC chondrogenesis, 5 or 6 for hMSC osteogenesis, 7 or 8 for hNSC, and 9 or 10 for HSkM differentiation assay. The last two numbers indicated the cluster number. The same method was used to generate control trios of clusters with seven random numbers. If the same differentiation assay was drawn twice, new numbers were drawn, as well as if the cluster number was higher than the actual number of clusters.

3.2.11.4. Statistics

Wilcoxon signed-rank tests were used to calculate whether the overlap of randomly drawn cluster pairs and manually selected cluster pairs were significantly different (see 4.1.3).

4. Results

4.1.   miRNome and transcriptome profiling by microarrays

To better comprehend the mechanisms involved in stem cell differentiation, the miRNA and gene expression of differentiating stem cells were profiled from 3 to 48 hours after induction of differentiation.

For this purpose, three cell types (hMSCs, hNSCs, and HSkMs) were cultured in five differentiation assays. HSkMs and hNSCs were differentiated in a non-directed manner, whereas differentiation of hMSCs into adipocytes, chondrocytes, or osteoblasts was specifically induced. Total RNA was isolated from cells 3 h, 6 h, 9 h, 12 h, 24 h, and 48 h after induction of differentiation, and from undifferentiated cells from the same batches (0 h). Microarrays were used to quantify the expression levels of 50,038 transcripts and 2,549 miRNAs from the same total RNA samples. After averaging the signals, the value matrices were normalized, log2 transformed, and filtered (see 3.2.11.1).

4.1.1.   Detected RNAs

Overall, the number of miRNAs detected in each differentiation assay was consistent across time points (see Figure 4.1 a). On average, 318 miRNAs were detected in the three hMSC differentiation assays (264-350), 524 (433-578) for the hNSC differentiation assay, and 616 (520-781) for HSkM cells. Figure 4.1 b shows that the majority (245) of miRNAs detected at 0 h were shared by all differentiation assays, 125 were shared by the hNSC and the HSkM differentiation assays, while 70 were identified only in hNSC and 62 only in the HSkM differentiation assay. This was expected as more miRNAs were detected in the hNSC and HSkM differentiation assays than in the hMSC differentiation assays.
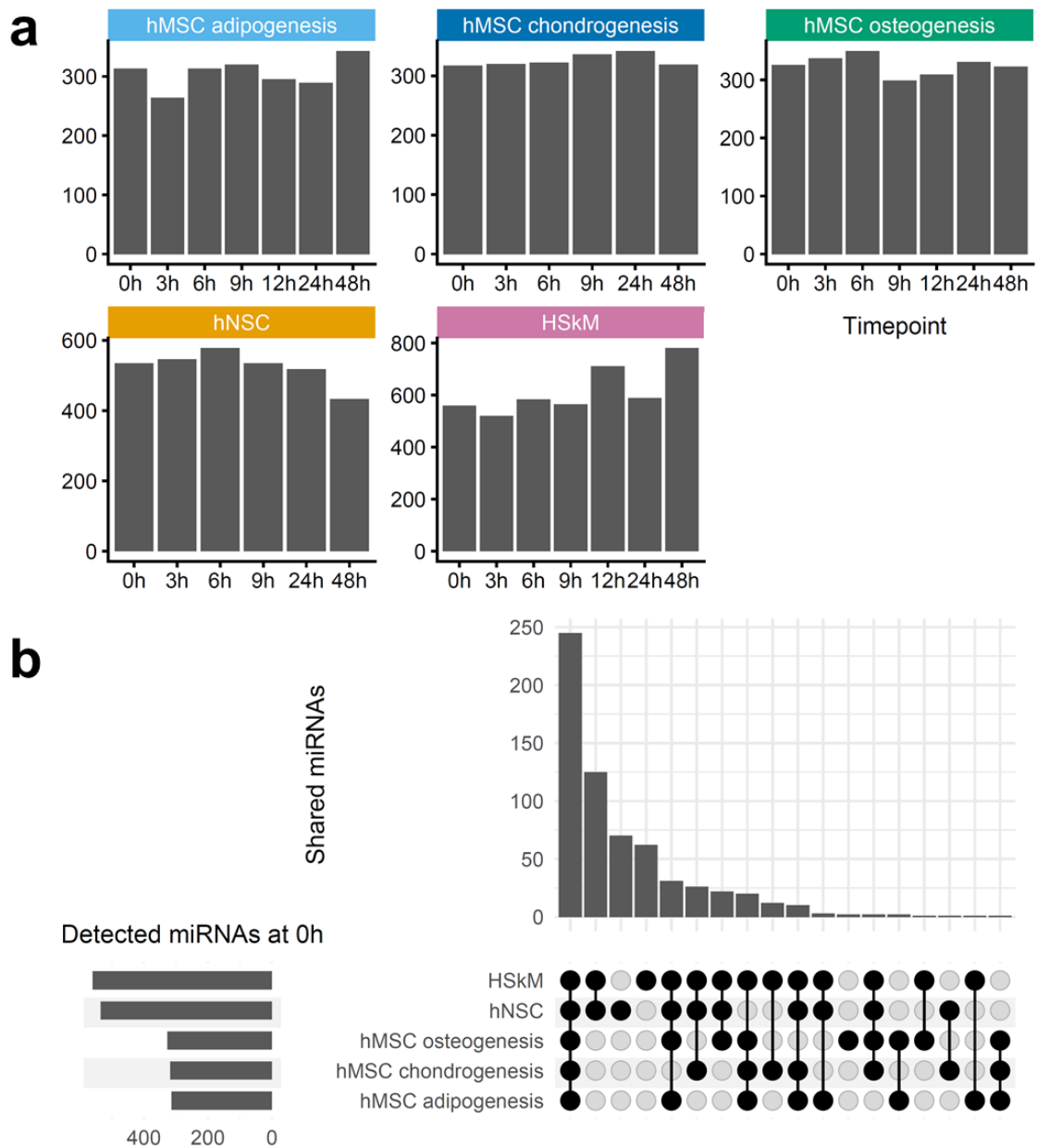
Figure 4.1: Detection levels of miRNAs. **a**: Numbers of miRNA detected for each time point in each differentiation assay. **b**: Upset plot (bottom right) showing how many of the miRNAs identified at 0 h (bottom left) were shared between differentiation assays. At the top of the upset plot are the numbers of shared miRNAs for each combination.

The numbers of genes detected were also homogeneous over time, averaging 32,038 (28,658-35,480) (see Figure 4.2 a). Almost 25,000 genes were shared by all five differentiation assays (see Figure 4.2 b). The second and third categories with the most genes in common were the three hMSC differentiation assays with and without the HSkM assay (2,037 and 1,505 respectively), which was expected because of the similarity of their lineage.
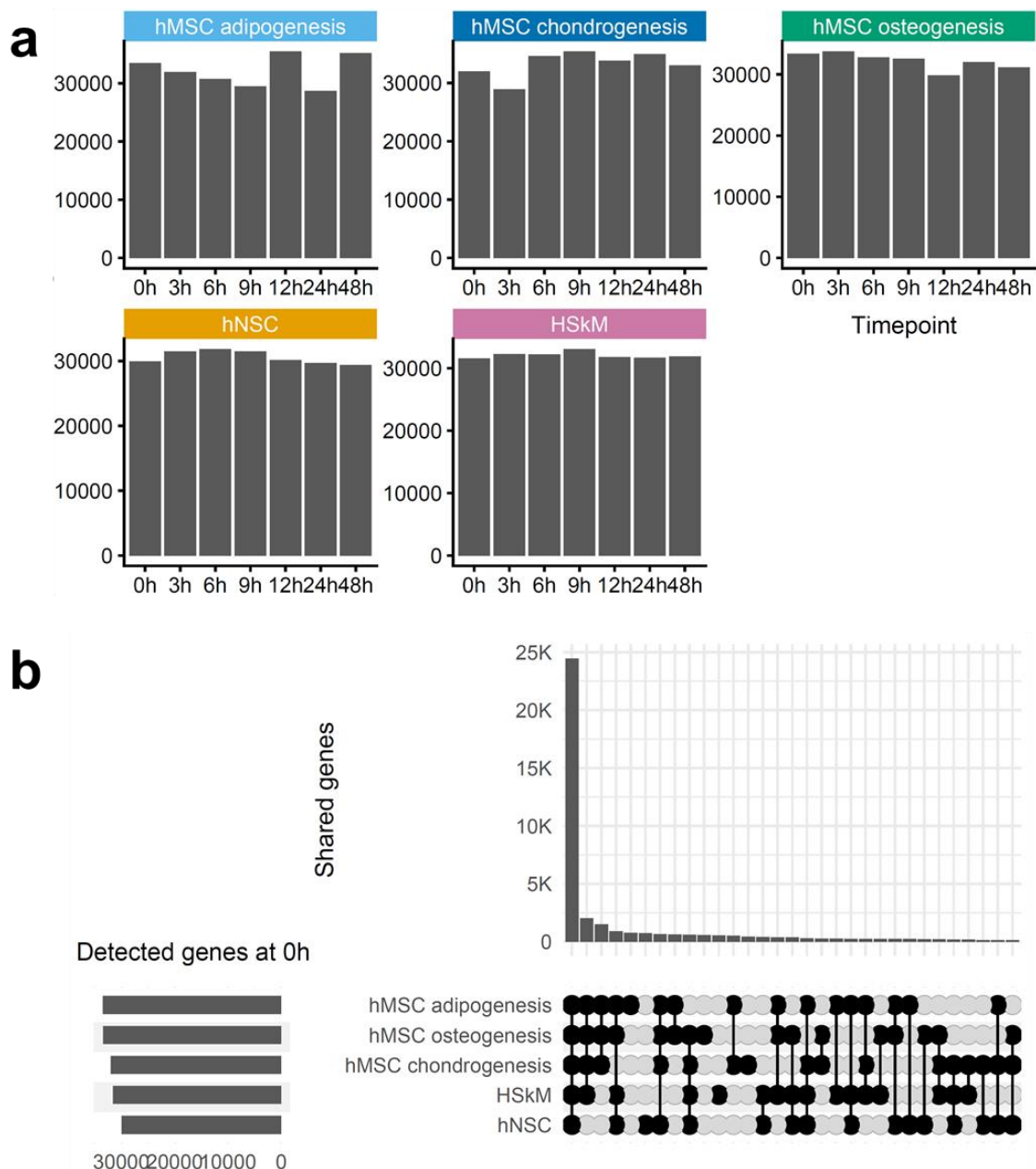
Figure 4.2: Detection levels of mRNAs. **a**: Numbers of genes detected for each time point in each differentiation assay. **b**: Upset plot (bottom right) showing how many of the genes identified at 0 h (bottom left) were shared between differentiation assays. At the top of the upset plot are the numbers of shared mRNAs for each combination.

4.1.2. Deregulated RNAs

RNAs were considered deregulated over the differentiation time course if the fold change between their minimum and maximum expression levels was at least 1.5. A total of 215 and 29,966 deregulated miRNAs and genes were observed respectively in the hMSC adipogenesis assay, 136 and 27,605 in the hMSC chondrogenesis assay, 267 and 29,433 in the hMSC osteogenesis assay, 354 and 18,866 in the hNSC differentiation assay, and 611 and 25,551 in the HSkM differentiation assay (see Figure 4.3).
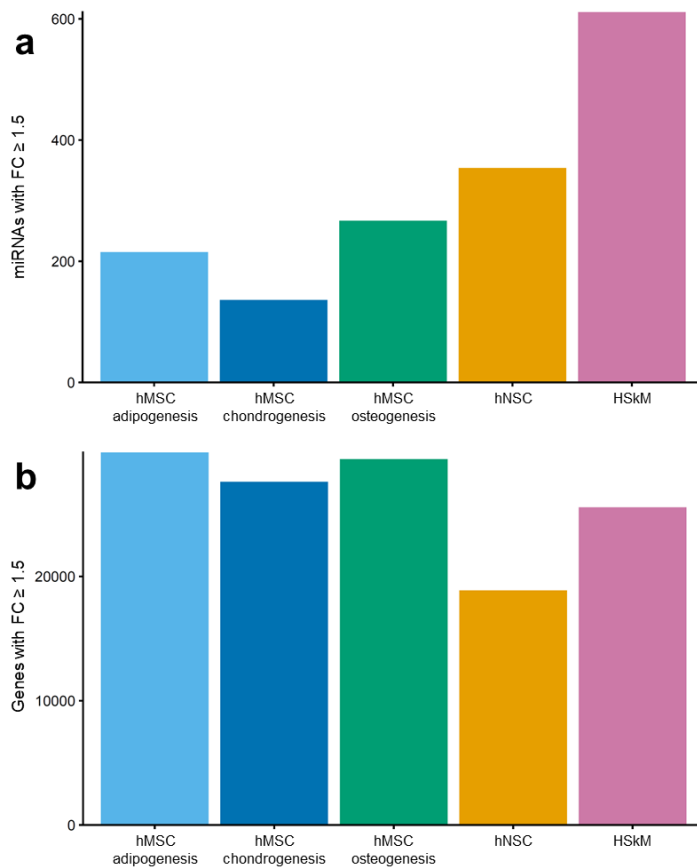
Figure 4.3: Total numbers of deregulated miRNAs (**a**) and transcripts (**b**) in each differentiation assay. miRNAs and transcripts were classified as deregulated if the fold change between their minimum and maximum expression values was at least 1.5.

When considering miRNAs that were deregulated compared to the onset of induction, particularly strong changes were noted at specific time points. In the HSkM and the hMSC osteogenesis assays, the 12 h and 48 h time points had the highest numbers of deregulated miRNAs (see Figure 4.4 a). These maxima for the hMSC adipogenesis assay were observed at time points 6 and 12 h, for the hMSC chondrogenesis assay at time point 48 h, and at time points 3 h and 48 h for the hNSC differentiation assay. The time points with the greatest changes in miRNA expression were comparable to those found for the genes, except in the case of the hMSC adipogenesis differentiation assay, for which the highest gene numbers were observed at 9 h and 24 h (see Figure 4.4 b). In general,

the numbers of up- and down-regulated miRNAs per time point were similar, but there were some exceptions, such as in the hMSC adipogenesis assay at 6 h or at several time points in the hMSC osteogenesis assay, where greater upregulation was found.
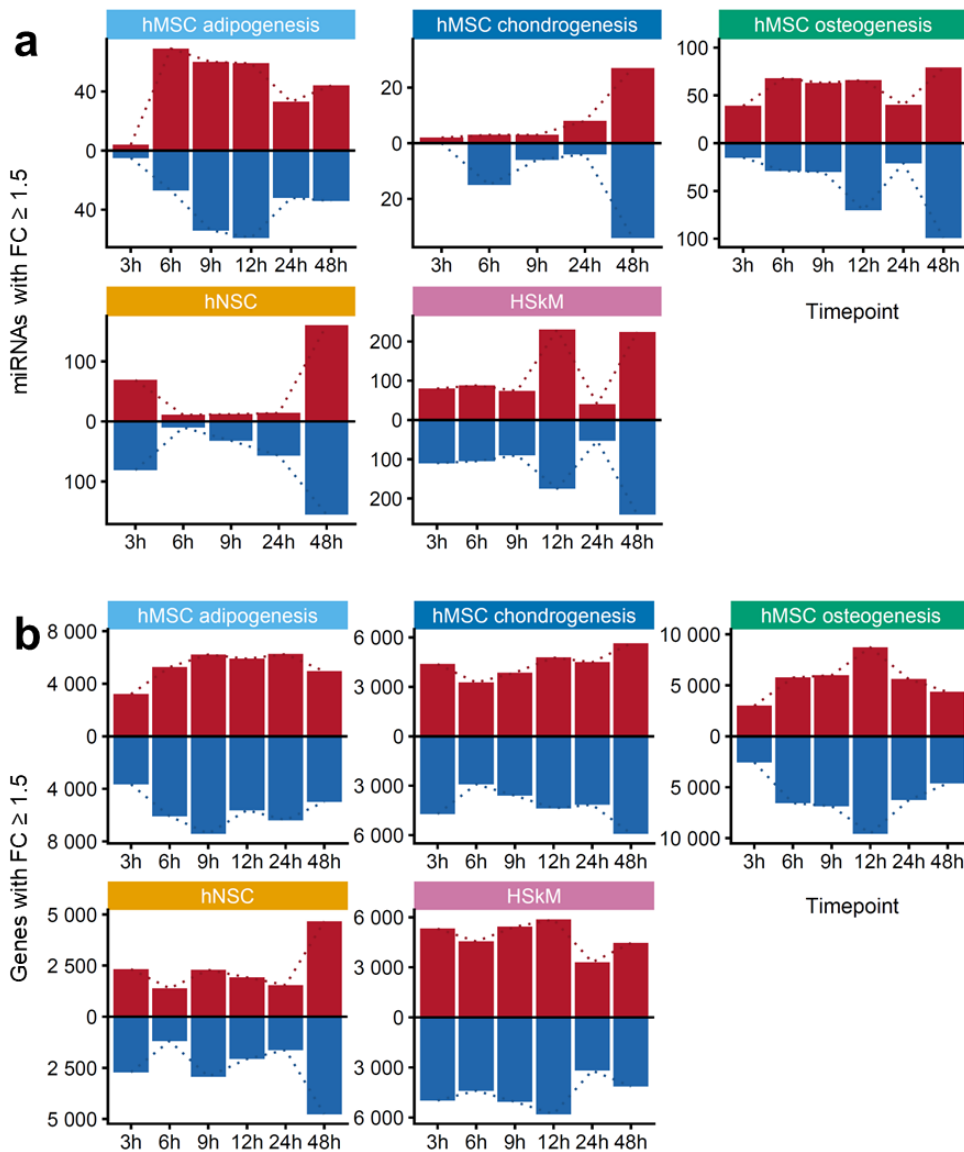
Figure 4.4: Time-resolved numbers of deregulated miRNAs and transcripts. **a**: Numbers of miRNAs for which the fold change between their maximum expression value and their value at 0 h was ≥ 1.5 in each differentiation assay, for each time point. **b**: Numbers of transcripts for which the fold change between their maximum expression value and their value at 0 h was ≥ 1.5 in each differentiation assay, for each time point.

The upset plots in Figure 4.5 show the numbers of shared deregulated RNAs for each combination of differentiation assay(s). The intersection of miRNAs found in all differentiation assays ranks third with 62 miRNAs, behind the "deregulated miRNAs found only in the HSkM differentiation assay" and the "deregulated miRNAs shared by the HSkM

and the hNSC differentiation assays" categories (215 and 177 miRNAs, respectively). This was not unexpected given the sheer number of deregulated miRNAs found in the hNSC and HSkM differentiation assays. There were no deregulated miRNAs unique to the hMSC differentiation assays, but 26 miRNAs were deregulated in all three hMSC differentiation assays and the HSkM differentiation assay. Since the numbers of deregulated genes are more similar than those of miRNAs, it was expected that the largest overlap would be found in the category "genes deregulated in all differentiation assays", with 9,158 genes. 2,873 deregulated genes are shared by the three hMSC differentiation assays only and 6,404 by the three hMSC differentiation assays and the HSkM differentiation assay.
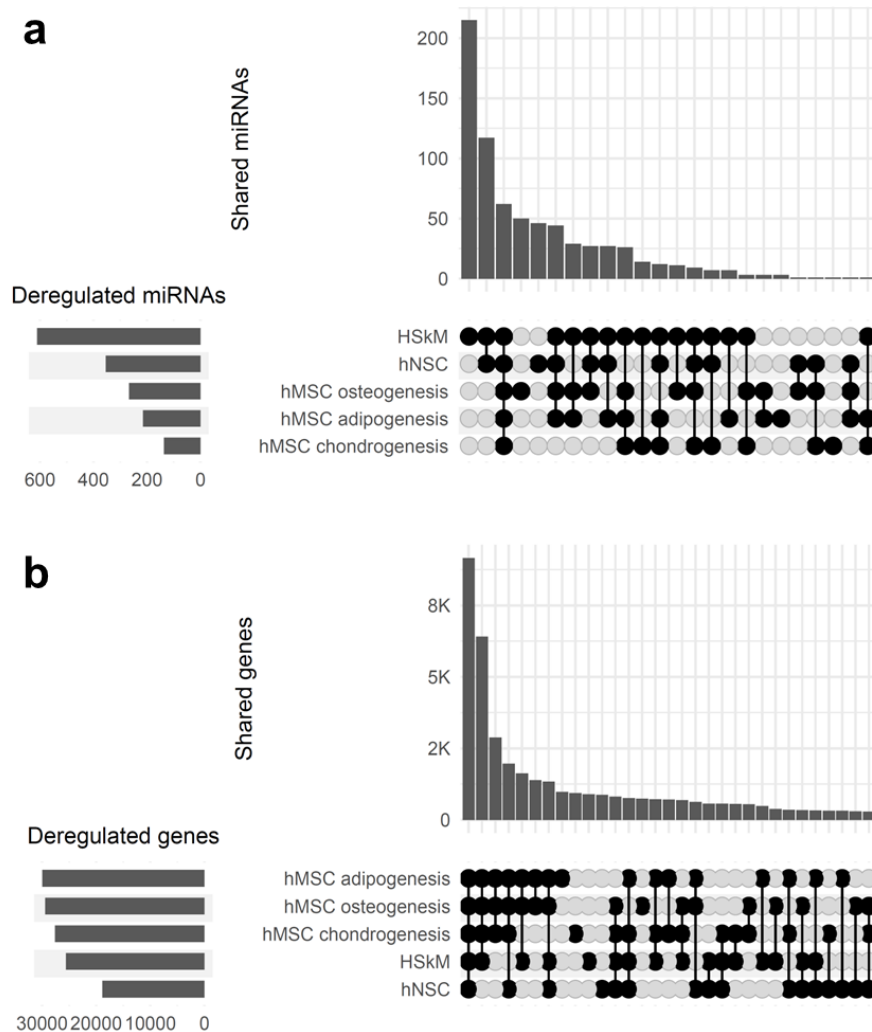
Figure 4.5: Overlaps of deregulated miRNAs and transcripts. miRNAs were classified as deregulated if the fold change between their minimum and maximum expression values was at least 1.5. Upset plot (bottom right) showing how many deregulated miRNAs (**a**) or transcripts (**b**) were shared between differentiation assays. At the top of the upset plot are the numbers of shared miRNAs or transcripts for each combination, and at the left are the numbers of deregulated miRNAs or transcripts in each assay.

4.1.3.   Cluster analysis

To better apprehend the expression patterns across time points, the deregulated RNAs were clustered using fuzzy c-means clustering. The number of clusters was determined manually based on the minimum cluster centroid distance plot (see Figure 4.6 a) and on the overlap plots (b-d). First, the number of clusters was determined via the elbow method based on the minimum cluster centroid distance plot, resulting in 6 identified clusters in the example of Figure 4.6. Then the overlap plots for 6 to 8 were examined and compared to identify the maximum number of clusters with enough dissimilarities. In the example shown in Figure 4.6, the distance between clusters 6 and 8 in Figure 4.6 d (8 clusters) is very small, which was confirmed by a visual assessment of the similarities between the two clusters (see Figure 4.6 e-f). The next nearest cluster is cluster 5, shown in Figure 4.6 g. In contrast to the difference between clusters 6 and 8, its pattern is different enough from both to be included as a separate cluster. Therefore, the number of clusters was set to 7.

This method identified 5 clusters for the miRNAs in the hMSC adipogenesis, chondrogenesis, and hNSC differentiation assays, 6 in the hMSC osteogenesis assay (miRNA), 7 for the miRNAs in the HSkM differentiation assay and for the mRNAs in the hMSC osteogenesis assay, 8 in the hMSC chondrogenesis assay (mRNAs), 9 in the hNSC and HSkM differentiation assays (mRNAs), and 10 for the mRNAs in the hMSC adipogenesis assay.
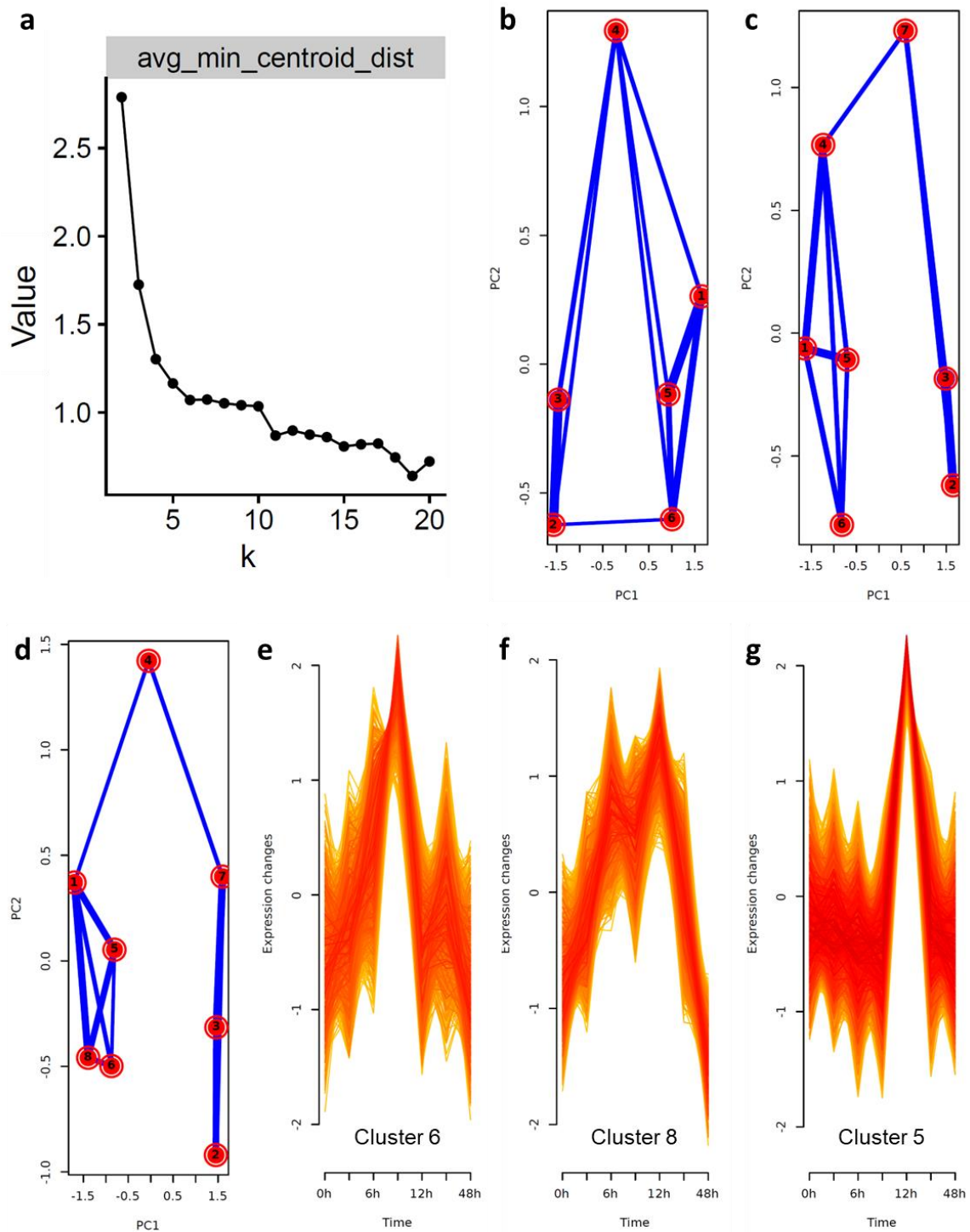
Figure 4.6: Determination of the number of clusters. Exemplary data from the hMSC osteogenesis assay (mRNA). **a**: Average minimum centroid distance (x-axis) for *k* clusters (y-axis). **b-d**: Overlap plots for 6 (**b**), 7 (**c**), or 8 (**d**) clusters. **e-g**: Expression patterns of genes with a membership of at least 0.5 across time points for clusters 6 (**e**), 8 (**f**), and 5 (**g**) in the case of 8 clusters.

Figure 4.7 shows all miRNAs clustered according to their pattern of expression across the time points. As expected, peaks of expression were observed in particular at time points that exhibited the highest numbers of deregulated miRNAs compared to induction start (see Figure 4.4 a). Interestingly, certain expression patterns seemed to reflect each other, such as miRNA clusters 1 vs. 4 and 2 vs. 3 of the hNSC differentiation assay (see Figure 4.7 d), or miRNA clusters 2 vs. 6 and 3 vs. 7 of the HSkM differentiation assay (see Figure 4.7 e).

Some clusters were especially well defined with nearly all miRNAs following the same pattern, shown by a high membership score, like the miRNA clusters 3 in the hMSC adipogenesis assay, 3 in the hMSC osteogenesis assay, and 2 and 3 in the HSkM differentiation assay (see Figure 4.7 a, c, e). These tended to be associated with few strong peaks of expression of the deregulated miRNAs, which also corresponded to the time points at which the greatest number of deregulated miRNAs compared to induction start were observed (see Figure 4.4 a).

Overall, the expression patterns of the deregulated miRNAs followed clear trends, except in the HSkM differentiation assay, where the expression levels increased and decreased at almost each time point.
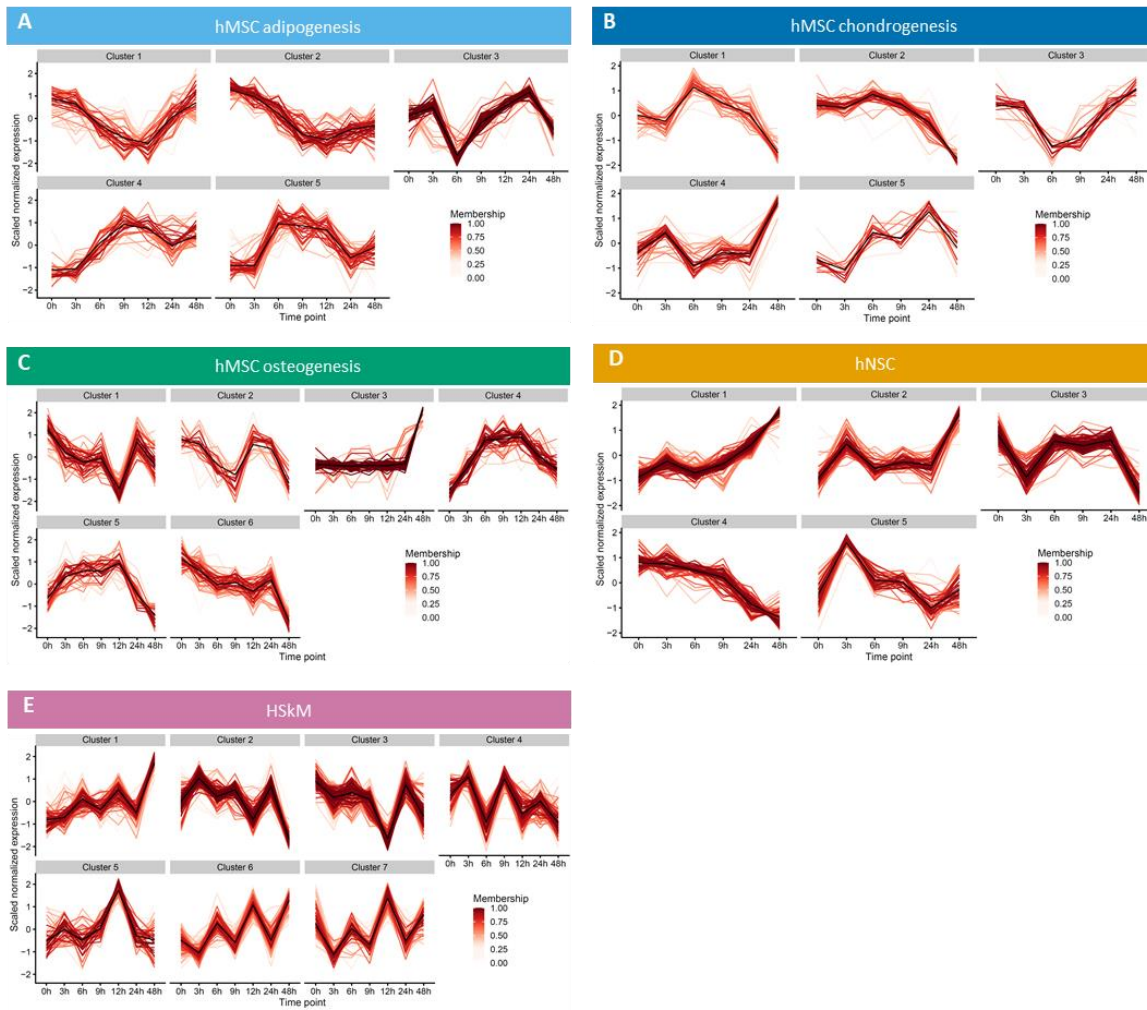
Figure 4.7: Clusters of patterns of expression of deregulated miRNAs, in each differentiation assay (**a-e**). Each miRNA is represented by a line, which is colored according to the cluster membership score of the miRNA. The black line symbolizes the centroid of the cluster for each time point.

The characteristics of the expression pattern clusters for the deregulated genes were similar to those for the miRNAs, although more complex patterns were also observed due to their greater number (see Figure 4.8). Here again, some clusters presented gene sets with a strong membership, such as clusters 3 in the hMSC adipogenesis assay and 7 in the hNSC differentiation assay (see Figure 4.8 a, d). Expression patterns that reflect each other were observed as well, such as in clusters 5 and 6 of the hMSC osteogenesis assay (see Figure 4.8 c). Certain time points were also associated with strong peaks of expression (such as 48 h in the hNSC differentiation assay; see Figure 4.8 d), and with the highest numbers of deregulated genes compared to induction start (see Figure 4.4 b).
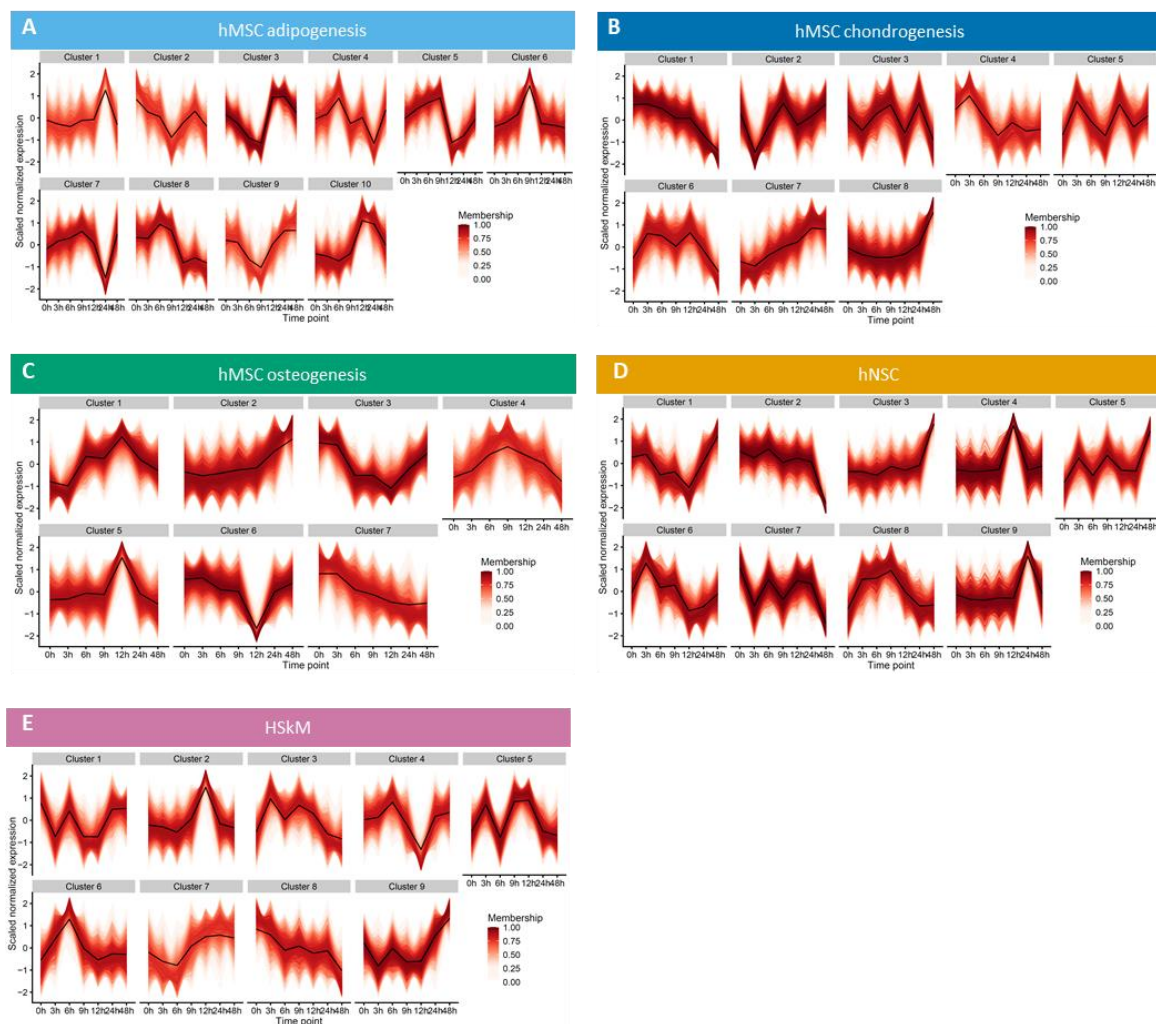
Figure 4.8: Clusters of patterns of expression of deregulated genes, in each differentiation assay (**a-e**). Each transcript is represented by a line, which is colored according to the cluster membership score of the transcript. The black line symbolizes the centroid of the cluster for each time point.

Some of the clusters have very similar expression patterns, such as cluster 1 of the hMSC osteogenesis assay and cluster 3 of the HSkM differentiation assay (miRNAs), or clusters 1 and 9 of the hMSC adipogenesis and hNSC differentiation assays respectively (genes). The member lists of these clusters were compared to identify possible overlaps. As a control, the same number of cluster pairs were randomly selected as described in 3.2.11.3, and the size of their overlaps was recorded. All lists and overlaps can be found in Appendix Table 7.1.

Some cluster pairs or trios with similar expression patterns had no overlap, as is the case for the miRNA clusters 3 and 3 of the hMSC adipogenesis and hNSC differentiation assays, and for the cluster 1 of the hMSC chondrogenesis assay (miRNAs) when compared to the clusters 5 or 4 of the hMSC adipogenesis and osteogenesis assays, respectively. In contrast, miRNA clusters 5 and 4 of the hMSC adipogenesis and osteogenesis assays shared 17 miRNAs (out of a total of 42 and 43 miRNAs, respectively). The miRNA clusters 2 and 4 of the hMSC chondrogenesis and hNSC differentiation assays shared only one miRNA, hsa-miR-1207-5p. In the trio comprising clusters 4, 2, and 1 of the hMSC chondrogenesis, hNSC, and HSkM differentiation assays respectively (miRNAs), hsa-miR-6875-5p was the only miRNA common to all three clusters, whereas six miRNAs belonged to both the clusters of the hMSC chondrogenesis and hNSC differentiation assays, four miRNAs to those of the hMSC chondrogenesis and HSkM differentiation assays, and eight to those of the hNSC and HSkM differentiation assays. The miRNA clusters 5 and 5 of the hMSC osteogenesis and HSkM differentiation assays had six miRNAs in common, and clusters 1 and 3 of the same assays shared 24 miRNAs (out of a total of 48 and 107 miRNAs, respectively).

The overlap of clusters 3 and 1 of the hMSC osteogenesis and hNSC differentiation assays, respectively, included 394 genes, out of a total of 4 547 (hMSC osteogenesis), and 2 085 genes (hNSC). The overlap between gene clusters 1 and 9 of the hMSC adipogenesis and hNSC differentiation assays consisted of 115 genes (out of a total of 2,534 and 1,285, respectively). Five genes were shared by the trio including clusters 5, 4, and 2 of the hMSC osteogenesis, hNSC, and HSkM differentiation assays, respectively (out of a total of 4,601, 1,283, and 2,893 genes, respectively), 183 by the clusters of the hMSC osteogenesis and hNSC differentiation assays, 296 by those of the hMSC osteogenesis and HSkM differentiation assays, and 63 by those of the hNSC and HSkM differentiation assays. Clusters 6 and 4 of the hMSC osteogenesis and HSkM differentiation assays had 637 genes in common out of a total of 4,489 and 2,621,

respectively, and 464 genes belonged to both clusters 6 and 4 of the hMSC adipogenesis and osteogenesis assays, respectively (out of a total of 3,139 and 3,986 genes, respectively). Clusters 1 and 2 of the hMSC chondrogenesis and hNSC differentiation assays shared 258 genes out of 3,766 and 2,507, respectively. In the trio comprising clusters 8, 2, and 3 of the hMSC chondrogenesis, osteogenesis, and hNSC differentiation assays, respectively, the overlap of the three clusters consisted of 30 genes, while 428 genes were common to the clusters of the hMSC differentiation assays, 286 to the clusters of the hMSC chondrogenesis and hNSC differentiation assays, and 266 to the clusters of the hMSC osteogenesis and hNSC differentiation assays, out of a total of 3,540 (hMSC chondrogenesis), 4 029 (hMSC osteogenesis), and 2,667 genes (hNSC). Finally, a total of 264 genes were shared by clusters 3 and 7 of the hMSC chondrogenesis and hNSC differentiation assays (out of a total of 2,976 and 2,810 genes, respectively).

The online tool Venny 2.1 was used to document the percentages of overlaps for each cluster pair or trio, which were then compared between randomly and manually selected ones. Figure 4.9 shows box plots of the overlaps in pairs (a), in pairs belonging to trios (b), and for three clusters (c). Although some overlaps were documented in control pairs of clusters, there were significantly bigger in cluster pairs that were manually selected for their pattern similarities (Wilcoxon signed-rank test, p-value of 0.02202, s.d. of 9.81). Cluster pairs in trios did not show significant differences (p-value of 0.18352). No significance could be calculated for overlaps of three clusters due to insufficient sample size, nonetheless, the same trend as with the cluster pairs could be observed.

Overall, there seems to be a correlation between pattern similarities of clusters and higher numbers of miRNAs or genes shared in these clusters.

a   Percentages of overlap (pairs)

b   Percentages of overlap (pairs in trios)

c   Percentages of overlap (trios)
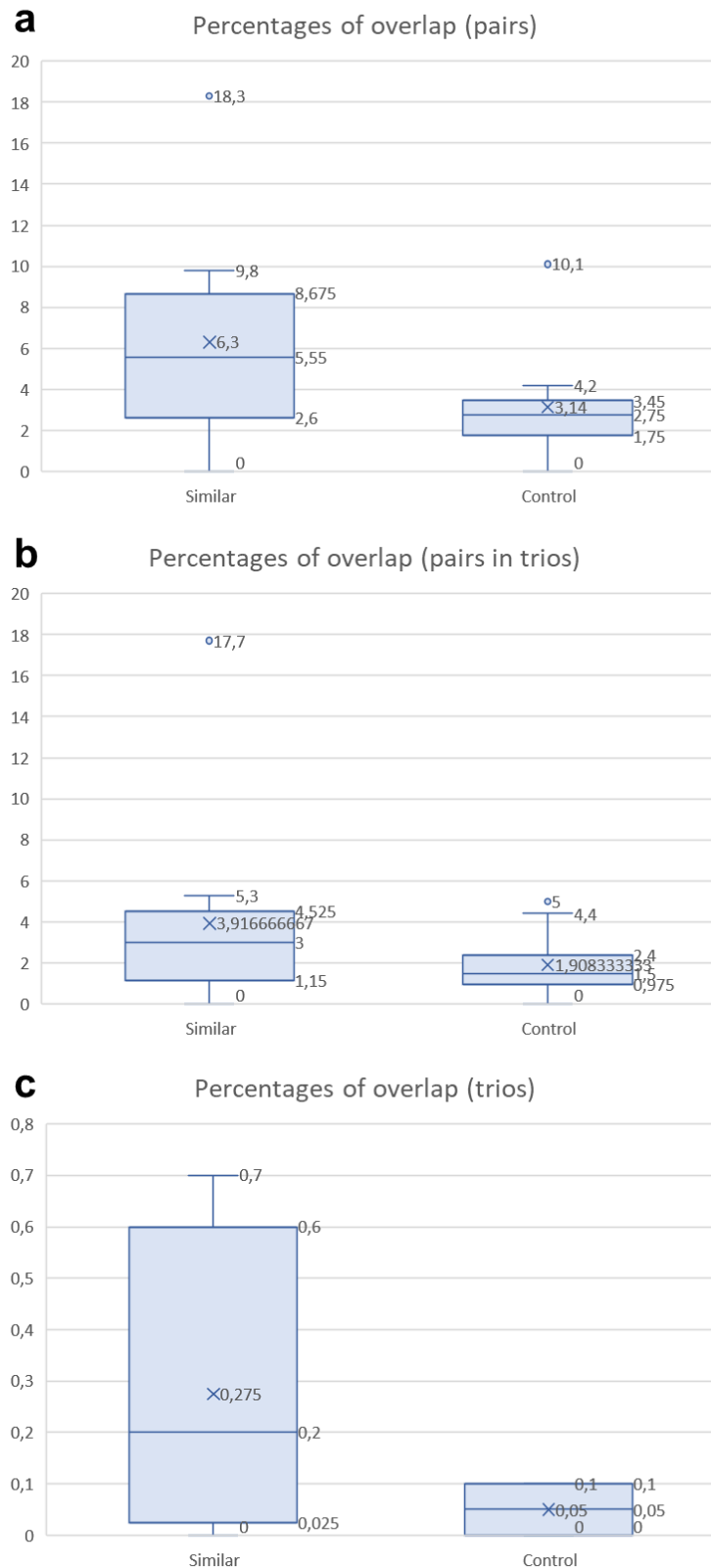
Figure 4.9: Boxplots showing the percentages of overlap between clusters selected for their pattern similarities or randomly selected clusters (control), in pairs (**a**), in pairs belonging to trios (**b**), or in three clusters (**c**). The percentage difference is significant in **a** according to a Wilcoxon signed-rank test (p-value of 0.02202, s.d. 9.81), but not significant in **b**. The sample size in **c** is too small to perform a test.

4.1.4.   Comparison of enriched pathways

For each cluster, biological pathways were analyzed and searched for enrichment (over-representation analysis) using the online tools miEAA (for miRNA clusters) and Gene Trail 3.2 (for gene clusters). This search for enriched pathways was designed to answer two questions:

- Are enriched pathways similar in miRNA-gene cluster pairs that appear to have anti-correlated patterns?
- Are expression patterns similar for clusters enriched in similar pathways?

To answer the first question, miRNA-gene cluster pairs whose expression patterns appeared anti-correlated for at least a portion of the timeframe studied were identified, and their respective enriched pathways were compared. For this purpose, the ten pathways with the lowest p-value were manually searched for broader categories. Table 4.1 lists which broad pathways categories were found to be enriched in both the miRNA cluster and the gene cluster of a pair. Cluster pairs that were investigated but for which no pathway similarity could be detected can be found in Appendix Table 7.2.

Table 4.1: Enriched pathways shared by both members of a miRNA-gene cluster pair with seemingly anti-correlated patterns of expression for at least a portion of the timeframe studied. Each cluster pair is represented by an overlap of the cluster centroids of the gene (in red) and the miRNA cluster (in blue). For each pair, the number of clusters is indicated by colored numbers.

Category	hMSC chondrogenesis	hMSC osteogenesis	hNSC	HSkM
Immune system signaling				-
Collagen & extracellular matrix	-		-	-
Membrane & channels	-	-		-
Chromatin	-		-	-
Translation	-	-		-
Cytoskeleton	-	-	-	
Muscle	-	Type — Gene — miRNA	-	
Cell differentiation & development	-	-	-	

Two cluster pairs from the hMSC chondrogenesis assay showed strong enrichment for pathways associated with immune system signaling (miRNA cluster 1 with gene cluster 8, miRNA cluster 2 with gene cluster 8). Two other cluster pairs, miRNA cluster 6 with gene cluster 2 of the hMSC osteogenesis assay and miRNA cluster 3 with gene cluster 6 of the hNSC differentiation assay, also presented enrichment for similar pathways.

The cluster pair from the hMSC osteogenesis assay was also associated with pathways related to collagen and the extracellular matrix. Additionally, the cluster pair formed by miRNA cluster 3 with gene cluster 6 of the hNSC differentiation assay also showed enrichment in pathways related to the membrane and transmembrane channels.

In the hMSC osteogenesis assay, the pair that includes miRNA cluster 1 and gene cluster 5 presents enrichment for chromatin-related pathways.

Another cluster pair of the hNSC differentiation assay, miRNA cluster 2 with gene cluster 2, is strongly associated with translation processes.

In the HSkM differentiation assay, the pair that includes miRNA cluster 2 and gene cluster 9 could be associated with both the cytoskeleton and muscles. The latter category is also strongly correlated with the pair that includes miRNA cluster 4 and gene cluster 9, as well as the cell differentiation category. Finally, the cluster pair formed by miRNA cluster 4 and gene cluster 1 was strongly linked with development, in particular muscle development.

To answer the question of the similarity of expression patterns for clusters enriched in similar biological pathways, such clusters had to be identified. The following general categories were considered: "cell cycle" (which includes pathways related to cell division, cell cycle phases, etc.), "cell differentiation & development", "collagen & extracellular matrix", "senescence", "signaling pathways of the immune system", "transcription".

Clusters enriched in "signaling pathways of the immune system" were miRNA clusters 2 of the hMSC adipogenesis, 1 and 2 of the hMSC chondrogenesis, 6 of the hMSC osteogenesis, 3 of the hNSC, and 3 and 4 of the HSkM differentiation assays, as well as gene clusters 3 of the hMSC adipogenesis, 3 and 8 of the hMSC chondrogenesis, 2, 3 and 6 of the hMSC osteogenesis, 6 and 8 of the hNSC, and 4, 6 and 7 of the HSkM differentiation assays. Most of these miRNA clusters had expression levels that decreased with time, especially the clusters of the hMSC chondrogenesis and osteogenesis assays. Strikingly, gene clusters 8 and 2 of the hMSC chondrogenesis and osteogenesis assays, respectively, showed a pattern that reflected the downward trend of the miRNA clusters.

The categories "cell cycle", "cell differentiation & development", and "senescence" were grouped. These included miRNA clusters 1 and 3 of the hMSC adipogenesis, 1 and 6 of the hMSC osteogenesis, 3 of the hNSC, and 3 and 4 of the HSkM differentiation assays, as well as the gene clusters 10 of the hMSC adipogenesis, 1 of the hMSC chondrogenesis, 2 of the hMSC osteogenesis, 3, 6 and 8 of the hNSC, and 1, 3, 8 and 9 of the HSkM differentiation assays. Three gene clusters, namely clusters 2, 3, and 9 of the hMSC osteogenesis, hNSC, and HSkM differentiation assays, respectively, showed an expression pattern with a clear upward trend at the 24 h and 48 h time points, whereas many miRNA clusters, especially miRNA cluster 6 of the hMSC osteogenesis assay, presented a clear downward trend at these time points. The miRNA cluster 1 was enriched in pathways for both the categories "cell cycle" and "senescence", and its pattern of expression with a downward trend from 0 h to 12 h, followed by a clear increase at 24 h and 48 h was reflected in gene cluster 10 of the hMSC adipogenesis assay.

The only miRNA clusters enriched in pathways from the category "transcription" were miRNA clusters 3 and 4 of the HSkM differentiation assay. Their mRNA counterparts were clusters 4 of the hMSC chondrogenesis, 3 and 6 of the hMSC osteogenesis, 6 of the hNSC, and 6 of the HSkM differentiation assay. Whereas miRNA cluster 3 of the HSkM

differentiation assay and gene cluster 6 of the hMSC osteogenesis assay showed similar expression patterns (a plateau until 9 h and a clear peak downward at the 12 h time point), miRNA cluster 4 and gene cluster 6 of the HSkM differentiation assay had more reflected patterns of expression, with a large peak at 6 h, downward for the miRNA cluster and upward for the gene cluster.

As expected, the category "collagen & extracellular matrix" was highly enriched in the hMSC chondrogenesis (1, 7, and 8) and hMSC osteogenesis (2 and 7) gene clusters. While clusters 1 of the hMSC chondrogenesis and 7 of the hMSC osteogenesis assays presented a decreasing trend from 0 h to 48 h, a steady increase of expression was observed in the other three clusters. This trend was reflected in miRNA cluster 6 of the hMSC osteogenesis assay, which was also enriched in pathways of the same category.

Overall, there seemed to be a positive trend between the similarity of enriched biological pathways and the similarity of cluster expression patterns in the same RNA class, or with mirrored expression patterns in the case of miRNA and gene clusters. Additionally, pathways with biological relevance to the future cell type of the differentiating stem cells could be found in some assays, especially in the hMSC osteogenesis and the HSkM differentiation assays.

4.1.5. Greatest increase or decrease in expression

Figures 4.10 through 4.13 are clustered heatmaps showing the miRNAs and transcripts for which expression decreased or increased the most between two of the time points (ten for each direction in each differentiation assay).

Interestingly, a few miRNAs or miRNA families were highly deregulated in more than one differentiation assay, like the hsa-miR-29 family with a total of nine hits (including four for hsa-miR-29b-3p and three for hsa-miR-29b-1-5p) in all five differentiation assays (decreased), or hsa-miR-221-5p, found in the top 10 decreased miRNAs of the hMSC adipogenesis and chondrogenesis assays (see Figure 4.10 a-c).

Figure 4.10 (next page): The ten miRNAs that showed the strongest decrease in expression across all time points in the hMSC adipogenesis (**a**), chondrogenesis (**b**), osteogenesis (**c**), hNSC (**d**), or HSkM differentiation assay (**e**).
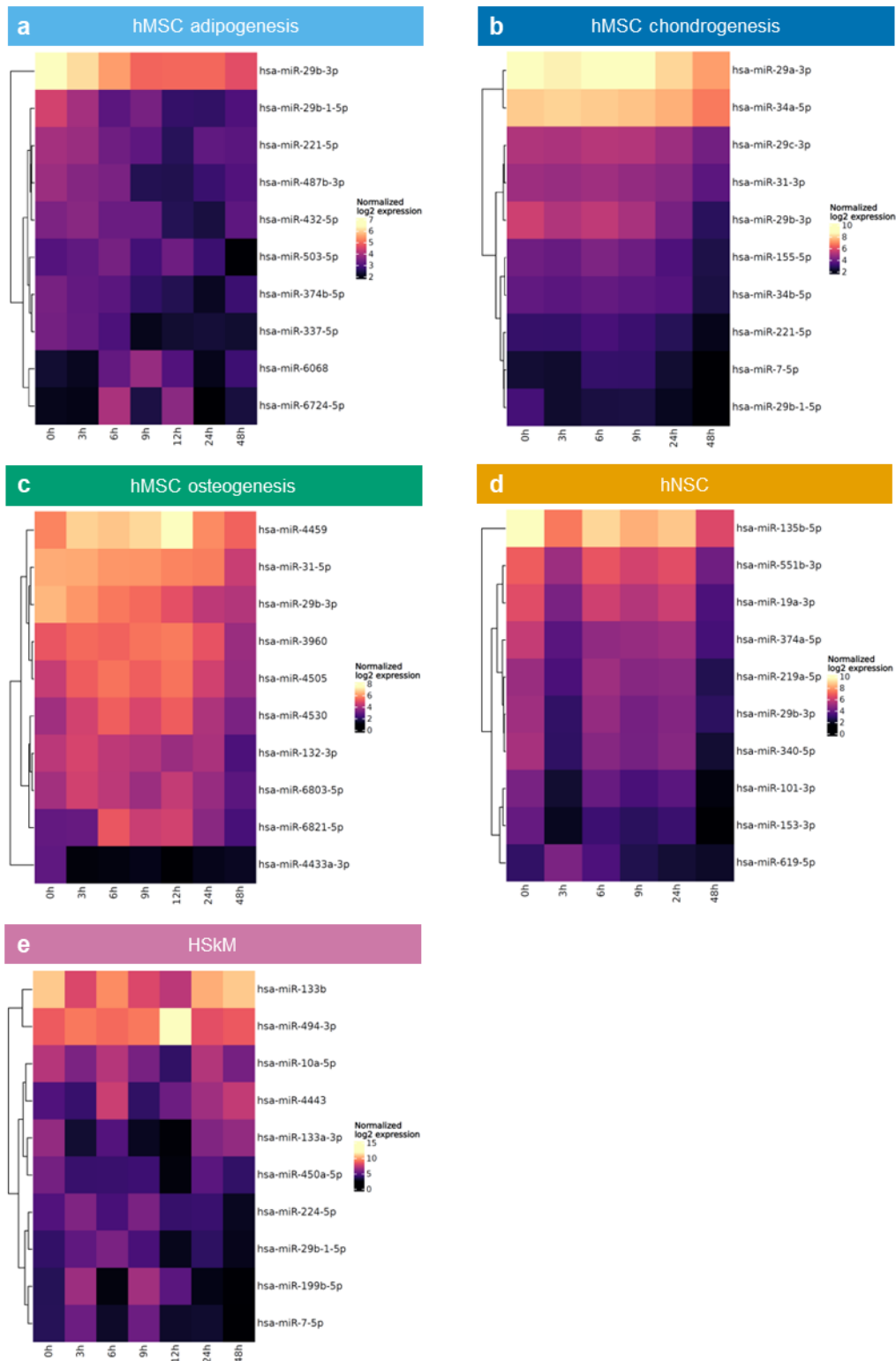
As for the top 10 increased miRNAs, the most abundant miRNA was hsa-miR-6785-5p, found in the hMSC adipogenesis, the hNSC, and the HSkM differentiation assays (see Figure 4.11 d-f). The ten most increased miRNAs in the hMSC osteogenesis assay all belonged to the same cluster (cluster 3 of Figure 4.7 c), and none of them was found in the top 10 of the other differentiation assays (see Figure 4.11).
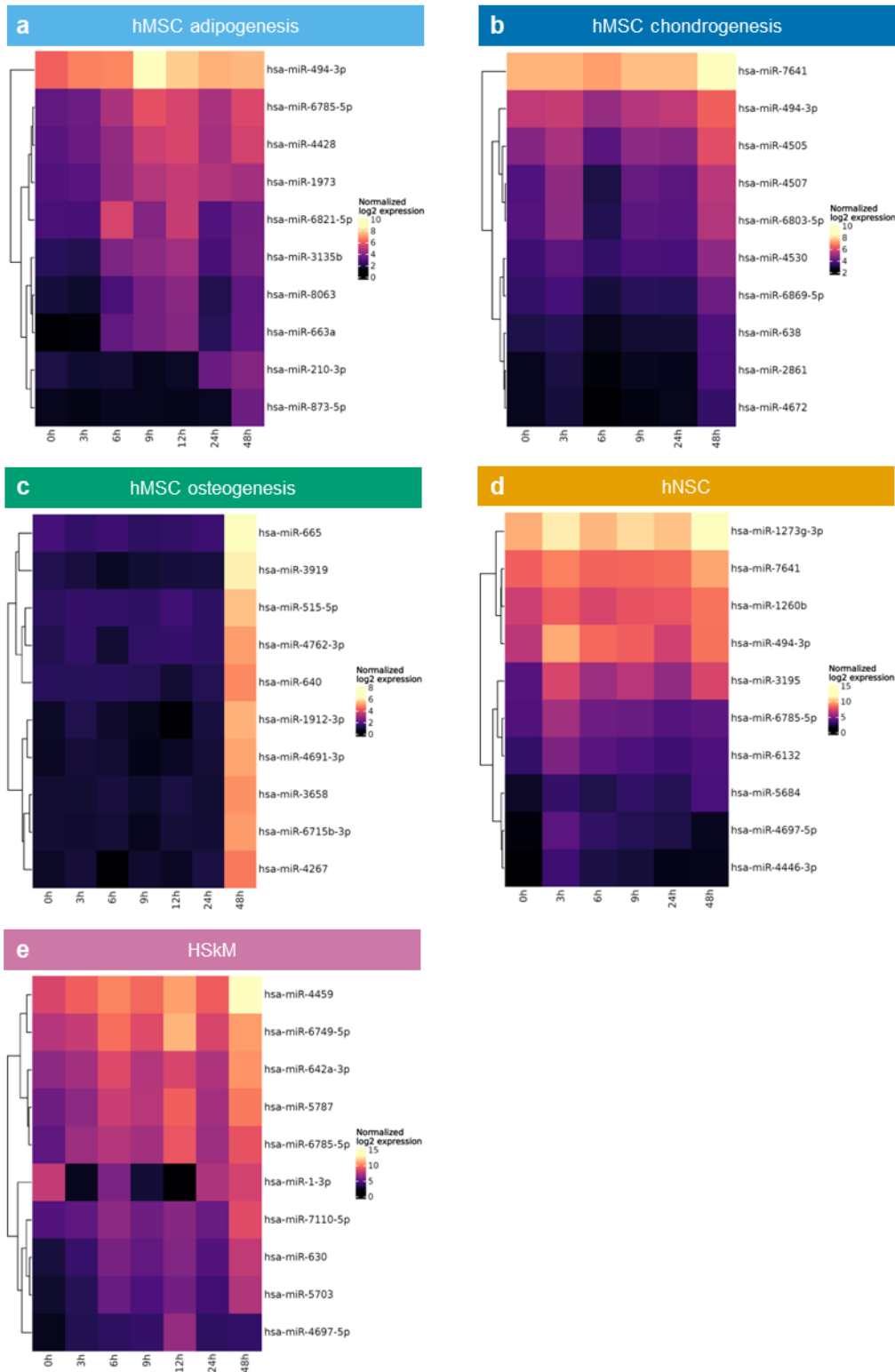
Figure 4.11: The ten miRNAs that showed the greatest increase across all time points in the hMSC adipogenesis (**a**), chondrogenesis (**b**), osteogenesis (**c**), hNSC (**d**), or HSkM differentiation assay (**e**).

Similarly, a few mRNAs showed greatly increased or decreased signals in multiple differentiation assays, such as *MMP1*, which was decreased in the hMSC chondrogenesis and osteogenesis assays (see Figure 4.12 b-c), or *FOSB*, which was decreased in the

hNSC and HSkM differentiation assay and increased in the hMSC adipogenesis assay (see Figure 4.12 d-e and Figure 4.13 a).
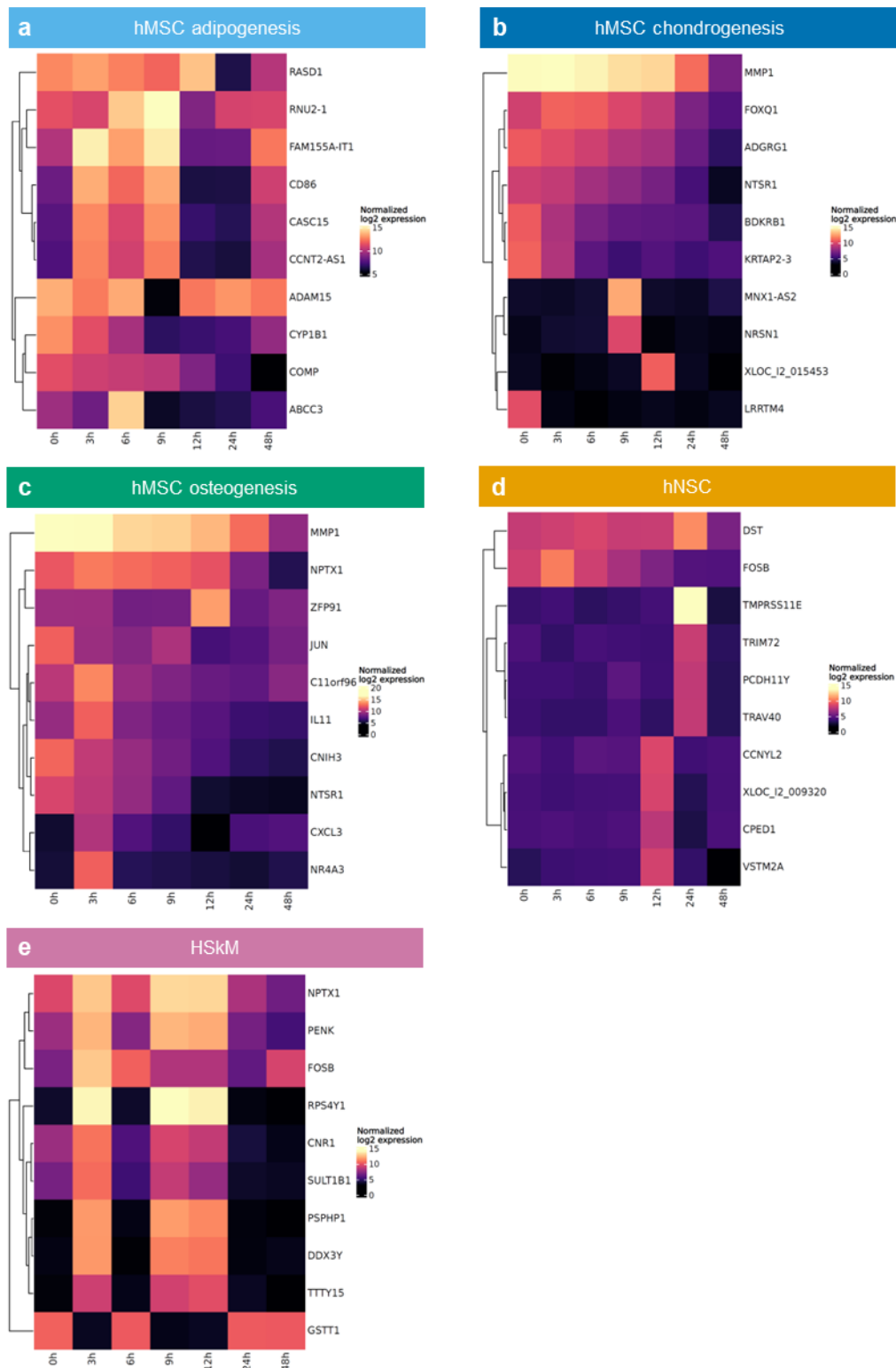
Figure 4.12: The ten genes that showed the strongest decrease across all time points in the hMSC adipogenesis (**a**), chondrogenesis (**b**), osteogenesis (**c**), hNSC (**d**), or HSkM differentiation assay (**e**).
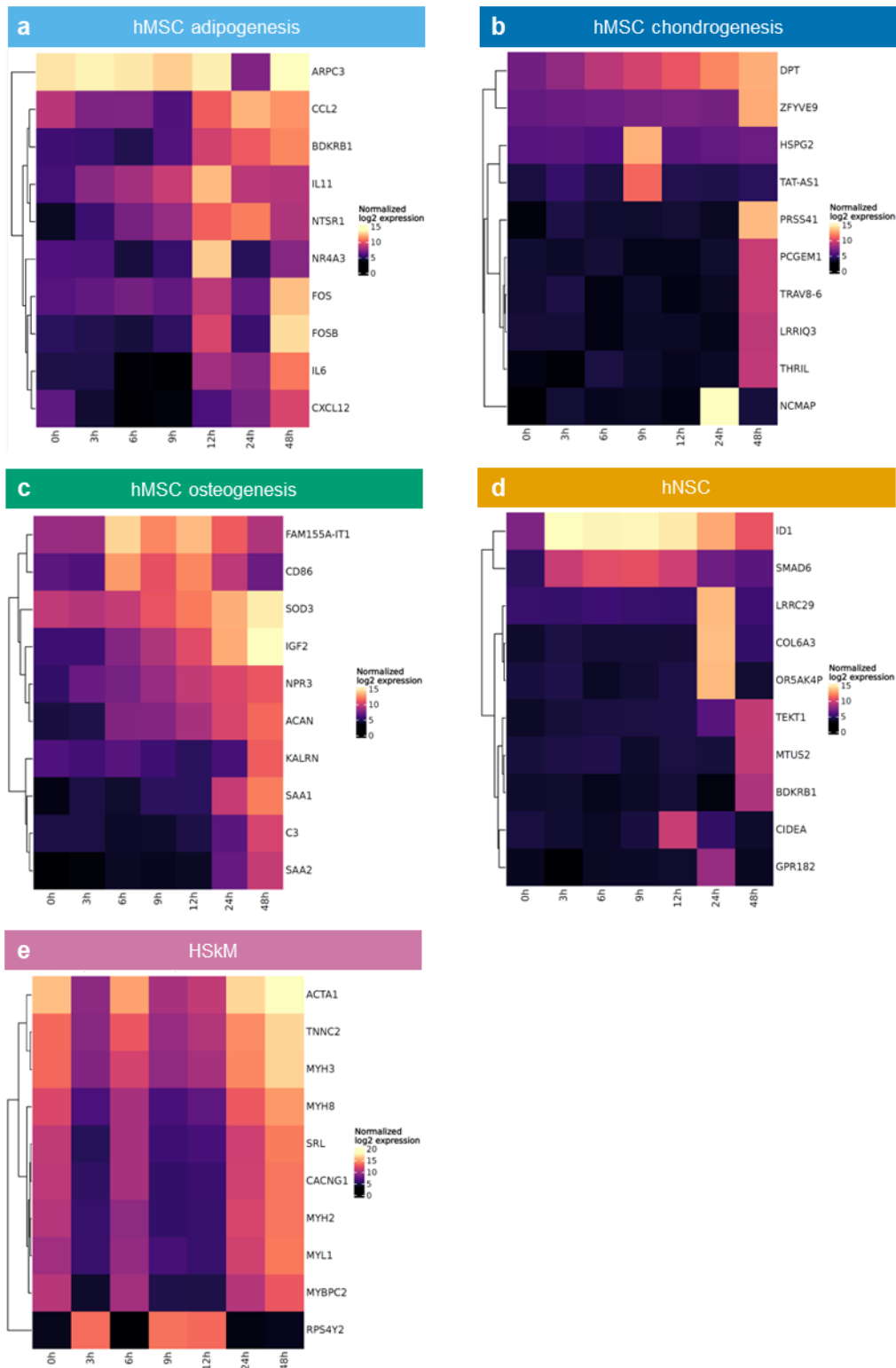
Figure 4.13: The ten genes that showed the greatest increase in expression across all time points in the hMSC adipogenesis (**a**), chondrogenesis (**b**), osteogenesis (**c**), hNSC (**d**), or HSkM differentiation assay (**e**).

To examine the distribution of pathways associated with the ten miRNAs and ten genes that showed the greatest increase or decrease in expression in the five differentiation assays, an over-representation analysis (ORA) was performed using the online tools miEAA (for the miRNAs) and Gene Trail 3.2 (for the genes). The resulting pathways were manually summarized into the following categories: "bacteria", "behavior", "biosynthesis and metabolism", "cancer", "cell death", "chromatin", "cytoskeleton", "development", "differentiation", "DNA repair", "drug", "extracellular matrix", "hormones and neurotransmitters", "immunity", "membrane", "(metal) ion", "mitosis and cell cycle", "pore and protein channel", "post-translational modifications", "replication", "reproduction", "RNA interference", "signaling", "stemness", "transcription and transcription factor", "translation", and "virus". When assigning a pathway to one or more categories, the more specific categories were preferred, and a pathway was assigned to the broader categories such as "biosynthesis and metabolism" only if no other category could be chosen.

In the hNSC differentiation assay, no overrepresentation of signaling pathways was detected for either genes or miRNAs. The same was true for the miRNAs of the hMSC adipogenesis and of the hMSC osteogenesis assays, and for the genes of the hMSC chondrogenesis assay.

Over-representation analysis of the hMSC adipogenesis assay revealed a high proportion of immunity-related and "(metal) ion"- associated pathways linked with the ten genes that experienced the greatest increase of expression.

In the hMSC chondrogenesis assay, the ten most decreased miRNAs were mainly associated with pathways of the "cytoskeleton", "development", "differentiation", and "stemness" categories.

Both the ten most increased and decreased genes of the hMSC osteogenesis assay were linked with a large proportion of immunity and signaling pathways.

In the HSkM differentiation assay, miRNAs were linked with pathways from the "membrane", "(metal) ion", and "pore and protein channel" categories. The ten genes with the greatest increase in expression were associated with a high number of pathways from the "behavior", "cytoskeleton", and "translation" categories. It should be noted that the "behavior" category in this case mainly included pathways related to muscle contraction, which is biologically linked to molecules of the cytoskeleton and calcium homeostasis.

4.1.6.   Correlations between miRNome and transcriptome

To start and evaluate possible expression correlations between miRNome and transcriptome, the interaction strength between miRNA and gene clusters of the same differentiation assay was calculated. For this purpose, interactions validated in the online miRNA-gene interaction database miRTarBase or predicted by at least three sources in the online miRNA-gene interaction prediction tool mirDIP (microRNA Data Integration Portal) that had a Spearman or Pearson correlation of at least -0.8 were compiled. Figures 4.14 through 4.18 display these interaction networks in the five differentiation assays, where the interaction strength is symbolized by the thickness and color of the bond between a miRNA cluster and a gene cluster. These networks were normalized by the size of the miRNA cluster, and non-normalized versions as well as interaction networks normalized by the percentage of regulated genes or of regulating miRNAs can be found in Appendix Figures 7.1 through 7.5.
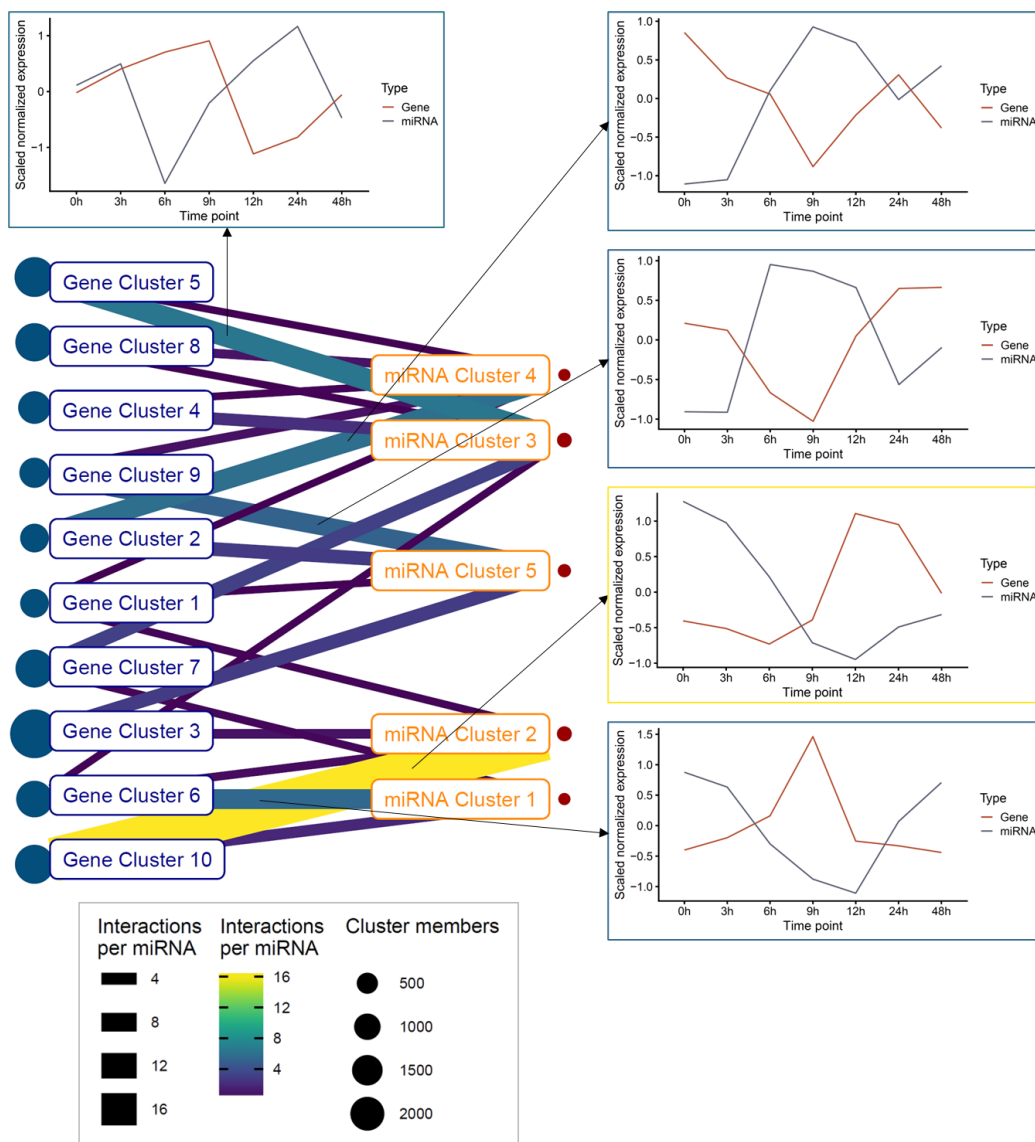
Figure 4.14 shows the network of interactions between gene and miRNA clusters of the hMSC adipogenesis assay, normalized by the size of the miRNA cluster. Five cluster pairs had a higher interaction count compared to the others, especially miRNA cluster 2 and gene cluster 10. The overlapped cluster centroids of these five cluster pairs are displayed on the right of Figure 4.14. In all cases, the miRNA centroid line mirrored the line of the gene cluster centroid quite well, which was to be expected. It is worth noting that the percentages of both regulating miRNAs and regulated genes of miRNA cluster 2 and gene cluster 10 were also the highest of this differentiation assay, but gene clusters 2 and 9 also exhibited higher percentages of regulated genes than expected by their interaction frequency, which might be explained by their smaller size (see Figure 7.1).
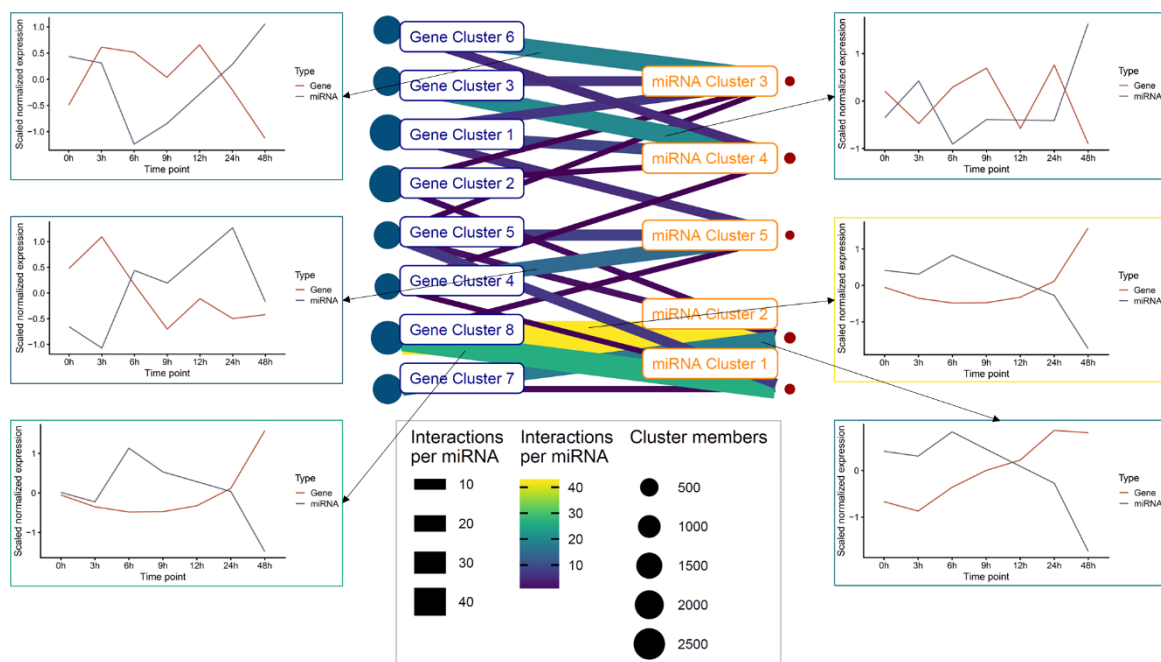
Figure 4.15: Network of interactions between gene clusters (left) and miRNA clusters (middle) of the hMSC chondrogenesis assay, normalized by the size of the miRNA cluster. The cluster centroids of the gene and miRNA clusters whose interactions are referred to by the arrows are shown on the right and bottom.

According to the interaction network of the hMSC chondrogenesis assay in Figure 4.15, six pairs of clusters had a high number of interactions. The microRNA cluster 1 strongly interacted with gene cluster 8, which was one of the two clusters heavily targeted by miRNA cluster 2, with gene cluster 7. The pair with the largest number of interactions, miRNA cluster 2 and gene cluster 8 was also the pair for which the cluster centroids best reflected each other, although other pairs with fewer interactions per miRNA also showed good concordance, like miRNA cluster 4 and gene cluster 3, and miRNA cluster 5 with gene cluster 4. It is worth noting that all or almost all miRNAs of each cluster were involved in interactions with at least one gene cluster (see Figure 7.2).
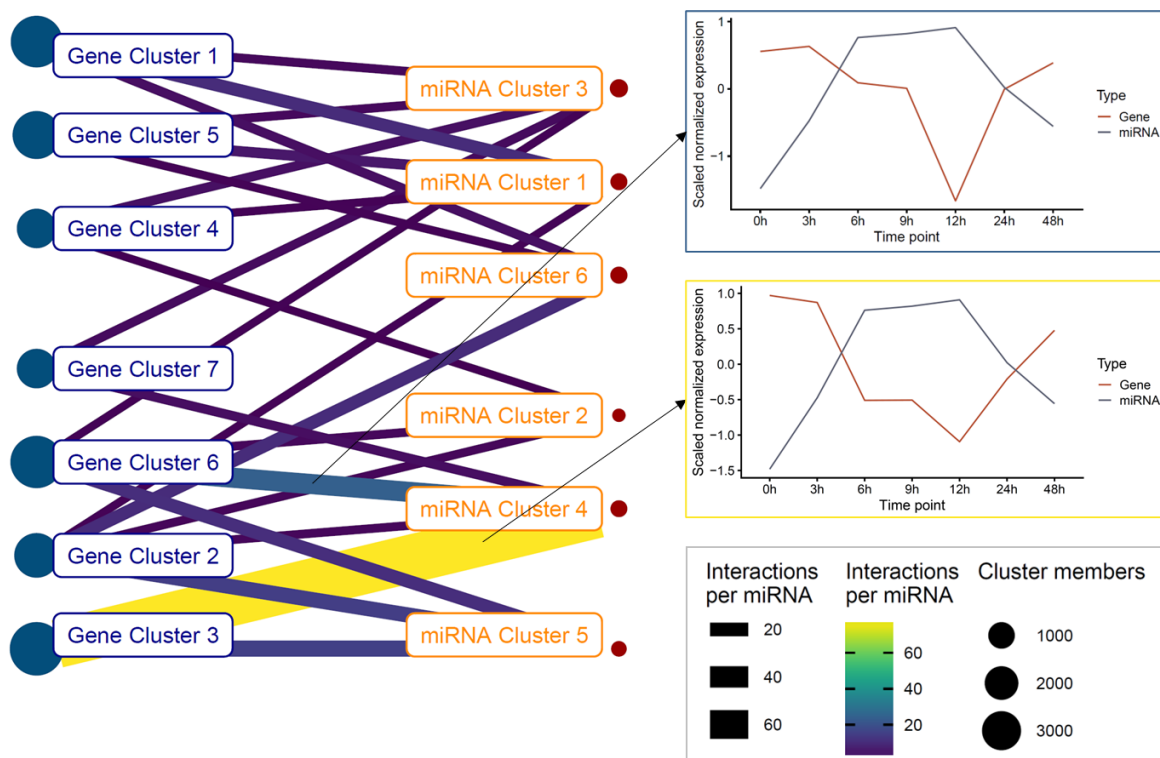
Figure 4.16: Network of interactions between gene clusters (left) and miRNA clusters (middle) of the hMSC osteogenesis assay, normalized by the size of the miRNA cluster. The cluster centroid of the gene and miRNA cluster whose interaction is referred to by the arrow is shown on the right.

In the network of cluster interactions of the hMSC osteogenesis assay (displayed in Figure 4.16), two cluster pairs were noticeable by their interaction frequency: miRNA cluster 4 with gene cluster 3 and with gene cluster 6. As already observed in other differentiation assays, the better concordance of the centroid lines could be found in the cluster pair with the highest interaction count per miRNA. When looking at the percentage

of regulating miRNAs and regulated genes, the pair formed by miRNA cluster 6 and gene cluster 2 stood out as involving all miRNAs from the not particularly small miRNA cluster but only about 10 % of the genes from the gene cluster (see Figure 7.3).
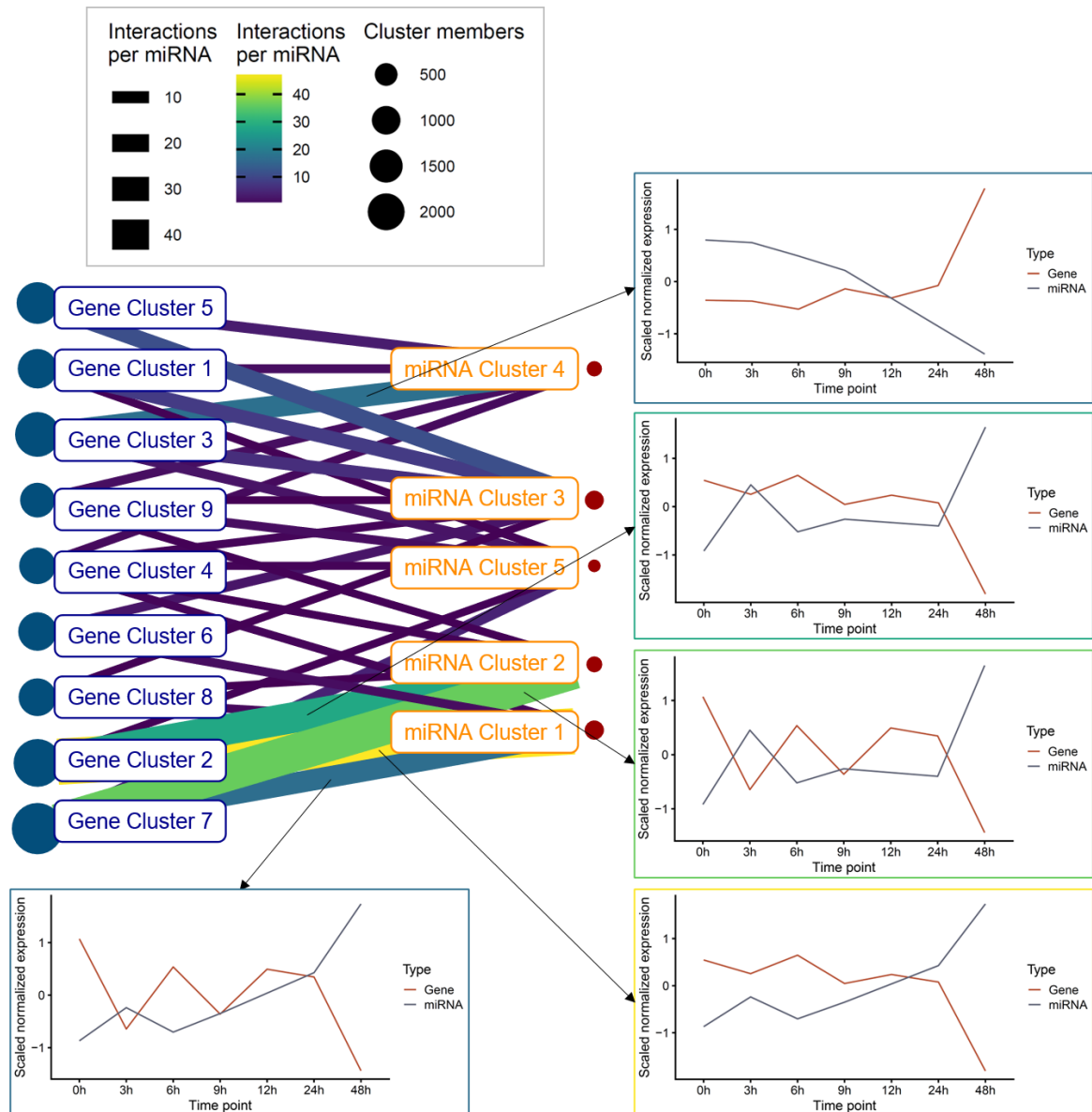
Figure 4.17: Network of interactions between gene clusters (left) and miRNA clusters (middle) of the hNSC differentiation assay, normalized by the size of the miRNA cluster. The cluster centroids of the gene and miRNA clusters whose interactions are referred to by the arrows are shown on the right.

Figure 4.17 shows the network of interactions of the hNSC differentiation assay, in which two miRNA clusters (1 and 2) and two gene clusters (2 and 7) had the highest interaction counts. The cluster centroids of these four pairs quite closely reflected each other,

particularly those of the miRNA cluster 1 and gene cluster 2, which together had the highest interaction proportion. Another cluster pair exhibited a high interaction count, miRNA cluster 4 with gene cluster 3. The miRNAs from the miRNA cluster were involved at a high percentage in regulation interactions (see Figure 7.4), although this cluster did not stand out in Figure 4.17.
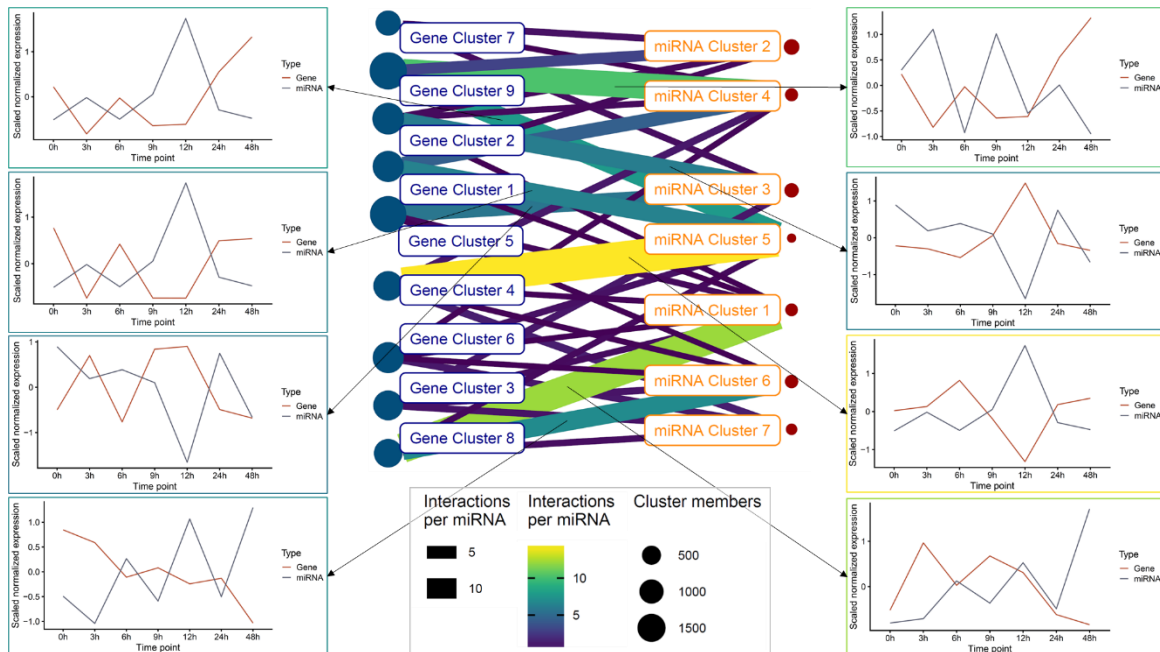
Figure 4.18: Network of interactions (middle) between gene clusters and miRNA clusters of the HSkM differentiation assay, normalized by the size of the miRNA cluster. The cluster centroids of the gene and miRNA clusters whose interactions are referred to by the arrows are shown on the right and left.

In the HSkM differentiation assay, whose interaction network is displayed in Figure 4.18, eight pairs of miRNA and gene clusters strongly interacted with each other. In this assay again, the centroids that best reflected each other were among the cluster pairs with the highest number of interactions per miRNA: miRNA cluster 5 with gene cluster 4 and miRNA cluster 4 with gene cluster 9, as well as miRNA cluster 3 with gene cluster 2. This last cluster pair was the only pair of this differentiation assay where all but one miRNA were regulating at least one gene (see Figure 7.5)

The interaction sets used for the above analysis were again restricted, this time to the interactions that contained the 10 miRNAs with the strongest increase or decrease in expression in the differentiation assays, or the 100 genes with the strongest increase or decrease, to identify specific miRNAs or genes driving these interactions. The resulting networks are shown in Figures 4.19 through 4.28. In this analysis, RNAs were considered not to belong to a cluster ("Cluster NA") if their membership score was less than 0.5. Unless otherwise stated, the miRNA-gene interaction percentages below do not include genes that could not be assigned a cluster.

The subset of interactions comprising the ten miRNAs with the strongest increase in expression in the hMSC adipogenesis assay is displayed in Figure 4.19 a-b and consists of two networks. In Figure 4.19 a, miRNAs are identified by their labels and the colored dots depict the cluster membership of their target genes, while in b the cluster membership of miRNAs is shown. Two miRNAs that were not part of any identified cluster, hsa-miR-210-3p and hsa-miR-873-5p, formed the first network and the targets of hsa-miR-210-3p belonged to gene clusters 8 (56.1 %) and 6 (42.9 %). The second network included seven members of miRNA cluster 4 (hsa-miR-1973, hsa-miR-3135b, hsa-miR-4428, hsa-miR-494-3p, hsa-miR-663a, hsa-miR-6785-5p, and hsa-miR-8063), and one member of miRNA cluster 5 (hsa-miR-6821-5p). Most of their targets that could be assigned to a cluster were members of gene cluster 2 (91.0 %), which is a moderately frequent interaction according to Figure 4.14.

Two networks could also be observed in the subset of interactions with the ten most decreasing miRNAs in the hMSC adipogenesis assay (Figure 4.19 c-d). The upper right network included two miRNAs (hsa-miR-6068 and hsa-miR-6724-5p), both members of miRNA cluster 5. Their targets belonged mostly to gene clusters 9 (64.7 %) and 2 (29.4 %), for which the interaction count is also moderately high in Figure 4.14. The other network in this subset comprised hsa-miR-503-5p and seven members of miRNA cluster 2 (hsa-miR-221-5p, hsa-miR-29b-1-5p, hsa-miR-29b-3p, hsa-miR-337-5p, hsa-miR-374b-5p, hsa-miR-432-5p, and hsa-miR-487b-3p). Most targets of this network were members of gene cluster 10 (92.8 %), which represent the highest cluster interaction count in Figure 4.14, and some targets of hsa-miR-432-5p belonged to gene cluster 3 (12.9 %).
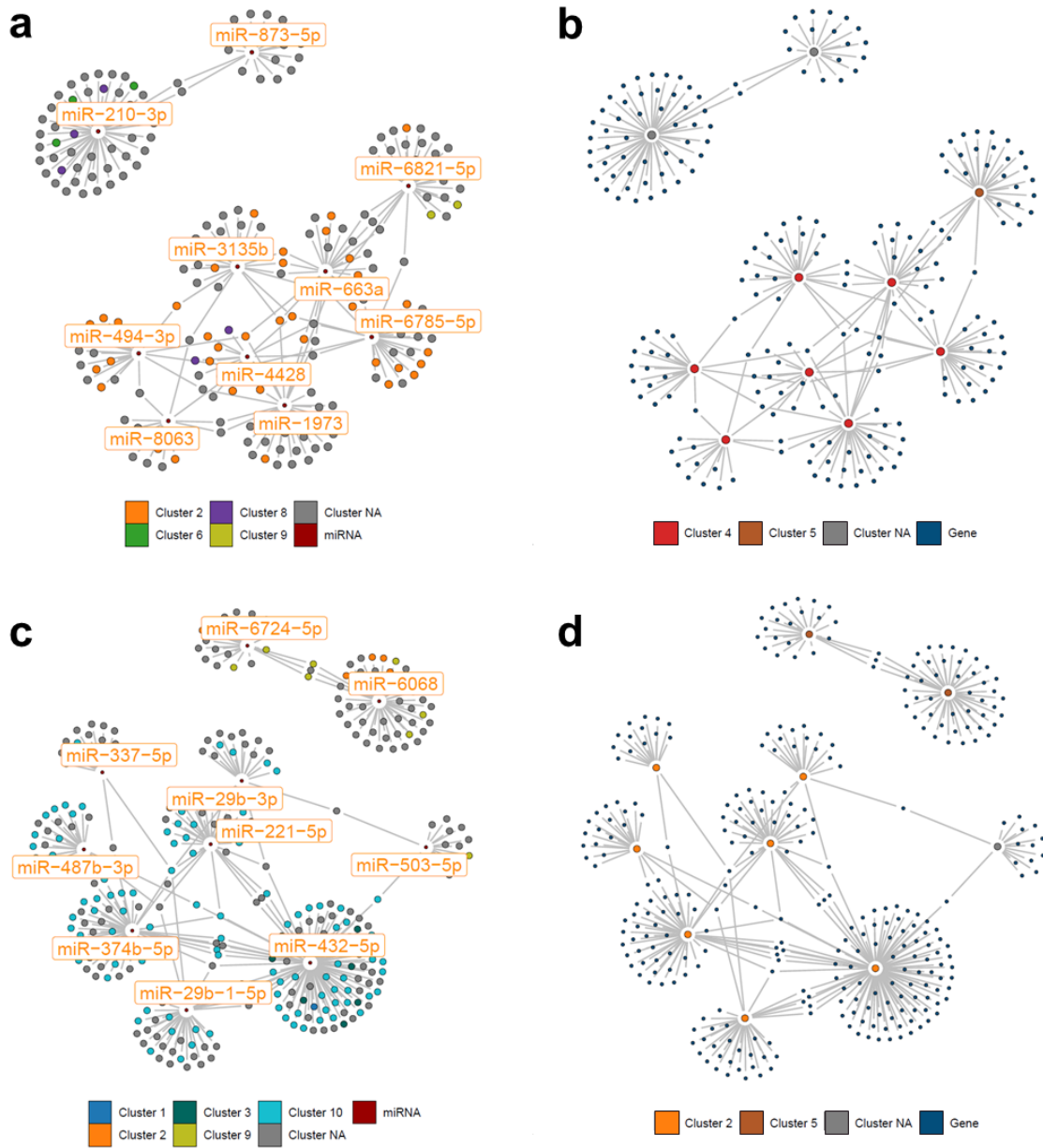
Figure 4.19: Interaction networks between the ten miRNAs with the strongest increase (**a-b**) or decrease in expression (**c-d**) in the hMSC adipogenesis assay and their targets. Each interaction was validated in the online miRNA-gene interaction database miRTarBase or predicted by at least three sources in the online miRNA-gene interaction prediction tool mirDIP (microRNA Data Integration Portal) and had a Spearman or Pearson correlation of at least -0.8. „Cluster NA" indicates that the membership score was less than 0.5.

The interaction networks focusing on the 100 most increasing genes in the hMSC adipogenesis assay were less well defined, since for most of these genes no miRNA-gene interactions were found (see Figure 4.20 a-b). The genes from cluster 9 (*CXCL12* and *IER3*) were targeted by the only member of miRNA cluster 5 (hsa-miR-3195). The other miRNAs mostly belonged to cluster 2 (77.3 %) and mainly targeted members of gene cluster 10 (90.9 %).

The interaction networks derived from the 100 most decreasing genes in the hMSC adipogenesis assay consisted of multiple networks with single genes targeted by one to five miRNAs (see Figure 4.20 c-d). Several miRNAs belonged to cluster 1 (27.8 %), and several others to miRNA cluster 4 (27.8 %). The latter group mostly targeted members of gene cluster 2 (60.0 % of all interactions), for which the interaction count in Figure 4.14 is moderately high.

Figure 4.20 (next page): Interaction networks between genes in the top 100 increased (**a-b**) or decreased expression (**c-d**) in the hMSC adipogenesis assay and the miRNAs that target them. Each interaction was validated in the online miRNA-gene interaction database miRTarBase or predicted by at least three sources in the online miRNA-gene interaction prediction tool mirDIP and demonstrated a Spearman or Pearson correlation of at least -0.8. "Cluster NA" indicates that the membership score was less than 0.5.
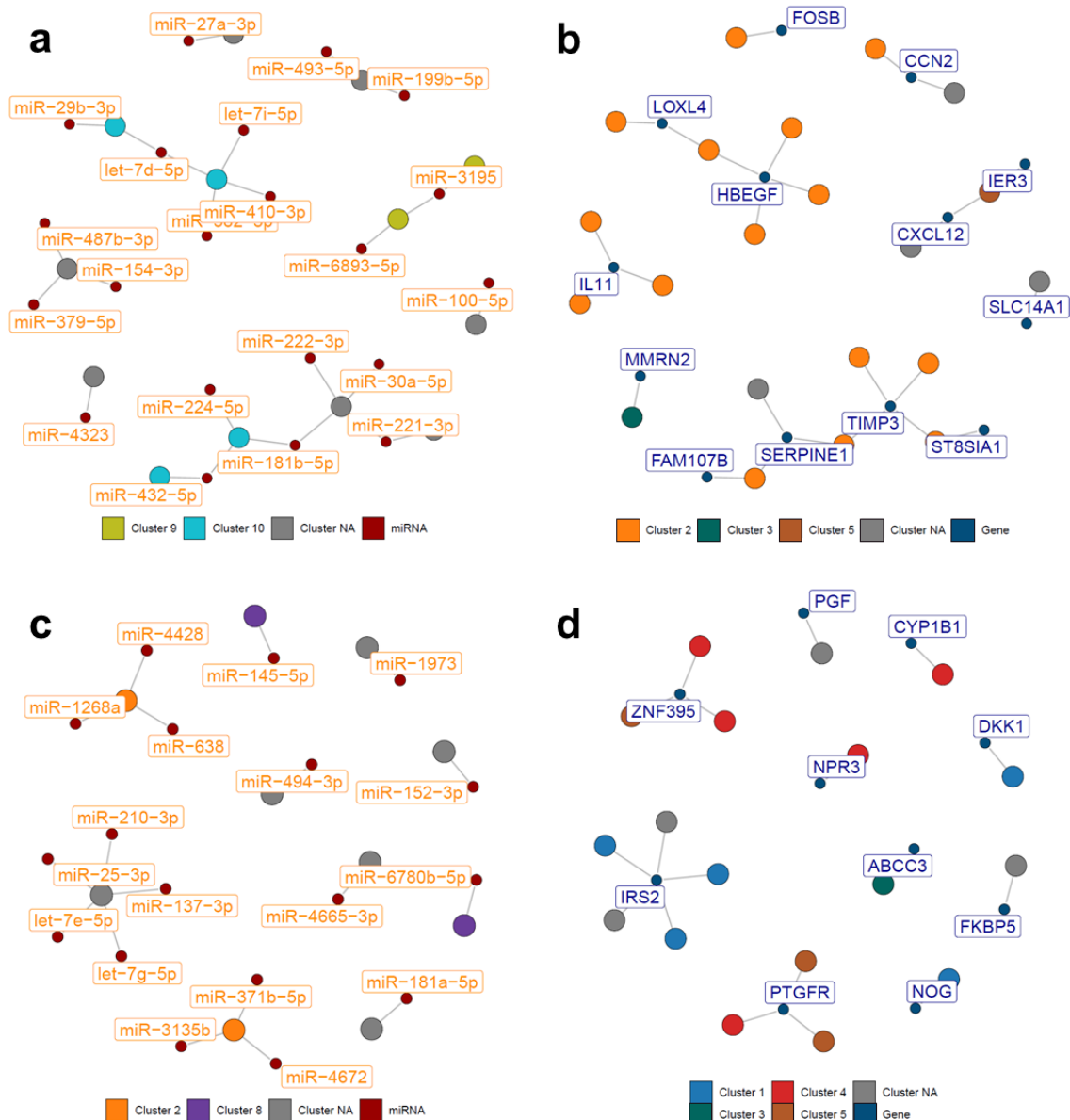
The subset of interactions of the ten most increasing miRNAs in the hMSC chondrogenesis assay was composed of nine members of miRNA cluster 4 and formed a highly connected network (see Figure 4.21 a-b; hsa-miR-2861, hsa-miR-4505, hsa-miR-4507, hsa-miR-4530, hsa-miR-4672, hsa-miR-494-3p, hsa-miR-638, hsa-miR-6803-5p, and hsa-miR-6869-5p). They mostly targeted members of gene cluster 3 (62.9 %), which is a common interaction according to Figure 4.15. For the remaining miRNA, hsa-miR-7641, no known target was found.

The network of the ten miRNAs with the strongest decrease in expression in the hMSC chondrogenesis assay is shown in Figure 4.21 c-d. All ten miRNAs were quite well connected, and eight were members of miRNA cluster 2 (hsa-miR-155-5p, hsa-miR-221-5p, hsa-miR-29a-3p, hsa-miR-29b-3p, hsa-miR-29c-3p, hsa-miR-31-3p, hsa-miR-34a-5p,

and hsa-miR-34b-5p). Their targets mainly belonged to gene clusters 8 (60.4 %) and 7 (35.0 %), except for the targets of hsa-miR-7-5p, the only member of miRNA cluster 1, who mostly belonged to gene clusters 8 (74.4 %) and 5 (25.6 %). These interaction counts are among the highest in Figure 4.15.

Figure 4.21: Interaction networks between the ten miRNAs with the strongest increase (**a-b**) or decrease in expression (**c-d**) in the hMSC chondrogenesis assay and their targets. Each interaction was validated in the online miRNA-gene interaction database miRTarBase or predicted by at least three sources in the online miRNA-gene interaction prediction tool mirDIP and had a Spearman or Pearson correlation of at least -0.8. „Cluster NA" indicates that the membership score was less than 0.5.

The network focusing on the 100 most increasing genes in the hMSC chondrogenesis assay, displayed in Figure 4.22 a-b, also supported a strong association between miRNA cluster 2 (81.8 % of all miRNAs) and gene cluster 8 (66.7 % of all genes).

In contrast, the interactions of the 100 most decreasing genes in the hMSC chondrogenesis assay (see Figure 4.22 c-d) mostly differed from the global interaction landscape observed in Figure 4.15. Most miRNAs in this subset belonged to miRNA cluster 4, and they mainly targeted members of gene cluster 1 (66.7 %). *PODXL*, the only member of gene cluster 4 in this subset, was targeted by the only two members of miRNA cluster 5 (hsa-miR-148a-3p and hsa-miR-199a-5p).
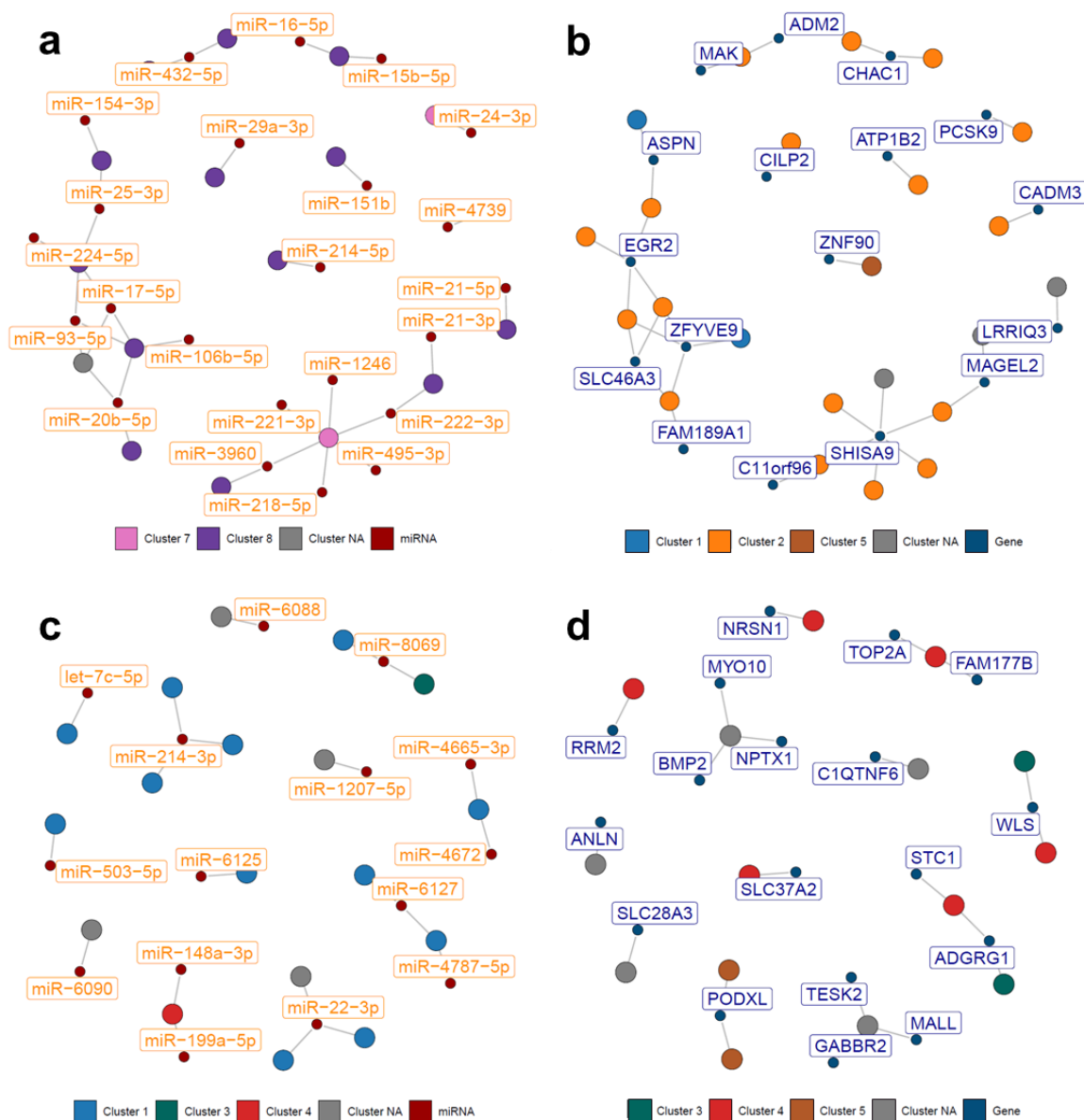
Figure 4.22 (previous page): Interaction network between genes in the top 100 increased (**a-b**) or decreased expression (**c-d**) in the hMSC chondrogenesis assay and the miRNAs that target them. Each interaction was validated in the online miRNA-gene interaction database miRTarBase or predicted by at least three sources in the online miRNA-gene interaction prediction tool mirDIP and demonstrated a Spearman or Pearson correlation of at least -0.8. "Cluster NA" indicates that the membership score was less than 0.5.

The interaction network derived from the ten most increasing miRNAs in the hMSC osteogenesis assay, shown in Figure 4.23 a-b, formed a fairly well-connected network. All ten miRNAs (hsa-miR-1912-3p, hsa-miR-3658, hsa-miR-3919, hsa-miR-4267, hsa-miR-4691-3p, hsa-miR-4762-3p, hsa-miR-515-5p, hsa-miR-640, hsa-miR-665, hsa-miR-6715b-3p) belonged to miRNA cluster 3, and the majority of their targets were members of gene clusters 4 (34.7 %) and 5 (27.7 %). These interaction counts are not particularly high in Figure 4.16.

The well-interconnected network formed by the ten most decreasing miRNAs in the hMSC osteogenesis assay was composed of nine miRNAs (see Figure 4.23 c-d). The three miRNAs situated in the upper left (hsa-miR-132-3p, hsa-miR-29b-3p, and hsa-miR-31-5p) were members of miRNA cluster 6, and their targets mostly belonged to gene cluster 2 (84.1 %). Three miRNAs (hsa-miR-3960, hsa-miR-4505, and hsa-miR-4530) were members of miRNA cluster 5, and mainly targeted members of gene cluster 3 (43.2 %) and 2 (33.5 %). Members of gene clusters 3, 6, and 2 were also targeted by hsa-miR-6821-5p, which was the only member of miRNA cluster 4 in this subset. For the remaining miRNA, hsa-miR-4459, no interactions were found. Most of these interactions are not particularly frequent according to Figure 4.16.

Figure 4.23 (next page): Interaction networks between the ten miRNAs with the strongest increase (**a-b**) or decrease in expression (**c-d**) in the hMSC osteogenesis assay and their targets. Each interaction was validated in the online miRNA-gene interaction database miRTarBase or predicted by at least three sources in the online miRNA-gene interaction prediction tool mirDIP and had a Spearman or Pearson correlation of at least -0.8. „Cluster NA" indicates that the membership value was less than 0.5.
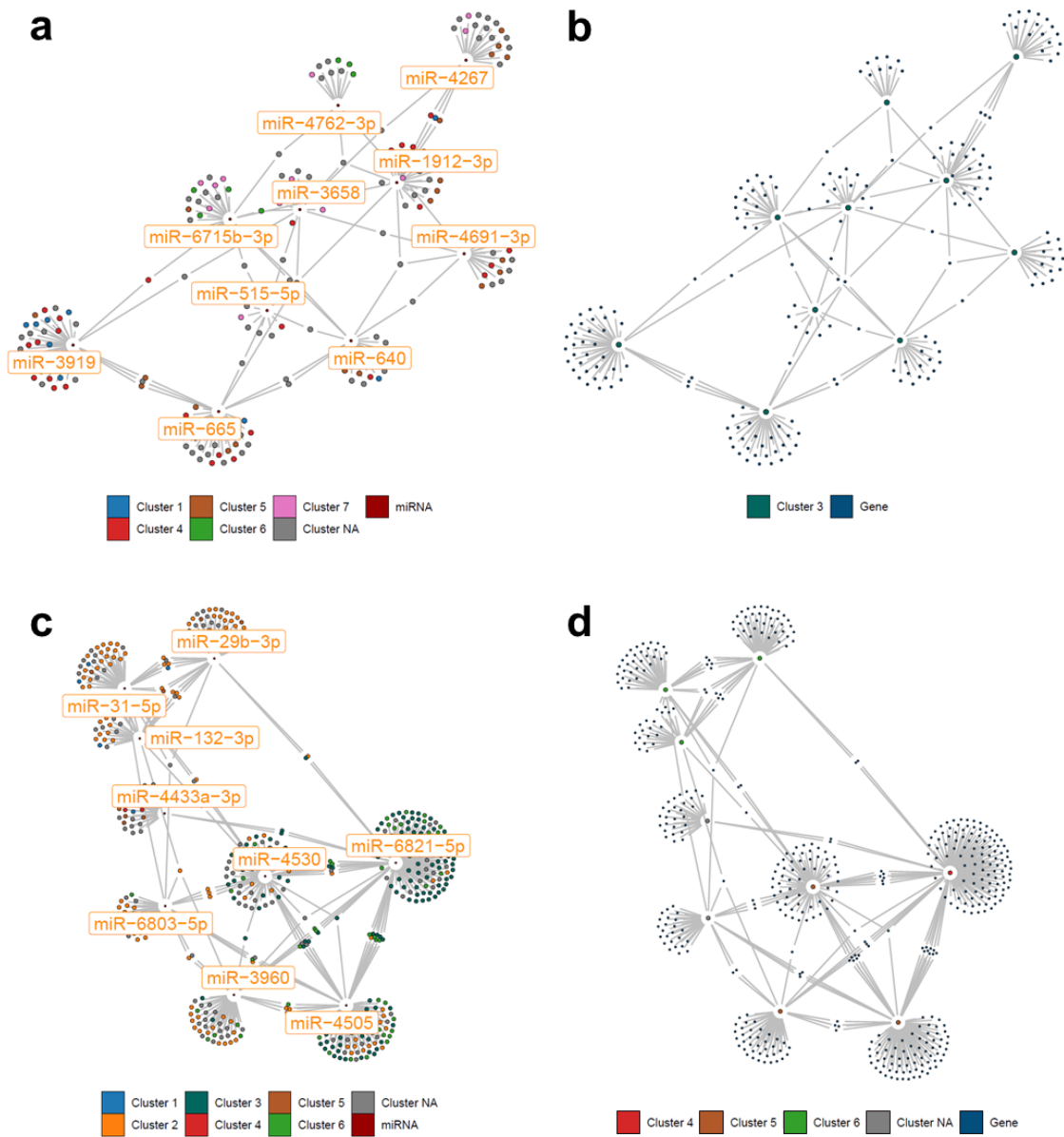
Focusing on the network formed by the 100 most increasing genes in the hMSC osteogenesis assay revealed a moderately interconnected topology (see Figure 4.24 a-b). Nevertheless, some trends were apparent: ten genes, including nine members of gene cluster 2 were targeted by eleven miRNAs belonging to miRNA cluster 6. Additionally, a network composed of three members of gene cluster 2 (*ABCC3*, *ADAMTS9*, and *PTK2B*), *FAM20A,* and *TNS3*, and of members of miRNA clusters 4 and 5 was visible on the bottom left of the subset, this interaction being not particularly common according to Figure 4.16.

The interaction network spanned by the 100 most decreasing genes in the hMSC osteogenesis assay (see Figure 4.24 c-d), was characterized by a principal network (bottom left) consisting of members of miRNA cluster 4, and their targets, most of which belonged to gene cluster 3 (75.0 %). This represents the most frequent interaction in

Figure 4.16. Another miRNA cluster was well represented in this subset: *NPTX1* was targeted by six miRNAs, of which five belonged to miRNA cluster 3, and *TFPI2* was targeted by three members of the same miRNA clusters.

Figure 4.24: Interaction network between genes in the top 100 increased (**a-b**) or decreased expression (**c-d**) in the hMSC osteogenesis assay and the miRNAs that target them. Each interaction was validated in the online miRNA-gene interaction database miRTarBase or predicted by at least three sources in the online miRNA-gene interaction prediction tool mirDIP and demonstrated a Spearman or Pearson correlation of at least -0.8. "Cluster NA" indicates that the membership score was less than 0.5.

The network formed by the ten most increasing miRNAs in the hNSC differentiation assay is shown in Figure 4.25 a-b. It included a high proportion of members from miRNA clusters 5 (mainly bottom left, 62.5 %; hsa-miR-4446-3p, hsa-miR-4697-5p, hsa-miR-494-3p, hsa-miR-6132, and hsa-miR-6785-5p) and 2 (upper right, 37.5 %; hsa-miR-1260b, hsa-miR-3195, and hsa-miR-5684). The genes targeted by miRNAs in the upper right corner mainly belonged to gene clusters 7 (70.7 %) and 2 (27.2 %), which were frequent interactions according to Figure 4.17. The targets of the members of miRNA cluster 5 mostly belonged to gene clusters 7 (55.0 %) and 3 (22.5 %), which are not particularly frequent interactions in Figure 4.17.

The interaction network of the ten most decreasing miRNAs in the hNSC differentiation assay was split into two parts. The main network comprised nine members of miRNA cluster 3 (hsa-miR-101-3p, hsa-miR-135b-5p, hsa-miR-153-3p, hsa-miR-19a-3p, hsa-miR-219a-5p, hsa-miR-29b-3p, hsa-miR-340-5p, hsa-miR-374a-5p, and hsa-miR-551b-3p) and was highly interconnected (Figure 4.25 c-d). A high proportion (57.1 %) of their multiple targets belonged to gene cluster 5, and 18.1 % to gene cluster 1, for which the interaction counts were moderately high according to Figure 4.17. The second part was formed by the member of miRNA cluster 5 (hsa-miR-619-5p), situated in the upper right corner, and mainly targeted members of gene cluster 3.
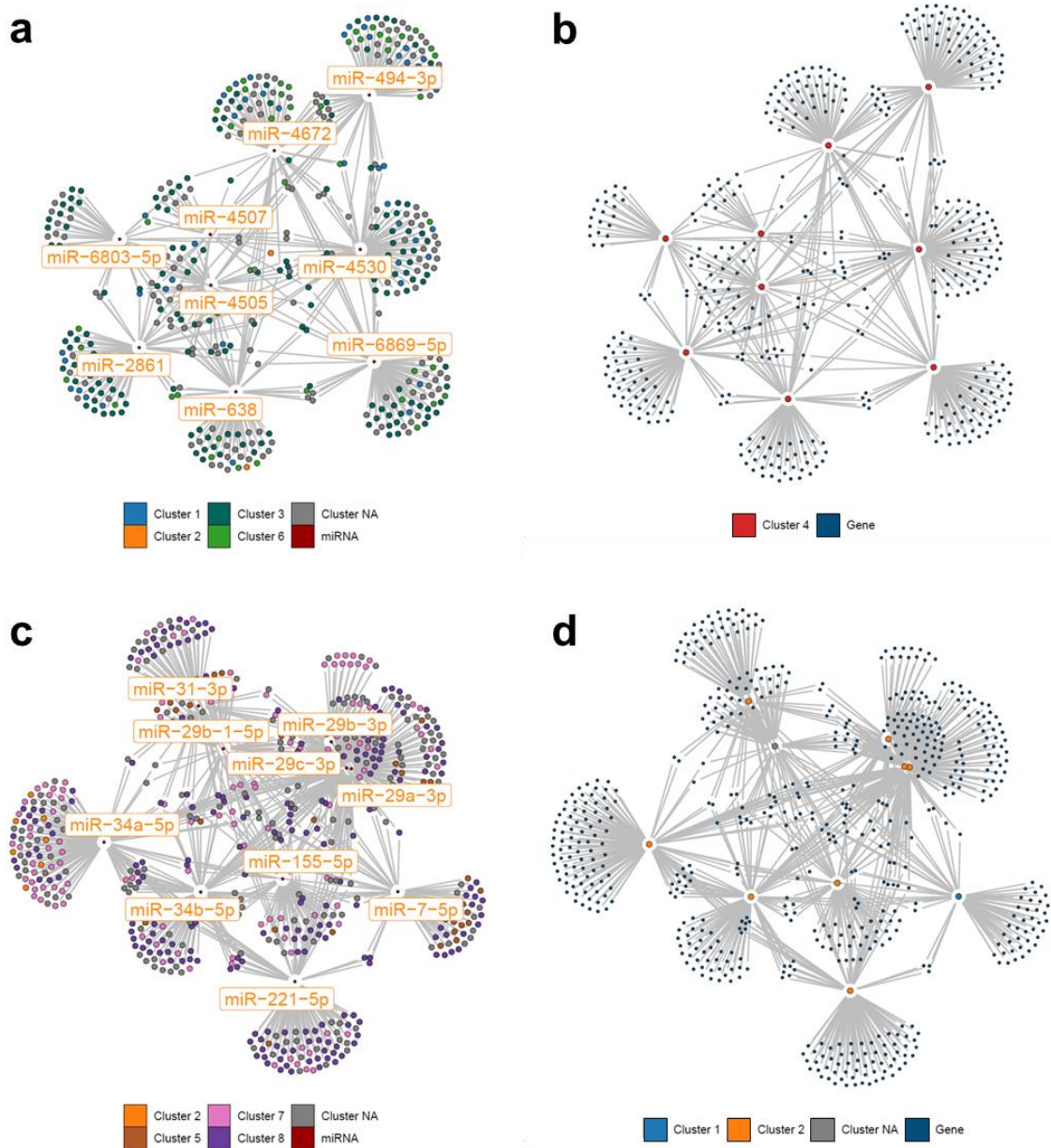
Figure 4.25 (next page): Interaction networks between the ten miRNAs with the strongest increase (**a-b**) or decrease in expression (**c-d**) in the hNSC differentiation assay and their targets. Each interaction was validated in the online miRNA-gene interaction database miRTarBase or predicted by at least three sources in the online miRNA-gene interaction prediction tool mirDIP and had a Spearman or Pearson correlation of at least -0.8. „Cluster NA" indicates that the membership value was less than 0.5.
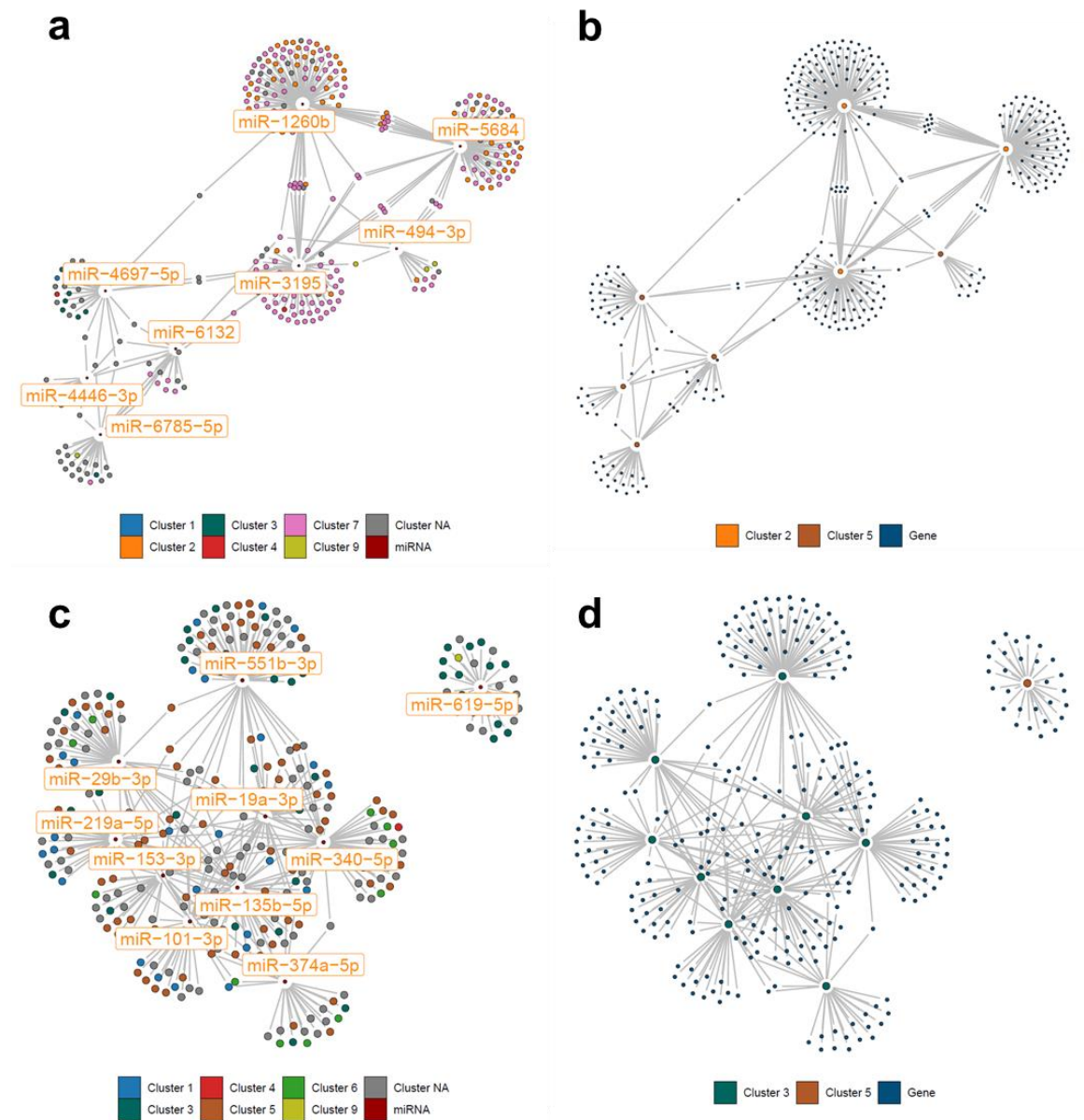
The interaction network focusing on the top 100 most increasing in the hNSC differentiation assay, shown in Figure 4.26 a-b, was mainly composed of members of gene cluster 3 (72.9 %), and associated with 19 members of miRNA cluster 3, and with five members of miRNA cluster 4. The only members of miRNA cluster 5 (hsa-miR-1275, hsa-miR-2861, hsa-miR-4728-5p, hsa-miR-638, and hsa-miR-6800-5p), and 2 (hsa-miR-4428, and hsa-miR-6780b-5p) all targeted *SPTB*, who belonged to gene cluster 9. These interactions are moderately frequent according to Figure 4.17.

The subset of interaction resulting from the 100 most decreasing genes in the hNSC differentiation assay was mostly disconnected and regulated by a few miRNAs. The largest

network was spanned by *FRMD4A*, a member of gene cluster 7, and the nine miRNAs targeting it, all of which belonged to miRNA cluster 2 (see Figure 4.26 c-d; hsa-miR-1260b, hsa-miR-1305, hsa-miR-149-5p, hsa-miR-320e, hsa-miR-342-3p, hsa-miR-4284, hsa-miR-432-5p, hsa-miR-4716-3p, and hsa-miR-6780b-5p). Two other members of this miRNA cluster were present in this subset (hsa-miR-4443, and hsa-miR-6740-5p), along with six members of miRNA cluster 1 (hsa-miR-1281, hsa-miR-4701-5p, hsa-miR-563, hsa-miR-6731-3p, hsa-miR-6784-3p, and hsa-miR-98-3p), one member of miRNA cluster 5 (hsa-miR-6800-5p), and two other miRNAs (hsa-miR-5739, and hsa-miR-6826-5p). These miRNA proportions are frequent according to Figure 4.17.

The interactions of the ten most increasing miRNAs in the HSkM differentiation assay, shown in Figure 4.27 a-b, included a contiguous network of eight miRNAs (hsa-miR-4697-5p, hsa-miR-5703, hsa-miR-5787, hsa-miR-630, hsa-miR-642a-3p, hsa-miR-6749-5p, hsa-miR-6785-5p, and hsa-miR-7110-5p), five of which belonged to miRNA cluster 1. A high proportion (95.8 %) of the targets in this network belonged to gene cluster 8, which is the second highest interaction count according to Figure 4.18. The only member of miRNA cluster 5 in this subset, hsa-miR-4697-5p, targeted the only four members of gene cluster 4 (*CNGB1*, *EFNA2*, *LSM4*, and *SLC39A3/ZIP3*), the interaction counts of these clusters being among the highest in Figure 4.18. One miRNA, hsa-miR-1-3p was situated in the upper left corner, disconnected from the rest and its numerous targets were mostly members of gene clusters 5 (57.6 %) and 3 (40.0 %). For the remaining miRNA, hsa-miR-4459, no known interactions were found.

The network spanned by the ten most decreasing miRNAs in the HSkM differentiation assay formed a sparsely connected network (Figure 4.27 c-d). Four of these belonged to miRNA clusters 4 and 5 (hsa-miR-199b-5p, hsa-miR-224-5p, hsa-miR-494-3p, and hsa-miR-7-5p) and targeted members of gene clusters 9 and 1. These interactions are frequent according to Figure 4.18. Two (hsa-miR-10a-5p, and hsa-miR-450a-5p) and one (hsa-miR-29b-1-5p) miRNAs belonged to miRNA clusters 3 and 2 respectively, and mainly targeted members of gene cluster 2 (66.7 %) and 7 (57.9 %) respectively. These interactions are less common according to Figure 4.18.

In the interaction network derived from the 100 most increasing genes in the HSkM differentiation assay, all but one gene (97.6 %) were members of gene cluster 9 (see Figure 4.28 a-b). They were mostly targeted by members of miRNA clusters 4 and 5, or in the case of *PCSK9*, by the only four members of miRNA cluster 2 present in this subset (hsa-miR-100-5p, hsa-miR-129-1-3p, hsa-miR-129-2-3p, and hsa-miR-99a-5p), which is common according to Figure 4.18. The only member of gene cluster 5 in this subset (*CCN5*) was targeted by the only miRNA of this subset belonging to miRNA cluster 3 (hsa-miR-455-3p).

The network focusing on the 100 most decreasing genes in the HSkM differentiation assay is shown in Figure 4.28 c-d. A high proportion (37.2 %) of miRNAs belonging to miRNA cluster 3 was found in this subset, and their targets were mainly members of gene cluster 5

(93.8 % of all interactions). The interaction count of these clusters is moderately high in Figure 4.18.
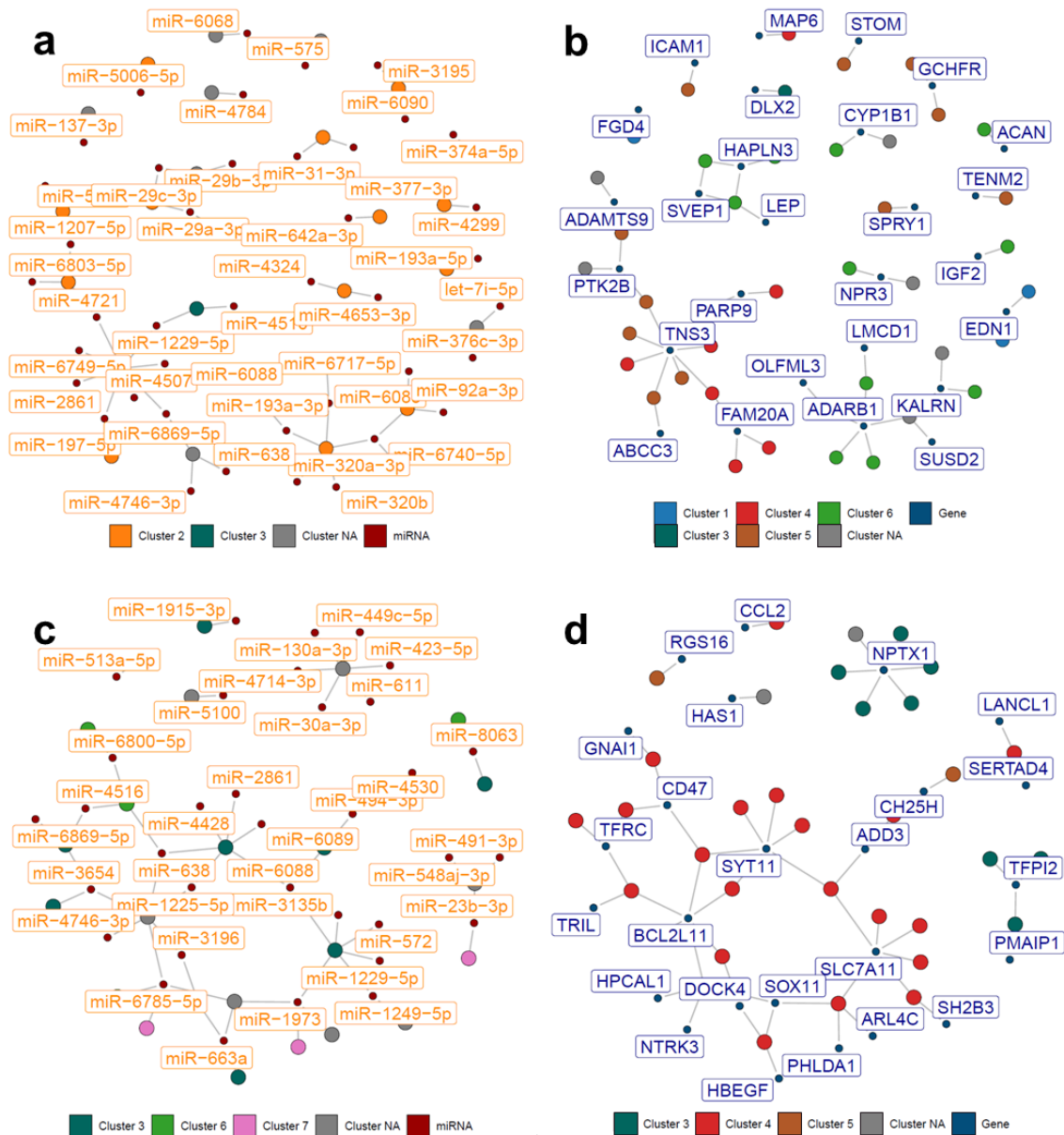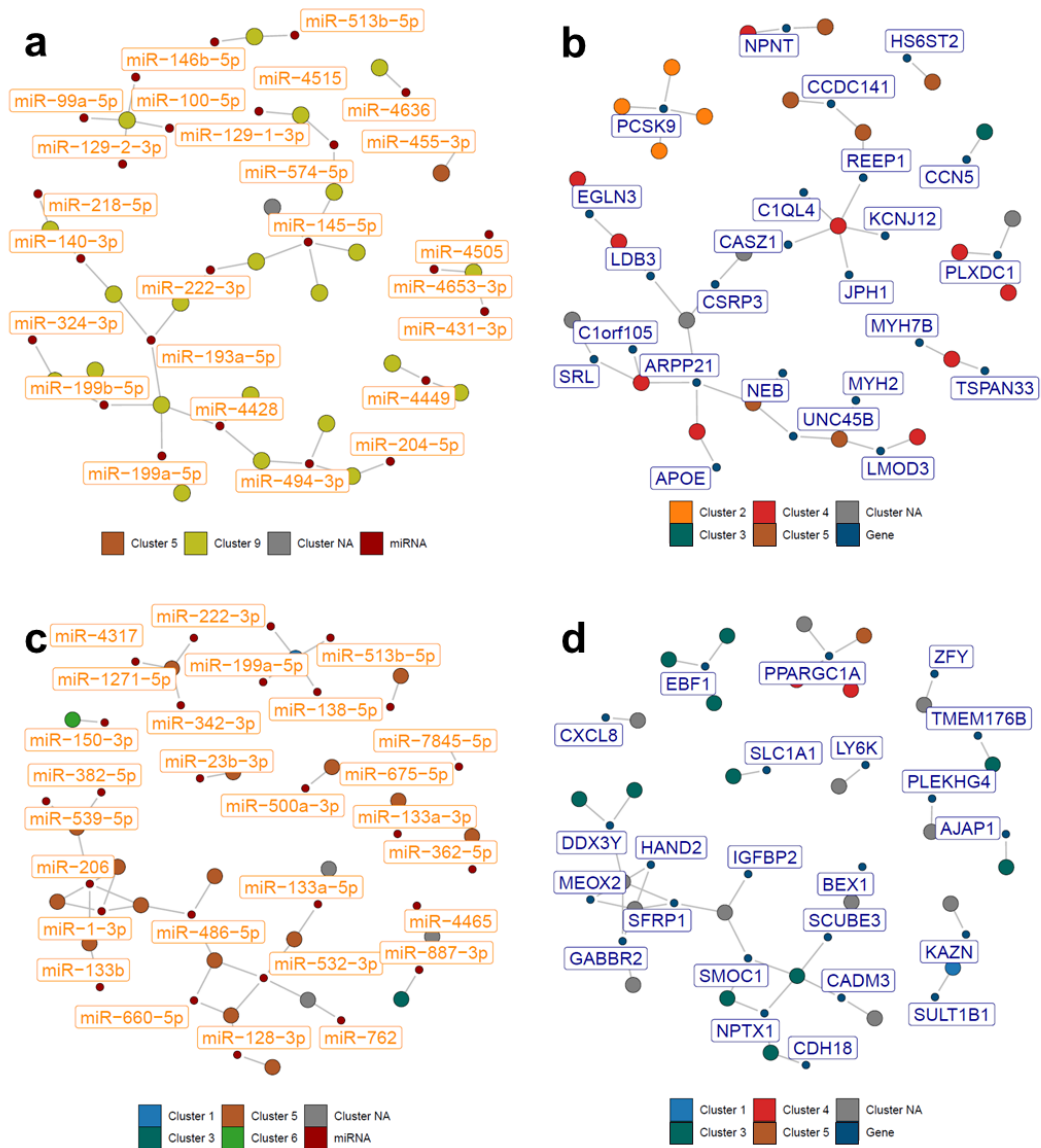

Figure 4.28: Interaction network between genes in the top 100 increased (**a-b**) or decreased expression (**c-d**) in the HSkM differentiation assay and the miRNAs that target them. Each interaction was validated in the online miRNA-gene interaction database miRTarBase or predicted by at least three sources in the online miRNA-gene interaction prediction tool mirDIP and demonstrated a Spearman or Pearson correlation of at least -0.8. "Cluster NA" indicates the membership score was less than 0.5.

In summary, a large proportion of interactions involving one miRNA or gene from the 10 or 100, respectively, that experienced the strongest increase or decrease in expression were frequent according to the networks of interactions between miRNA and gene clusters. Of note, mostly connected networks were observed when investigating the most increasing or decreasing miRNAs, while networks focusing on the most increasing or decreasing genes were more often split into multiple components.

4.1.7. Hints of the adipogenesis-osteogenesis balance

According to Scheideler *et al.* 2008, it is possible to detect the adipogenesis-osteogenesis balance in gene expression data of hMSCs undergoing adipogenesis and osteogenesis even before commitment, which happens between 2 and 5 days after the onset of the differentiation process [465].

To investigate whether hints of the adipogenesis-osteogenesis balance could be found in the gene expression data of this work, lists of genes involved in adipogenesis and/or osteogenesis processes were assembled from the existing literature (full lists available in Appendix Table 7.3). Then the expression data of genes promoting or inhibiting adipogenesis were collected from the hMSC adipogenesis assay and the expression data of genes promoting or inhibiting osteogenesis were collected from the hMSC osteogenesis assay. Figures 4.29 through 4.33 show selected gene expression data relative to 0 h for all available time points, in the hMSC adipogenesis assay (see Figures 4.29 and 4.30) and the hMSC osteogenesis assay (see Figures 4.31 and 4.32). Figures with all gene expression data can be found in Appendix Figures 7.6 through 7.9.

For genes known to promote adipogenesis (see Figure 4.29), three genes, *Schnurri-2* (*HIVEP2*), *PPARG*, and *SRC*, showed a decrease of expression at the 6 h and/or 9 h time points compared to 0 h. The expression of *BMP4* and *DKK2* also decreased at earlier time points but rose well above 2 times more compared with 0 h at the 24 h time point. Their counterparts *BMP2* and *DKK1* both showed an increase in expression between 0 h and 3 h and between 9 h and 12 h.

Figure 4.29 (next page): Selected time-resolved gene expression relative to 0 h for genes known to promote adipogenesis, in the hMSC adipogenesis assay. The color scale indicates the maximum fold change in gene expression between two time points.
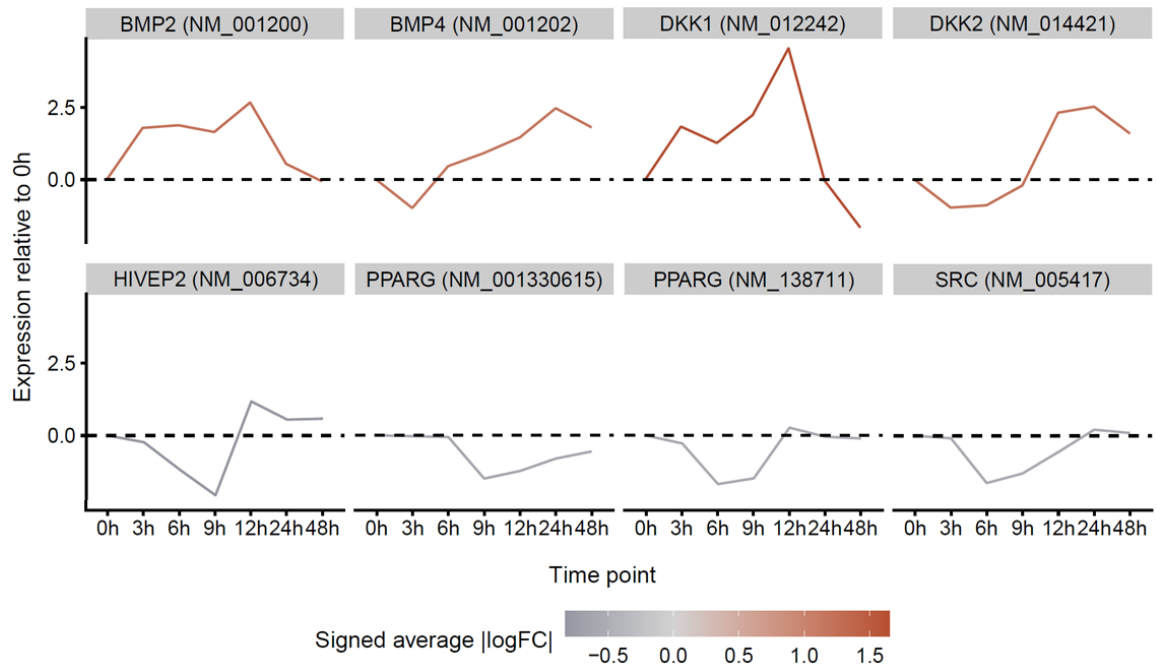
The category of genes known to inhibit adipogenesis was characterized by four genes whose expression strongly decreased: *CTNNB1*, *GLI3*, *RUNX2*, *SMAD6*, and only one gene showing a strong increase in expression, *GLI1* (see Figure 4.30).
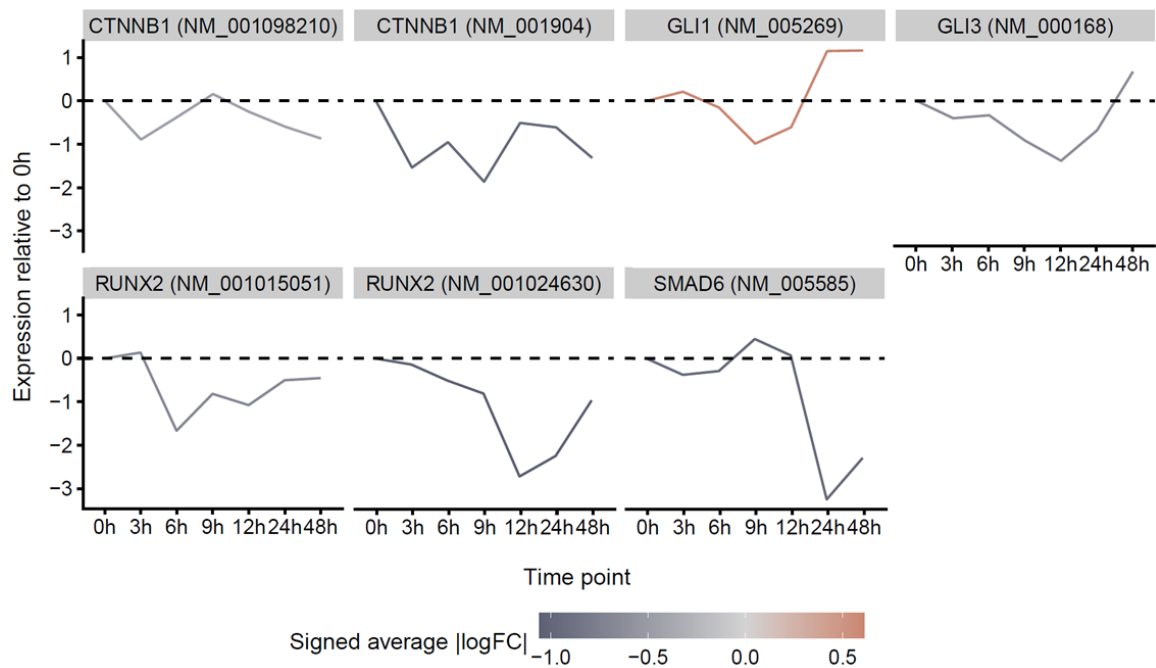
Figure 4.30: Selected time-resolved gene expression relative to 0 h for genes known to inhibit adipogenesis, in the hMSC adipogenesis assay. The color scale indicates the maximum fold change in gene expression between two time points.

Some of the genes known to promote osteogenesis demonstrated sharp decreases in expression, like *BMP2*, *BMP4*, *GLI1*, and *JUN* (see Figure 4.31). Although unexpected, these results were not particularly surprising considering that commitment to the osteogenic process is slower than commitment to adipogenesis [452]. Some genes, such as *IGFBP2* and *IGFBP4*, showed greatly increased expression after the 9 h time point.
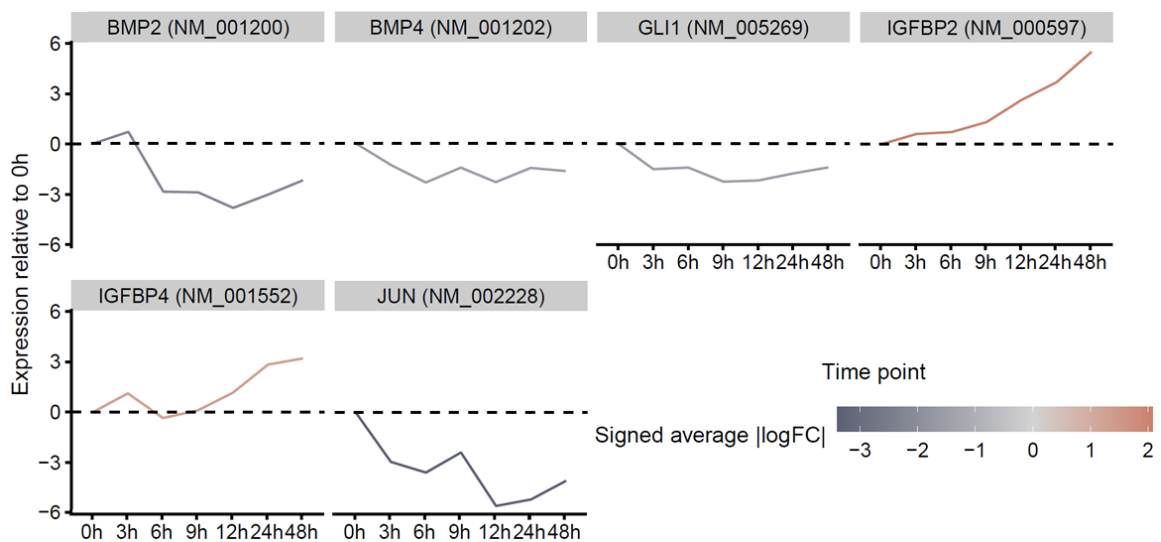
Figure 4.31: Selected time-resolved gene expression relative to 0 h for genes known to promote osteogenesis, in the hMSC osteogenesis assay. The color scale indicates the maximum fold change in gene expression between two time points.

In the category of genes known to inhibit osteogenesis (see Figure 4.32), two genes showed a counterintuitive expression pattern: adipsin (*CFD*) and leptin (*LEP*). Other genes, such as *ADIPOQ*, *DKK1*, or *NOG*, had a more expected pattern of expression characterized by higher expression levels at earlier time points that decreased over time.
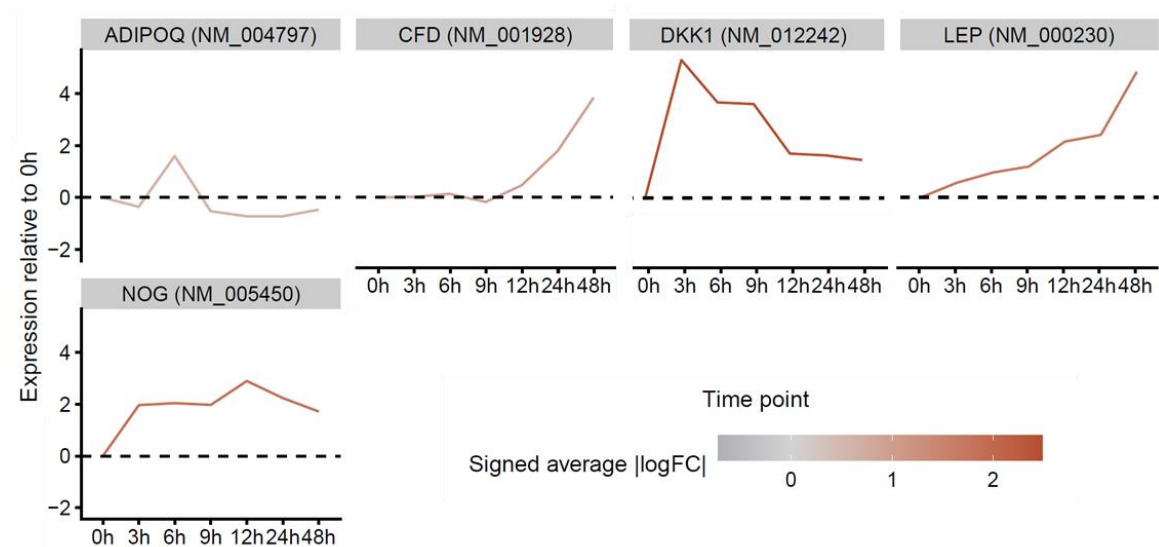
Figure 4.32: Selected time-resolved gene expression relative to 0 h for genes known to inhibit osteogenesis, in the hMSC osteogenesis assay. The color scale indicates the maximum fold change in gene expression between two time points.

Although anticipated alterations in gene expression levels were observed, an equal number of unexpected changes were also noted. Additionally, the majority of genes exhibited no significant modifications, suggesting a potential random nature of these observations in the studied time frame.

4.1.8.   Investigation of miRNAs important for embryonic stem cells

ESC-specific miRNA signatures have been described in both mouse and human cell lines [26,214,397,504]. Human embryonic stem cells (hESCs) show enrichment in a few miRNA groups: miRNAs from the miR-17 family, miRNAs from the chromosome 19 miRNA cluster, miRNAs from the miR-302 cluster, and miRNAs from the miR-371/373 cluster [89,122]. Most of these clusters are transcribed as polycistronic transcripts, meaning that two or more miRNAs are found on one transcript, suggesting common regulators and expression patterns. Moreover, the seed sequences of several of these ESC-enriched miRNAs are similar or identical, suggesting that they may target the same mRNA pool [504]. Some studies also found the miR-130 and miR-200 families to be enriched in hESCs [504]. Several miRNAs involved in regulating the ESC transcriptome and in the differentiation of ESC have been also described [31,536].

The goal of this analysis was to explore the expression patterns of specific miRNAs that are known to play crucial roles in the stemness and maintenance of the ESC profile, as well as those involved in ESC differentiation and regulation of the ESC transcriptome. The expectation was that miRNAs associated with stemness would exhibit reduced expression levels following differentiation induction, while miRNAs involved in differentiation processes and ESC transcriptome regulation would display increased expression. The expression levels of 168 mature miRNAs, originating from 91 miRNA genes, were investigated. A detailed list of these miRNAs can be found in Appendix Table 7.4.

Figure 4.33 displays heatmaps depicting the normalized expression levels of all identified miRNAs from the 168 across the five differentiation assays. The cluster memberships of the miRNAs are indicated on the right side of each heatmap. In the cluster column, a grey square signifies that the miRNA did not exhibit a fold change over 1.5 between two time points, indicating it was not considered deregulated and was not attributed to a cluster. Additional heatmaps with only the deregulated miRNAs and/or scaled and normalized can be found in Appendix Figures 7.10 through 7.12.

It should be noted that not all of the 168 miRNAs were detected, with varying numbers found in each differentiation assay: 19 in the hMSC adipogenesis, 18 in the hMSC chondrogenesis, 26 in the hMSC osteogenesis, 32 in the hNSC, and 31 in the HSkM differentiation assay. Overall, 41 of the 168 unique miRNAs were observed.
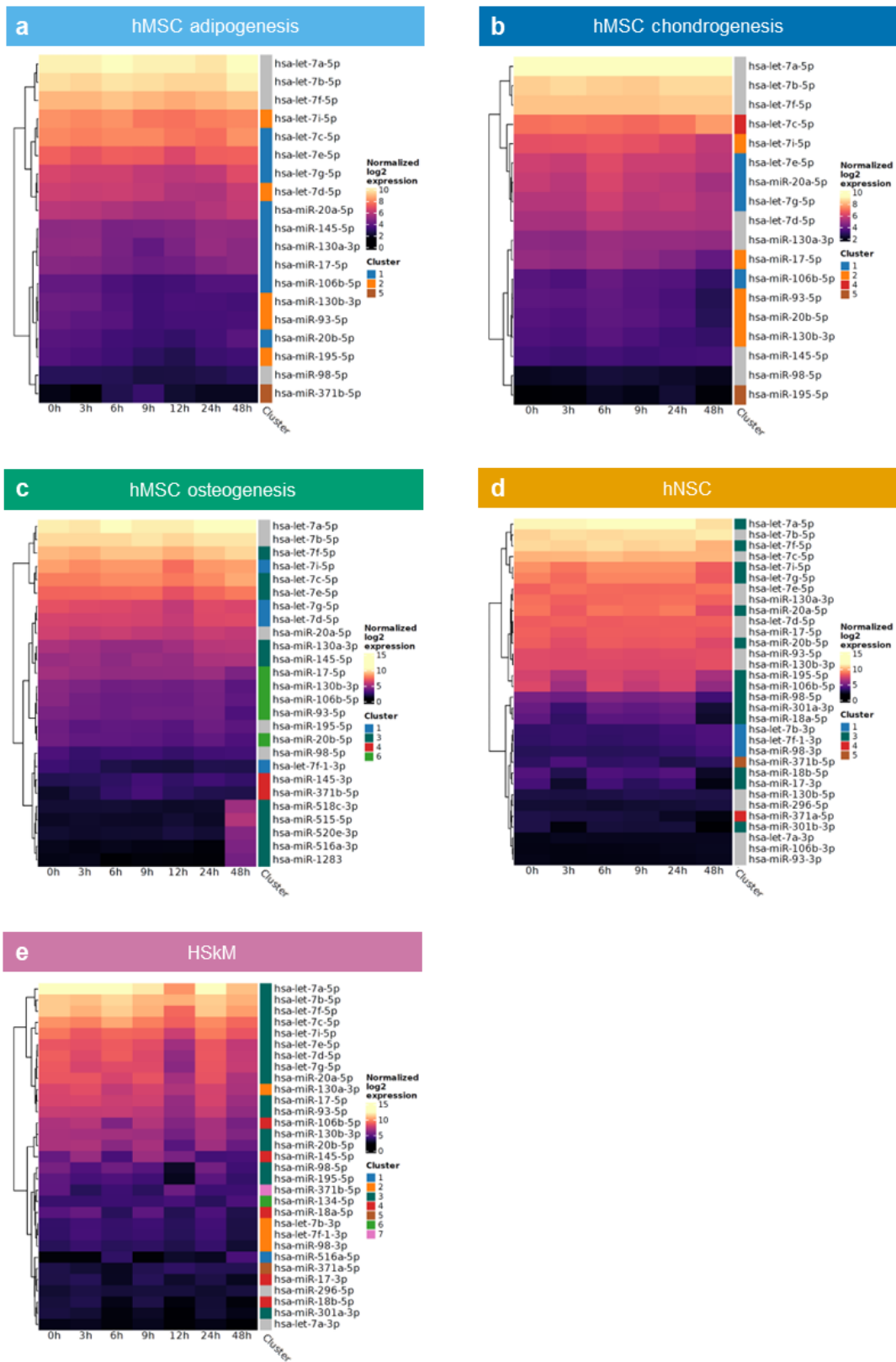
Figure 4.33: Heatmaps of the normalized expression levels of miRNAs known to be important in embryonic stem cells (ESCs) in the hMSC adipogenesis (a), chondrogenesis (b), osteogenesis (c), hNSC (d), and HSkM (e) differentiation assays. The cluster memberships of the miRNAs are shown at the right of each heatmap. A grey square in the cluster column indicates that the miRNA did not present a fold change over 1.5 between two time points.

Among the six groups of ESC-enriched miRNAs, four were observed in the analysis, specifically the miR-17 family, the chromosome 19 miRNA cluster, the miR-371/373 cluster, and the miR-130 family.

Five members of the miR-17 family were detected in all differentiation assays: hsa-miR-106b-5p, hsa-miR-17-5p, hsa-miR-20a-5p, hsa-miR-20b-5p, and hsa-miR-93-5p. Three other members were detected in the hNSC and HSkM differentiation assays (hsa-miR-17-3p, hsa-miR-18a-5p, and hsa-miR-18b-5p), while hsa-miR-106b-3p and hsa-miR-93-3p were only detected in the hNSC differentiation assay. All presented a downward trend, except four out of the five miRNAs detected in the hMSC adipogenesis assay (hsa-miR-106b-5p, hsa-miR-17-5p, hsa-miR-20a-5p, and hsa-miR-20b-5p), whose expression tended to increase, and three miRNAs that were more or less constantly expressed in the hNSC differentiation assay (hsa-miR-106b-3p, hsa-miR-93-5p, and hsa-miR-93-3p).

Members of the chromosome 19 miRNA cluster were detected five times in the hMSC osteogenesis assay (hsa-miR-1283, hsa-miR-515-5p, hsa-miR-516a-3p, hsa-miR-518c-3p, and hsa-miR-520e-3p) and once in the HSkM differentiation assay (hsa-miR-516a-5p), all with an upward trend in expression.

Two members of the miR-371/373 cluster were detected six times total in the hMSC adipogenesis, osteogenesis, hNSC, and HSkM differentiation assays: hsa-miR-371a-5p and hsa-miR-371b-5p. Their expression tended to increase in the earlier time points and then decrease, staying overall quite low.

The miR-130 family was detected in all five differentiation assays. The expression of hsa-miR-130b-3p decreased when it was deregulated, while hsa-miR-130a-3p showed an upward trend in expression in the hMSC adipogenesis and osteogenesis assays, and a downward trend in the HSkM differentiation assay. Additionally, hsa-miR-130b-5p was detected but not considered deregulated in the hNSC differentiation assay, with an increasing expression level. Furthermore, the expression of hsa-miR-301a-3p decreased in the hNSC and HSkM differentiation assays, as did the expression of hsa-miR-301b-3p in the HSkM differentiation assay.

Other miRNAs known to play a role in ESCs were detected as well. For example, hsa-miR-195-5p was detected in all five differentiation assays and considered deregulated everywhere except in the hMSC osteogenesis assay. Its expression was low in the other hMSC differentiation assays and tended to decrease overall, after peaks at the 6 h and 24 h time points in most assays.

Detected in the hNSC and HSkM differentiation assays, hsa-miR-296-5p presented an overall increasing trend.

In the hMSC adipogenesis and osteogenesis assays, the expression of hsa-miR-145-5p tended to increase, while it remained consistently high in the hMSC chondrogenesis assay, and it decreased in the HSkM differentiation assay. On the other hand, hsa-miR-145-3p was detected and deregulated only in the hMSC osteogenesis assay, where its expression increased at the last two time points.

Expression levels of the let-7 family were varied. All the members of this family that were detected in the HSkM differentiation assay decreased in expression, as did hsa-let-7i-5p in all assays and hsa-let-7g-5p and hsa-miR-98-5p in all assays except one (hMSC adipogenesis and osteogenesis respectively). However, expression levels in the hMSC differentiation assays increased for the most part. In the hNSC differentiation assay, five members of the let-7 family presented a downward trend, while six showed an upward trend in expression.

Some of the miRNAs known to be enriched in ESCs or to regulate their transcriptome could be detected in the differentiating stem cells characterized in this work. Interestingly, some miRNAs exhibited consistent trends across assays, while others displayed more diverse expression patterns, suggesting complex regulation during differentiation.

4.1.9.   The miR-29 family

A notable miRNA family in the 10 miRNAs that showed the strongest decrease across all time points was the hsa-miR-29 family. This family includes four members: hsa-miR-29a-3p, hsa-miR-29b-1-5p, hsa-miR-29b-3p, and hsa-miR-29c-3p. All of these miRNAs were found at least once in the top 10 decreased miRNAs, with hsa-miR-29b-1-5p found in the top 10 of the three hMSC and hNSC differentiation assays, and hsa-miR-29a-3p in the top 10 of the hMSC adipogenesis, chondrogenesis, and HSkM differentiation assays.

First, we investigated the cluster membership of each hsa-miR-29 family member and detected a striking result. In the three hMSC differentiation assays, all members belonged to the same cluster (clusters 2, 2, and 6 in the adipogenesis, chondrogenesis, and osteogenesis assay, respectively; see Table 4.2). In the hNSC and the HSkM differentiation assays, hsa-miR-29b-1-5p was the only one of the four miRNAs that belonged to another cluster, but with a much lower membership score than its family members counterparts. As expected, since they were among the 10 miRNAs that exhibited the strongest decrease, all patterns of expression showed a downward trend, except for the cluster to which hsa-miR-29b-1-5p belonged in the hNSC differentiation assay (cluster 5; Table 4.2).

Table 4.2: Cluster membership of the members of the hsa-miR-29 family. For each differentiation assay, the clusters to which the members of the hsa-miR-29 family belong are indicated with their respective membership scores and the corresponding cluster patterns.

	hMSC adipogenesis		hMSC chondrogenesis		hMSC osteogenesis		hNSC		HSkM	
	Cluster	Membership	Cluster	Membership	Cluster	Membership	Cluster	Membership	Cluster	Membership
hsa-miR-29b-1-5p	2	0,722922348	2	0,428989363	6	0,522732077	5	0,285257052	2	0,507328898
hsa-miR-29a-3p	2	0,638344543	2	0,836853453	6	0,672914252	3	0,974740907	4	0,747804413
hsa-miR-29b-3p	2	0,867756926	2	0,749747678	6	0,533980225	3	0,930771498	4	0,903036666
hsa-miR-29c-3p	2	0,887177739	2	0,887386585	6	0,830205811	3	0,982691670	4	0,669996689
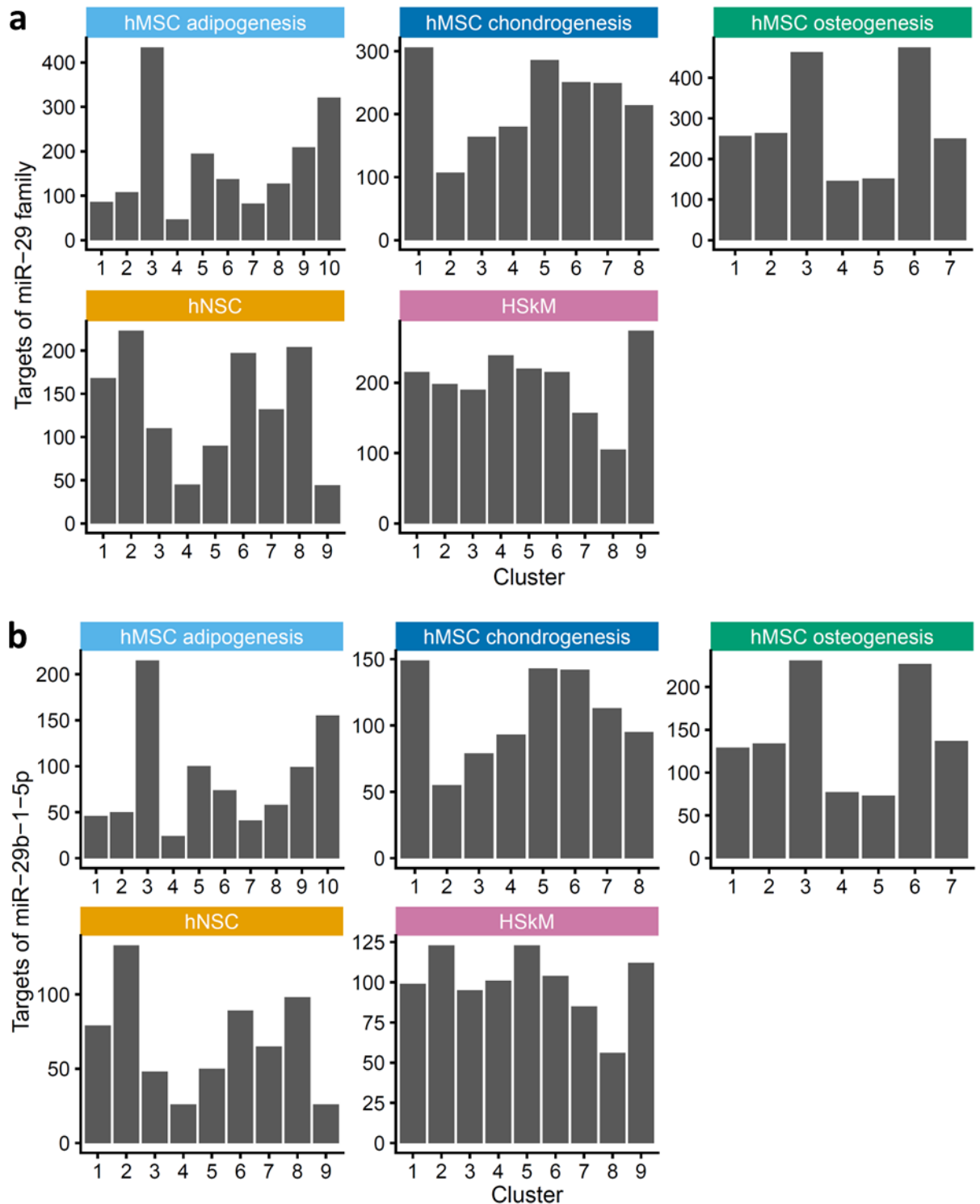
Figure 4.34: Cluster membership of targets of hsa-miR-29 family members. For each differentiation assay, the clusters to which the targets of hsa-miR-29 family members (**a**) or the targets of hsa-miR-29b-1-5p (**b**) belong are shown.

Next, potential targets of the hsa-miR-29 family were searched using the online tool mirDIP, which yielded 1 098 targets with high or very high confidence for hsa-miR-29a-3p,

922 for hsa-miR-29b-1-5p, 797 for hsa-miR-29b-3p, and 786 for hsa-miR-29c-3p. Figure 4.34 shows the cluster membership of all these targets in each differentiation assay (a), and the cluster membership of all hsa-miR-29b-1-5p targets (b). These cluster membership profiles were similar for both sets of targets. In both cases, some clusters were overrepresented, like cluster 3 in the hMSC adipogenesis assay, clusters 3 and 6 in the hMSC osteogenesis assay, or cluster 2 in the hNSC differentiation assay.

In the hMSC adipogenesis assay, all members of the hsa-miR-29 family belonged to cluster 2, which was characterized by a downward trend from 0 h to 9 h followed by a plateau of expression (see Figure 4.7 a). The gene clusters that included most of the hsa-miR-29 family targets and most of the hsa-miR-29b-1-5p targets were clusters 3, 10, 9, and 5 in descending order (see Figure 4.34). All four gene clusters showed a strong change of expression between 9 h and 12 h, increasing in all except gene cluster 5. In addition, as shown in Figure 4.13, miRNA cluster 2 was strongly associated with gene cluster 10.

In the hMSC chondrogenesis assay, cluster 2, to which the members of the hsa-miR-29 family belonged, showed a plateau of expression from 0 h to 9 h, followed by a sharp decrease of expression at the 24 h and 48 h time points (see Figure 4.7 b). The gene clusters with the highest proportion of both the hsa-miR-29 family and hsa-miR-29b-1-5p targets were clusters 1, 5, 6, and 7 in descending order (see Figure 4.34). Gene clusters 1 and 6 showed expression patterns similar to miRNA cluster 2, which was unexpected, while gene clusters 7 and 5 displayed an upward trend, which was more expected. In Figure 4.15, miRNA cluster 2 interacted strongly with clusters 7 and 8.

In the hMSC osteogenesis assay, all members of the hsa-miR-29 family belonged to miRNA cluster 6, which displayed a slight and steady decrease of expression from 0 h to 12 h, and a sharp decrease between 24 h and 48 h (see Figure 4.7 c). Most of the hsa-miR-29 family and hsa-miR-29b-1-5p targets belonged to gene clusters 3 and 6 (see Figure 4.34). These two clusters showed greatly decreased expression at 12 h, followed by an increase at the 24 h and 48 h time points. The patterns of these clusters were reflected in gene clusters 4 and 5, which included the smallest proportion of the hsa-miR-29 family and hsa-miR-29b-1-5p targets.

In the hNSC differentiation assay, three members of the hsa-miR-29 family belonged to miRNA cluster 3, which was characterized by two sharp peaks of decreased expression, at 3 h and 48 h (see Figure 4.7 d). The gene clusters with the highest proportion of hsa-

miR-29 family targets were clusters 2, 8, 6, and 1 in descending order (see Figure 4.34). Clusters 6 and 1 both showed peaks of increased expression at 3 h and 48 h (highest at 3 h in cluster 6 and 48 h in cluster 1), but the pattern of expression of gene cluster 8 did not correlate with that of miRNA cluster 3, and gene cluster 2 also presented a strongly decreased expression at 48 h. The miRNA cluster 5, which included hsa-miR-29b-1-5p, albeit with a very low membership score of 0.29, had a pattern of expression that reflected that of miRNA cluster 3 and gene cluster 6 (see Figures 4.7 d and 4.8 d).

In the HSkM differentiation assay too, hsa-miR-29b-1-5p did not belong to the same miRNA cluster as its family members, but to the miRNA cluster 2 (with a membership score of 0.51). This cluster showed an alternating increase and decrease of expression, with two strong peaks of decreased expression at 12 h and 48 h (see Figure 4.7 e). Gene clusters 2, 5, and 9 included the highest proportion of hsa-miR-29b-1-5p targets (see Figure 4.34). The expression patterns of these gene clusters were quite different, but they each anti-correlated well with the pattern of miRNA cluster 2 during a portion of the timeframe studied: 6 h to 24 h for gene cluster 2, 12 h to 24 h for gene cluster 5, and 0 h to 9 h and 24 h to 48 h for gene cluster 9 (see Figures 4.7 e and 4.8 e). This last cluster was expected to interact strongly with both miRNA clusters 2 and 4, as shown in Figure 4.18. The three remaining members of the hsa-miR-29 family (hsa-miR-29a-3p, hsa-miR-29b-3p, and hsa-miR-29c-3p) belonged to miRNA cluster 4 (with membership scores from 0.67 to 0.90), whose expression pattern was similar to that of miRNA cluster 2, albeit with stronger peaks of expression at earlier time points. The gene clusters containing the highest numbers of hsa-miR-29 family targets were gene clusters 9 and 4 (see Figure 4.34). The expression pattern of gene cluster 9 again anti-correlated quite well with that of miRNA cluster 4, as did that of gene cluster 4 with its sharp decrease of expression from 6 h to 12 h (see Figure 4.8 e).

The data obtained from searching for enrichment in particular biological pathways (4.1.4) were extracted for each of the previously mentioned clusters and compared in each differentiation assay. Figures 4.35 through 4.40 are grid plots showing the distribution of these pathways among the databases and broad categories considered in the hMSC adipogenesis (see Figure 4.35), hMSC chondrogenesis (see Figure 4.36), hMSC osteogenesis (see Figure 4.37), hNSC (see Figure 4.38) and HSkM differentiation assays (see Figures 4.39 and 4.40). The size of each circle corresponds to the number of pathways at each intersection of the grid, while the colors indicate the enriched cluster, as shown in the legend on the right.

In the hMSC adipogenesis assay, miRNA cluster 2 was enriched in pathways from the broad categories of "cell cycle & differentiation", "extracellular matrix", and "immunity" (see Figure 4.35). The four associated gene clusters, 3, 5, 9, and 10 also showed enrichment for the broad categories "cell cycle & differentiation" and "immunity", but also for "membrane" and "nucleic acid binding".
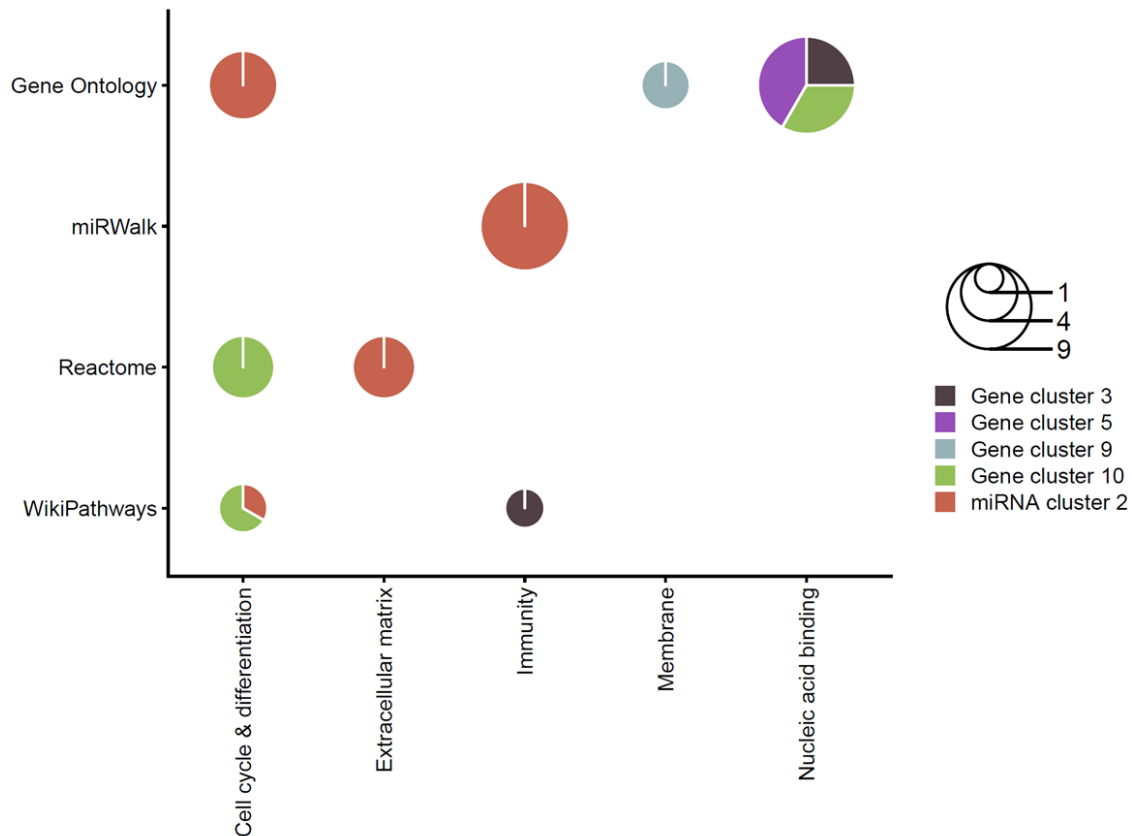
Figure 4.54: Enrichment of biological pathways in the miRNA cluster that comprised the members of the hsa-miR-29 family (cluster 2) and gene clusters enriched in hsa-miR-29 family targets in the hMSC adipogenesis assay. Databases are listed on the y-axis, and broad biological pathway categories are listed on the x-axis. The size of each circle indicates the number of pathways at each intersection of the grid, and the colors represent the cluster that is enriched, as shown by the legend on the right.

In miRNA cluster 2 of the hMSC chondrogenesis assay, the over-represented pathways belonged to the broad categories "cell cycle & differentiation", "DNA damage response", and "immunity". Two of the four gene clusters with the highest numbers of hsa-miR-29 family targets, clusters 5 and 6, displayed enrichment only in kinase and oxidoreductase activity, respectively, and were therefore not shown in Figure 4.36. The other two gene clusters (1 and 7) were enriched in pathways from the broad categories "cell cycle & differentiation" (cluster 1), "DNA damage response" (cluster 1), and "extracellular matrix" (cluster 7).
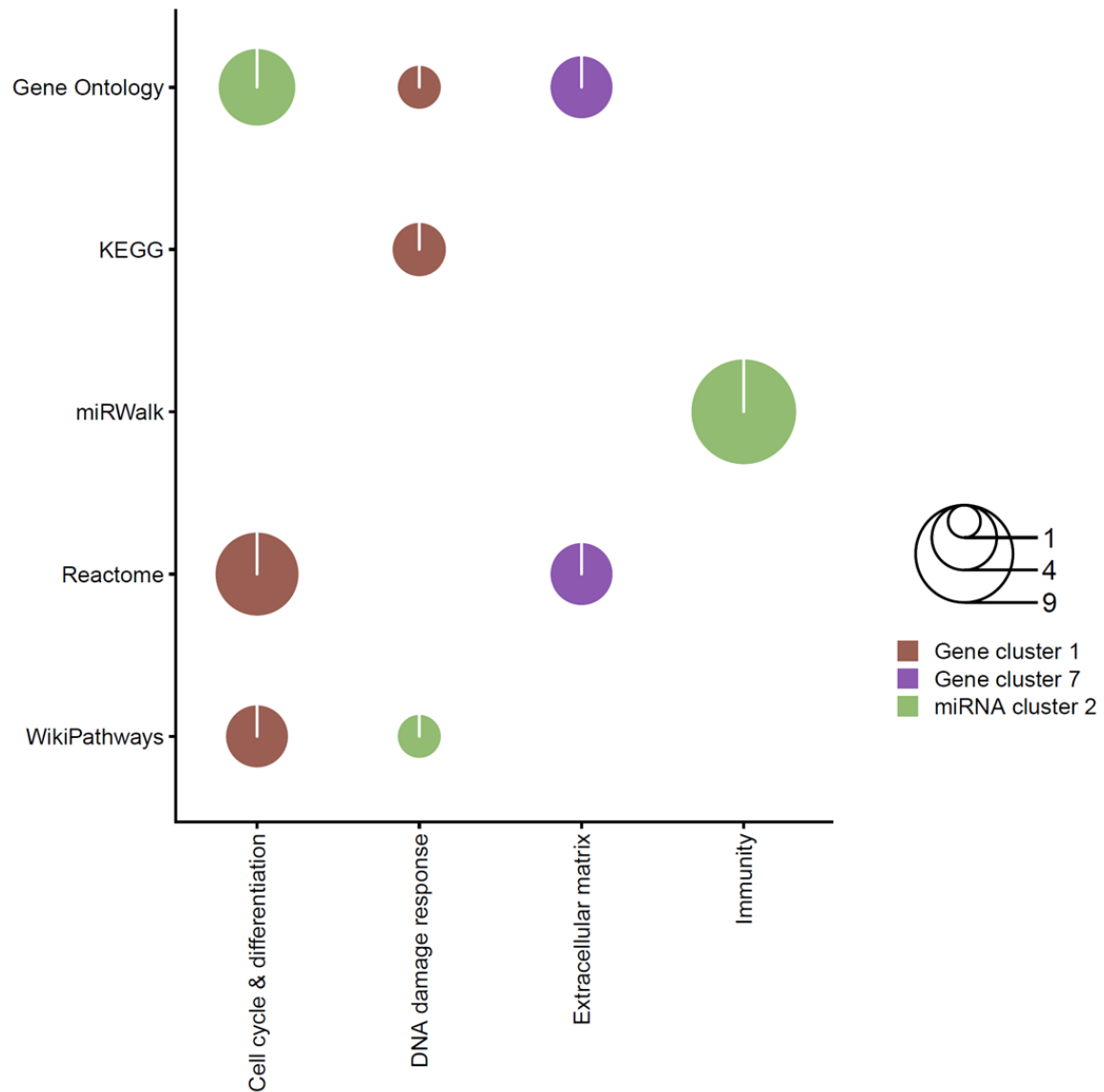
Figure 4.36: Enrichment of biological pathways in the miRNA cluster that comprised the members of the hsa-miR-29 family (cluster 2) and gene clusters enriched in hsa-miR-29 family targets in the hMSC chondrogenesis assay. Databases are listed on the y-axis, and broad biological pathway categories are listed on the x-axis. The size of each circle indicates the number of pathways at each intersection of the grid, and the colors represent the cluster that is enriched, as indicated by the legend on the right.

In the hMSC osteogenesis assay, miRNA cluster 6 was enriched for pathways from the broad categories "cell cycle & differentiation", "immunity", and "transcription". The latter two categories were also overrepresented in the associated gene clusters 3 and 6, as well as the "translation" category (see Figure 4.37).
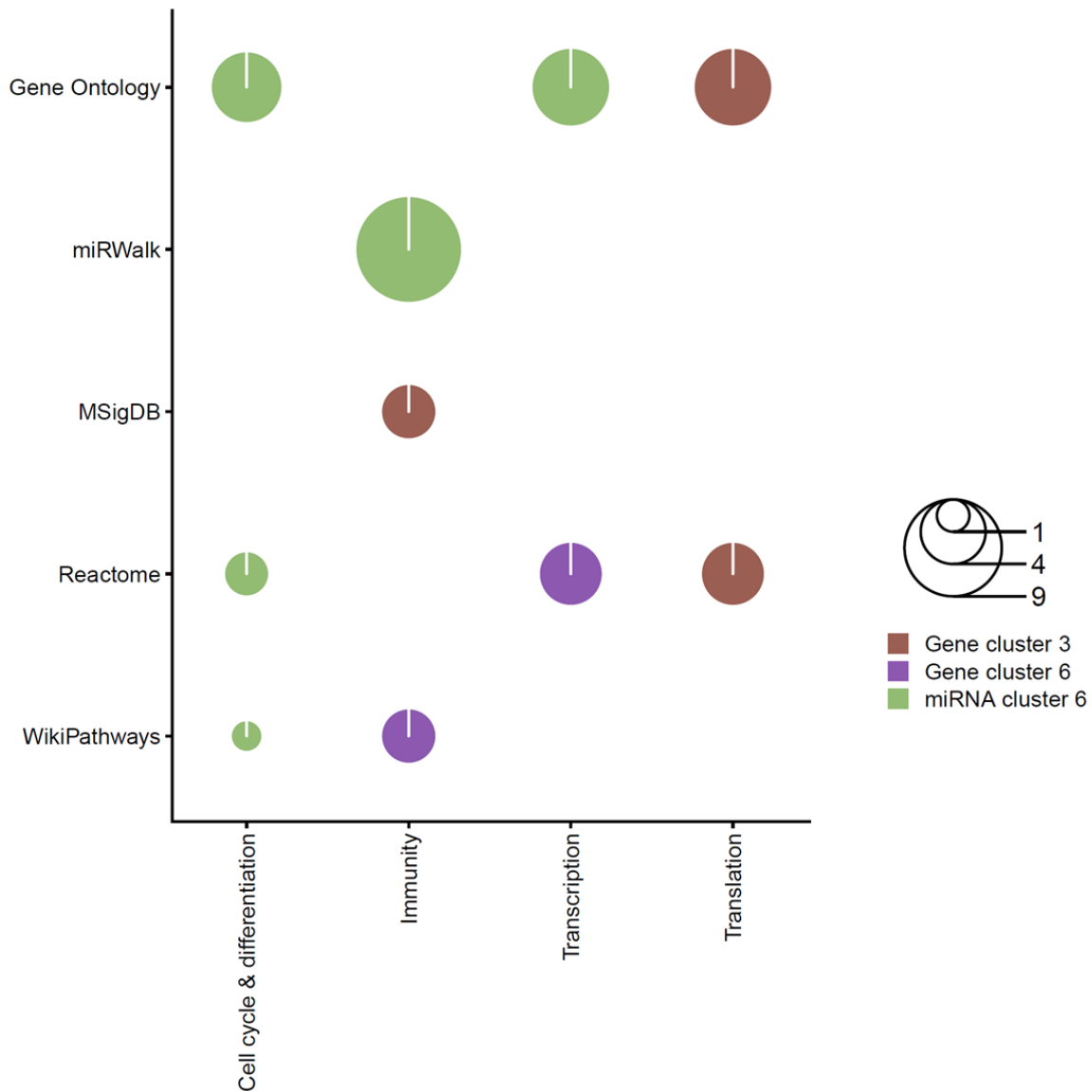
Figure 4.37: Enrichment of biological pathways in the miRNA cluster that comprised the members of the hsa-miR-29 family (cluster 6) and gene clusters enriched in hsa-miR-29 family targets in the hMSC osteogenesis assay. Databases are listed on the y-axis, and broad biological pathway categories are listed on the x-axis. The size of each circle indicates the number of pathways at each intersection of the grid, and the colors represent the cluster that is enriched, as indicated by the legend on the right.

In the hNSC differentiation assay, the miRNA cluster to which hsa-miR-29b-1-5p belonged, cluster 5, did not show any particular enrichment, in contrast to miRNA cluster 3, which included the other hsa-miR-29 family members. This cluster was enriched in pathways from the broad categories "cell cycle & differentiation", "immunity", and "membrane" (see Figure 4.38). These three broad categories were also overrepresented in gene clusters 1, 6, and 8, as is the category "transcription", which was also the only

category enriched in gene cluster 2. Strikingly, gene cluster 6 also showed enrichment in the category "adipogenesis" (with four overrepresented pathways), which was unexpected in this particular assay.
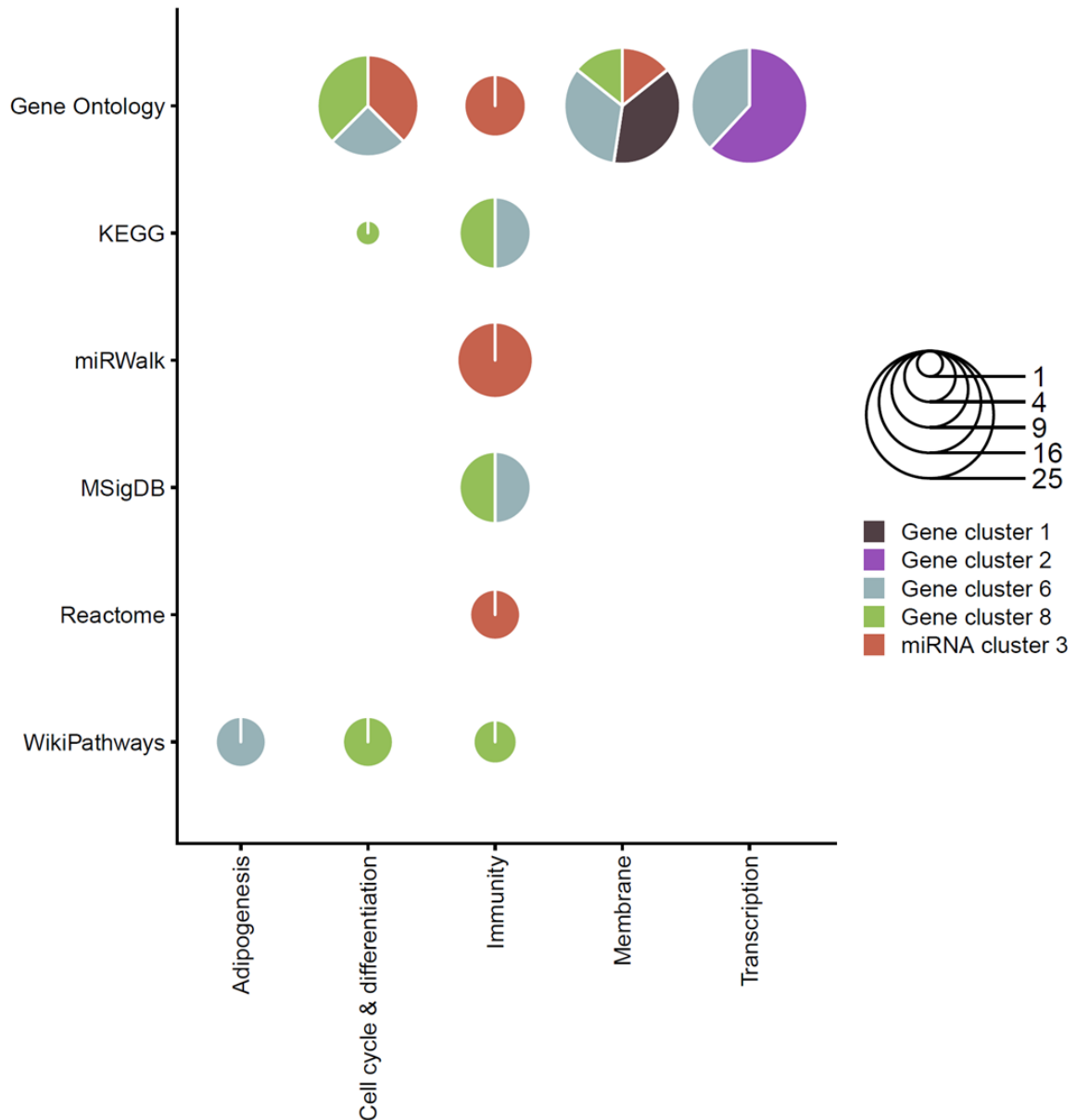
Figure 4.38: Enrichment of biological pathways in the miRNA cluster that comprised most members of the hsa-miR-29 family (cluster 3) and gene clusters enriched in hsa-miR-29 family targets in the hNSC differentiation assay. Databases are listed on the y-axis, and broad biological pathway categories are listed on the x-axis. The size of each circle indicates the number of pathways at each intersection of the grid, and the colors represent the cluster that is enriched, as indicated by the legend on the right.

In the HSkM differentiation assay, hsa-miR-29b-1-5p belonged to miRNA cluster 2, in which pathways from the broad category "translation" were overrepresented (see Figure 4.39). Three gene clusters, 2, 5, and 9, were enriched in hsa-miR-29b-1-5p targets. Gene cluster 2 was not particularly enriched in pathways, whereas gene cluster 5 was enriched in pathways from the broad categories "extracellular matrix" and "membrane". Gene cluster 9 was highly enriched in pathways from the "myogenesis" category.
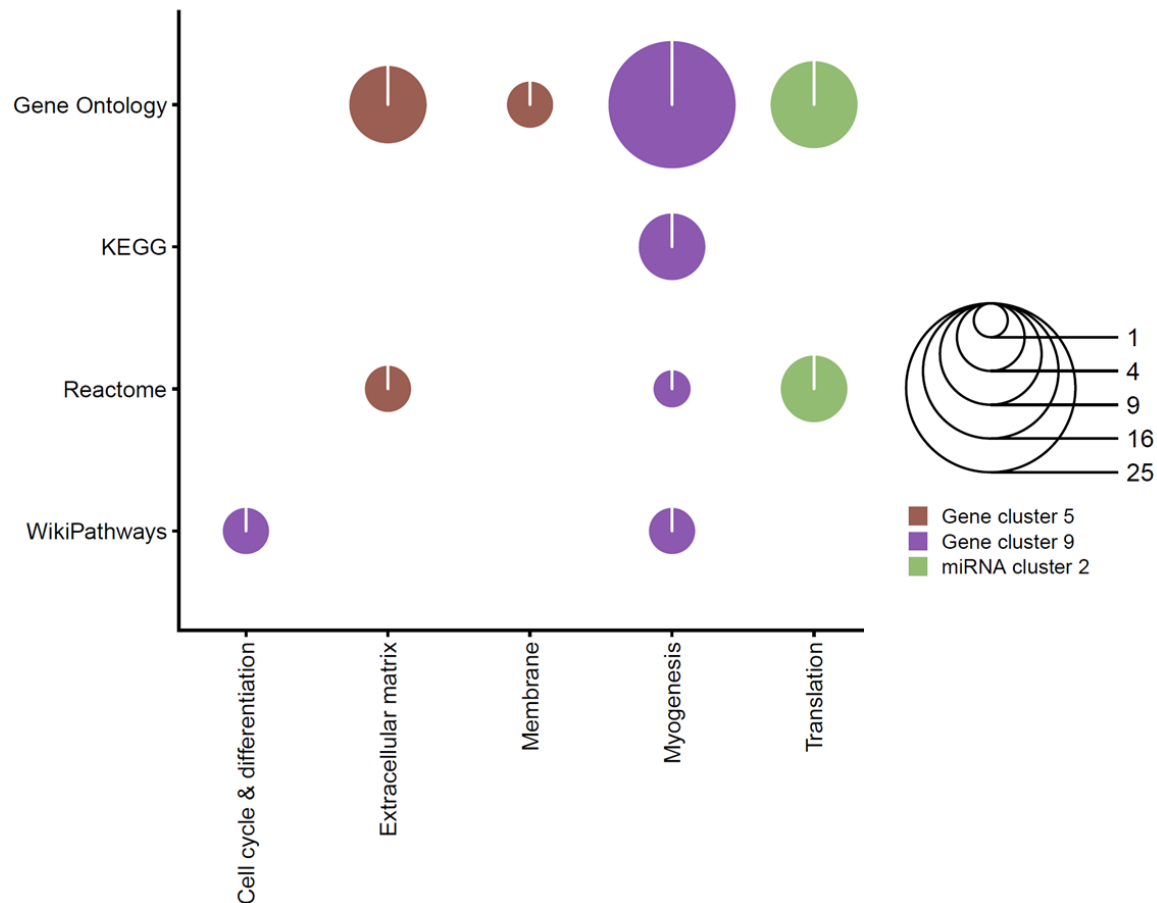
Figure 4.39: Enrichment of biological pathways in the miRNA cluster that comprised hsa-miR-29b-1-5p (cluster 2) and gene clusters enriched in hsa-miR-29b-1-5p targets in the HSkM differentiation assay. Databases are listed on the y-axis, and broad biological pathway categories are listed on the x-axis. The size of each circle indicates the number of pathways at each intersection of the grid, and the colors represent the cluster that is enriched, as indicated by the legend on the right.

The other three members of the hsa-miR-29 family belonged to miRNA cluster 4, in which pathways from the categories "cell cycle & differentiation", "immunity", "myogenesis", and "transcription" were overrepresented (see Figure 4.40). The associated gene clusters 4 and 9 were enriched in pathways from the same broad categories: "immunity" and "transcription" for gene cluster 4, and "cell cycle & differentiation" and "myogenesis" for gene cluster 9.
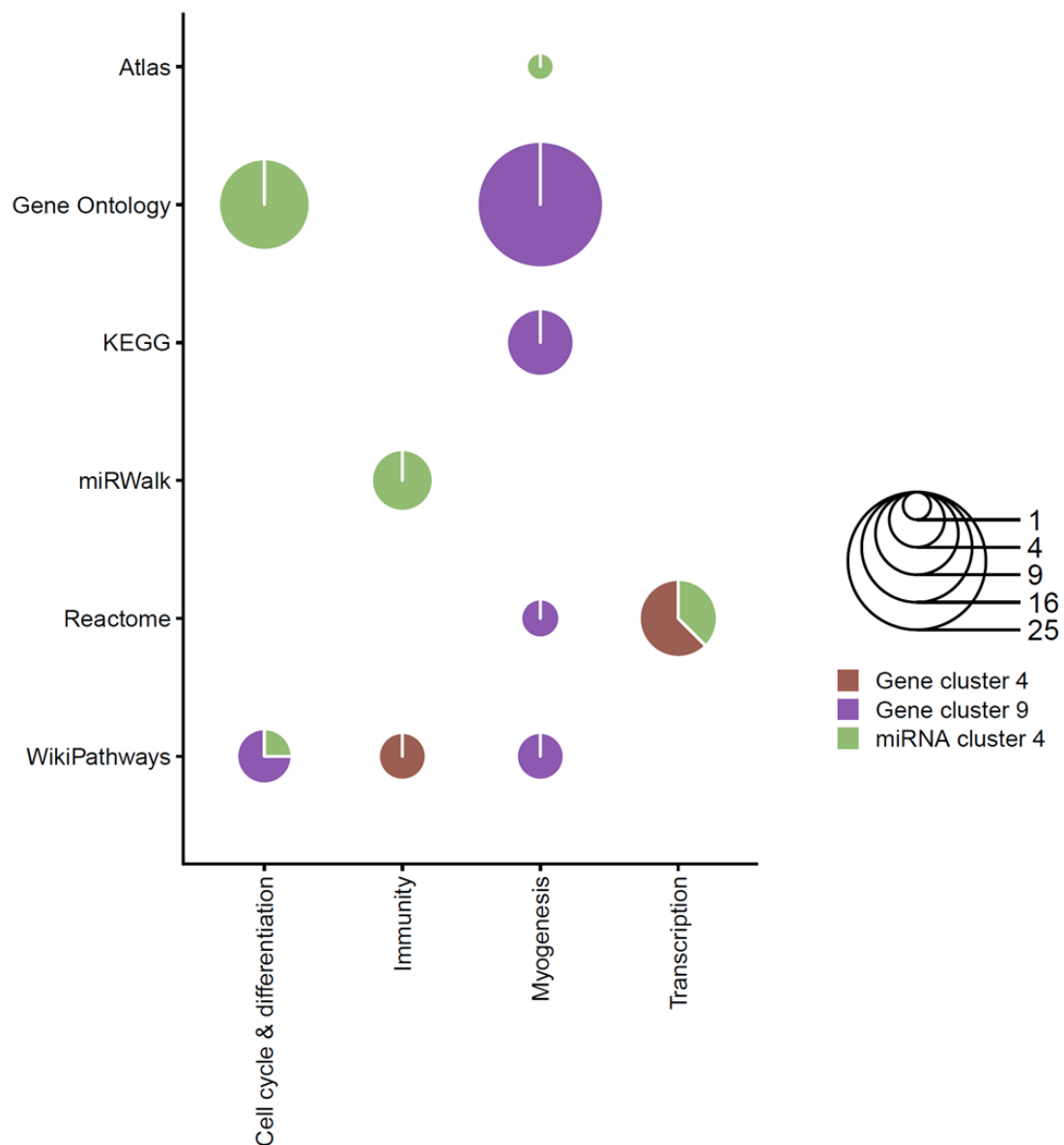
Figure 4.40: Enrichment of biological pathways in the miRNA cluster that comprised most members of the hsa-miR-29 family (cluster 4) and gene clusters enriched in hsa-miR-29 family targets in the HSkM differentiation assay. Databases are listed on the y-axis, and broad biological pathway categories are listed on the x-axis. The size of each circle indicates the number of pathways at each intersection of the grid, and the colors represent the cluster that is enriched, as indicated by the legend on the right.

The Venn diagram in Figure 4.41 shows which target from the high or very high confidence mirDIP sets was shared by members of the hsa-miR-29 family. While hsa-miR-29b-3p and hsa-miR-29c-3p did not have specific targets, 238 and 791 mRNAs were targeted only by hsa-miR-29a-3p and hsa-miR-29b-1-5p, respectively. The highest degree of overlap was observed among the shared targets of hsa-miR-29a-3p, hsa-miR-29b-3p, and hsa-miR-29c-3p, accounting for 657 mRNAs. However, it is worth noting that 94 mRNAs are still targeted by all members of the hsa-miR-29 family.
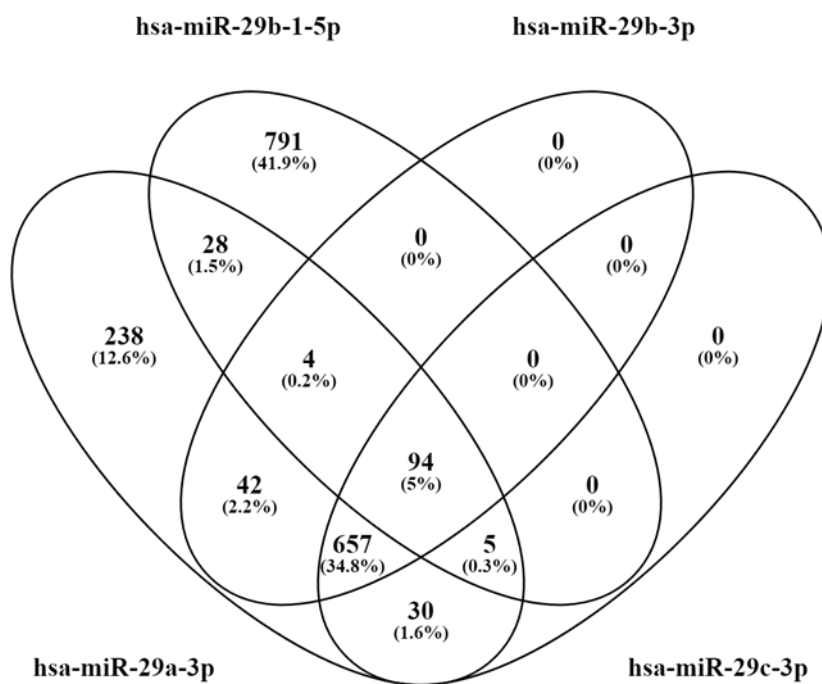
Figure 4.41: Venn diagram of the distribution of mirDIP predicted targets of hsa-miR-29 family members. Created with Venny 2.1.

Enriched pathways in this set of 94 genes were searched for by overrepresentation analysis using the Gene Trail 3.2 online tool. Figure 4.42 shows the summarized distribution of these enriched pathways. In the five databases (Reactome, KEGG, Gene Ontology Biological Processes, Gene Ontology Molecular Function, WikiPathways), a total of 47 pathways were involved directly in transcription processes, and 35 could be linked to either organ development, stem cell differentiation, cell proliferation or aging.
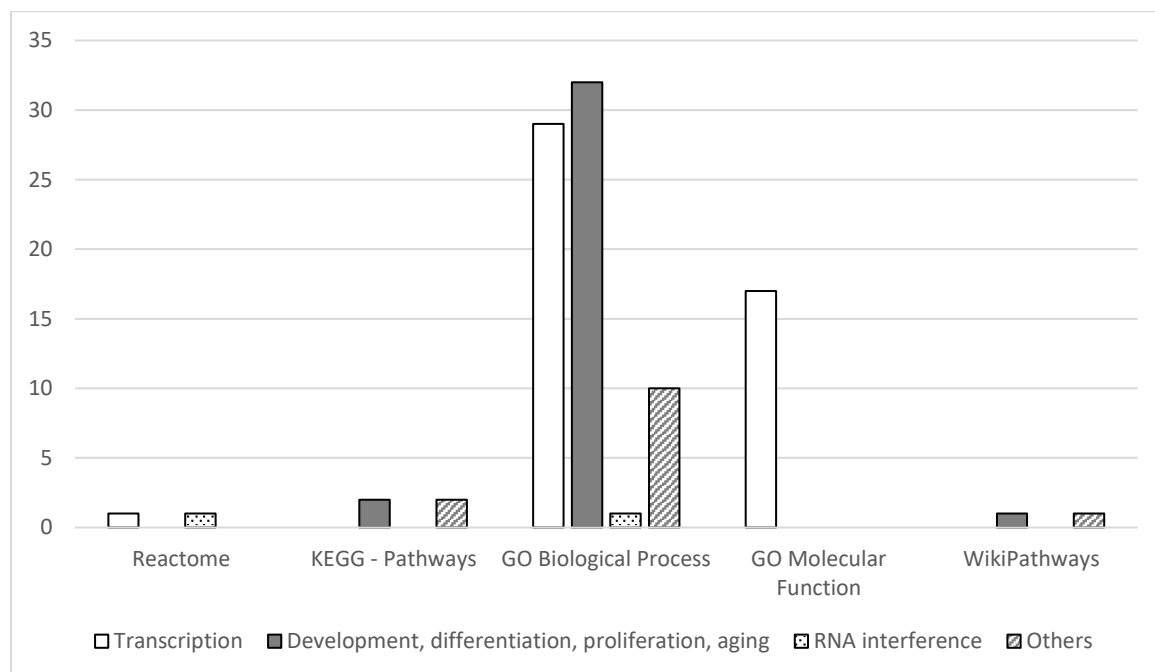
Figure 4.42: Distribution of enriched pathways from the set of 94 mRNAs predicted to be targeted by all members of the hsa-miR-29 family. Over-representation analysis was performed with Gene Trail 3.2.

The miR-29 family has also been shown to be involved in aging [274,561]. These two studies investigated data from the Tabula Muris Senis or "Mouse Ageing Cell Atlas", a comprehensive resource that focuses on bulk and single-cell RNA sequencing data from various tissues and organs of mice over the aging process [6]. Both studies noted that members of the mmu-miR-29 family had an increase in expression with age in various tissues. When plotting the miR-29 data of the Tabula Muris Senis for the seven organs or tissues corresponding to the differentiation processes studied in this thesis, the same trend was observed. Figure 4.43 shows a selection of these time-resolved expression data, and the others can be found in Appendix Figure 7.13.
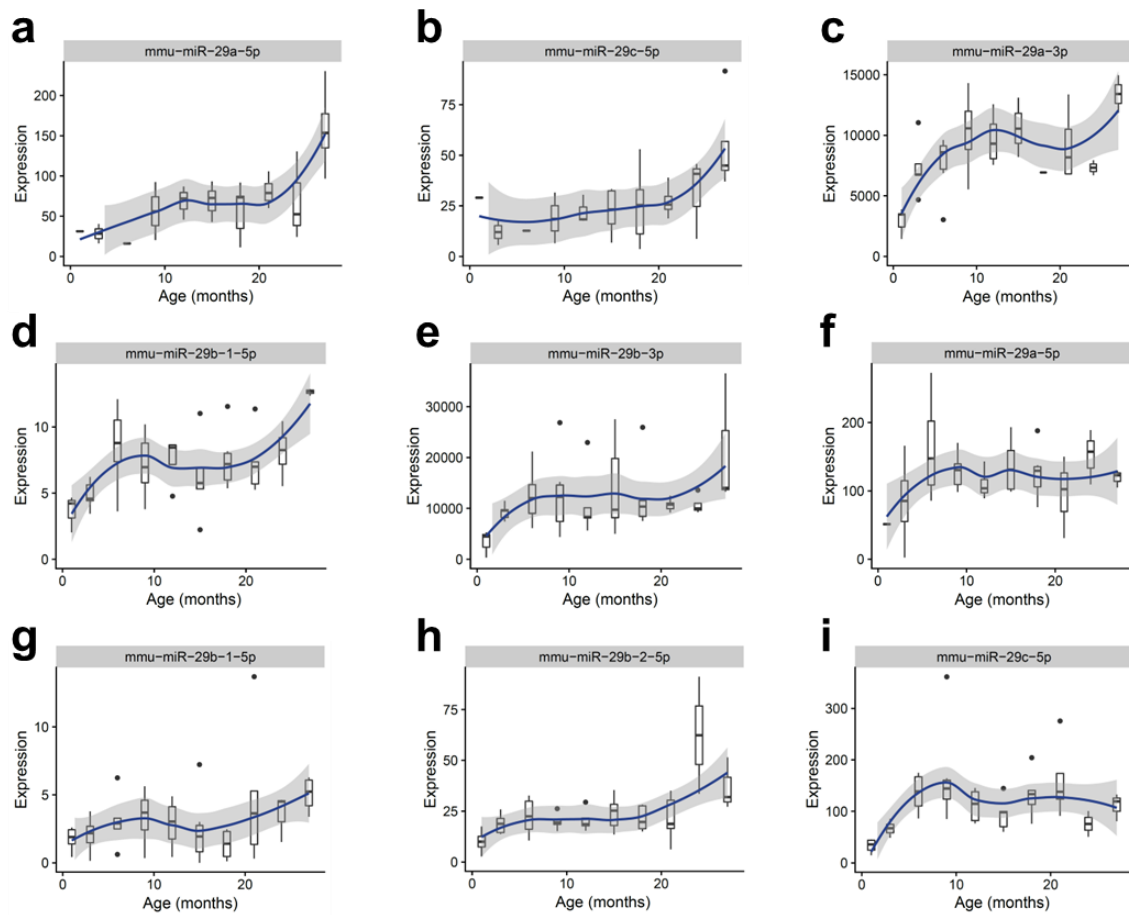
Figure 4.43: Selected time-resolved boxplots of the expression levels of members of the mmu-miR-29 family in various organs or tissues. **a** and **b** are from the brown adipose tissue (BAT), **c** from the gonadal adipose tissue (GAT), **d** and **e** from the marrow adipose tissue (MAT), **f** from the subcutaneous tissue (SCAT), **g** from the bone, and **h** and **i** from the skeletal limb muscle. The data were obtained from the Tabula Muris Senis dataset. The line was fitted with a loess formula (s.e. 95%).

Kern and colleagues also noted that their interpretation of the data supported the theory that the miR-29 family would participate in the inhibition of adipogenesis, a finding consistent with the results of the present work [274].

Overall, the hsa-miR-29 family appears to play a common, possibly redundant, role during the early differentiation of the studied stem cells.

4.2. Re-replication

*Some results of this dissertation work have already been published within the framework of a publication ("*A Temporary Pause in the Replication Licensing Restriction Leads to Re-replication during Early Human Cell Differentiation*") in the scientific journal* Cells [389].

4.2.1. Preliminary work

To investigate the possibility of re-replication as a mechanism for generating gene amplifications in differentiating stem cells, it was decided to use the molecular combing method in conjunction with thymidine analogs. The method called "molecular combing" was first published in 1994 [30,573]. It allows the combing of DNA fibers via a receding meniscus, resulting in a series of parallel and uniformly stretched single DNA molecules. Combined with sequential pulses of thymidine analogs, this method makes it possible to study replication dynamics. The thymidine analogs are incorporated into the newly replicated DNA, allowing it to be distinguished from the template DNA. If thymidine analogs are administered to cells only during successive time periods, some temporal discrimination is possible. In particular, in normal replication events as in Figure 4.44 a, the thymidine analog tracts are distinct from one another, stained red for EdU and stained green for CldU. In the case of re-replication events as in Figure 4.44 b, the thymidine analogs would be incorporated into the newly formed DNA at the locus of the replication origin at each activation, so that both thymidine analogs would be incorporated in case the origin is fired during both pulse treatments. The tracts would then overlap, producing yellow on merge images.
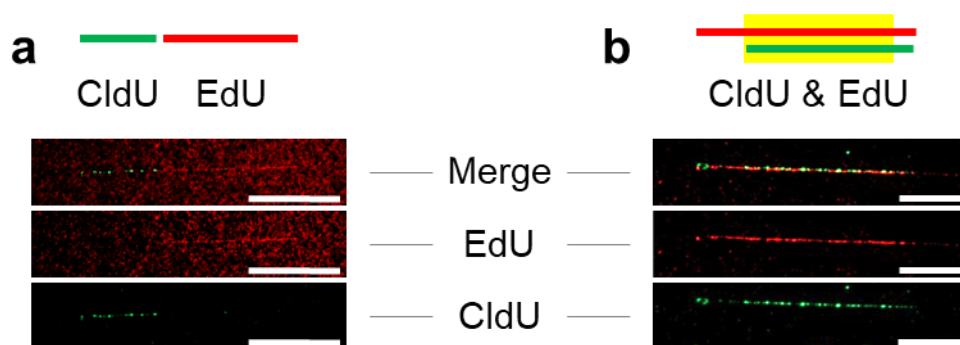
Figure 4.44: Examples of tracts obtained with thymidine analogs and molecular combing in HSkM cells. A normal replication event is displayed on **a** (HSkM 1 h differentiation assay), and a re-replication event is shown in **b** (HSkM 2 h differentiation assay). CldU-containing DNA is stained green, EdU-containing DNA in red, with the merged image at the top, followed by the EdU and the CldU staining. The scale bars correspond to 20 (**a**) and 10 μm (**b**).

Spontaneously differentiating HSkMs and hMSCs undergoing chondrogenesis were used to study re-replication with proliferating HSkM and hMSC cells serving as negative controls. Cells were allowed to differentiate for a predetermined period (0 to 7 hours), then were pulse-labeled. After harvesting and processing, DNA fibers were combed.

To ensure that the quality of the combed fibers was sufficient for subsequent experiments, one test coverslip was stained with YOYO-1, a green intercalating dye that binds mainly to double-stranded DNA. Example results of this staining are shown in Figure 4.45.
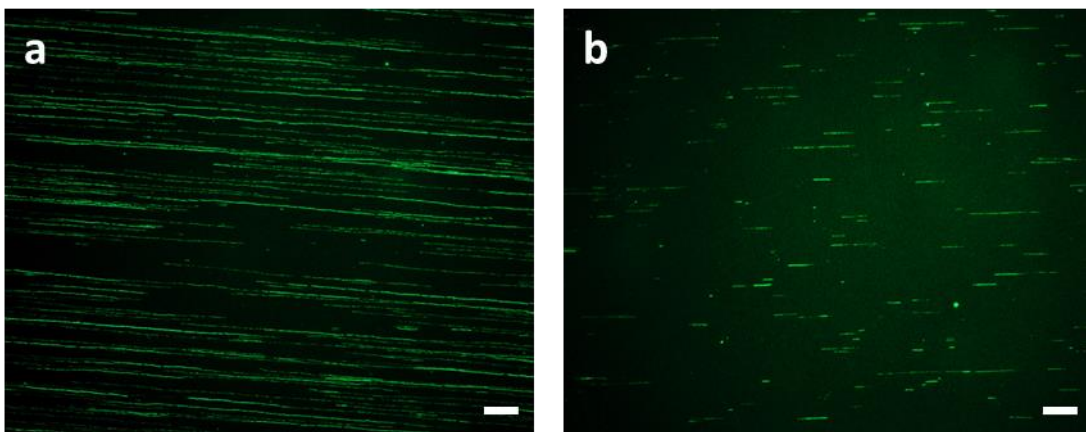
Figure 4.45: Two representative examples of YOYO-1 staining on DNA fibers from the HSkM 4 h differentiation assay, prepared with molecular combing. In **a**, the DNA fibers are longer and more numerous than in **b**. Scale bars correspond to 20 µm.

Several problems were encountered in establishing the staining protocol. As described in the literature, the two thymidine analogs initially used for these experiments were IdU (2'-deoxy-5-iodouridine) and CldU (5-chloro-2'-deoxyuridine). Both were stained by immunofluorescence, but the IdU antibody used was not specific enough and also bound to CldU. A stringency buffer wash between the antibodies directed against CldU and IdU was tested, without success.

To overcome this problem, it was decided to use a combination of EdU (5-ethynyl-2′-deoxyuridine) together with CldU. EdU is stained with a Click-iT® reaction that adds an Alexa Fluor® azide to the analog, making it fluorescent, but also allowing further immunofluorescence staining, which was still the method of choice for CldU.

Figure 4.46 shows that there is no cross-reaction between the two stainings, as the DNA fibers containing only CldU were not colored red by the EdU Click-iT staining (a), and vice versa for the EdU-containing fibers (b).
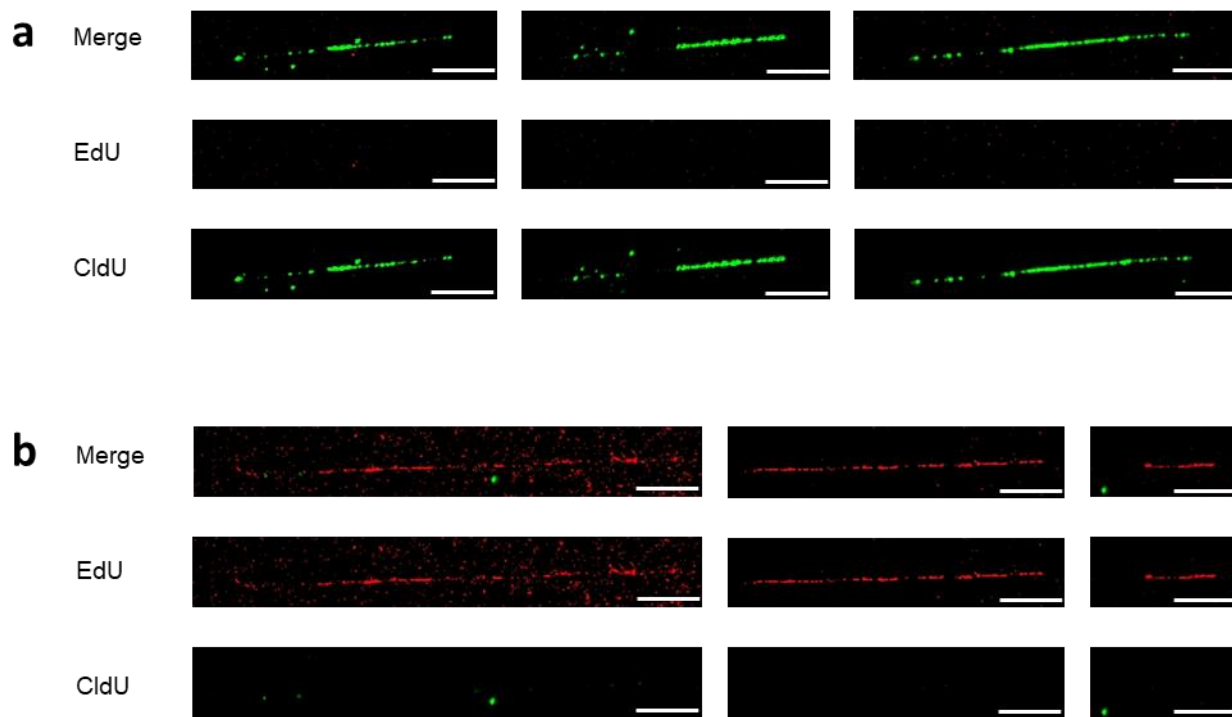
Figure 4.46: Representative images of DNA fibers obtained by molecular combing, containing one type of thymidine analog (CldU, in **a**, or EdU, in **b**) but stained for both. Each fiber is shown three times, with the merged image at the top, followed by EdU and CldU staining. Scale bars correspond to 10 μm.

DNA counterstaining with the standard intercalating dye DAPI (4′,6-diamidino-2-phenylindole, maximum emission at 461 nm) is not recommended with combed DNA fibers, due to the dimness of the dye. DNA staining by immunofluorescence was tested but the antibodies chosen did not allow sufficient brightness for this work.

Instead, the three filters of the confocal fluorescence microscope were used unconventionally: the blue filter, usually associated with DNA counterstaining, was used for immunofluorescent detection of CldU (secondary antibody coupled with Alexa350®, which has a maximum emission at 442 nm), and DNA was stained with the intercalating dye YOYO™-1, which fluoresces green (maximum emission at 508 nm). However, in the following pictures, the DNA counterstain is artificially rendered blue for standardization purposes and the CldU stain is green.

4.2.2. Qualitative analysis in differentiating HSkMs

Previous work [151] has shown that stem cells exhibit gene amplifications during the first 24 h after induction of differentiation. Therefore, it was hypothesized that the mechanism by which these gene amplifications occur is re-replication. To examine possible re-replication events during early stem cell differentiation in a time-resolved manner, it was decided to treat HSkM cells with thymidine analog pulses in 1-hour increments 0 h to 7 h after thawing (two biological replicates; see Figure 4.47). Because most HSkM cells begin differentiation right after thawing, these time points ensured that the first replication event of the differentiating stem cells would be captured.
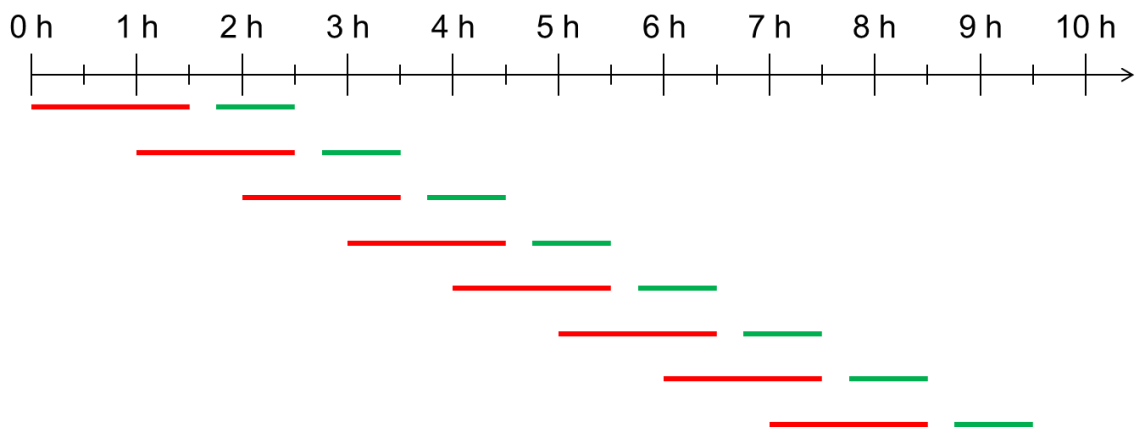
Figure 4.47: Schematic of the EdU and CldU pulse treatments, started at eight different time points, ranging from 0 h to 7 h after differentiation induction in HSkM cells.

In cells pulse-treated 0 h, 1 h, and 7 h after thawing (see Figure 4.48), long stretches of EdU-stained (red) DNA and smaller CldU-stained (green) stretches could be observed, sometimes at intervals that undoubtedly indicate normal replication events, as in Figure 4.48 b. No overlapping red and green stretches were observed, so no re-replication event could be described for these time points.
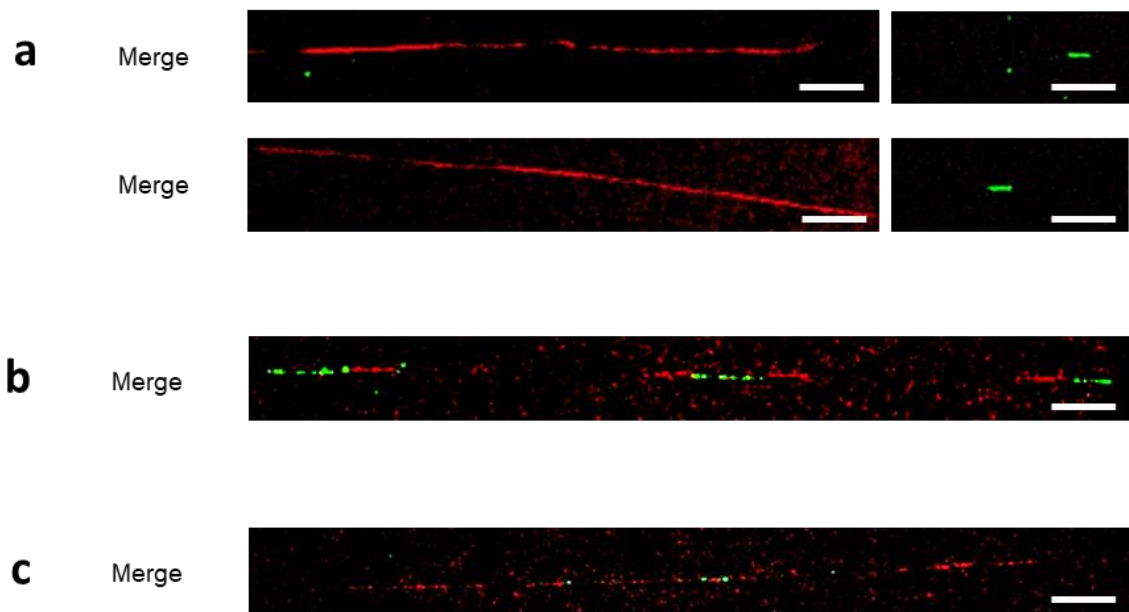
Figure 4.48: Representative images from time points 0 h (**a**), 1 h (**b**), and 7 h (**c**) of the HSkM differentiation assay. Cells were pulse-treated with EdU and CldU and stained for both thymidine analogs. Images are shown as a merge of both channels. Scale bars correspond to 10 µm.
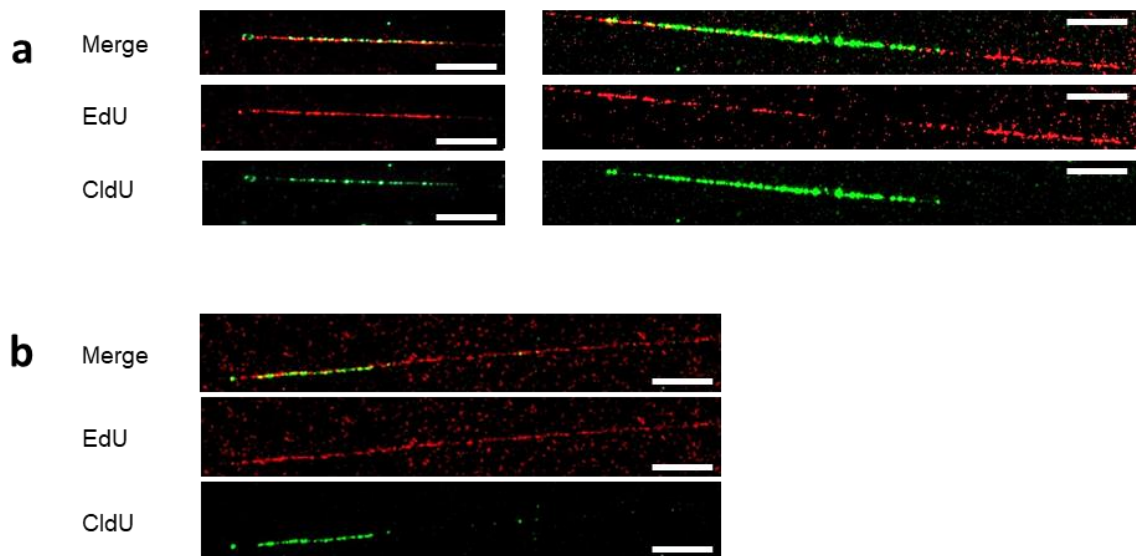
Figure 4.49: Representative images from time points 2 h (**a**), and 6 h (**b**) of the HSkM differentiation assay. Cells were pulse-treated with EdU and CldU and stained for both thymidine analogs. Each fiber is shown three times, with the merged image at the top, followed by EdU and CldU staining. Scale bars correspond to 10 µm.

At all time points from 2 h to 6 h (included), both normal replication and re-replication events were detected. Figure 4.49 shows three representative examples of re-replication events from the 2 h and 6 h HSkM differentiation assays, with the merged image at the top, and then the EdU and the CldU channels, respectively.

Although this was a qualitative analysis, it appeared that the number of observed re-replication events peaked at the 4 h time point (representative examples are shown in Figure 4.50).
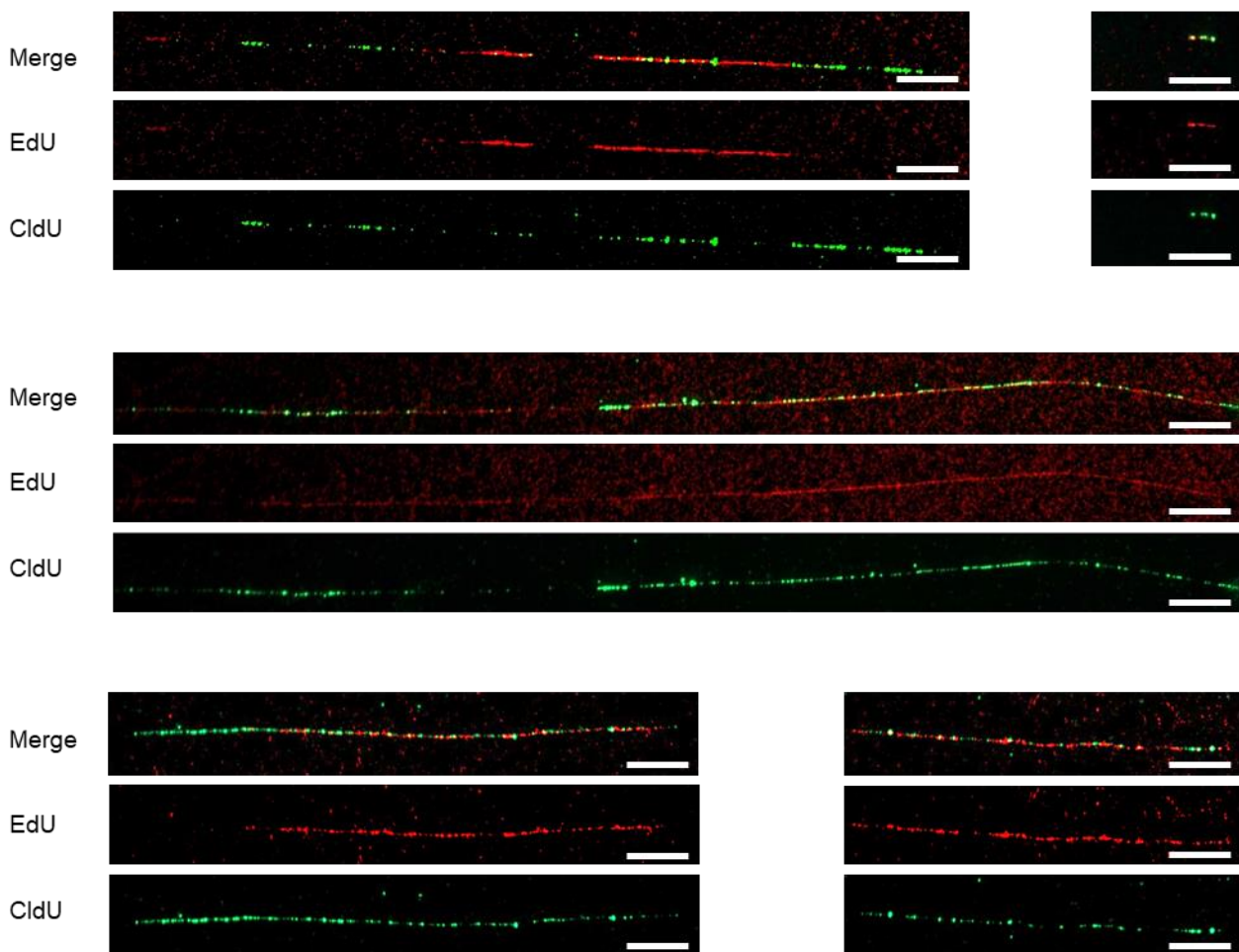
Figure 4.50: Representative images from the 4 h time point of the HSkM differentiation assay. Cells were pulse-treated with EdU and CldU and stained for both thymidine analogs. Each fiber is shown three times, with the merged image at the top, followed by EdU and CldU staining. Scale bars correspond to 10 μm.

4.2.3. Quantitative analysis in differentiating HSkMs

To investigate this possibility quantitatively, higher numbers of replication and re-replication events were required. For this reason, and because Zhao and colleagues have described a possible deleterious effect of EdU on human cells [628], some conditions were replicated with the thymidine analogs IdU and CldU and sent to the company Genomic Vision. This allowed the comparison of results between the two conditions and evaluation of the potential toxicity of EdU in our differentiation experiments. The numbers of re-replication events could also be recorded and analyzed, as well as the frequency and length of tracts containing incorporated thymidine analogs.

The service purchased from Genomic Vision is called EasyComb. The usual procedure for obtaining DNA fibers using the molecular combing method was followed until washing the agarose plugs after the overnight proteinase digestion. The plugs were sent to the company, which is based in France. After the remaining steps of the molecular combing method were performed and the coverslips were stained by immunofluorescence, they were scanned, and the images were merged into a composite image and provided to the customer. Figure 4.51 shows an example of a scanned coverslip, with DNA in blue, CldU in red, and IdU in green. The full image is displayed in Figure 4.51 a. The red rectangle outlines the edge of the image presented in Figure 4.51 b, and similarly the blue rectangle and Figure 4.51 c.
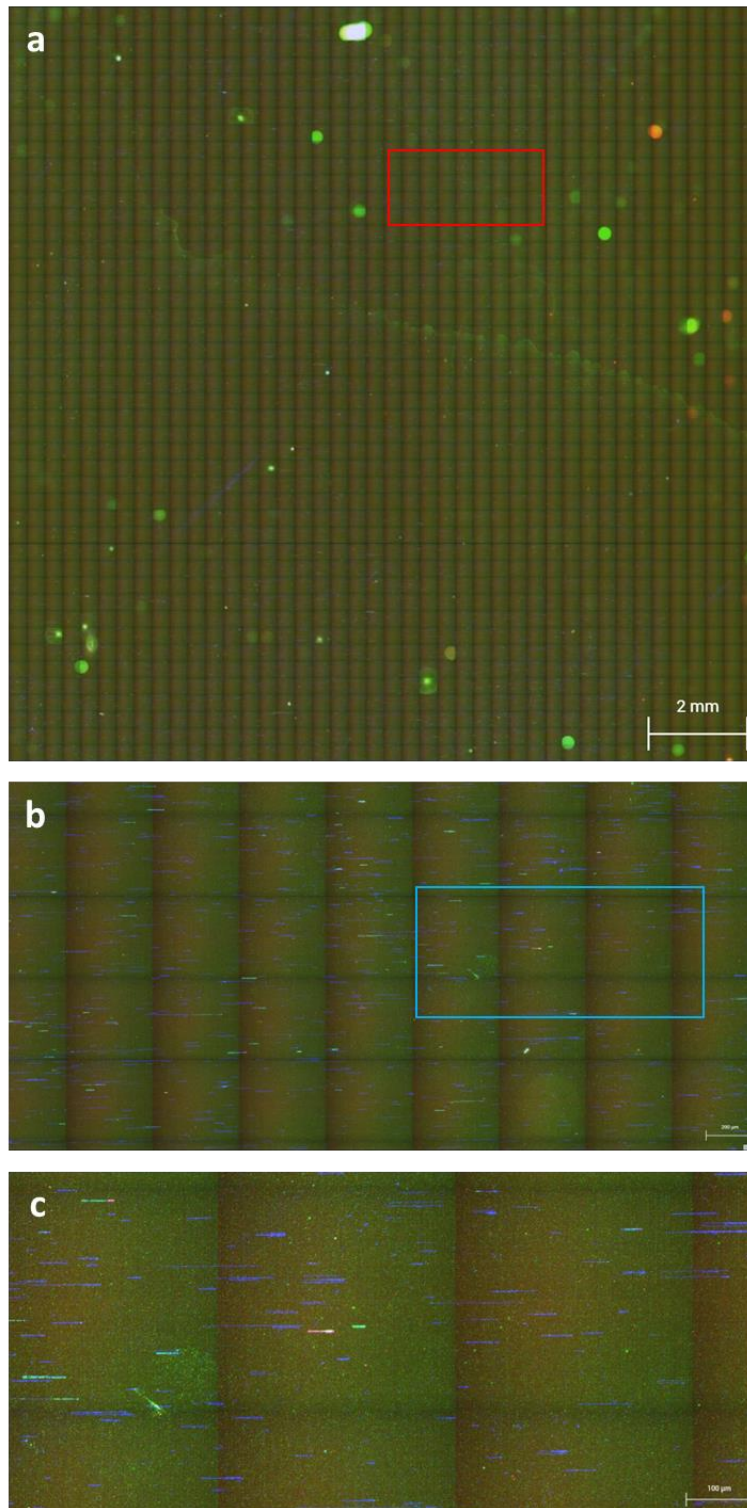
Figure 4.51: Example of a scanned coverslip as displayed in the FiberStudio® online tool (screenshots). DNA is shown in blue, CldU in red, and IdU in green. All images are from the hMSC 6 h chondrogenesis assay. **a**: The entire slide is shown, each square represents one scanned portion of the slide. The red rectangle outlines the edge of **b**. The blue rectangle in **b** outlines the edge of the image shown in **c**. Scale bars correspond to 2 mm (**a**), 200 µm (**b**), and 100 µm (**c**).

With the EasyComb service, the customer also receives time-limited access to Genomic Vision's proprietary online tool, FiberStudio®. This tool is used to analyze the fibers on the scanned coverslips. The fibers are automatically recognized by the tool and assigned ROIs (regions of interest) if they appear to be associated with tracts positive for thymidine analog incorporation. However, manual verification of the fibers and ROIs is necessary. For the work presented in this dissertation, the following criteria were used to discard ROIs during the manual inspection: they are on two or more DNA fibers, or there is a possibility that this is the case, or it is on a fiber that forms a U-shaped loop because both ends adhered to the silanized surface while combing. Figure 4.52 shows representative examples of such cases.
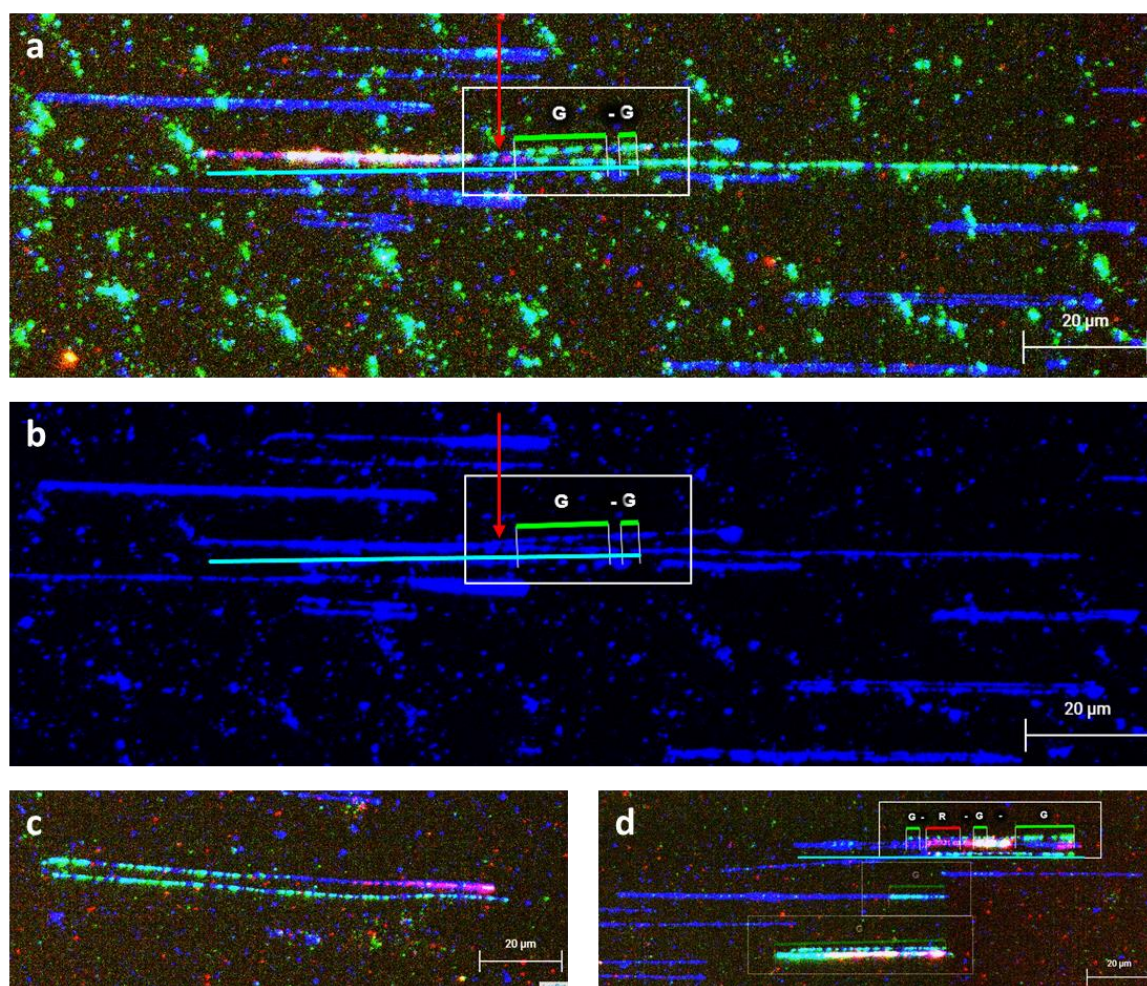
Figure 4.52: Examples of FiberStudio® images of discarded regions of interest (ROIs). DNA is shown in blue, CldU in red, and IdU in green. All images (screenshots) are from the hMSC proliferation 0 h assay. **a-b**: Example of two fibers overlapping to the left of the red arrow and not overlapping to the right. **c**: Example of a fiber whose ends both adhered to the silanized surface while combing. **d**: Examples of fiber aggregates. Scale bars correspond to 20 µm.

According to Genomic Vision representatives and the existing literature, FiberStudio® is commonly used to analyze qualitatively and quantitatively replication events and is calibrated to automatically detect initiation and termination events such as those shown in Figure 4.53. It is however possible to use this tool to document re-replication events, for example by repurposing the color code B during the manual review of the ROIs.

In Figure 4.53 a, three distinct thymidine analogs tracts can be seen on one of the fibers, which are shown in blue. IdU was administered to HSkM cells during the first pulse treatment and is shown in green. The replication origin in the center of the fiber was fired during this first pulse, and IdU was incorporated by both replication forks to the left and right of the origin. CldU, which was given to the cells during the second pulse, and is shown in red, was incorporated next, again by both replication forks. For the fibers shown in Figure 4.53 b, the scenario is similar: activation of the origin of replication during the first pulse and continued incorporation of thymidine analogs until after the beginning of the second pulse treatment. In the case of the lower fiber, the small green dot to the left of the center could be another replication origin that was also fired during the first pulse and subsequently silenced by the replication fork of its neighbor. In the fiber shown in Figure 4.53 c, replication was terminated shortly after the beginning of the second pulse treatment, as inferred from the long green IdU stretches flanking a short red CldU tract.
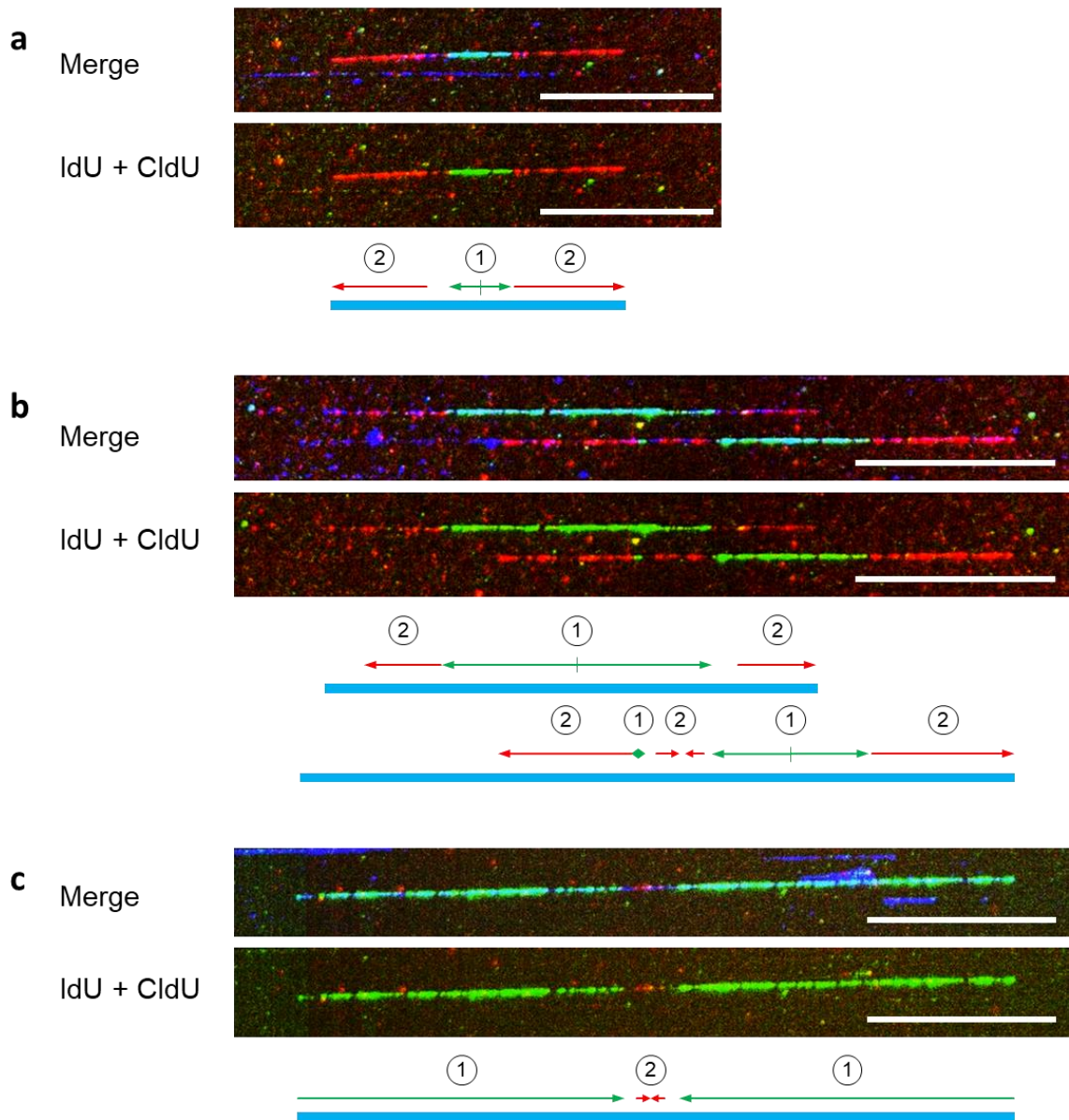
Figure 4.53: Representative images of normal replication events as seen in FiberStudio®. DNA is shown in blue, CldU in red, and IdU in green. Each fiber is shown twice, with the merged image at the top, followed by the IdU and CldU channels together. Below each image pair is a schematic representation of the fiber(s) with the numbers indicating the order in which the thymidine analogs were incorporated. Scale bars correspond to 50 µm. **a**. Example of replication initiation in the HSkM 6 h differentiation assay. **b**. Two examples of replication initiation in the HSkM 6 h differentiation assay. The green dot on the left arm of the lower fiber might be an origin of replication that was activated and subsequently silenced. **c**. Example of a termination of replication event in the hMSC 6 h chondrogenesis assay.

Three conditions were repeated with IdU and CldU and sent to Genomic Vision: HSkM cells pulse-treated 1 h, 4 h, and 6 h after differentiation induction (see Figure 4.54 a). Additionally, as a control, HSkM cells were proliferated and pulse-treated after 4 h with EdU and CldU, and further processed in-house to obtain combed fibers (see Figure 4.54 b).
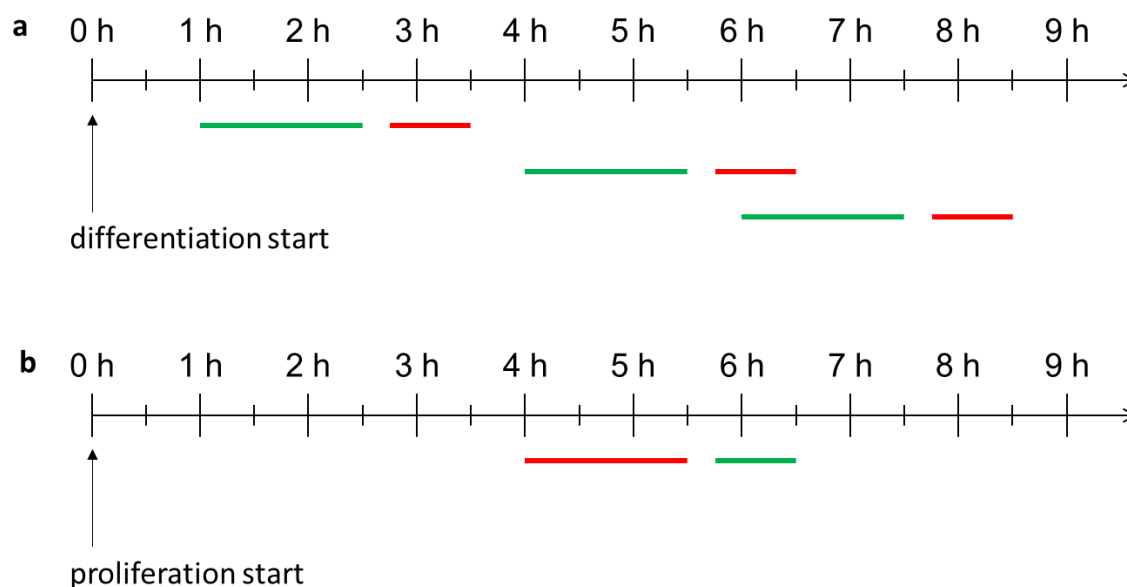
Figure 4.54: Schematic of the thymidine analog pulse treatments in HSkM cells, started at four different time points: 1 h, 4 h, and 6 h after differentiation start (**a**), and 4 h after proliferation start (**b**). CldU (in red) and IdU (in green) were used in the differentiation assays (**a**), and EdU (in red) and CldU (in green) were used in the proliferation assay (**b**).

Figure 4.55 shows a representative image of fibers of the HSkM 4 h differentiation assay as seen in FiberStudio®, with either the three channels visible (see Figure 4.55 a) or without DNA counterstaining (see Figure 4.55 b). Some fiber aggregates can be observed, but enough fibers do not overlap with others to allow analyses.
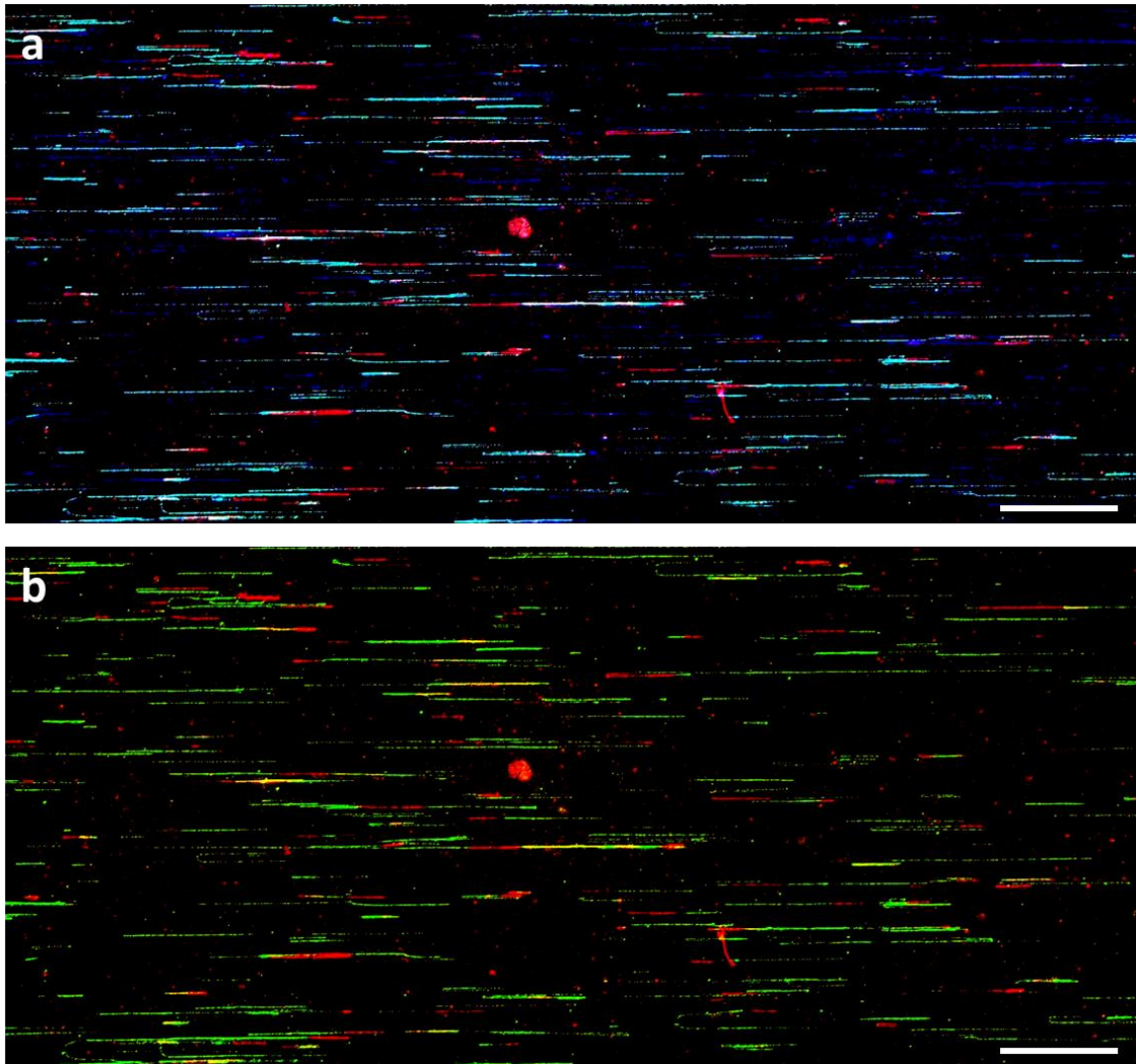
Figure 4.55: Representative images of combed fibers from the HSkM 4 h differentiation assay as seen in FiberStudio®. DNA is shown in blue, CldU in red, and IdU in green. The same image is shown twice, with (**a**) and without (**b**) DNA counterstaining. Scale bars correspond to 100 μm = 200 kb.

As shown in the representative examples of all four conditions in Figure 4.56, re-replication events were observed in all three differentiation assays (see Figures 4.56, 4.57, and 4.58), but not in the HSkM proliferation assay (see Figure 4.59). Each fiber is displayed twice, first as merge images of the three channels (with DNA shown in blue, and thymidine analogs in red and green: IdU (green) and CldU (red) in a-c, EdU (red) and CldU (green) in d), then without DNA counterstaining. Although re-replication events were already observed in the HSkM 1 h differentiation assay (see Figure 4.56), the yellow overlaps appeared to be shorter than those in the HSkM 4 h (see Figure 4.57) and 6 h differentiation assay (see Figure 4.58). In many fibers, numerous (up to four) distinct yellow traces were found.
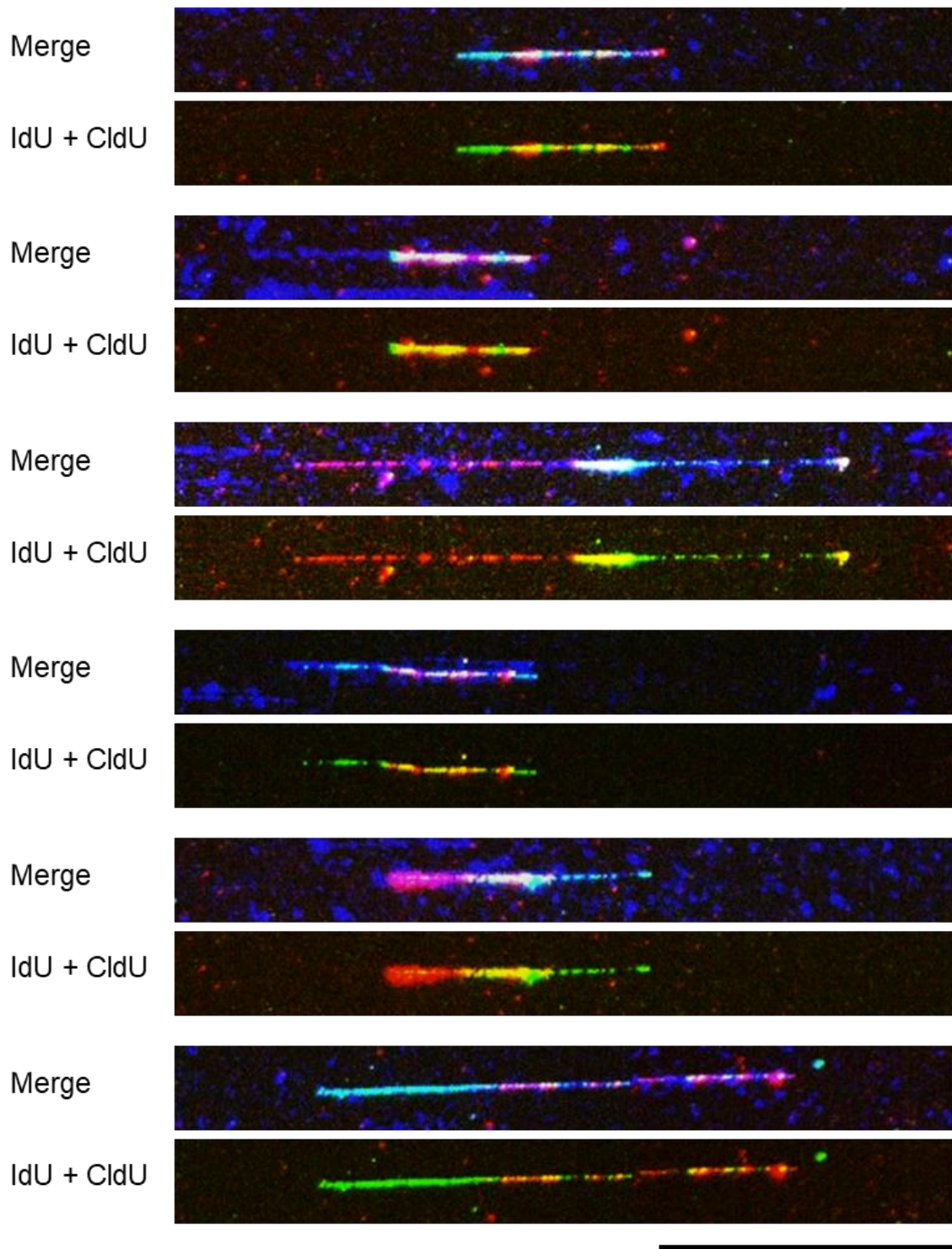
Figure 4.56: Representative examples of combed fibers exhibiting overlaps of red and green tracts in the HSkM 1 h differentiation assay. DNA is shown in blue, CldU in red, and IdU in green. Each image is shown twice, with and without DNA counterstaining. Scale bars correspond to 50 µm = 100 kb.
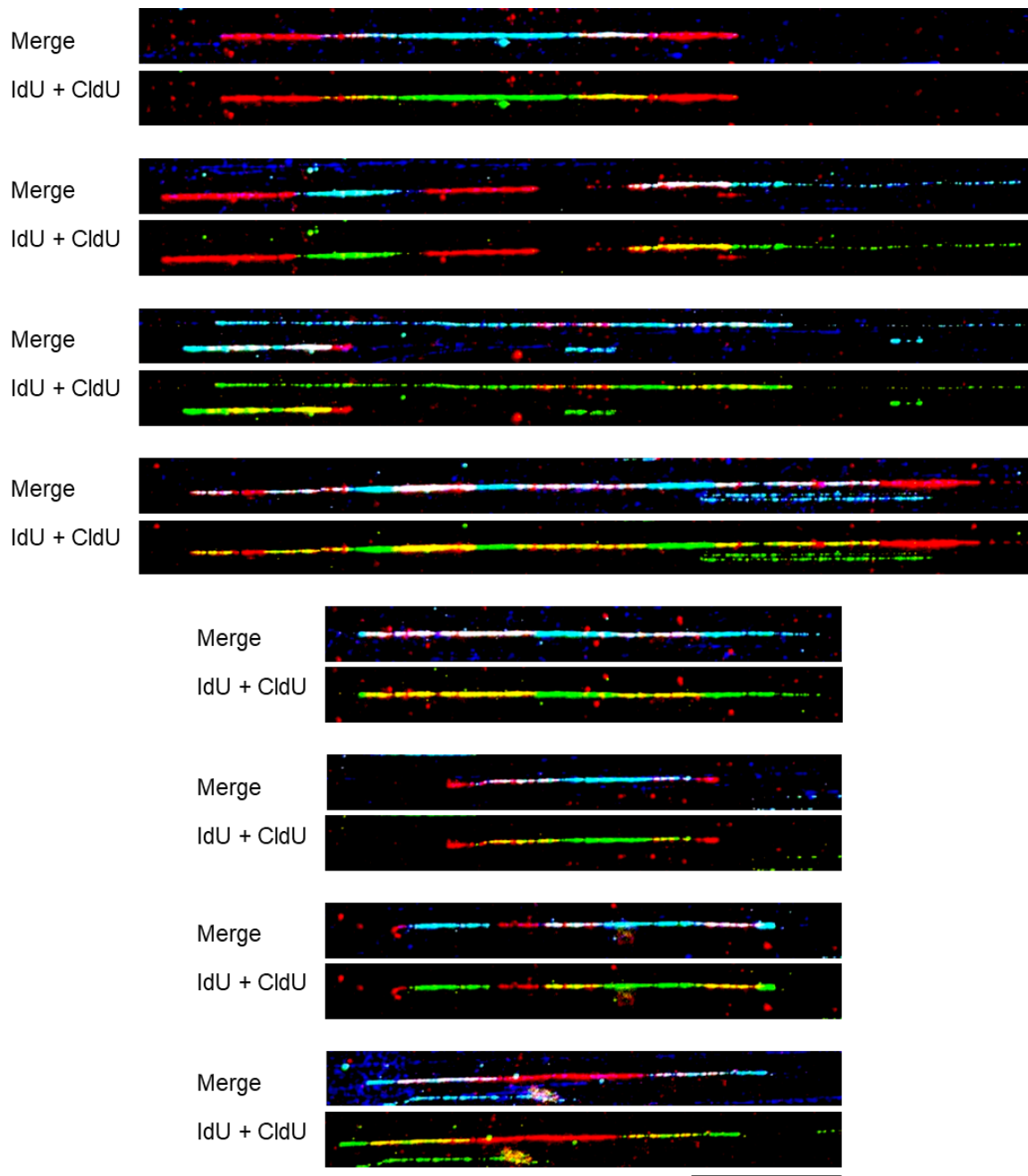
Figure 4.57: Representative examples of combed fibers exhibiting overlaps of red and green tracts in the HSkM 4 h differentiation assay. DNA is shown in blue, CldU in red, and IdU in green. Each image is shown twice, with and without DNA counterstaining. Scale bars correspond to 50 μm = 100 kb.
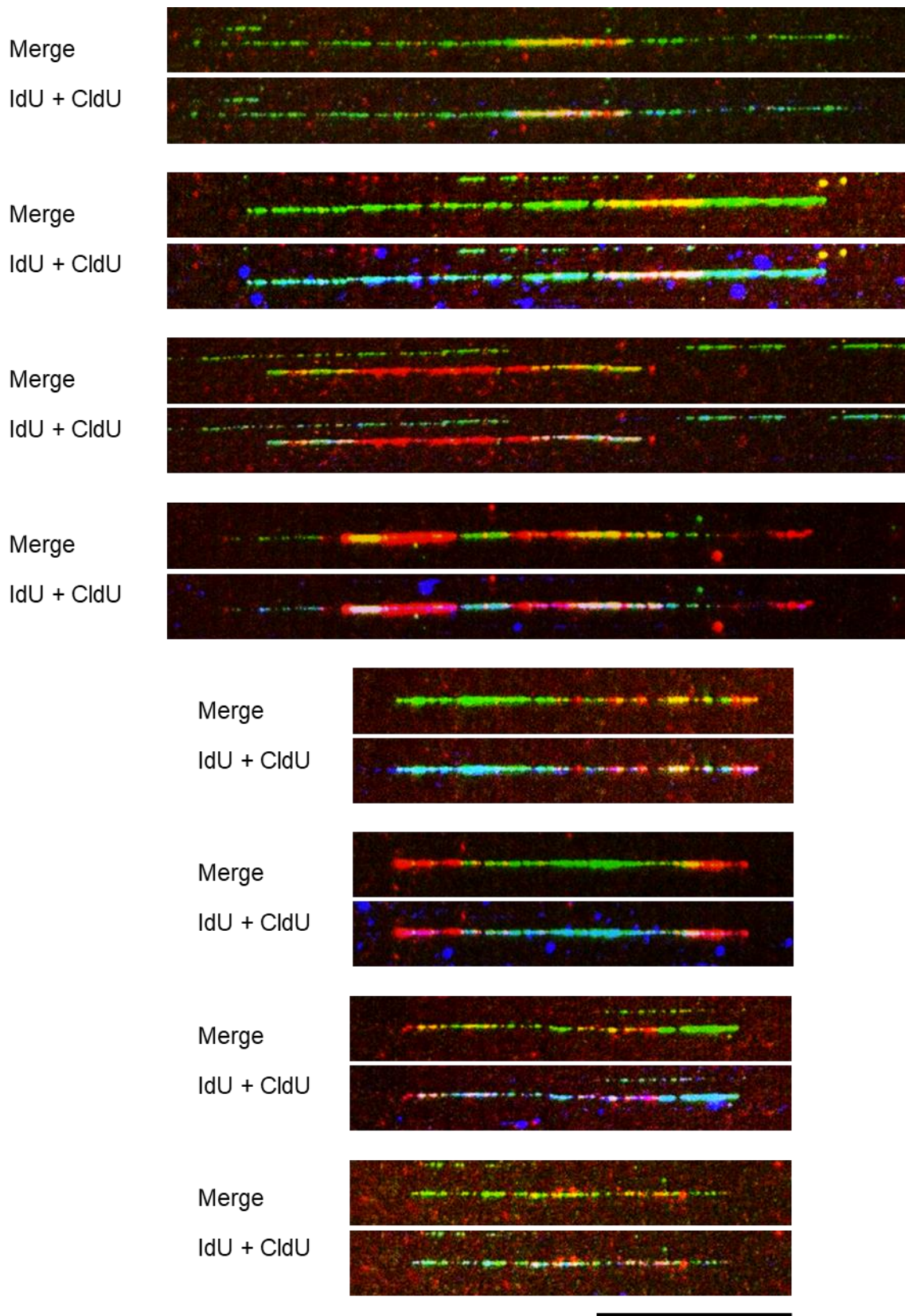
Figure 4.58: Representative examples of combed fibers exhibiting overlaps of red and green tracts in the HSkM 6 h differentiation assay. DNA is shown in blue, CldU in red, and IdU in green. Each image is shown twice, with and without DNA counterstaining. Scale bars correspond to 50 μm = 100 kb.
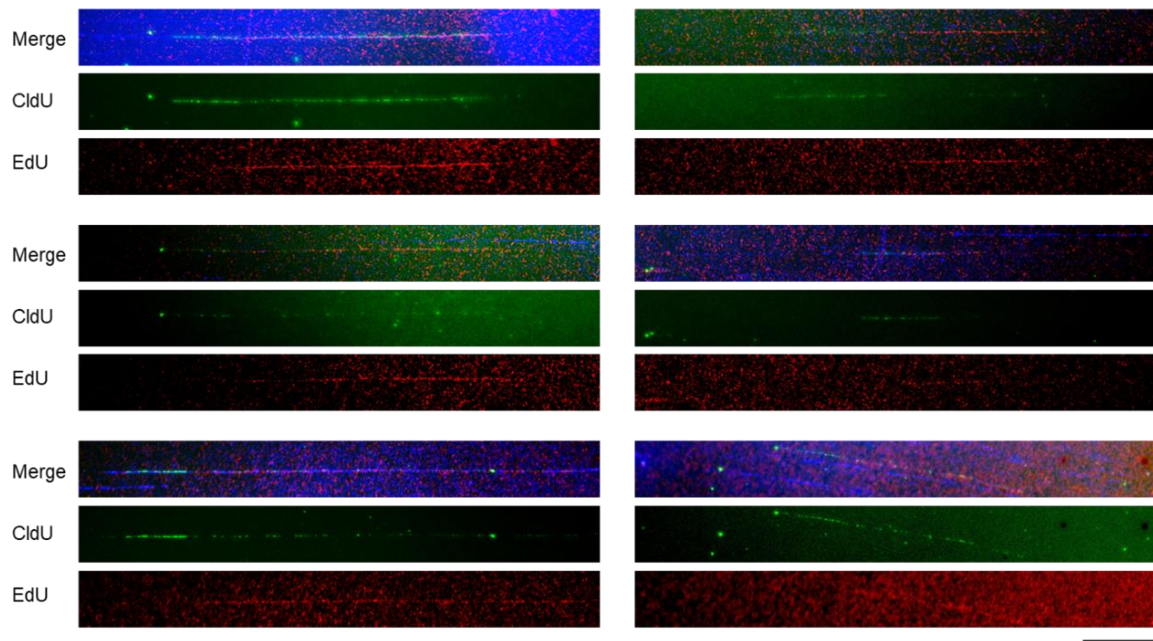
Figure 4.59: Representative examples of combed fibers exhibiting overlaps of red and green tracts in the HSkM 4 h proliferation assay. DNA is shown in blue, CldU in red, and IdU in green. Each image is shown twice, with and without DNA counterstaining. Scale bars correspond to 50 μm = 100 kb.

Table 4.3 summarizes the numbers of fibers for each condition in the quantitative analysis (520 for the HSkM proliferation assay, 221, 196, and 182 for the HSkM 1 h, 4 h, and 6 h differentiation assays, respectively), as well as the number of yellow, red, and green positive fibers.

Table 4.3: Frequency of thymidine analog incorporation in proliferating or differentiating HSkM cells.

	Fibers n	Yellow n (%)	Red n (%)	Green n (%)	Red and Green n (%)
4 h proliferation	520	0 (0.0 %)	9 (1.7 %)	15 (2.9 %)	17 (3.3 %)
1 h differentiation	221	5 (2.3 %)	3 (1.4 %)	3 (1.4 %)	3 (1.4 %)
4 h differentiation	196	14 (7.0 %)	11 (5.6 %)	51 (26.0 %)	17 (8.7 %)
6 h differentiation	182	11 (6.0 %)	6 (3.3 %)	94 (52.0 %)	19 (10.0 %)

This confirms the absence and lower number of yellow-positive fibers, i.e., containing a re-replication event, in the HSkM proliferation (0 % of fibers) and 1 h differentiation assays (2.3 % of fibers), respectively, compared to the HSkM 4 h and 6 h differentiation assays (7 % and 6 % of fibers, respectively). In general, fewer fibers were positive for thymidine analog incorporation in cells pulse-treated 1 h after the start of the experiment than at later time points.

When comparing the HSkM 4 h proliferation and differentiation assays, far fewer thymidine analogs were incorporated in proliferating cells than in differentiating cells (1.7 % versus 5.6 % of red positive fibers, 2.9 % versus 26 % of green positive fibers, and 3.3 % versus 8.7 % of red and green positive fibers).

The number of yellow, red, and red-green positive fibers is similar in the HSkM 4 h and 6 h differentiation assays, but there were two times more green-positive fibers (52 % versus 26 %) in the cells pulse-treated 6 h after differentiation induction than in the cells pulse-treated two hours earlier. Since green positive DNA portions were replicated during the first pulse treatment, this may indicate that more replication was initiated between 6 h and 7 h 30 than between 4 h and 5 h 30 after the differentiation was started. Assuming similar replication speed in all three differentiation assays, this greater ratio of re-replication to replication events at the 4 h time point may suggest that re-replication occurs very early in this replication process of these cells.

Because the fibers generated by molecular combing are stretched by a uniform factor (2 kb/μm), this method allows measurement and comparison of the lengths of thymidine analog-positive tracts. All red, green, and yellow traces documented in Table 4.3 were measured and are displayed as violin and box plots in Figure 4.60. The lengths of red or green-positive tracts were similar in all HSkM assays, whether they were proliferation or differentiation assays. Yellow overlaps were observed in all three differentiation assays (HSkM 1 h, 4 h, and 6 h differentiation assays), although they tended to be longer in the HSkM 4 h and 6 h differentiation assays compared with cells pulse-treated 1 h after differentiation induction (median 32, 38, and 14 kb, respectively). Shorter yellow stretches indicate shorter time periods during which the DNA portion was replicated during each incorporation pulse.
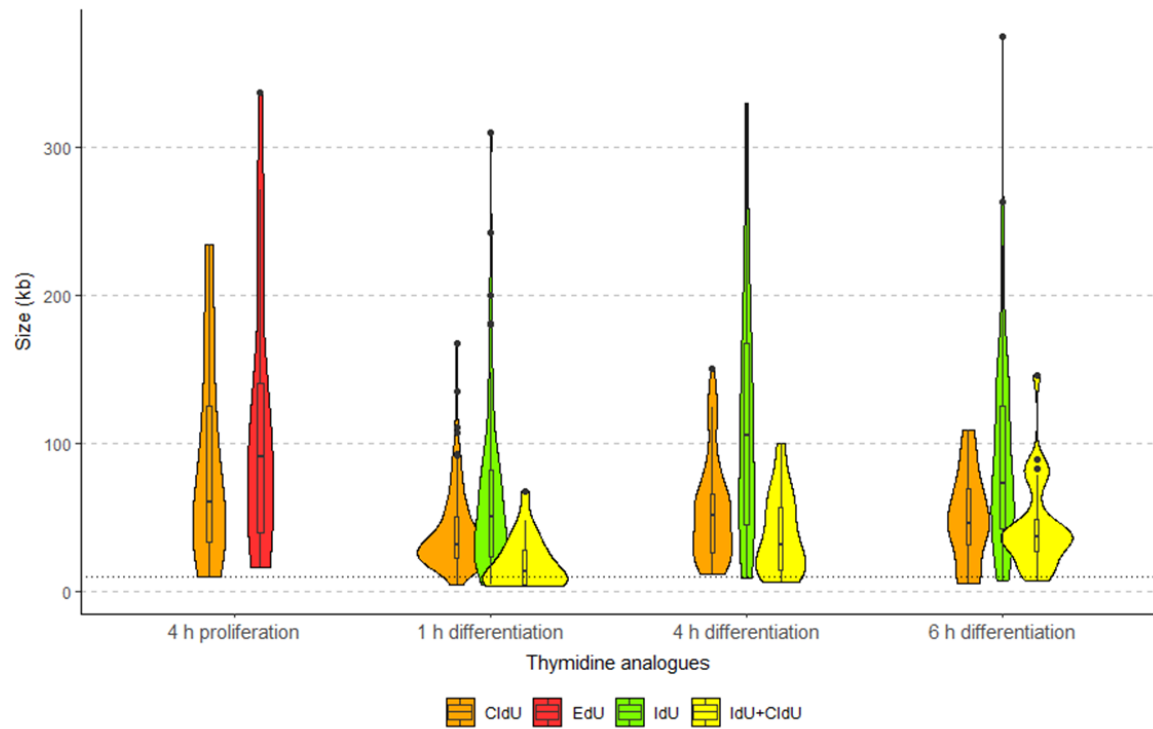
Figure 4.60: Quantitative distribution of thymidine analogs incorporation during HSkM proliferation and differentiation assays. HSkM cells were proliferated for 4 h or differentiated for 1 h, 4 h, or 6 h, and subsequently pulse-treated with thymidine analogs. CldU stretches are shown in orange, EdU stretches are shown in red, IdU stretches are shown in green, and stretches in which IdU and CldU overlap are shown in yellow. The boxes within the violin plots indicate the mean and the 2nd and 3rd quartiles. The lengths of the stretches where thymidine analogs are incorporated are shown on the y-axis. The black horizontal dotted line corresponds to 10 kb.

4.2.4. Quantitative analysis in hMSCs undergoing chondrogenesis

Since re-replication appears to occur at different time points in different cell types, the experiment was repeated with hMSCs undergoing chondrogenesis. Proliferating hMSCs were used as negative controls. Four conditions were prepared and sent to Genomic Vision: hMSC 0 h, 4 h, and 6 h chondrogenesis, and hMSC 0 h proliferation.

Table 4.4 provides an overview of the number of ROIs obtained, reviewed, validated, and discarded for each assay. In general, a very high number of ROIs were discarded, according to the criteria shown in Figure 4.51 (83.28 to 60.47 %). At least 600 ROIs were validated and measured in each assay.

Table 4.4: Numbers of the total, reviewed, validated regions of interest (ROIs) and percentage of discarded ROIs for each hMSC proliferation or chondrogenesis assay.

Assay	Total ROIs	Reviewed ROIs	Validated ROIs	% discarded ROIs
hMSC proliferation 0 h	14 955	3 589	600	83.28
hMSC chondrogenesis 0 h	11 903	2 500	600	76.00
hMSC chondrogenesis 4 h	9 664	3 866	836	78.37
hMSC chondrogenesis 6 h	3 530	1 518	600	60.47

Table 4.5 summarizes the number of fibers for each condition in the quantitative analysis, as well as the number of yellow, red, and green positive segments. More than one segment could be found on one fiber, with up to 13 segments interspersed with DNA without incorporated thymidine analogues in two cases.

The quantitative analysis revealed differences in thymidine analog incorporation between the hMSC proliferation and chondrogenesis timepoints. The percentages of DNA segments positive for CldU (red) or IdU (green) incorporation were greater at earlier timepoints, decreasing progressively from 0 h to 6 h in differentiating hMSCs. Proliferating cells were similar to differentiating ones at the same time points.

Interestingly, despite higher overall incorporation rates at the 0 h time point, the number of re-replication events detected was similar between proliferating hMSCs and those undergoing chondrogenesis. Approximately 1.5-2.5 % of analyzed fibers showed evidence

of re-replication across the 0 h, 4 h, and 6 h timepoints in both conditions. The lack of a substantial difference in re-replication incidence between proliferating and differentiating states suggests that re-replication may be an intrinsic phenomenon in these cells, rather than specifically triggered by differentiation signals.

Table 4.5: Frequency of thymidine analog incorporation in proliferating or differentiating (chondrogenesis) hMSC cells.

	Fibers n	Yellow n (%)	Red n (%)	Green n (%)
0 h proliferation	600	10 (1.7 %)	209 (34.9 %)	864 (144.0 %)
0 h differentiation	600	9 (1.5 %)	338 (56.3 %)	877 (146.2 %)
4 h differentiation	836	3 (0.4 %)	300 (35.9 %)	1061 (126.9 %)
6 h differentiation	600	15 (2.5 %)	171 (28.5 %)	662 (110.3 %)

Figure 4.61 shows violin and box plots of the lengths of all traces positive for thymidine analog incorporation in all validated ROIs. Similar to the HSkM proliferation and differentiation assays, the lengths of DNA segments into which CldU or IdU was incorporated were comparable in all hMSC chondrogenesis assays (medians of 15.7 to 24.2 kb for the CldU positive tracts, medians of 35.5 to 49.5 kb for the IdU positive tracts). More discrepancy was found in the yellow tracts: only three of the fibers reviewed in the hMSC 4 h chondrogenesis assay contained potential re-replication events, all three very small (2.9, 3.3, and 3.3 kb). Ten of the fibers reviewed in the hMSC 0 h proliferation assay also presented overlaps, including two that were longer than 9 kb (see Figure 4.62 a and b). The tracts positive for both thymidine analogs were similar in length in the hMSC 0 h chondrogenesis assay (median of 5.5 kb versus 5.0 kb in the proliferating cells), with two tracts longer than 9 kb (see Figure 4.62 e and f). However, in the hMSC 6 h chondrogenesis assay, 15 yellow stretches were observed with a median length of 16.9 kb; eleven stretches were longer than 9 kb (two of which are shown in Figure 4.62 m and n).
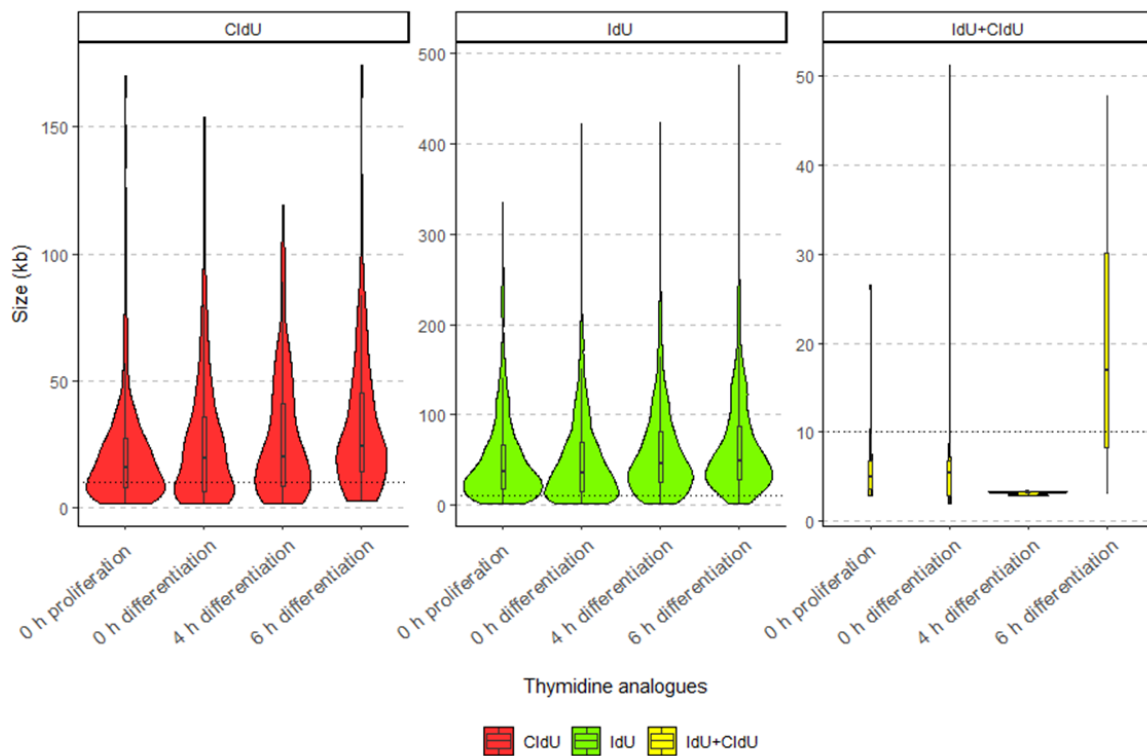
Figure 4.61: Quantitative distribution of thymidine analogs incorporation during the hMSC proliferation and chondrogenesis assays. hMSC cells were proliferated for 0 h or differentiated for 0 h, 4 h, or 6 h, and subsequently pulse-treated with thymidine analogs. CldU stretches are shown in red, IdU stretches are shown in green and stretches in which IdU and CldU overlap are shown in yellow. The boxes inside the violin plots indicate the mean and the 2nd and 3rd quartiles. The lengths of the stretches where thymidine analogs are incorporated are shown on the y-axis. The black horizontal dotted line corresponds to 10 kb.

Figure 4.62 shows four representative examples of fibers having incorporated thymidine analogs in each hMSC assay: hMSC 0 h proliferation (a-d), hMSC 0 h (e-h), 4 h (i-l), or 6 h (m-p) chondrogenesis assay. Each fiber is displayed twice, first as merge images of the three channels (with DNA shown in blue, IdU in green, and CldU in red), then without DNA counterstaining. In addition to normal initiation (g, h, j, and o) and termination events (i, l, and p), seven examples of possible re-replication events are shown (a-c, e, f, m, and n).
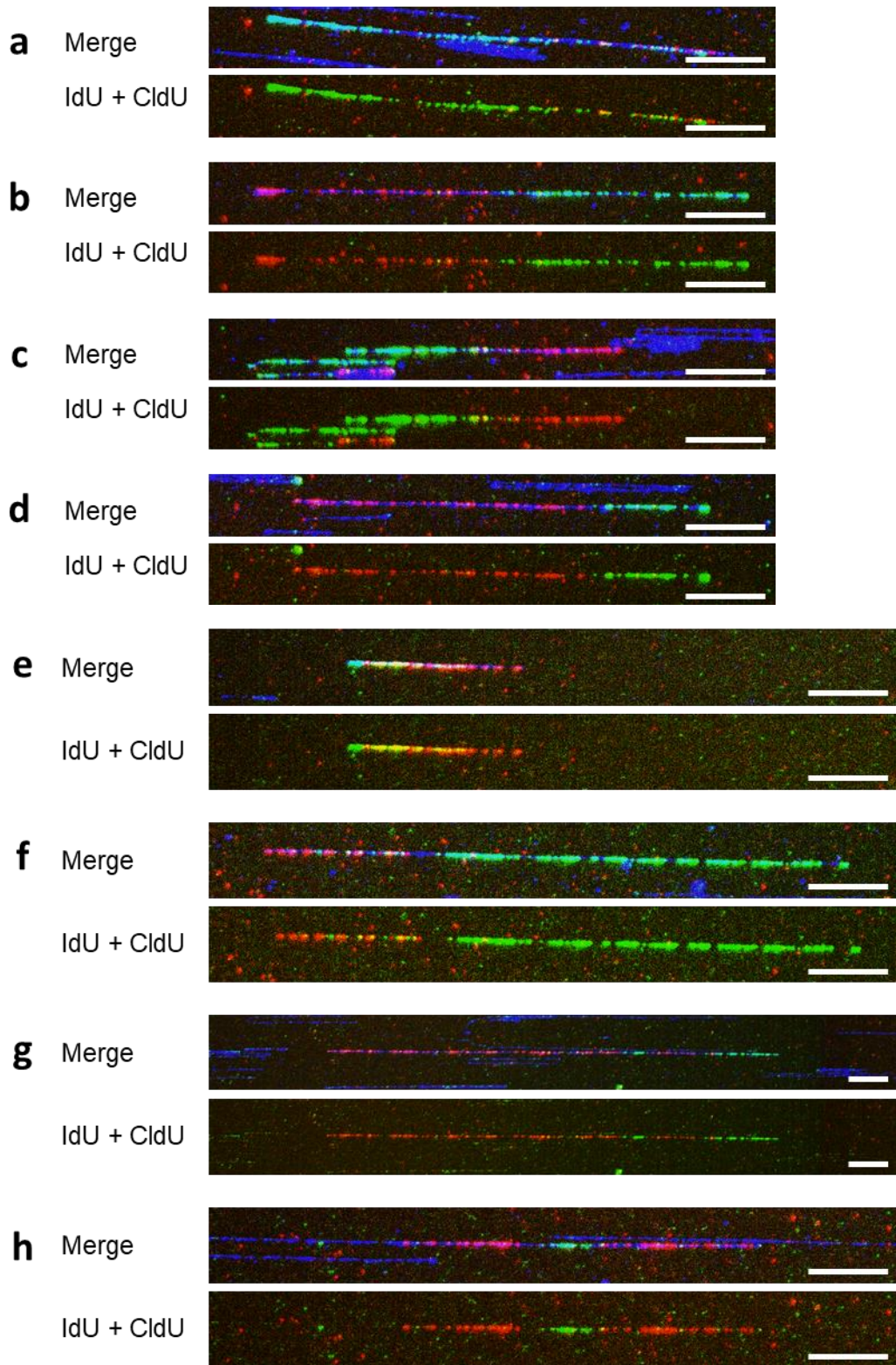
Figure 4.62: Representative examples of combed fibers in the hMSC 0 h proliferation (**a-d**), or 0 h (**e-h**), 4 h (**i-l**), 6 h (**m-p**) chondrogenesis assay. DNA is shown in blue, CldU in red, and IdU in green. Each image is shown twice, with and without DNA counterstaining. Fibers displayed in **a**, **b**, **c**, **e**, **f**, **m**, and **n** exhibit overlaps of red and green tracts; fibers shown in **g**, **h**, **j**, and **o** are examples of normal replication initiation events; fibers shown in **i**, **l**, and **p** are examples of normal replication termination events. Scale bars correspond to 20 μm = 40 kb.

i Merge

IdU + CldU

j Merge

IdU + CldU

k Merge

IdU + CldU

l Merge

IdU + CldU

m Merge

IdU + CldU

n Merge

IdU + CldU

o Merge

IdU + CldU

p Merge

IdU + CldU
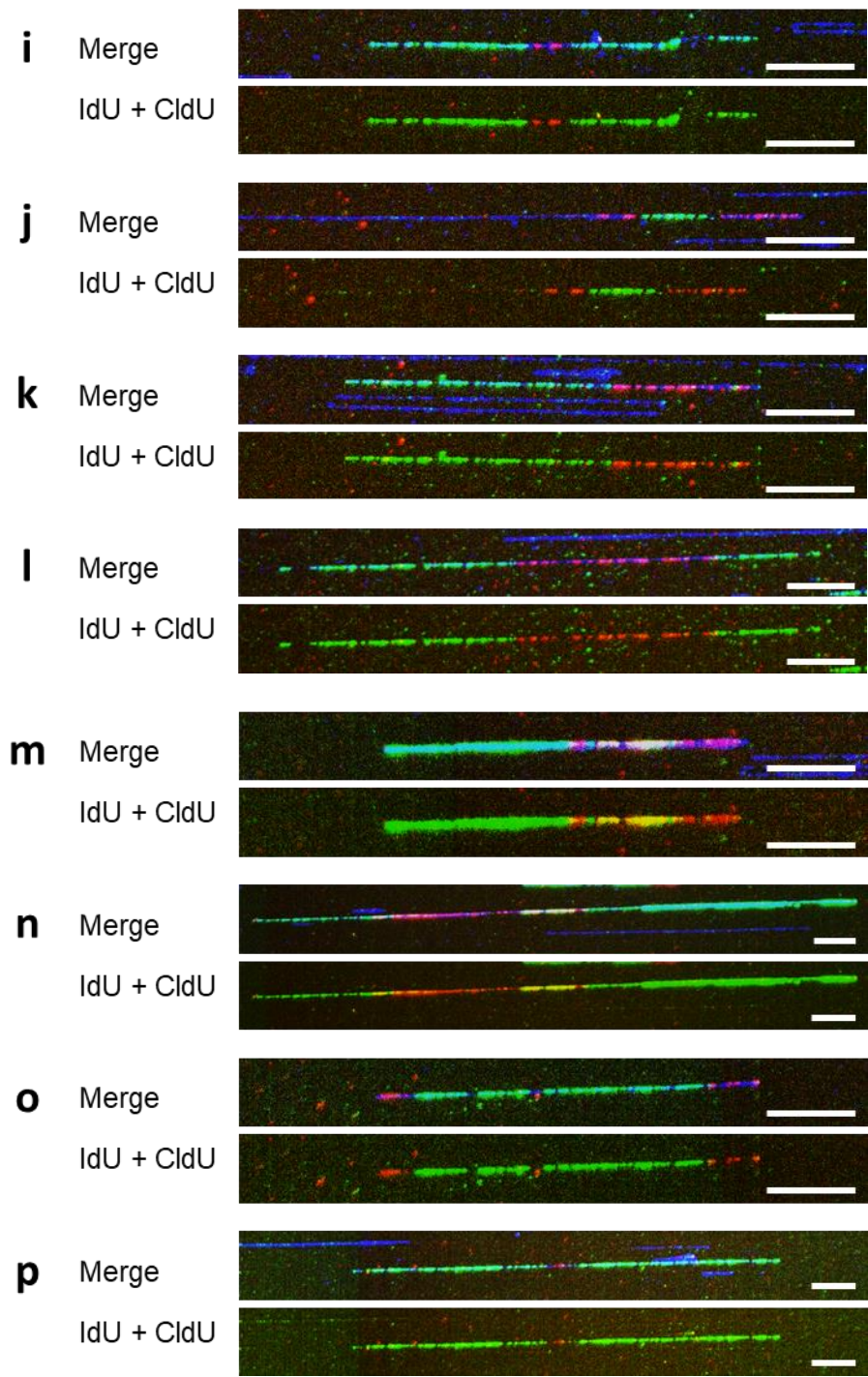
Figure 4.62 continued

5. Discussion

This work aimed to characterize the miRNome, transcriptome, and re-replication events during the initial hours of stem cell differentiation and focused on the first hours after the induction of differentiation in healthy human stem cells, which are understudied in the current literature. Instead, these cells are typically characterized after one or a few days of differentiation. Understanding the internal processes of early differentiating stem cells might be of help to the scientific community, especially in the domains of cancer research and stem cell therapies. Studying the first 48 hours could provide unique insights into the immediate molecular changes triggered by differentiation induction, as opposed to reflecting downstream effects.

Gene amplifications, which are present in both stem cells and cancer cells, were shown to be a good prognostic tool for certain types of cancer, including breast, colon, ovarian, neuroblastoma, and small-cell lung cancer [471]. Studies by the Pan-Cancer Analysis of Whole Genomes Consortium and The Cancer Genome Atlas have confirmed the link between gene amplification and cancer [329]. Understanding the mechanisms behind gene amplifications in stem cells could potentially lead to new approaches or targets for overcoming chemotherapy and radiotherapy resistance in cancers like ovarian and lung cancer. Additionally, more research on human stem cells is necessary to improve patient safety and potentially use these cells in future therapeutic approaches.

Stem cell therapies include regenerative medicine approaches, and only a few such treatments are currently approved [80,433]. The research for new stem cell therapies is a very active field, with researchers trying to develop therapies against numerous cancer types, neurodegenerative diseases like Alzheimer's disease, blood disorders, and many others [24,154,190].

The stem cells used in therapeutic approaches are either derived from the patient (autologous) or another person (allogeneic). Currently, stem cell therapies mainly use blood stem cells, sometimes derived from umbilical cords and skin stem cells, but many researchers also have high hopes for mesenchymal stem cells (MSCs) in this context [79,171,236].

Apart from ethical issues, most therapeutic applications of stem cells face obstacles related to the nature of these cells, including tumorigenicity and phenotypic instability of differentiated stem cells, which are both linked to their genomic stability.

When introduced into an organism, some stem cells such as embryonal stem cells (ESCs) and induced pluripotent stem cells (iPSCs) can form tumors called teratomas. This problematic ability of ESCs and iPSCs appears to be linked to their pluripotency [401,415]. Some procedures to ensure that injected stem cells are fully differentiated are being considered [235,497]. Another option for iPSCs could be to adjust their reprogramming cocktail, for example with miRNAs like hsa-miR-302 [336,337,556]. Because iPSCs must undergo a high number of cell divisions before being used, they may exhibit genomic abnormalities such as single-nucleotide variations (SNVs) or copy number variations (CNVs). Yamamoto and colleagues demonstrated that there was no correlation between the presence of SNVs and the growth of abnormal tissue in immunodeficient mice that received injections of iPSCs filtered or not for SNVs, but they found a positive correlation with copy numbers higher than three [593].

Currently, MSCs are solid candidates for stem cell therapy. Although they were initially thought to be potential promoters of tumor growth and metastasis, recent studies have shown that this is not the case. Instead, they tend to play a tumorigenesis-inhibiting role under certain conditions [161,533]. The main concern with MSCs is the stability of their phenotype: whether they maintain their naïve, differentiating, or differentiated characteristics and functional properties over time. Some patients who sought treatment at "stem cell clinics", where claims were made that are not supported by current science, had unexpected and unfortunate results with these cells [295]. Another obstacle with MSCs is their short and transient transplantation period, the timeframe during which they can be transplanted into the recipient's organism [269].

Another hurdle for the development of stem cell therapies is the potential response of the recipient's immune system to the graft, in short, the immunogenicity of the stem cell graft. In the case of hematopoietic stem cells, HLA (human leukocyte antigen) matching of donor and patient is always of the utmost importance, although stem cells derived from cord blood appear to be less immunogenic [308,416]. Graft-versus-host disease, which has been known for decades in other medical procedures, is also a risk in stem cell therapies. MSCs might help in this area as they have the potential to reduce inflammation in the body and thus the severity of the immune system response [194,309,631,633,636].

5.1. Goals

This thesis focused on two questions related to the characterization of healthy human stem cells during the initial hours of differentiation:

1. The transcriptional and miRNA profiles of differentiating hMSCs, hNSCs, and HSkMs were analyzed using microarrays and bioinformatic tools. This allowed for the investigation of a) clusters of RNA expression; b) pathways enriched after induction of differentiation; c) correlations between miRNA and mRNA levels of expression; and d) a miRNA family potentially involved in differentiation in all cell types studied. These results are presented in Part 4.1.
2. Gene amplifications, which are present in differentiating stem cells [10,150–153,193,362], have not yet been fully understood in terms of their mechanism of occurrence. Part 4.2 of this work aimed to investigate whether this mechanism may involve re-replication, by examining hMSCs undergoing chondrogenesis and differentiating HSkMs to determine: a) whether re-replication occurs in these cells; and b) if so, in what time frame.

5.2. Methods used

To answer the first question, the miRNA and gene expression of differentiating stem cells were studied up to 48 hours after induction of differentiation. Three cell types (hMSCs, hNSCs, and HSkMs) were cultured in five different differentiation assays. HSkMs and hNSCs were allowed to differentiate in a non-directed manner, while hMSCs were differentiated into adipocytes, chondrocytes, or osteoblasts. Total RNA was collected from the cells at 3 h, 6 h, 9 h, 12 h, 24 h, and 48 h after induction of differentiation, as well as from undifferentiated cells from the same batches (0 h). Microarrays were used to quantify the expression levels of 50,038 transcripts and 2,549 miRNAs from the same total RNA samples.

To find an answer to the second question, the molecular combing method was used in conjunction with sequential pulses of thymidine analogs to study DNA replication in HSkM cells treated with thymidine analogs in 1-hour increments from 0 h to 7 h after thawing. DNA counterstaining with the intercalating dye YOYO™-1 allowed for visualization of the replicating DNA. In addition, DNA replication events were studied in hMSCs, at 0h, 4h, and 6h after chondrogenesis induction, and during proliferation.

Figure 5.1 recapitulates the different methods and analyses performed for this thesis.
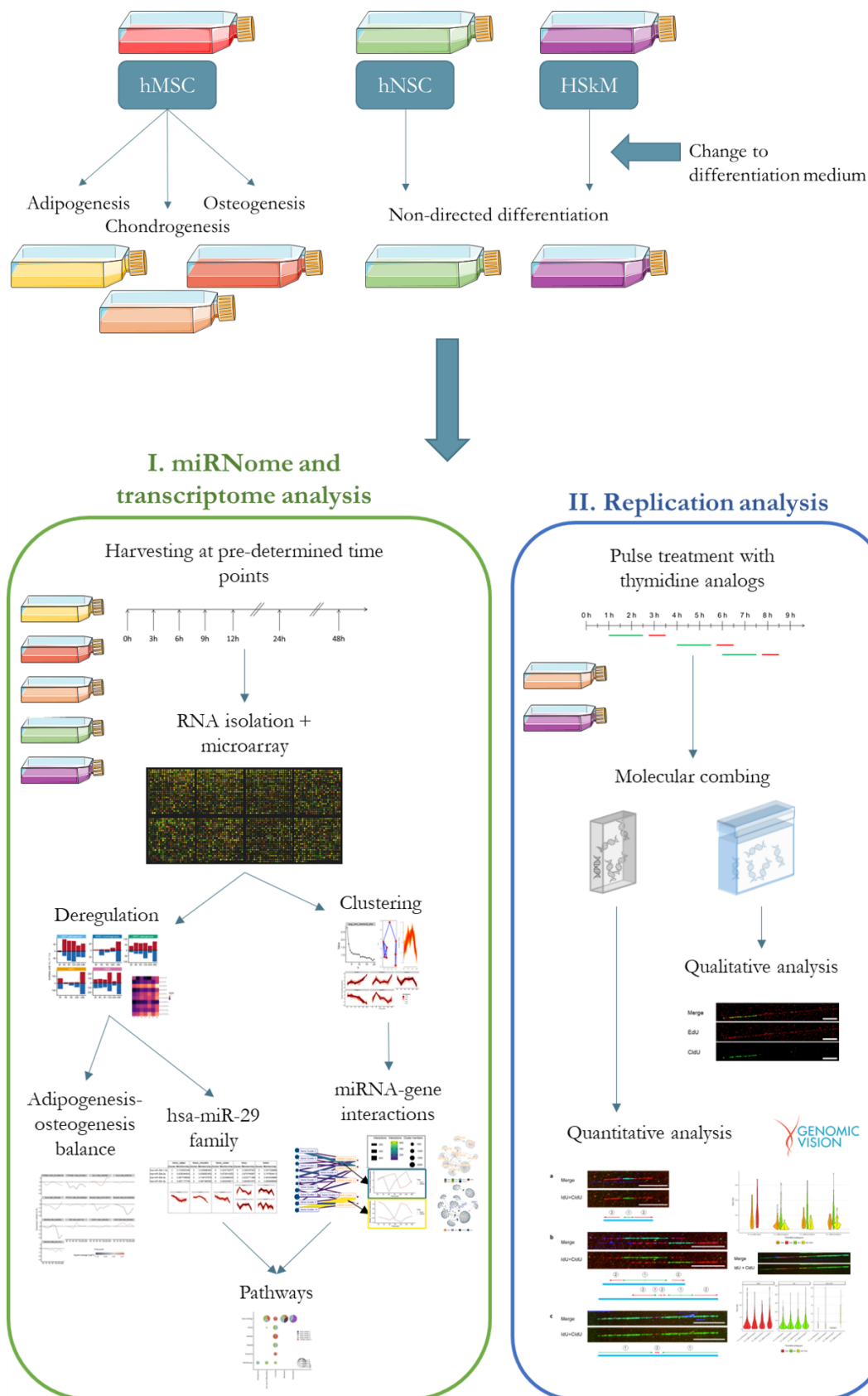
Figure 5.1: Summary of the methods and analyses used in this work. Three stem cell types were differentiated in five distinct differentiation assays, and time-resolved analyses were performed after I. miRNA and mRNA microarrays (presented in 4.1) or II. thymidine incorporation and molecular combing of DNA fibers (presented in 4.2).

5.3.　　Major findings

This work produced three major findings. First, it showed positive trends between the similarity of pattern expression in clusters and the overlap of miRNAs or genes, as well as between the similarity of expression pattern and enriched biological pathways. Second, it demonstrated the participation of the hsa-miR-29 family in the early differentiation of stem cells. Second, it revealed significant correlations and pathway associations between miRNAs and genes during this differentiation process. Finally, it uncovered the occurrence of re-replication events in differentiating human skeletal myoblasts and human mesenchymal stem cells undergoing chondrogenesis.

Positive trends that shed light on the relationship between the similarity of expression patterns in clusters and the overlap of miRNAs or genes were observed. This observation implies that miRNAs and genes within these clusters may play essential roles in driving specific cellular processes and functional outcomes during differentiation. Additionally, reciprocated positive trends between enrichment in certain biological pathways and similarity of pattern of expression were also observed in several analyses. Notably, pathways with functional biological relevance to the future cell type of the differentiating cells were found. For example, differentiating HSkMs were associated with pathways from broad categories like "muscle" and "muscle contraction", and differentiating hNSCs were found to be enriched in pathways from the "membrane & channels" category. Clusters enriched in pathways related to cell cycle and differentiation were consistently associated with the early stages of differentiation assays.

The miR-29 family, a group of four miRNAs, was found to be among the top 10 decreased miRNAs in all differentiation assays and almost always in the same cluster. The targets of these miRNAs were overrepresented in certain clusters, most of which showed increased expression. Pathways related to cell cycle and differentiation were enriched in all differentiation assays in clusters including the members of the hsa-miR-29 family or including a majority of their targets, as well as in the 94 shared targets among those known for the members of this family.

Re-replication was observed between 2 h and 6 h in spontaneously differentiating HSkM cells, but not at 0 h, 1 h, or 7 h, indicating that re-replication occurs only within a defined time frame. No re-replication events were observed in proliferating HSkM cells.

5.4. Interpretation of the findings

5.4.1. Transcriptome and miRNome analysis during early differentiation of hMSC, hNSC, and HSkM

Analysis of the microarray experiments revealed that the number of miRNAs detected in each differentiation assay was consistent across time points, ranging from 300 in the hMSC differentiation assays to 600 in the HSkM differentiation assay. The majority of miRNAs detected at 0 h were found to be shared by all differentiation assays. Similarly, the number of genes detected was also found to be relatively uniform over time, with an average of 32,038 genes. Nearly 25,000 genes were found to be shared by all five differentiation assays.

RNAs were considered deregulated if their expression levels exhibited a fold change of at least 1.5 between their minimum and maximum values. Strikingly strong changes in the number of deregulated RNAs were observed at specific time points, often in both miRNAs and transcripts. These time points did not correspond to particularly high numbers of detected RNAs. In the hMSC osteogenesis and the HSkM differentiation assays, the 12 h and 48 h time points showed the highest numbers of deregulated miRNAs. In the hMSC adipogenesis assay, the 6 and 12 h time points had the highest numbers of deregulated miRNAs, while in the hMSC chondrogenesis assay, the highest numbers were observed at 48 h, and in the hNSC differentiation assay at 3 and 48 h. These time points of highest deregulation were different between differentiation assays, as expected based on previous literature [453,465]. In general, there were comparable numbers of up and down-regulated miRNAs at each time point, with some exceptions. Similar time points for deregulated genes were observed, except for the hMSC adipogenesis assay, where the highest numbers were recorded at 9 and 24 h, and for the hMSC osteogenesis assay, where the gene numbers were the second lowest at 48 h. This may be because the measurements were taken at intervals of 3 to 24 hours, which would be enough time for miRNA-mediated repression of translation or miRNA-mediated mRNA degradation, which can occur within minutes to hours [37].

The scale of the numbers of deregulated miRNAs and genes was overall different between the assays, as expected from the numbers of detected RNAs. However, the number of deregulated genes did not always reflect the number of deregulated miRNAs. For example, the HSkM differentiation assay showed the highest number of deregulated miRNAs and only an average number of deregulated transcripts. The three hMSC

differentiation assays and particularly the hMSC chondrogenesis assay had low numbers of deregulated miRNAs but large numbers of deregulated genes. This suggests that different cell types and differentiation processes may rely on distinct regulatory mechanisms, where the relationship between miRNAs and their target genes can vary significantly and underscores the complexity of gene regulation during cell differentiation.

A significant number of shared RNAs were also observed. The biggest shared miRNA category was those deregulated in the HSkM and hNSC differentiation assays, which was expected, due to the much higher numbers of detected miRNAs in these differentiation assays. The biggest shared gene category was the genes deregulated in all differentiation assays, which was also expected. High numbers of shared genes were observed between all hMSCs differentiation assays (with or without HSkM differentiation assay), which was also expected, due to their common origin.

Overall, high proportions of detected RNAs were categorized as deregulated when considering all time points (62 to 93 % of transcripts, and 42 to 99 % of miRNAs). This was anticipated as differentiating stem cells exhibit significantly distinct expression profiles in comparison to their proliferating counterparts.

To note, Marcon and colleagues conducted polysomal profiling on human adipose tissue-derived stem cells undergoing adipogenesis and osteogenesis and observed a significant reduction in translational efficiency 24 hours after induction of differentiation. These results do not necessarily oppose the findings of this work; however, they are considered significant and, therefore, warrant mentioning [363,364].

To further analyze the microarray data, groups of miRNAs (or genes) following similar expression trajectories were determined via fuzzy c-means clustering, which was further refined through manual analysis of the minimum cluster centroid distance plot and overlap plots.

Overlap analysis revealed that manual selection of pairs or trios of clusters with similar expression patterns resulted in significantly more overlap in the numbers of shared miRNAs or genes, compared to randomly drawn pairs or trios of clusters. Thus, clusters with very similar expression patterns in different differentiation assays tended to share more RNAs than random control pairs or trios from different differentiation assays, indicating a possible overlap in the underlying regulatory mechanisms of differentiation in the stem cell types studied.

Analysis of the patterns showed that well-defined clusters with a high mean membership score, indicating well-defined expression patterns, tended to be associated with a small number of strong expression peaks, which also correspond to the time points where the highest number of deregulated miRNAs were observed compared to the start of induction. This observation supports the notion that miRNAs play a crucial role in repressing mRNA expression during early differentiation processes. Several genes have been linked to stemness and the process of stem cell differentiation in various cell types. Notable examples include Oct4/POU5F1, Sox2, c-Myc, and Nanog, which are some of the key factors used for the reprogramming of induced pluripotent stem cells [115,209,275,522,523,608,624]. Other important regulators of stem cell differentiation include Wnt, Notch, ERK/MAPK1, GSK3, and BMP signaling pathways, but also p63, Pax6, and Runx2 [114,209,417,453,596,624].

Alternatively, these genes might be associated with other changes happening concomitantly in these cells, like cell division and therefore replication, or reacting to temperature or medium changes, but probably not directly with confluency changes, since re-plating of the cells was conducted 24 h before induction of differentiation.

The patterns of expression of some miRNA-mRNA cluster pairs seemed anti-correlated, which was studied further by comparing enrichment in biological pathways. The results showed a tendency (significant in one case) towards similarity in both enriched pathways and expression patterns for clusters enriched in similar pathways.

Clusters exhibiting mirrored expression patterns might also suggest that genes included in these clusters are associated with differentiation (upregulated) or associated with stemness processes (downregulated). Overall, the timeframe for expression changes in genes related to differentiation or stemness upon induction of differentiation is complex and context-dependent. In some cases, changes in gene expression can be observed within a few hours of the initiation of differentiation or reprogramming, while in other cases, it may take several days or even weeks for significant changes to occur [240,398,452,465].

The comparison of enriched pathways in the microarray data aimed to answer two primary questions: 1) Are enriched pathways similar in miRNA-mRNA cluster pairs that appear to have anti-correlated patterns? 2) Are expression patterns similar for clusters enriched in similar pathways?

While there were no pathway similarities in the hMSC adipogenesis assay, there were two miRNA-mRNA cluster pairs in the hMSC chondrogenesis assay that were enriched in

immune system-associated signaling pathways, one pair of the hMSC osteogenesis assay enriched in both immune system-associated signaling and collagen or ECM pathways. There was also one pair of the hNSC differentiation assay enriched in translation-associated pathways and another pair of the same assay enriched in both immune system-associated and membrane pathways, and three pairs of the HSkM differentiation assay enriched in both cytoskeleton and muscle-associated pathways, muscle and cell differentiation-associated pathways, and muscle development pathways respectively.

To answer the second question, pathway similarities were considered across a few broad categories. A miRNA cluster and two gene clusters of the hMSC osteogenesis assay, as well as three gene clusters of the hMSC chondrogenesis assay were enriched in pathways from the category "collagen and extracellular matrix", and their expression patterns presented some similarities. Pathways from the category "immune system signaling" were enriched in at least one miRNA and one gene cluster in all differentiation assays, with overall trends very similar in the miRNA clusters. Two miRNA clusters and one gene cluster of the HSkM differentiation assay were found to be enriched in pathways from the "transcription" category, as well as gene clusters of the hMSC chondrogenesis, osteogenesis, and hNSC differentiation assays. The expression pattern of the HSkM gene cluster mirrored the pattern of one of the miRNA clusters from the same assay. Pathways from the categories "cell cycle", "differentiation and development", and "senescence" were enriched in miRNAs clusters from the hMSC adipogenesis, osteogenesis, hNSC, and HSkM differentiation assays, and in gene clusters from all differentiation assays. Three gene clusters showed increased expression levels at 24 and 48 hours, while many miRNA clusters were found to have low expression levels at these time points. The expression pattern of a gene cluster of the hMSC adipogenesis assay mirrored the pattern of one of the miRNA clusters from the same assay.

Overall, this suggests that there is a tendency towards similarity in both enriched pathways and expression patterns for miRNA and gene clusters. Additionally, pathways with biological relevance to future cell types were found to already be enriched in the hMSC chondrogenesis, osteogenesis, hNSC, and HSkM differentiation assays, as well as pathways associated with cell cycle, differentiation, and development in all differentiation assays. These findings suggest early activation of the different fates in the differentiating cells. This can also be found in studies profiling differentially expressed genes of differentiating hMSCs [137] and HSkMs [100,569], although at later time points. Upregulation of muscle contraction transcripts in differentiating HSkMs and thereby a

potential early activation of the muscle differentiation program would not be unexpected since these cells are already more specialized stem cells than hMSCs for example.

Interestingly, immune system-associated pathways were also enriched in multiple differentiation assays, which correlates well with the current literature [69,100,612]. However, this might be due to a bias in reported pathways in the literature, due to some miRNAs, genes, and pathways being more extensively studied than others.

When considering the ten miRNAs and transcripts that showed the greatest increase or decrease in expression between two time points, a few RNAs were found in more than one differentiation assay. Members of the miR-29 family were downregulated in all 5 assays (nine times in total), while hsa-miR-221-5p was downregulated in the hMSC adipogenesis and chondrogenesis assays, and hsa-miR-6785-5p was upregulated in the hMSC adipogenesis, hNSC, and HSkM differentiation assay. MMP1 was downregulated in the hMSC chondrogenesis and osteogenesis assays, while FOSB was downregulated in two differentiation assays (hNSC and HSkM) but upregulated in the hMSC adipogenesis assay. This might indicate that these transcripts and miRNAs play a role in differentiation processes, not specifically in only one process. Examples of miRNAs involved in more than one differentiation process are numerous in the literature: hsa-miR-155-5p (adipogenesis: Liu, Yang and Wu, 2011; chondrogenesis: Lee *et al.*, 2015; odontogenesis: Zhu *et al.*, 2022; osteogenesis: Liu *et al.*, 2018), hsa-miR-221-5p (adipogenesis: Xie, Lim and Lodish, 2009; chondrogenesis: Lolli *et al.*, 2014; myogenesis: Cardinali *et al.*, 2009; neurogenesis: Cheng *et al.*, 2014; osteogenesis: Yeh *et al.*, 2016), hsa-miR-29a-3p (chondrogenesis: Guérit *et al.*, 2014; myogenesis: Galimov *et al.*, 2016; neurogenesis: Li *et al.*, 2014; osteogenesis: Tan, Peng and Guo, 2018), hsa-miR-4459 (stemness: Lu *et al.*, 2015), hsa-miR-7-5p (adipogenesis/osteogenesis balance: Chen *et al.*, 2020), etc. At the moment of writing this thesis, hsa-miR-494-3p has only been associated with myogenesis [237], hsa-miR-6785-5p with osteogenesis [113], and hsa-miR-7641 with endothelial differentiation [606]. However, these greatly increased or decreased RNAs could be involved in other processes happening simultaneously in the differentiating stem cells, as discussed previously.

Some specific RNAs or pathways also suffer from reporting bias in the literature, some being largely more studied than others, and negative results being mostly unreported [276,418].

The miRNA cluster 3 of the hMSC osteogenesis assay contained all ten most strongly upregulated miRNAs, which did not overlap with any highly upregulated miRNAs of the other differentiation assays. This cluster is characterized by a strong upregulation between 24h and 48h after induction of differentiation and might be comprised of miRNAs specifically involved in osteogenesis. Seven of the ten miRNAs have not yet been described in the literature as associated with any differentiation process, and the other three, hsa-mir-3658, hsa-miR-640, and hsa-miR-665, have only been correlated with osteogenesis as of the time of writing [333,498].

Analysis of enriched pathways based on the ten most strongly deregulated transcripts and miRNAs of each differentiation assay showed that hMSCs undergoing adipogenesis strongly upregulated transcripts linked to immune system signaling pathways and to metal ions. HMSCs in the chondrogenesis assay strongly downregulated miRNAs associated with the cytoskeleton, organism development, differentiation, and stemness; while hMSCs undergoing osteogenesis both up- and downregulated transcripts related to signaling pathways, including from the immune system. Differentiating HSkM strongly upregulated transcripts linked to muscle contraction, cytoskeleton, and translation, and both up- and downregulated miRNAs associated with membrane, metal ion, and pore and protein channel.

Interestingly, the results of both enrichment pathway analyses overlapped in part: signaling pathways of the immune system and pathways with physiological relevance in the future cell type. While there is a bias in reported pathways in the literature and therefore in these enrichment analyses, these results might hint at significant pathways for the early differentiation of the cell types studied.

Several miRNA clusters showed strong connections to specific mRNA clusters in each differentiation assay, and their centroid lines often exhibited mirrored patterns, which is expected due to the regulatory role of miRNAs in repressing mRNA expression or promoting their degradation [28,193].

In previous studies profiling miRNome or transcriptome during stem cell differentiation, clusters with recognizable expression patterns were already observed, for example by Ghila and colleagues [176] or by Ng and colleagues [407]. However, the most interesting study to compare these results to might be by Li and Wang [330]. In their scientific paper, they profiled the transcriptome of hMSCs undergoing osteogenesis 2, 8, 12, and 25 days

after differentiation induction and compared it to undifferentiated hMSCs. Although they used a much higher number of clusters, some were similar to the clusters obtained during the present thesis. Interestingly, well-defined clusters with a high mean membership score and associated with a strong expression peak were also observed, mostly between the undifferentiated and day 2 cells, which corresponds to the time frame used in the present work.

The comparison of the centroid lines of strongly interacting cluster pairs showed that these often exhibited mirrored expression patterns and that peaks in these patterns were mainly observed at the same time points. While the dissociation rate of miRNA and mRNA is usually in the range of a few hours, it highly depends on the RNA themselves, their respective concentrations, and the binding strength (which itself depends on the RNA sequences, and therefore the k-mer used) [256]. Bisaria and colleagues described the miRNA-induced cleavage rate of mRNA as very quick, in the range of 1 to 10 minutes^{-1} [37], which would agree with our findings of quasi-simultaneous changes in miRNA and mRNA expression.

Further analysis of interactions involving the top-ranked miRNAs and genes revealed the presence of both previously identified and novel cluster pairs, suggesting a potentially influential role from a few miRNAs or genes in these previously unidentified cluster pairs in driving the observed effects. Specifically, notable associations were observed in the hMSC adipogenesis assay between the miRNA clusters 4 and 5 with gene cluster 2, miRNA cluster 5 with gene cluster 9, and miRNA clusters 1 and 4 with gene cluster 2. In the hMSC chondrogenesis assay, miRNA cluster 4 was associated with gene cluster 1, and in the hMSC osteogenesis assay, miRNA cluster 6 was connected with gene cluster 2, and miRNA cluster 5 with gene cluster 3, while no significant associations were found in the hNSC and HSkM differentiation datasets.

Almost 60% of the miRNAs in the interaction networks across all five differentiation assays have been reported as involved in at least one differentiation process, although not always the one in the context in which they were identified in this work. As expected, most of the miRNAs previously described in the literature were members of strongly interconnected cluster pairs, except for the miRNA cluster 4 and gene cluster 3 of the hMSC osteogenesis assay, in which most miRNAs have not yet been described as contributing to differentiation. Another cluster pair, miRNA cluster 3 and gene cluster 3 of the hNSC differentiation assay, also stood out during this comparison, as manual searches indicated reports of many of the miRNAs of this cluster regulating differentiation, but the pair was

not strongly interacting according to the interaction strength diagram. Some note-worthy miRNAs in the interaction networks include miR-221-3p, which has been shown to play a role in the five differentiation processes studied here, the miR-29 family, collectively involved in all five differentiation processes investigated in this work according to literature, and miR-222-3p, which has been shown to regulate adipogenesis, osteogenesis, neurogenesis, and myogenesis, but was found in the HSkM differentiation assay as well as in the hMSC chondrogenesis and adipogenesis assay.

The microarray data of the hMSC adipogenesis and osteogenesis assays were examined for hints of the adipogenesis-osteogenesis balance. While some expected changes in gene expression levels were visible, a similar number of unexpected changes were also observed. Furthermore, the majority of genes did not display any significant alterations, which could indicate a random occurrence.

Perhaps the experimental timeframe of this study was too early compared to the study by Scheideler and colleagues, which may explain why their results could not be replicated (Scheideler et al., 2008). Other researchers observed changes in expression levels related to the adipogenesis-osteogenesis balance at later time points (Beresford et al., 1992; James et al., 2010; Robert et al., 2020; Yi et al., 2022).

Additionally, the balance between adipogenesis and osteogenesis is not a clear-cut matter, and some signaling pathways, such as the BMPs and IGF-1 pathways, are involved in both differentiation directions. For instance, BMP-2 can induce adipogenesis at low levels while promoting osteogenesis at higher levels (Kang et al., 2009; James, 2013). Moreover, some partial PPAR-γ agonists support adipogenesis without inhibiting osteogenesis, while others inhibit osteogenesis without promoting adipogenesis (Lecka-Czernik et al., 2002).

An alternative explanation is that the regulation of the adipogenesis-osteogenesis balance and possibly other essential biological processes during stem cell differentiation could be happening at another level. Studies by Van de Peppel and colleagues and Marcon and colleagues using polysomal profiling in human adipose tissue-derived stem cells undergoing osteogenesis and adipogenesis respectively revealed significant changes in the polysomal fraction but no change in total RNA expression levels. Furthermore, they showed that protein synthesis as a whole was reduced (Marcon et al., 2017; van de Peppel et al., 2017). This suggests that the regulation of essential biological processes during stem cell differentiation may occur primarily at the translational level.

It may be worthwhile to investigate the post-transcriptional regulation level by miRNAs as well, due to their general role in differentiating stem cells.

The microarray data were analyzed to identify miRNAs previously described in the literature as enriched in ESCs or involved in their differentiation and transcriptome regulation. Out of the 168 miRNAs examined, a total of 41 were detected, with some being present in more than one or even in all differentiation assays.

Among the six groups of ESC-enriched miRNAs, four were represented in the stem cells studied here, which is consistent with the specialization and therefore reduced potency of these stem cells compared to ESCs. The absence of the miR-200 family and miR-302 cluster in the microarray may indicate their specificity to ESCs. It was anticipated that these miRNAs would be downregulated upon differentiation induction, which was true for the miR-17 family (except in the hMSC adipogenesis assay) and miR-371/373 cluster. These findings raise intriguing questions about the potential roles of the miR-17 family and miR-371/373 cluster in stem cells in general. Further investigation is warranted to unravel their precise contributions to stem cell biology and differentiation.

However, the results regarding the chromosome 19 miRNA cluster and miR-130 family were not as expected. Contrary to the anticipated downregulation, the chromosome 19 miRNA cluster exhibited an upregulation, while the miR-130 family displayed varying expression patterns. The primate-specific chromosome 19 miRNA cluster is considered to be exclusively expressed in ESCs and the reproductive system and is known to be transcribed from a common long noncoding transcript [153,396]. The detection of these miRNAs in the context of this study raises intriguing questions, especially the limited detection of only one or five members, rather than the entire cluster. Notably, the miR-130 family has been reported to stimulate the reprogramming of induced pluripotent stem cells (iPSCs) [432], indicating its relevance to pluripotency.

Additionally, it is known that ESC-enriched miRNAs are also enriched in certain cancers [21,163,175,253,254,362,409,477,566,614], as cancer cells often re-express stem cell-related factors as part of their aberrant behavior [287]. This highlights the complex and dynamic relationship between stem cells and cancer, which warrants further investigation to unveil the underlying mechanisms driving these connections.

Additional miRNAs critical for the self-renewal and proliferation of human ESCs include hsa-miR-195 and hsa-miR-372 [437]. Although hsa-miR-372 is part of the miR-371/373 cluster, it was not detected in the microarray data, which could suggest a more specialized role or possibly a limitation of the microarray method in capturing its expression. hsa-miR-195 showed low expression levels but exhibited first an upregulation followed by downregulation. This dynamic expression pattern may be attributed to its role in replication and proliferation processes, implying that it is essential during specific stages of ESC differentiation.

The low expression of certain miRNAs, such as members of the let-7 family and hsa-miR-145, might also contribute to the maintenance of the ESC phenotype [369]. Interestingly, hsa-miR-145 was upregulated, as expected, supporting its potential role in maintaining the ESC characteristics at a low expression level and in regulating the ESC transcriptome at a higher level [504,590]. On the other hand, the let-7 family showed diverse expression patterns, making it challenging to discern a common theme, except for a potential upregulation in hMSC differentiation assays. The varied expression of let-7 miRNAs might indicate their involvement in regulating specific processes during differentiation and warrant further investigation to understand their precise roles in stem cell fate determination.

Numerous miRNAs have been reported to be involved in regulating the ESC transcriptome and influencing ESC differentiation [31,536]. Notable examples include mmu-miR-200c, mmu- and hsa-miR-203, mmu-miR-183 [575], mmu-let-7 [383], hsa-miR-134, mmu- and hsa-miR-296, and mmu-miR-470 (which lacks a direct human homolog) [532]. Interestingly, among the miRNAs mentioned, only hsa-miR-296-5p was identified in this study. It was detected in the hNSC and HSkM differentiation assays, exhibiting an upregulated expression pattern, which aligns with the expectations based on its previously reported roles in stem cell regulation.

These findings highlight the need for further exploration to fully understand the intricate regulatory roles of these miRNAs in the context of ESC differentiation.

The miR-29 family, consisting of hsa-miR-29a-3p, hsa-miR-29b-1-5p, hsa-miR-29b-3p, and hsa-miR-29c-3p, was found in this study to be among the most sharply decreased miRNAs in all differentiation assays. Additionally, the expression patterns of this miRNA family were consistent across all differentiation assays, except for hsa-miR-29b-1-5p in the hNSC and HSkM differentiation assays. Their targets, which overlap broadly, were

over-represented in certain clusters, mostly exhibiting increased expression levels. The set of 94 mRNAs predicted to be targeted by all members of the hsa-miR-29 family, showed enrichment in pathways from the broad category of "cell cycle and differentiation" in all five differentiation assays. The same pathway enrichment was found in all differentiation assays in the cluster comprising the members of the hsa-miR-29 family or a high proportion of their targets.

This might mean that these miRNAs act as inhibitors of differentiation, and therefore downregulation of this miRNA family at the beginning of differentiation is necessary. Alternatively, this miRNA family might be associated with other changes happening concomitantly. The scientific literature is also divided on this subject. On one hand, some studies suggested that rodent and human miRNAs from this family inhibit adipogenesis, chondrogenesis, and neurogenesis [192,204,281,594]. On the other hand, other researchers proposed that members of this family promoted chondrogenesis, myogenesis, neurogenesis, and osteogenesis in human and mouse models [99,187,282,332]. To note, the time frames considered vary between studies, making the direct comparison more challenging. Further investigation is warranted to elucidate the role of this miRNA family during differentiation.

The role of the miR-29 family during aging is less ambiguous: they exhibit an increase in expression levels with age, as exemplified by the Tabula Muris Senis dataset [273,561]. The miR-29 data from the tissues and organs of the Tabula Muris Senis that most closely match the stem cell types used in this work all present the same trend. These miRNAs have also been described as involved in multiple processes pertaining to aging and senescence, as well as in cancer [10,218].

In conclusion, the findings in this work regarding the miR-29 family's role in early stem cell differentiation suggest that these miRNAs may function as inhibitors of differentiation, necessitating their downregulation at the onset of differentiation. Further research is needed to fully understand the precise role of the miR-29 family during differentiation, considering the variation in time frames among different studies. Understanding the role of the miR-29 family in differentiation and aging could have significant implications for regenerative medicine and therapeutic interventions in age-related diseases and conditions.

5.4.2. Re-replication analysis during HSkM and hMSC early differentiation

A combination of incorporation of thymidine analogs and the molecular combing method was used to explore the potential role of re-replication in the generation of gene amplifications during stem cell differentiation.

Qualitative analysis of HSkM differentiation revealed no evidence of re-replication events at the time points 0 h, 1 h, and 7 h, only normal replication events were observed. However, re-replication events were detected between time points 2 h and 6 h, with the highest incidence at 4 hours.

In the quantitative analysis of HSkM cells, no re-replication events were observed in proliferating cells. However, re-replication events were detected at time points 1 h (2.3 % of recorded events), 4 h (7 % of recorded events), and 6 h (6 % of recorded events) during differentiation. Interestingly, there were more cells positive for thymidine analog incorporation at the 4 h differentiation time point compared to the 4 h proliferation time point. The length of thymidine analog incorporation stretches indicative of re-replication events was shorter at the 1 h timepoint compared to the 4 h and 6 h timepoints in differentiating HSkM cells.

These observations suggest that re-replication in these cells only occurs during a specific period following the induction of differentiation. Assuming replication takes at least 10 hours in HSkM (approximate mean value for quickly dividing human cells, [35,186]) and since replication events were observed as early as in the 1 h time point, re-replication appears to happen early during the replication process, possibly during the first half or even quarter of the S phase. Furthermore, more replication occurred in HSkM cells undergoing differentiation at the 4 h time point than in proliferating cells, indicating that differentiation induces replication. Additionally, differentiation also induces re-replication within a specific time frame (between the 1 h and 6 h time points, with the highest incidence at the 4 h time point). This specific time window suggests it is induced by early differentiation signals but tightly regulated.

A key technical limitation of the molecular combing approach is the potential for overlap of fibers on the silanized coverslips, which can complicate analysis. Although extensive

efforts were made to manually validate each quantified fiber and discard ambiguous ROIs with possible overlap, there remains a chance of overlap bias influencing the frequency of re-replication event detection. Overlapping fibers could allow analog pulses in different fibers to appear as re-replication events within a single fiber. This could lead to an overestimation of re-replication frequency. However, the differentiation time points exhibited substantially more re-replication events compared to proliferating controls. Given proliferating and differentiating cells were prepared identically, overlap biases should theoretically impact both. The significant differences observed between conditions suggest true biological differences exist in re-replication incidence. Nonetheless, the potential impacts of fiber overlap must be considered. Applying more stringent criteria for fiber validation may further minimize artifacts, although reducing analyzed events. Overall, while fiber overlap bias remains a technical limitation, the relative differences between conditions likely reflect meaningful biological phenomena worthy of further investigation into re-replication during early stem cell differentiation.

Research has demonstrated that GEMININ (GMNN) is necessary to prevent re-replication in proliferating cells, including embryonic stem cells [222,427], and to regulate chromatin remodeling to maintain undifferentiated states of stem cells [600]. Additionally, the depletion of GMNN has been shown to induce terminal differentiation into nonproliferating giant cells in trophoblast stem cells [102]. This might suggest that GMNN expression decreases after differentiation induction, which was observed in the accompanying experiments of this work [389].

Quantitative analysis of hMSCs (human mesenchymal stem cells) undergoing chondrogenesis showed replication-typical thymidine analog incorporation in all assays, including proliferating cells at timepoint 0 h. Re-replication events were visible in all assays, including proliferating cells at timepoint 0 h. Of note, the segments indicative of re-replication events were relatively short at the 4 h timepoint during hMSC chondrogenesis (median length of 3.3 kb), while they were longest at the 6 h timepoint with a median length of 16.9 kb.

In these cells, induction of differentiation does not seem to increase the replication rate compared to proliferating cells. Re-replication events appear to be ubiquitous, occurring in proliferating as well as in cells undergoing chondrogenesis, and in all three time points tested. This might indicate that the re-replication time frame may be broader, or even that

re-replication might happen naturally in these cells. This could hint at a potential cell-type specific regulation.

In the existing literature, re-replication has been consistently linked to adverse effects, such as DNA damage and apoptosis [5,17]. However, a potential tolerance for a small amount of re-replication events has already been proposed in the literature [460] and is discussed in 5.7.2. Alternatively, similar to the HSkM quantitative analysis, there is still a possibility of bias due to overlapping fibers, despite the manual validation of each fiber and the high numbers of discarded fibers. In contrast to HSkMs, the culture conditions for hMSCs did not permit any discernible degree of synchronization of the cell cycle, potentially accounting for the wider time frame of re-replication events.

Induction of differentiation seems to induce replication in HSkMs, as seen when comparing the 4 h time point in differentiating and proliferating cells. In hMSCs undergoing chondrogenesis, the effect is less clear between differentiating and proliferating cells. The effect of differentiation on replication induction has been described in multiple studies using various stem cell types.

As an example, Ikeda and colleagues reported seeing upregulation of cell proliferation at initial time points during chondrogenesis [233]. Satellite cells, another type of muscle stem cells, seem to proliferate immediately after muscle injury, accompanied by a transient drop in the expression of miR-1 and miR-206, which are known to suppress cell proliferation [110,202,246,609]. According to Marquez and colleagues and Patel and Lane, preadipocytes undergo clonal expansion until confluence [366,426]. On the other hand, Hung and colleagues found genes related to growth arrest to be upregulated three days after adipogenic induction [225]. Adipocytes were also described as having stopped proliferation at later time points [452]. Marcon and colleagues also reported that adipogenesis was associated with the downregulation of cell cycle-related genes and with lower proliferative activity 24 h after induction of differentiation [363,364], although their 24-hour-long treatment with EdU might have been too long for the cells. Finally, there is conflicting evidence regarding the effect of osteogenesis on the cell cycle. Some studies suggest that it stops cell cycle progression [64,249], while others report that it leads to increased cell proliferation [452]. In the adult brain, neural stem cells are one of the few cell types still dividing, and their proliferation is the first stage in the neurogenesis process [45,181].

Overall, in the stem cell types studied in this work, differentiation induction appears to trigger cell proliferation and therefore replication, at least in the timeframe studied here.

5.5. Strengths and limitations of this work

This work has generated novel time-resolved data on miRNA and gene expression changes in the initial 48 hours of stem cell differentiation. The high-resolution view of early molecular events provides unique insights not captured in most prior studies, which typically characterize later differentiation stages. The use of primary cells and differentiation of healthy human stem cells is a significant strength, providing findings that more closely reflect normal biology compared to cancer or model cell lines. This will aid the understanding of human development and disease.

The analysis of multiple human stem cell types (hMSCs, hNSCs, HSkMs) differentiating into distinct lineages allows for interesting comparisons of the dynamics and mechanisms underlying fate transitions across cell types. Few studies have examined miRNA and transcriptome changes so broadly. The unbiased analysis of all expressed miRNAs and genes, without pre-selecting candidates, allowed novel patterns, clusters, and families to emerge, revealing new candidate regulators like the miR-29 family that warrant future investigation.

The multi-level approach integrating miRNome, transcriptome, and replication timing analyses provides a systems perspective. The ability to correlate miRNA and mRNA expression changes is a key advantage, yielding insights into miRNA-mediated regulation.

This thesis capitalizes on the molecular combing technique, which offers enhanced sensitivity and resolution to directly visualize replication and re-replication events at the single DNA molecule level. To the best of our knowledge, this method has not been previously used to study re-replication.

Overall, the complementary multi-omics analyses of healthy differentiating human stem cells in this work provide novel, timely, and valuable contributions to the understanding of molecular processes regulating cell fate.

Despite the challenges brought about by the COVID-19 pandemic; this research has successfully been completed with a limited but valuable number of replicates. Although conditions did not permit the replication of microarray experiments, this opens up exciting avenues for further investigations into the reproducibility of our findings. Due to circumstances, we focused our efforts and resources on the most promising aspects of our work. Additional replicates would allow statistical analysis to confirm reproducibility. Nevertheless, clear patterns were observed in the datasets obtained. While the planned study of re-replication during the differentiation of hNSCs and hMSCs into adipocytes and osteocytes was not feasible this time, it is part of future objectives, offering promising potential for further exploration and understanding in these areas.

Moreover, the inherent limitations of transcriptome analysis, which do not facilitate the direct assessment of protein levels, necessitate careful interpretation of findings. Augmenting this approach with protein quantification techniques, such as Western Blotting, would offer a more comprehensive validation of mRNA results.

Some biological assumptions were made in this work, including the fact that replication forks containing re-replication events are symmetrical, although it was shown by Osheim and colleagues that this is not always the case, at least in *D. melanogaster* [420]. This may have implications for the measurements of replicated and re-replicated DNA segments. However, given the current uncertainty about its frequency, it was deemed less critical for the scope of this exploration study.

Another assumption that should be put in perspective is that the mechanism(s) for the formation of gene amplification is similar between human cells, namely stem and cancer cells. While we do not currently have information about this particular question, it was suggested that the mechanisms for gene amplification were different between *Drosophila* and mammals [199].

In recent works, the term eccDNAs, or "extrachromosomal circular DNA", has emerged [395]. According to these works, double minutes constitute one class of eccDNAs [284]. The formation process of eccDNAs remains somewhat enigmatic; while some studies indicate a replication-dependent mechanism, others report the occurrence of eccDNAs in the absence of replication [82,428,517]. They have been linked to gene amplifications and copper resistance in *S. cerevisiae* and therefore may benefit from investigations of these mechanisms [224].

5.6. Future directions

5.6.1. miRNome and transcriptome profiling

Replicating the miRNome and transcriptome profiling of healthy differentiating human stem cells using single-cell sequencing methods like the co-sequencing of miRNAs and mRNAs described by Wang and colleagues might be a good approach to further characterize miRNA-gene correlations [567]. However, it might be necessary to synchronize the cells to hopefully obtain a higher number of differentiating stem cells, and this might influence their metabolism in non-physiological ways. This method might also be less sensitive to less strongly expressed miRNAs and genes than conventional single-cell sequencing methods, which themselves have low sensitivity.

To further validate and extend the transcriptomic findings of this work, quantification of protein levels is an important future direction. While mRNA expression provides insights into gene regulation, protein levels more directly indicate functional impacts. Techniques such as Western blotting could be utilized to quantify changes in protein abundance of key miRNA targets and genes associated with differentiation or stemness at multiple time points. Comparing miRNA and mRNA trajectories with protein dynamics would allow stronger validation of regulatory relationships. If discordant trends are observed, it may indicate regulation at the translational level. Proteomics could also help corroborate if transcriptional changes related to the adipogenesis-osteogenesis balance manifest at the protein level. Overall, augmenting the transcriptomics approach of this study with targeted protein quantification will be key to gaining a multi-dimensional understanding of the signaling networks and post-transcriptional regulation governing early stem cell differentiation.

Another interesting approach to consider is polysomal profiling, which involves isolating and profiling the mRNA fraction bound to polysomes - clusters of ribosomes that are actively translating an mRNA strand [157]. This method has been successfully implemented in human adipose tissue-derived stem cells undergoing adipogenesis and osteogenesis, although not in a time-resolved manner [363,364,452,501].

To validate the functional impact of the hsa-miR-29 family in differentiating stem cells, a comprehensive approach involving both RNA and protein quantification of miR-29 targets at multiple time points would be essential. This would provide valuable insights into the

direct regulatory effects exerted by the miR-29 family on its target genes during the differentiation process. Additionally, employing gene knockdown or overexpression experiments specifically targeting the miR-29 family could further corroborate their roles in modulating stem cell fate and differentiation.

5.6.2. Re-replication timing

Studies of re-replication in almost physiological conditions report this phenomenon happening at early replicating regions [159,549], which is consistent with the fact that re-replication must occur in previously replicated regions and, therefore, is more likely to occur in regions that undergo replication earlier in the cell cycle. It could be insightful to identify which regions are re-replicated in the model used in this thesis and compare these with known early replicating regions. The observation that gene amplifications frequently occur in similar regions also raises questions regarding their association with early origins or regions that have undergone re-replication and might be tested with the same data. A method that might be used for this purpose, Rerep-Seq, was described by Menzel and colleagues in 2020 and is currently being implemented by a member of the Institute for Human Genetics. This technique uses thymidine analogues to isolate re-replicated sequences [387]. It could identify genomic sites of re-replication and determine if they correlate to common amplification regions.

In this thesis, naturally occurring re-replication during the S phase of the cell cycle was studied. However, the timing of re-replication is not yet clear, and there is conflicting evidence in the literature. Re-replication caused by re-licensing of origins during the G2 and M phases has been described in three studies [29,280,410]. However, these results do not describe physiological situations. Nguyen and colleagues deregulated expressions of ORC, MCM2-7, or CDC6, although to moderate levels. For example, they transiently induced the expression of a modified, more stable CDC6 for 1 or 2 hours, which allowed them to reach levels less than twofold higher than the highest levels of endogenous CDC6 they measured [410]. Nevertheless, this induction was high enough to observe high levels of re-replication. Klotz-Noack and colleagues ablated Geminin altogether and observed that no specific genomic regions were re-replicated, which correlated with the fact that cells in the G2 phase have no replication timing information left [280]. In these two scientific articles, cells in which re-replication was induced remained blocked in the G2/M phase. Bellanger and colleagues knocked down cyclins B1 and B2 by RNA interference and

reported that the knockdown of only one cyclin did not show significant alteration of the cell cycle. But when both cyclins were depleted, multiple cell cycle and replication errors occurred, including endoreplication (that they called re-replication) [29].

Studies reporting re-replication under physiological conditions are much sparser, thus it is much harder to estimate the timing of naturally occurring re-replication. One hypothesis to explain the discrepancy between the phases during which re-replication is observed might be that the effects of deregulated or depleted proteins are too strong to mimic physiological situations. Under these circumstances, there seems to be a certain level of DNA damage due to colliding forks that can be tolerated before the ATM/ATR checkpoint is activated [460,482]. Considering the limited availability of studies reporting re-replication under physiological conditions, further research is essential to gain a more comprehensive understanding of the timing and occurrences of naturally induced re-replication events. Investigating the effects of deregulated or depleted proteins in more physiologically relevant settings may provide valuable insights into the factors influencing re-replication dynamics. Moreover, exploring the mechanisms of DNA damage tolerance and its implications for ATM/ATR checkpoint activation could shed light on the thresholds of tolerable DNA damage during replication. Continued investigation in these areas will contribute to a deeper comprehension of re-replication processes in the context of natural cell differentiation and replication, potentially uncovering new avenues for therapeutic interventions or disease prevention.

5.6.3. Applications, recommendations, implications

Based on the results of the present work, re-replication appears to occur in the first hours of replication following differentiation induction. This finding holds significant implications for future investigations focused on understanding the early stages of the differentiation process. To delve deeper into the safety and efficacy of stem cell therapies, it becomes imperative to explore the potential impact of re-replication on stem cell fate and functionality.

In particular, unraveling the interplay between re-replication and the reprogramming of induced pluripotent stem cells (iPSCs) is a compelling avenue for future research. The implications of re-replication during the iPSC reprogramming process hold crucial significance, given the promising potential of these cells in regenerative medicine and therapeutic applications. Delving into the dynamics of re-replication during iPSC

reprogramming might shed light on how gene amplifications influence the cellular identity and functional characteristics of iPSC-derived cells.

The implications of gene amplifications, which can result from re-replication events, are multifaceted and might carry implications for cellular behavior and fate determination. As we strive to harness the full potential of stem cells and gene-editing technologies for therapeutic purposes, comprehending the occurrence and regulation of re-replication becomes increasingly essential. This knowledge will not only enhance our understanding of stem cell biology but also pave the way for more precise and effective therapeutic interventions.

6. Bibliography

1. Agarwal V, Bell GW, Nam J-W, Bartel DP (2015) Predicting effective microRNA target sites in mammalian mRNAs. eLife 4:

2. Akiyama H (2008) Control of chondrogenesis by the transcription factor Sox9. Mod Rheumatol 18:213–219

3. Aladjem MI, Redon CE (2017) Order from clutter: selective interactions at mammalian replication origins. Nat Rev Genet 18:101–116

4. Albertson DG (2006) Gene amplification in cancer. Trends Genet TIG 22:447–455

5. Alexander JL, Orr-Weaver TL (2016) Replication fork instability and the consequences of fork collisions from rereplication. Genes Dev 30:2241–2252

6. Almanzar N, Antony J, Baghel AS, Bakerman I, Bansal I, Barres BA, Beachy PA, Berdnik D, Bilen B, Brownfield D, Cain C, Chan CKF, Chen MB, Clarke MF, Conley SD, Darmanis S, Demers A, Demir K, de Morree A, Divita T, du Bois H, Ebadi H, Espinoza FH, Fish M, Gan Q, George BM, Gillich A, Gòmez-Sjöberg R, Green F, Genetiano G, Gu X, Gulati GS, Hahn O, Haney MS, Hang Y, Harris L, He M, Hosseinzadeh S, Huang A, Huang KC, Iram T, Isobe T, Ives F, Jones RC, Kao KS, Karkanias J, Karnam G, Keller A, Kershner AM, Khoury N, Kim SK, Kiss BM, Kong W, Krasnow MA, Kumar ME, Kuo CS, Lam J, Lee DP, Lee SE, Lehallier B, Leventhal O, Li G, Li Q, Liu L, Lo A, Lu W-J, Lugo-Fagundo MF, Manjunath A, May AP, Maynard A, McGeever A, McKay M, McNerney MW, Merrill B, Metzger RJ, Mignardi M, Min D, Nabhan AN, Neff NF, Ng KM, Nguyen PK, Noh J, Nusse R, Pálovics R, Patkar R, Peng WC, Penland L, Pisco AO, Pollard K, Puccinelli R, Qi Z, Quake SR, Rando TA, Rulifson EJ, Schaum N, Segal JM, Sikandar SS, Sinha R, Sit RV, Sonnenburg J, Staehli D, Szade K, Tan M, Tan W, Tato C, Tellez K, Dulgeroff LBT, Travaglini KJ, Tropini C, Tsui M, Waldburger L, Wang BM, van Weele LJ, Weinberg K, Weissman IL, Wosczyna MN, Wu SM, Wyss-Coray T, Xiang J, Xue S, Yamauchi KA, Yang AC, Yerra LP, Youngyunpipatkul J, Yu B, Zanini F, Zardeneta ME, Zee A, Zhao C, Zhang F, Zhang H, Zhang MJ, Zhou L, Zou J, The Tabula Muris Consortium (2020) A single-cell transcriptomic atlas characterizes ageing tissues in the mouse. Nature 583:590–595

7. Alt FW, Kellems RE, Bertino JR, Schimke RT (1978) Selective multiplication of dihydrofolate reductase genes in methotrexate-resistant variants of cultured murine cells. J Biol Chem 253:1357–1370

8. Altmayer NC, Galata V, Warschburger N, Keller A, Meese E, Fischer U (2018) Gene amplification in mesenchymal stem cells and during differentiation towards adipocytes or osteoblasts. Oncotarget 9:1803–1812

9. Ambele MA, Dhanraj P, Giles R, Pepper MS (2020) Adipogenesis: A Complex Interplay of Multiple Molecular Determinants and Pathways. Int J Mol Sci 21:4283

10. Amirian M, Jafari-Nozad AM, Darroudi M, Farkhondeh T, Samarghandian S (2023) Overview of the miR-29 family members' function in breast cancer. Int J Biol Macromol 230:123280

11. Anglana M, Apiou F, Bensimon A, Debatisse M (2003) Dynamics of DNA replication in mammalian somatic cells: nucleotide pool modulates origin choice and interorigin spacing. Cell 114:385–394

12. Anokye-Danso F, Trivedi CM, Juhr D, Gupta M, Cui Z, Tian Y, Zhang Y, Yang W, Gruber PJ, Epstein JA, Morrisey EE (2011) Highly efficient miRNA-mediated reprogramming of mouse and human somatic cells to pluripotency. Cell Stem Cell 8:376–388

13. Arai Y, Choi B, Kim BJ, Park S, Park H, Moon JJ, Lee S-H (2021) Cryptic ligand on collagen matrix unveiled by MMP13 accelerates bone tissue regeneration via MMP13/Integrin α3/RUNX2 feedback loop. Acta Biomater 125:219–230

14. Arentson E, Faloon P, Seo J, Moon E, Studts JM, Fremont DH, Choi K (2002) Oncogenic potential of the DNA replication licensing protein CDT1. Oncogene 21:1150–1158

15. Arias EE, Walter JC (2005) Replication-dependent destruction of Cdt1 limits DNA replication to a single round per cell cycle in Xenopus egg extracts. Genes Dev 19:114–126

16. Arias EE, Walter JC (2006) PCNA functions as a molecular platform to trigger Cdt1 destruction and prevent re-replication. Nat Cell Biol 8:84–90

17. Arias EE, Walter JC (2007) Strength in numbers: preventing rereplication via multiple mechanisms in eukaryotic cells. Genes Dev 21:497–518

18. Ayyagari R, Gomes XV, Gordenin DA, Burgers PMJ (2003) Okazaki fragment maturation in yeast. I. Distribution of functions between FEN1 AND DNA2. J Biol Chem 278:1618–1625

19. Azvolinsky A, Giresi PG, Lieb JD, Zakian VA (2009) Highly transcribed RNA polymerase II genes are impediments to replication fork progression in Saccharomyces cerevisiae. Mol Cell 34:722–734

20. Bae SC, Ito Y (1999) Regulation mechanisms for the heterodimeric transcription factor, PEBP2/CBF. Histol Histopathol 14:1213–1221

21. Bai X, Hua S, Zhang J, Xu S (2019) The MicroRNA Family Both in Normal Development and in Different Diseases: The miR-17-92 Cluster. BioMed Res Int 2019:9450240

22. Balaban-Malenbaum G, Gilbert F (1980) The proposed origin of double minutes from Homogeneously Staining Region (HSR)-marker chromosomes in human neuroblastoma hybrid cell lines. Cancer Genet Cytogenet 2:339–348

23. Balakrishnan L, Bambara RA (2013) Okazaki fragment metabolism. Cold Spring Harb Perspect Biol 5:a010173

24. Balistreri CR, De Falco E, Bordin A, Maslova O, Koliada A, Vaiserman A (2020) Stem cell therapy: old challenges and new solutions. Mol Biol Rep 47:3117–3131

25. Ballabeni A, Melixetian M, Zamponi R, Masiero L, Marinoni F, Helin K (2004) Human geminin promotes pre-RC formation and DNA replication by stabilizing CDT1 in mitosis. EMBO J 23:3122–3132

26. Bar M, Wyman SK, Fritz BR, Qi J, Garg KS, Parkin RK, Kroh EM, Bendoraite A, Mitchell PS, Nelson AM, Ruzzo WL, Ware C, Radich JP, Gentleman R, Ruohola-Baker

H, Tewari M (2008) MicroRNA discovery and profiling in human embryonic stem cells by deep sequencing of small RNA libraries. Stem Cells Dayt Ohio 26:2496–2505

27. Barateiro A, Fernandes A (2014) Temporal oligodendrocyte lineage progression: In vitro models of proliferation, differentiation and myelination. Biochim Biophys Acta BBA - Mol Cell Res 1843:1917–1929

28. Bartel DP (2009) MicroRNAs: target recognition and regulatory functions. Cell 136:215–233

29. Bellanger S, de Gramont A, Sobczak-Thépot J (2007) Cyclin B2 suppresses mitotic failure and DNA re-replication in human somatic cells knocked down for both cyclins B1 and B2. Oncogene 26:7175–7184

30. Bensimon A, Simon A, Chiffaudel A, Croquette V, Heslot F, Bensimon D (1994) Alignment and sensitive detection of DNA by a moving interface. Science 265:2096–2098

31. Berardi E, Pues M, Thorrez L, Sampaolesi M (2012) miRNAs in ESC differentiation. Am J Physiol Heart Circ Physiol 303:H931-939

32. Beresford JN, Bennett JH, Devlin C, Leboy PS, Owen ME (1992) Evidence for an inverse relationship between the differentiation of adipocytic and osteogenic cells in rat marrow stromal cell cultures. J Cell Sci 102 (Pt 2):341–351

33. Bernstein E, Caudy AA, Hammond SM, Hannon GJ (2001) Role for a bidentate ribonuclease in the initiation step of RNA interference. Nature 409:363–366

34. Besnard E, Babled A, Lapasset L, Milhavet O, Parrinello H, Dantec C, Marin J-M, Lemaitre J-M (2012) Unraveling cell type-specific and reprogrammable human replication origin signatures associated with G-quadruplex consensus motifs. Nat Struct Mol Biol 19:837–844

35. Bialic M, Al Ahmad Nachar B, Koźlak M, Coulon V, Schwob E (2022) Measuring S-Phase Duration from Asynchronous Cells Using Dual EdU-BrdU Pulse-Chase Labeling Flow Cytometry. Genes 13:408

36. Biedler JL, Spengler BA (1976) Metaphase chromosome anomaly: association with drug resistance and cell-specific products. Science 191:185–187

37. Bisaria N, Jarmoskaite I, Herschlag D (2017) Lessons from Enzyme Kinetics Reveal Specificity Principles for RNA-Guided Nucleases in RNA Interference and CRISPR-Based Genome Editing. Cell Syst 4:21–29

38. Bitgood MJ, McMahon AP (1995) Hedgehog and Bmp genes are coexpressed at many diverse sites of cell-cell interaction in the mouse embryo. Dev Biol 172:126–138

39. Bleichert F, Botchan MR, Berger JM (2015) Crystal structure of the eukaryotic origin recognition complex. Nature 519:321–326

40. Blow JJ, Gillespie PJ, Francis D, Jackson DA (2001) Replication origins in Xenopus egg extract Are 5-15 kilobases apart and are activated in clusters that fire at different times. J Cell Biol 152:15–25

41. Blow JJ, Dutta A (2005) Preventing re-replication of chromosomal DNA. Nat Rev Mol Cell Biol 6:476–486

42. Blow JJ, Gillespie PJ (2008) Replication licensing and cancer--a fatal entanglement? Nat Rev Cancer 8:799–806

43. Blumenfeld B, Ben-Zimra M, Simon I (2017) Perturbations in the Replication Program Contribute to Genomic Instability in Cancer. Int J Mol Sci 18:E1138

44. Bohnsack MT, Czaplinski K, Gorlich D (2004) Exportin 5 is a RanGTP-dependent dsRNA-binding protein that mediates nuclear export of pre-miRNAs. RNA N Y N 10:185–191

45. Bordiuk OL, Smith K, Morin PJ, Semënov MV (2014) Cell Proliferation and Neurogenesis in Adult Mouse Brain. PLoS ONE 9:e111453

46. Bowers RR, Kim JW, Otto TC, Lane MD (2006) Stable stem cell commitment to the adipocyte lineage by inhibition of DNA methylation: Role of the BMP-4 gene. Proc Natl Acad Sci 103:13022–13027

47. Breuer ME, Pavan C (1955) Behavior of polytene chromosomes of Rhynchosciara angelae at different stages of larval development. Chromosoma 7:341–386

48. Brewer BJ, Fangman WL (1987) The localization of replication origins on ARS plasmids in S. cerevisiae. Cell 51:463–471

49. Brodeur GM, Green AA, Hayes FA, Williams KJ, Williams DL, Tsiatis AA (1981) Cytogenetic features of human neuroblastomas and cell lines. Cancer Res 41:4678–4686

50. Broughton JP, Lovci MT, Huang JL, Yeo GW, Pasquinelli AE (2016) Pairing beyond the Seed Supports MicroRNA Targeting Specificity. Mol Cell 64:320–333

51. Brown C, McKee C, Bakshi S, Walker K, Hakman E, Halassy S, Svinarich D, Dodds R, Govind CK, Chaudhry GR (2019) Mesenchymal stem cells: Cell therapy and regeneration potential. J Tissue Eng Regen Med 13:1738–1755

52. Brown DD, Dawid IB (1968) Specific gene amplification in oocytes. Oocyte nuclei contain extrachromosomal replicas of the genes for ribosomal RNA. Science 160:272–280

53. Brown JP, Couillard-Després S, Cooper-Kuhn CM, Winkler J, Aigner L, Kuhn HG (2003) Transient expression of doublecortin during adult neurogenesis. J Comp Neurol 467:1–10

54. Bruno IG, Karam R, Huang L, Bhardwaj A, Lou CH, Shum EY, Song H-W, Corbett MA, Gifford WD, Gecz J, Pfaff SL, Wilkinson MF (2011) Identification of a microRNA that activates gene expression by repressing nonsense-mediated RNA decay. Mol Cell 42:500–510

55. Byun MR, Jeong H, Bae SJ, Kim AR, Hwang ES, Hong J-H (2012) TAZ is required for the osteogenic and anti-adipogenic activities of kaempferol. Bone 50:364–372

56. Caburet S, Conti C, Bensimon A (2002) Combing the genome for genomic instability. Trends Biotechnol 20:344–350

57. Cacchiarelli D, Martone J, Girardi E, Cesana M, Incitti T, Morlando M, Nicoletti C, Santini T, Sthandier O, Barberi L, Auricchio A, Musarò A, Bozzoni I (2010) MicroRNAs Involved in Molecular Circuitries Relevant for the Duchenne Muscular Dystrophy Pathogenesis Are Controlled by the Dystrophin/nNOS Pathway. Cell Metab 12:341–351

58. Cadoret J-C, Meisch F, Hassan-Zadeh V, Luyten I, Guillet C, Duret L, Quesneville H, Prioleau M-N (2008) Genome-wide studies highlight indirect links between human replication origins and gene regulation. Proc Natl Acad Sci U S A 105:15837–15842

59. Callan HG (1966) Chromosomes and nucleoli of the axolotl, Ambystoma mexicanum. J Cell Sci 1:85–108

60. Cardinali B, Castellani L, Fasanaro P, Basso A, Alemà S, Martelli F, Falcone G (2009) Microrna-221 and microrna-222 modulate differentiation and maturation of skeletal muscle cells. PloS One 4:e7607

61. Carroll SM, DeRose ML, Gaudray P, Moore CM, Needham-Vandevanter DR, Von Hoff DD, Wahl GM (1988) Double minute chromosomes can be produced from precursors derived from a chromosomal deletion. Mol Cell Biol 8:1525–1533

62. Case N, Rubin J (2010) Beta-catenin--a supporting role in the skeleton. J Cell Biochem 110:545–553

63. Cayrou C, Coulombe P, Vigneron A, Stanojcic S, Ganier O, Peiffer I, Rivals E, Puy A, Laurent-Chabalier S, Desprat R, Méchali M (2011) Genome-scale analysis of metazoan replication origins reveals their organization in specific but flexible sites defined by conserved features. Genome Res 21:1438–1449

64. Chang C-C, Venø MT, Chen L, Ditzel N, Le DQS, Dillschneider P, Kassem M, Kjems J (2018) Global MicroRNA Profiling in Human Bone Marrow Skeletal—Stromal or Mesenchymal–Stem Cells Identified Candidates for Bone Regeneration. Mol Ther 26:593–605

65. Chawla A, Lazar MA (1994) Peroxisome proliferator and retinoid signaling pathways co-regulate preadipocyte phenotype and survival. Proc Natl Acad Sci U S A 91:1786–1790

66. Chen C, Uludağ H, Wang Z, Jiang H (2012) Noggin suppression decreases BMP-2-induced osteogenesis of human bone marrow-derived mesenchymal stem cells in vitro. J Cell Biochem 113:3672–3680

67. Chen F, Walder B, James AW, Soofer DE, Soo C, Ting K, Zhang X (2012) NELL-1-dependent mineralisation of Saos-2 human osteosarcoma cells is mediated via c-Jun N-terminal kinase pathway activation. Int Orthop 36:2181–2187

68. Chen G, Wang Q, Li Z, Yang Q, Liu Y, Du Z, Zhang G, Song Y (2020) Circular RNA CDR1as promotes adipogenic and suppresses osteogenic differentiation of BMSCs in steroid-induced osteonecrosis of the femoral head. Bone 133:115258

69. Chen J, Chen L, Hua J, Song W (2021) Long-term dynamic compression enhancement TGF-β3-induced chondrogenesis in bovine stem cells: a gene expression analysis. BMC Genomic Data 22:13

70. Chen J-F, Mandel EM, Thomson JM, Wu Q, Callis TE, Hammond SM, Conlon FL, Wang D-Z (2006) The role of microRNA-1 and microRNA-133 in skeletal muscle proliferation and differentiation. Nat Genet 38:228–233

71. Chen J-F, Tao Y, Li J, Deng Z, Yan Z, Xiao X, Wang D-Z (2010) microRNA-1 and microRNA-206 regulate skeletal muscle satellite cell proliferation and differentiation by repressing Pax7. J Cell Biol 190:867–879

72. Chen Q, Shou P, Zheng C, Jiang M, Cao G, Yang Q, Cao J, Xie N, Velletri T, Zhang X, Xu C, Zhang L, Yang H, Hou J, Wang Y, Shi Y (2016) Fate decision of mesenchymal stem cells: adipocytes or osteoblasts? Cell Death Differ 23:1128–1139

73. Chen W, Chen L, Zhang Z, Meng F, Huang G, Sheng P, Zhang Z, Liao W (2016) MicroRNA-455-3p modulates cartilage development and degeneration through modification of histone H3 acetylation. Biochim Biophys Acta 1863:2881–2891

74. Chen X, Wang K, Chen J, Guo J, Yin Y, Cai X, Guo X, Wang G, Yang R, Zhu L, Zhang Y, Wang J, Xiang Y, Weng C, Zen K, Zhang J, Zhang C-Y (2009) In vitro evidence suggests that miR-133a-mediated regulation of uncoupling protein 2 (UCP2) is an indispensable step in myogenic differentiation. J Biol Chem 284:5362–5369

75. Cheng H, Jiang W, Phillips FM, Haydon RC, Peng Y, Zhou L, Luu HH, An N, Breyer B, Vanichakarn P, Szatkowski JP, Park JY, He T-C (2003) Osteogenic activity of the fourteen types of human bone morphogenetic proteins (BMPs). J Bone Joint Surg Am 85:1544–1552

76. Cheng H, Zhou L, Li B, Zhu M, Too H-P, Choi WK (2014) Nano-topology guided neurite outgrowth in PC12 cells is mediated by miRNAs. Nanomedicine Nanotechnol Biol Med 10:1871–1875

77. Cheng L-C, Pastrana E, Tavazoie M, Doetsch F (2009) miR-124 regulates adult neurogenesis in the subventricular zone stem cell niche. Nat Neurosci 12:399–408

78. Cheung TH, Rando TA (2013) Molecular regulation of stem cell quiescence. Nat Rev Mol Cell Biol 14:329–340

79. Chevalier S, Blow JJ (1996) Cell cycle control of replication initiation in eukaryotes. Curr Opin Cell Biol 8:815–821

80. Childs PG, Reid S, Salmeron-Sanchez M, Dalby MJ (2020) Hurdles to uptake of mesenchymal stem cells and their progenitors in therapeutic products. Biochem J 477:3349–3366

81. Christov CP, Gardiner TJ, Szüts D, Krude T (2006) Functional requirement of noncoding Y RNAs for human chromosomal DNA replication. Mol Cell Biol 26:6993–7004

82. Cohen S, Mechali M (2001) A novel cell-free system reveals a mechanism of circular DNA formation from tandem repeats. Nucleic Acids Res 29:2542–2548

83. Conti C, Caburet S, Schurra C, Bensimon A (2001) Molecular combing. Curr Protoc Cytom Chapter 8:Unit 8.10

84. Conti C, Saccà B, Herrick J, Lalou C, Pommier Y, Bensimon A (2007) Replication fork velocities at adjacent replication origins are coordinately modified during DNA replication in human cells. Mol Biol Cell 18:3059–3067

85. Cook JG, Chasse DAD, Nevins JR (2004) The regulated association of Cdt1 with minichromosome maintenance proteins and Cdc6 in mammalian cells. J Biol Chem 279:9625–9633

86. Coquelle A, Pipiras E, Toledo F, Buttin G, Debatisse M (1997) Expression of fragile sites triggers intrachromosomal mammalian gene amplification and sets boundaries to early amplicons. Cell 89:215–225

87. Courbet S, Gay S, Arnoult N, Wronka G, Anglana M, Brison O, Debatisse M (2008) Replication fork movement sets chromatin loop size and origin choice in mammalian cells. Nature 455:557–560

88. Coverley D, Wilkinson HR, Downes CS (1996) A protein kinase-dependent block to reinitiation of DNA replication in G2 phase in mammalian cells. Exp Cell Res 225:294–300

89. Cross JC (2016) Gene Amplification: Trophoblast Giant Cells Use All the Tricks. Curr Biol CB 26:R177-179

90. Crouse HV, Keyl HG (1968) Extra replications in the "DNA-puffs" of Sciara coprophila. Chromosoma 25:357–364

91. Cupp JD, Nielsen BL (2014) Minireview: DNA replication in plant mitochondria. Mitochondrion 19 Pt B:231–237

92. Dai L, Zhang X, Hu X, Zhou C, Ao Y (2012) Silencing of microRNA-101 prevents IL-1β-induced extracellular matrix degradation in chondrocytes. Arthritis Res Ther 14:R268

93. Dai Z, Jin Y, Zheng J, Liu K, Zhao J, Zhang S, Wu F, Sun Z (2019) MiR-217 promotes cell proliferation and osteogenic differentiation of BMSCs by targeting DKK1 in steroid-associated osteonecrosis. Biomed Pharmacother Biomedecine Pharmacother 109:1112–1119

94. D'Alimonte I, Lannutti A, Pipino C, Di Tomo P, Pierdomenico L, Cianci E, Antonucci I, Marchisio M, Romano M, Stuppia L, Caciagli F, Pandolfi A, Ciccarelli R (2013) Wnt signaling behaves as a "master regulator" in the osteogenic and adipogenic commitment of human amniotic fluid mesenchymal stem cells. Stem Cell Rev Rep 9:642–654

95. Darlington GJ, Ross SE, MacDougald OA (1998) The role of C/EBP genes in adipocyte differentiation. J Biol Chem 273:30057–30060

96. Darzacq X, Jády BE, Verheggen C, Kiss AM, Bertrand E, Kiss T (2002) Cajal body-specific small nuclear RNAs: a novel class of 2'-O-methylation and pseudouridylation guide RNAs. EMBO J 21:2746–2756

97. Das SP, Borrman T, Liu VWT, Yang SC-H, Bechhoefer J, Rhind N (2015) Replication timing is regulated by the number of MCMs loaded at origins. Genome Res 25:1886–1892

98. Davidson IF, Li A, Blow JJ (2006) Deregulated replication licensing causes DNA fragmentation consistent with head-to-tail fork collision. Mol Cell 24:433–443

99. De Mattei M, Grassilli S, Pellati A, Brugnoli F, De Marchi E, Contartese D, Bertagnolo V (2020) Pulsed Electromagnetic Fields Modulate miRNAs During Osteogenic Differentiation of Bone Mesenchymal Stem Cells: a Possible Role in the Osteogenic-angiogenic Coupling. Stem Cell Rev Rep 16:1005–1012

100. De Micheli AJ, Spector JA, Elemento O, Cosgrove BD (2020) A reference single-cell transcriptomic atlas of human skeletal muscle tissue reveals bifurcated muscle stem cell populations. Skelet Muscle 10:19

101. De Pietri Tonelli D, Pulvers JN, Haffner C, Murchison EP, Hannon GJ, Huttner WB (2008) miRNAs are essential for survival and differentiation of newborn neurons but not for expansion of neural progenitors during early neurogenesis in the mouse embryonic neocortex. Dev Camb Engl 135:3911–3921

102. de Renty C, Kaneko KJ, DePamphilis ML (2014) The dual roles of geminin during trophoblast proliferation and differentiation. Dev Biol 387:49–63

103. Delaloy C, Liu L, Lee J-A, Su H, Shen F, Yang G-Y, Young WL, Ivey KN, Gao F-B (2010) MicroRNA-9 coordinates proliferation and migration of human embryonic stem cell-derived neural progenitors. Cell Stem Cell 6:323–335

104. Demczuk A, Gauthier MG, Veras I, Kosiyatrakul S, Schildkraut CL, Busslinger M, Bechhoefer J, Norio P (2012) Regulation of DNA replication within the immunoglobulin heavy-chain locus during B cell commitment. PLoS Biol 10:e1001360

105. Denoth-Lippuner A, Jaeger BN, Liang T, Royall LN, Chie SE, Buthey K, Machado D, Korobeynyk VI, Kruse M, Munz CM, Gerbaulet A, Simons BD, Jessberger S (2021) Visualization of individual cell division history in complex tissues using iCOUNT. Cell Stem Cell 28:2020-2034.e12

106. Deo M, Yu J-Y, Chung K-H, Tippens M, Turner DL (2006) Detection of mammalian microRNA expression by in situ hybridization with RNA oligonucleotides. Dev Dyn Off Publ Am Assoc Anat 235:2538–2548

107. DePamphilis ML (1993) Origins of DNA replication in metazoan chromosomes. J Biol Chem 268:1–4

108. Dershowitz A, Newlon CS (1993) The effect on chromosome stability of deleting replication origins. Mol Cell Biol 13:391–398

109. Dewar JM, Walter JC (2017) Mechanisms of DNA replication termination. Nat Rev Mol Cell Biol 18:507–516

110. Dey BK, Gagan J, Dutta A (2011) miR-206 and -486 induce myoblast differentiation by downregulating Pax7. Mol Cell Biol 31:203–214

111. Dey BK, Gagan J, Yan Z, Dutta A (2012) miR-26a is required for skeletal muscle differentiation and regeneration in mice. Genes Dev 26:2180–2191

112. Di G, Kong L, Zhao Q, Ding T (2018) MicroRNA-146a knockdown suppresses the progression of ankylosing spondylitis by targeting dickkopf 1. Biomed Pharmacother Biomedecine Pharmacother 97:1243–1249

113.   Di Pietro L, Barba M, Palacios D, Tiberio F, Prampolini C, Baranzini M, Parolini O, Arcovito A, Lattanzi W (2021) Shaping modern human skull through epigenetic, transcriptional and post-transcriptional regulation of the RUNX2 master bone gene. Sci Rep 11:21316

114.   Diacou R, Nandigrami P, Fiser A, Liu W, Ashery-Padan R, Cvekl A (2022) Cell fate decisions, transcription factors and signaling during early retinal development. Prog Retin Eye Res 91:101093

115.   Diamante L, Martello G (2022) Metabolic regulation in pluripotent stem cells. Curr Opin Genet Dev 75:101923

116.   Dieci G, Preti M, Montanini B (2009) Eukaryotic snoRNAs: a paradigm for gene expression flexibility. Genomics 94:83–88

117.   Dileep V, Gilbert DM (2018) Single-cell replication profiling to measure stochastic variation in mammalian replication timing. Nat Commun 9:427

118.   Ding Q, MacAlpine DM (2010) Preferential re-replication of Drosophila heterochromatin in the absence of geminin. PLoS Genet 6:e1001112

119.   Diril MK, Ratnacaram CK, Padmakumar VC, Du T, Wasser M, Coppola V, Tessarollo L, Kaldis P (2012) Cyclin-dependent kinase 1 (Cdk1) is essential for cell division and suppression of DNA re-replication but not for liver regeneration. Proc Natl Acad Sci U S A 109:3826–3831

120.   Dominici M, Le Blanc K, Mueller I, Slaper-Cortenbach I, Marini FC, Krause DS, Deans RJ, Keating A, Prockop DJ, Horwitz EM (2006) Minimal criteria for defining multipotent mesenchymal stromal cells. The International Society for Cellular Therapy position statement. Cytotherapy 8:315–317

121.   Donato R (2001) S100: a multigenic family of calcium-modulated proteins of the EF-hand type with intracellular and extracellular functional roles. Int J Biochem Cell Biol 33:637–668

122.   Dong P, Mai Y, Zhang Z, Mi L, Wu G, Chu G, Yang G, Sun S (2014) MiR-15a/b promote adipogenesis in porcine pre-adipocyte via repressing FoxO1. Acta Biochim Biophys Sin 46:565–571

123.   Dorman LJ, Tucci M, Benghuzzi H (2012) In vitro effects of bmp-2, bmp-7, and bmp-13 on proliferation and differentation of mouse mesenchymal stem cells. Biomed Sci Instrum 48:81–87

124.   Dorn ES, Chastain PD, Hall JR, Cook JG (2009) Analysis of re-replication from deregulated origin licensing by DNA fiber spreading. Nucleic Acids Res 37:60–69

125.   Dugas JC, Cuellar TL, Scholze A, Ason B, Ibrahim A, Emery B, Zamanian JL, Foo LC, McManus MT, Barres BA (2010) Dicer1 and miR-219 Are required for normal oligodendrocyte differentiation and myelination. Neuron 65:597–611

126.   Duursma A, Agami R (2005) p53-Dependent regulation of Cdc6 protein stability controls cellular proliferation. Mol Cell Biol 25:6937–6947

127.   Eichhorn SW, Guo H, McGeary SE, Rodriguez-Mias RA, Shin C, Baek D, Hsu S-H, Ghoshal K, Villén J, Bartel DP (2014) mRNA destabilization is the dominant effect

of mammalian microRNAs by the time substantial repression ensues. Mol Cell 56:104–115

128. Ekholm-Reed S, Méndez J, Tedesco D, Zetterberg A, Stillman B, Reed SI (2004) Deregulation of cyclin E in human cells interferes with prereplication complex assembly. J Cell Biol 165:789–800

129. Emery B (2010) Regulation of oligodendrocyte differentiation and myelination. Science 330:779–782

130. Esau C, Kang X, Peralta E, Hanson E, Marcusson EG, Ravichandran LV, Sun Y, Koo S, Perera RJ, Jain R, Dean NM, Freier SM, Bennett CF, Lollo B, Griffey R (2004) MicroRNA-143 regulates adipocyte differentiation. J Biol Chem 279:52361–52365

131. Eskildsen T, Taipaleenmäki H, Stenvang J, Abdallah BM, Ditzel N, Nossent AY, Bak M, Kauppinen S, Kassem M (2011) MicroRNA-138 regulates osteogenic differentiation of human stromal (mesenchymal) stem cells in vivo. Proc Natl Acad Sci U S A 108:6139–6144

132. Evans MJ, Kaufman MH (1981) Establishment in culture of pluripotential cells from mouse embryos. Nature 292:154–156

133. Evrony GD, Cordero DR, Shen J, Partlow JN, Yu TW, Rodin RE, Hill RS, Coulter ME, Lam A-TN, Jayaraman D, Gerrelli D, Diaz DG, Santos C, Morrison V, Galli A, Tschulena U, Wiemann S, Martel MJ, Spooner B, Ryu SC, Elhosary PC, Richardson JM, Tierney D, Robinson CA, Chibbar R, Diudea D, Folkerth R, Wiebe S, Barkovich AJ, Mochida GH, Irvine J, Lemire EG, Blakley P, Walsh CA (2017) Integrated genome and transcriptome sequencing identifies a noncoding mutation in the genome replication factor DONSON as the cause of microcephaly-micromelia syndrome. Genome Res 27:1323–1335

134. Fakhry M, Hamade E, Badran B, Buchet R, Magne D (2013) Molecular mechanisms of mesenchymal stem cell differentiation towards osteoblasts. World J Stem Cells 5:136–148

135. Falck J, Petrini JHJ, Williams BR, Lukas J, Bartek J (2002) The DNA damage-dependent intra-S phase checkpoint is regulated by parallel pathways. Nat Genet 30:290–294

136. Falkenberg M, Gustafsson CM (2020) Mammalian mitochondrial DNA replication and mechanisms of deletion formation. Crit Rev Biochem Mol Biol 55:509–524

137. Fan T, Qu R, Yu Q, Sun B, Jiang X, Yang Y, Huang X, Zhou Z, Ouyang J, Zhong S, Dai J (2020) Bioinformatics analysis of the biological changes involved in the osteogenic differentiation of human mesenchymal stem cells. J Cell Mol Med 24:7968–7978

138. Ferenbach A, Li A, Brito-Martins M, Blow JJ (2005) Functional domains of the Xenopus replication licensing factor Cdt1. Nucleic Acids Res 33:316–324

139. Findeisen M, El-Denary M, Kapitza T, Graf R, Strausfeld U (1999) Cyclin A-dependent kinase activity affects chromatin binding of ORC, Cdc6, and MCM in egg extracts of Xenopus laevis. Eur J Biochem 264:415–426

140.   Finn KJ, Li JJ (2013) Single-stranded annealing induced by re-initiation of replication origins provides a novel and efficient mechanism for generating copy number expansion via non-allelic homologous recombination. PLoS Genet 9:e1003192

141.   Fischer U, Sattler H, Bonkhoff H, Herrmann M, Wullich B, Meese E (1994) Amplification on chromosomes 1p31, 1q21-24, 5p13-14, and 11p12-14 in ovarian-carcinoma detected by reverse chromosome painting. Oncol Rep 1:1069–1073

142.   Fischer U, Meltzer P, Meese E (1996) Twelve amplified and expressed genes localized in a single domain in glioma. Hum Genet 98:625–628

143.   Fischer U, Meese E (2007) Glioblastoma multiforme: the role of DSB repair between genotype and phenotype. Oncogene 26:7809–7815

144.   Fischer U, Keller A, Leidinger P, Deutscher S, Heisel S, Urbschat S, Lenhof H-P, Meese E (2008) A different view on DNA amplifications indicates frequent, highly complex, and stable amplicons on 12q13-21 in glioma. Mol Cancer Res MCR 6:576–584

145.   Fischer U, Radermacher J, Mayer J, Mehraein Y, Meese E (2008) Tumor hypoxia: Impact on gene amplification in glioblastoma. Int J Oncol 33:509–515

146.   Fischer U, Leidinger P, Keller A, Folarin A, Ketter R, Graf N, Lenhof H-P, Meese E (2010) Amplicons on chromosome 12q13-21 in glioblastoma recurrences. Int J Cancer 126:2594–2602

147.   Fischer U, Keller A, Voss M, Backes C, Welter C, Meese E (2012) Genome-wide gene amplification during differentiation of neural progenitor cells in vitro. PloS One 7:e37422

148.   Fischer U, Backes C, Raslan A, Keller A, Meier C, Meese E (2015) Gene amplification during differentiation of mammalian neural stem cells in vitro and in vivo. Oncotarget 6:7023–7039

149.   Fischer U, Ludwig N, Keller A, Backes C, Meese E (2015) Genome-wide copy number profiling of mouse neural stem cells during differentiation. Genomics Data 5:3–6

150.   Fischer U, Ludwig N, Raslan A, Meier C, Meese E (2016) Gene amplification during myogenic differentiation. Oncotarget 7:6864–6877

151.   Fischer U, Kim E, Keller A, Meese E (2017) Specific amplifications and copy number decreases during human neural stem cells differentiation towards astrocytes, neurons and oligodendrocytes. Oncotarget 8:25872–25884

152.   Fontaine C, Cousin W, Plaisant M, Dani C, Peraldi P (2008) Hedgehog signaling alters adipocyte maturation of human mesenchymal stem cells. Stem Cells Dayt Ohio 26:1037–1046

153.   Fóthi Á, Biró O, Erdei Z, Apáti Á, Orbán TI (2021) Tissue-specific and transcription-dependent mechanisms regulate primary microRNA processing efficiency of the human chromosome 19 MicroRNA cluster. RNA Biol 18:1170–1180

154. Fouad GI (2019) Stem cells as a promising therapeutic approach for Alzheimer's disease: a review. Bull Natl Res Cent 43:52

155. França GS, Hinske LC, Galante PAF, Vibranovski MD (2017) Unveiling the Impact of the Genomic Architecture on the Evolution of Vertebrate microRNAs. Front Genet 8:34

156. Friedman RC, Farh KK-H, Burge CB, Bartel DP (2009) Most mammalian mRNAs are conserved targets of microRNAs. Genome Res 19:92–105

157. Fromm-Dornieden C, von der Heyde S, Lytovchenko O, Salinas-Riester G, Brenig B, Beissbarth T, Baumgartner BG (2012) Novel polysome messages and changes in translational activity appear after induction of adipogenesis in 3T3-L1 cells. BMC Mol Biol 13:9

158. Fu H, Maunakea AK, Martin MM, Huang L, Zhang Y, Ryan M, Kim R, Lin CM, Zhao K, Aladjem MI (2013) Methylation of histone H3 on lysine 79 associates with a group of replication origins and helps limit DNA replication once per cell cycle. PLoS Genet 9:e1003542

159. Fu H, Redon CE, Thakur BL, Utani K, Sebastian R, Jang S-M, Gross JM, Mosavarpour S, Marks AB, Zhuang SZ, Lazar SB, Rao M, Mencer ST, Baris AM, Pongor LS, Aladjem MI (2021) Dynamics of replication origin over-activation. Nat Commun 12:3448

160. Fu L, Wang H, Liao Y, Zhou P, Xu Y, Zhao Y, Xie S, Zhao S, Li X (2020) miR-208b modulating skeletal muscle development and energy homoeostasis through targeting distinct targets. RNA Biol 17:743–754

161. Fu Y, Li J, Li M, Xu J, Rong Z, Ren F, Wang Y, Sheng J, Chang Z (2022) Umbilical Cord Mesenchymal Stem Cells Ameliorate Inflammation-Related Tumorigenesis via Modulating Macrophages. Stem Cells Int 2022:1–13

162. Futcher AB (1986) Copy number amplification of the 2 micron circle plasmid of Saccharomyces cerevisiae. J Theor Biol 119:197–204

163. Fuziwara CS, Kimura ET (2015) Insights into Regulation of the miR-17-92 Cluster of miRNAs in Cancer. Front Med 2:64

164. Gaillard H, García-Muse T, Aguilera A (2015) Replication stress and cancer. Nat Rev Cancer 15:276–289

165. Galimov A, Merry TL, Luca E, Rushing EJ, Mizbani A, Turcekova K, Hartung A, Croce CM, Ristow M, Krützfeldt J (2016) MicroRNA-29a in Adult Muscle Stem Cells Controls Skeletal Muscle Regeneration During Injury and Exercise Downstream of Fibroblast Growth Factor-2. Stem Cells Dayt Ohio 34:768–780

166. Gambus A, Jones RC, Sanchez-Diaz A, Kanemaki M, van Deursen F, Edmondson RD, Labib K (2006) GINS maintains association of Cdc45 with MCM in replisome progression complexes at eukaryotic DNA replication forks. Nat Cell Biol 8:358–366

167. Gatti D, Viapiana O, Fracassi E, Idolazzi L, Dartizio C, Povino MR, Adami S, Rossini M (2012) Sclerostin and DKK1 in postmenopausal osteoporosis treated with denosumab. J Bone Miner Res Off J Am Soc Bone Miner Res 27:2259–2263

168.   Gay I, Cavender A, Peto D, Sun Z, Speer A, Cao H, Amendt BA (2014) Differentiation of human dental stem cells reveals a role for microRNA-218. J Periodontal Res 49:110–120

169.   Ge XQ, Jackson DA, Blow JJ (2007) Dormant origins licensed by excess Mcm2-7 are required for human cells to survive replicative stress. Genes Dev 21:3331–3341

170.   Ge XQ, Lin H (2014) Noncoding RNAs in the regulation of DNA replication. Trends Biochem Sci 39:341–343

171.   Ge Y, Chen J (2011) MicroRNAs in skeletal myogenesis. Cell Cycle Georget Tex 10:441–448

172.   Ge Y, Sun Y, Chen J (2011) IGF-II is regulated by microRNA-125b in skeletal myogenesis. J Cell Biol 192:69–81

173.   Gebler A, Zabel O, Seliger B (2012) The immunomodulatory capacity of mesenchymal stem cells. Trends Mol Med 18:128–134

174.   George DL, Powers VE (1981) Cloning of DNA from double minutes of Y1 mouse adrenocortical tumor cells: evidence for gene amplification. Cell 24:117–123

175.   Ghasemi M, Samaei NM, Mowla SJ, Shafiee M, Vasei M, Ghasemian N (2018) Upregulation of miR-371-373 cluster, a human embryonic stem cell specific microRNA cluster, in esophageal squamous cell carcinoma. J Cancer Res Ther 14:S132–S137

176.   Ghila L, Bjørlykke Y, Legøy TA, Vethe H, Furuyama K, Chera S, Ræder H (2020) Bioinformatic Analyses of miRNA–mRNA Signature during hiPSC Differentiation towards Insulin-Producing Cells upon HNF4α Mutation. Biomedicines 8:179

177.   Gillespie PJ, Li A, Blow JJ (2001) Reconstitution of licensed replication origins on Xenopus sperm nuclei using purified proteins. BMC Biochem 2:15

178.   Gindin Y, Valenzuela MS, Aladjem MI, Meltzer PS, Bilke S (2014) A chromatin structure-based model accurately predicts DNA replication timing in human cells. Mol Syst Biol 10:722

179.   Glass CK, Rose DW, Rosenfeld MG (1997) Nuclear receptor coactivators. Curr Opin Cell Biol 9:222–232

180.   Gloor JW, Balakrishnan L, Campbell JL, Bambara RA (2012) Biochemical analyses indicate that binding and cleavage specificities define the ordered processing of human Okazaki fragments by Dna2 and FEN1. Nucleic Acids Res 40:6774–6786

181.   Gould E (2007) How widespread is adult neurogenesis in mammals? Nat Rev Neurosci 8:481–488

182.   Govoni KE (2012) Insulin-like growth factor-I molecular pathways in osteoblasts: potential targets for pharmacological manipulation. Curr Mol Pharmacol 5:143–152

183.   Granchi D, Ochoa G, Leonardi E, Devescovi V, Baglìo SR, Osaba L, Baldini N, Ciapetti G (2010) Gene expression patterns related to osteogenic differentiation of bone marrow-derived mesenchymal stem cells during ex vivo expansion. Tissue Eng Part C Methods 16:511–524

184. Greco S, De Simone M, Colussi C, Zaccagnini G, Fasanaro P, Pescatori M, Cardani R, Perbellini R, Isaia E, Sale P, Meola G, Capogrossi MC, Gaetano C, Martelli F (2009) Common micro-RNA signature in skeletal muscle damage and regeneration induced by Duchenne muscular dystrophy and acute ischemia. FASEB J Off Publ Fed Am Soc Exp Biol 23:3335–3346

185. Green BM, Finn KJ, Li JJ (2010) Loss of DNA replication control is a potent inducer of gene amplification. Science 329:943–946

186. Greenberg A, Simon I (2022) S Phase Duration Is Determined by Local Rate and Global Organization of Replication. Biology 11:718

187. Griffiths R, Woods S, Cheng A, Wang P, Griffiths-Jones S, Ronshaugen M, Kimber SJ (2020) The Transcription Factor-microRNA Regulatory Network during hESC-chondrogenesis. Sci Rep 10:4744

188. Grimson A, Farh KK-H, Johnston WK, Garrett-Engele P, Lim LP, Bartel DP (2007) MicroRNA targeting specificity in mammals: determinants beyond seed pairing. Mol Cell 27:91–105

189. Grishok A, Pasquinelli AE, Conte D, Li N, Parrish S, Ha I, Baillie DL, Fire A, Ruvkun G, Mello CC (2001) Genes and mechanisms related to RNA interference regulate expression of the small temporal RNAs that control C. elegans developmental timing. Cell 106:23–34

190. Grochowski C, Radzikowska E, Maciejewski R (2018) Neural stem cell therapy-Brief review. Clin Neurol Neurosurg 173:8–14

191. Grounds MD, Yablonka-Reuveni Z (1993) Molecular and cell biology of skeletal muscle regeneration. Mol Cell Biol Hum Dis Ser 3:210–256

192. Guérit D, Brondello J-M, Chuchana P, Philipot D, Toupet K, Bony C, Jorgensen C, Noël D (2014) FOXO3A regulation by miRNA-29a Controls chondrogenic differentiation of mesenchymal stem cells and cartilage formation. Stem Cells Dev 23:1195–1205

193. Guo H, Ingolia NT, Weissman JS, Bartel DP (2010) Mammalian microRNAs predominantly act to decrease target mRNA levels. Nature 466:835–840

194. Ha DH, Kim H-K, Lee J, Kwon HH, Park G-H, Yang SH, Jung JY, Choi H, Lee JH, Sung S, Yi YW, Cho BS (2020) Mesenchymal Stem/Stromal Cell-Derived Exosomes for Immunomodulatory Therapeutics and Skin Regeneration. Cells 9:E1157

195. Hall JR, Kow E, Nevis KR, Lu CK, Luce KS, Zhong Q, Cook JG (2007) Cdc6 stability is regulated by the Huwe1 ubiquitin ligase after DNA damage. Mol Biol Cell 18:3340–3350

196. Hamam D, Ali D, Vishnubalaji R, Hamam R, Al-Nbaheen M, Chen L, Kassem M, Aldahmash A, Alajez NM (2014) microRNA-320/RUNX2 axis regulates adipocytic differentiation of human mesenchymal (skeletal) stem cells. Cell Death Dis 5:e1499

197. Han H, Liu L (2021) Long noncoding RNA TUG1 regulates degradation of chondrocyte extracellular matrix via miR-320c/MMP-13 axis in osteoarthritis. Open Life Sci 16:384–394

198. Hannibal RL, Chuong EB, Rivera-Mulia JC, Gilbert DM, Valouev A, Baker JC (2014) Copy number variation is a fundamental aspect of the placental genome. PLoS Genet 10:e1004290

199. Hannibal RL, Baker JC (2016) Selective Amplification of the Genome Surrounding Key Placental Genes in Trophoblast Giant Cells. Curr Biol CB 26:230–236

200. Hassan MQ, Maeda Y, Taipaleenmaki H, Zhang W, Jafferji M, Gordon JAR, Li Z, Croce CM, van Wijnen AJ, Stein JL, Stein GS, Lian JB (2012) miR-218 directs a Wnt signaling circuit to promote differentiation of osteoblasts and osteomimicry of metastatic cancer cells. J Biol Chem 287:42084–42092

201. Hata K, Nishimura R, Ikeda F, Yamashita K, Matsubara T, Nokubi T, Yoneda T (2003) Differential roles of Smad1 and p38 kinase in regulation of peroxisome proliferator-activating receptor gamma during bone morphogenetic protein 2-induced adipogenesis. Mol Biol Cell 14:545–555

202. Hawke TJ, Garry DJ (2001) Myogenic satellite cells: physiology to molecular biology. J Appl Physiol Bethesda Md 1985 91:534–551

203. Hayles J, Fisher D, Woollard A, Nurse P (1994) Temporal order of S phase and mitosis in fission yeast is determined by the state of the p34cdc2-mitotic B cyclin complex. Cell 78:813–822

204. He A, Zhu L, Gupta N, Chang Y, Fang F (2007) Overexpression of Micro Ribonucleic Acid 29, Highly Up-Regulated in Diabetic Rats, Leads to Insulin Resistance in 3T3-L1 Adipocytes. Mol Endocrinol 21:2785–2794

205. He H, Chen K, Wang F, Zhao L, Wan X, Wang L, Mo Z (2015) miR-204-5p promotes the adipogenic differentiation of human adipose-derived mesenchymal stem cells by modulating DVL3 expression and suppressing Wnt/β-catenin signaling. Int J Mol Med 35:1587–1595

206. Hellman A, Zlotorynski E, Scherer SW, Cheung J, Vincent JB, Smith DI, Trakhtenbrot L, Kerem B (2002) A role for common fragile site induction in amplification of human oncogenes. Cancer Cell 1:89–97

207. Herrick J, Bensimon A (1999) Imaging of single DNA molecule: applications to high-resolution genomic studies. Chromosome Res Int J Mol Supramol Evol Asp Chromosome Biol 7:409–423

208. Higa LAA, Mihaylov IS, Banks DP, Zheng J, Zhang H (2003) Radiation-mediated proteolysis of CDT1 by CUL4-ROC1 and CSN complexes constitutes a new checkpoint. Nat Cell Biol 5:1008–1015

209. Honeycutt KA, Koster MI, Roop DR (2004) Genes involved in stem cell fate decisions and commitment to differentiation play a role in skin disease. J Investig Dermatol Symp Proc 9:261–268

210. Hook SS, Lin JJ, Dutta A (2007) Mechanisms to control rereplication and implications for cancer. Curr Opin Cell Biol 19:663–671

211. Horak M, Novak J, Bienertova-Vasku J (2016) Muscle-specific microRNAs in skeletal muscle development. Dev Biol 410:1–13

212. Hornstein E, Mansfield JH, Yekta S, Hu JK-H, Harfe BD, McManus MT, Baskerville S, Bartel DP, Tabin CJ (2005) The microRNA miR-196 acts upstream of Hoxb8 and Shh in limb development. Nature 438:671–674

213. Hou C, Yang Z, Kang Y, Zhang Z, Fu M, He A, Zhang Z, Liao W (2015) MiR-193b regulates early chondrogenesis by inhibiting the TGF-beta2 signaling pathway. FEBS Lett 589:1040–1047

214. Houbaviy HB, Murray MF, Sharp PA (2003) Embryonic stem cell-specific MicroRNAs. Dev Cell 5:351–358

215. Hu C-H, Sui B-D, Du F-Y, Shuai Y, Zheng C-X, Zhao P, Yu X-R, Jin Y (2017) miR-21 deficiency inhibits osteoclast function and prevents bone loss in mice. Sci Rep 7:43191

216. Hu J, McCall CM, Ohta T, Xiong Y (2004) Targeted ubiquitination of CDT1 by the DDB1-CUL4A-ROC1 ligase in response to DNA damage. Nat Cell Biol 6:1003–1009

217. Hu X, Tang J, Hu X, Bao P, Pan J, Chen Z, Xian J (2018) MiR-27b Impairs Adipocyte Differentiation of Human Adipose Tissue-Derived Mesenchymal Stem Cells by Targeting LPL. Cell Physiol Biochem Int J Exp Cell Physiol Biochem Pharmacol 47:545–555

218. Hu Z, Klein JD, Mitch WE, Zhang L, Martinez I, Wang XH (2014) MicroRNA-29 induces cellular senescence in aging muscle through multiple signaling pathways. Aging 6:160–175

219. Huang C -Y. C, Reuben PM, Cheung HS (2005) Temporal Expression Patterns and Corresponding Protein Inductions of Early Responsive Genes in Rabbit Bone Marrow–Derived Mesenchymal Stem Cells Under Cyclic Compressive Loading. Stem Cells 23:1113–1121

220. Huang H, Song T-J, Li X, Hu L, He Q, Liu M, Lane MD, Tang Q-Q (2009) BMP signaling pathway is required for commitment of C3H10T1/2 pluripotent stem cells to the adipocyte lineage. Proc Natl Acad Sci 106:12670–12675

221. Huang J, Zhao L, Xing L, Chen D (2010) MicroRNA-204 regulates Runx2 protein expression and mesenchymal progenitor cell differentiation. Stem Cells Dayt Ohio 28:357–364

222. Huang Y-Y, Kaneko KJ, Pan H, DePamphilis ML (2015) Geminin is Essential to Prevent DNA Re-Replication-Dependent Apoptosis in Pluripotent Cells, but not in Differentiated Cells. Stem Cells Dayt Ohio 33:3239–3253

223. Hulke ML, Siefert JC, Sansam CL, Koren A (2019) Germline Structural Variations Are Preferential Sites of DNA Replication Timing Plasticity during Development. Genome Biol Evol 11:1663–1678

224. Hull RM, King M, Pizza G, Krueger F, Vergara X, Houseley J (2019) Transcription-induced formation of extrachromosomal DNA during yeast ageing. PLoS Biol 17:e3000471

225. Hung S-C, Chang C-F, Ma H-L, Chen T-H, Low-Tone Ho L (2004) Gene expression profiles of early adipogenesis in human mesenchymal stem cells. Gene 340:141–150

226.   Hutvágner G, McLachlan J, Pasquinelli AE, Bálint E, Tuschl T, Zamore PD (2001) A cellular function for the RNA-interference enzyme Dicer in the maturation of the let-7 small temporal RNA. Science 293:834–838

227.   Huynh NPT, Zhang B, Guilak F (2019) High-depth transcriptomic profiling reveals the temporal gene signature of human mesenchymal stem cells during chondrogenesis. FASEB J Off Publ Fed Am Soc Exp Biol 33:358–372

228.   Hyrien O, Debatisse M, Buttin G, de Saint Vincent BR (1988) The multicopy appearance of a large inverted duplication and the sequence at the inversion joint suggest a new model for gene amplification. EMBO J 7:407–417

229.   Iaculli F, Di Filippo ES, Piattelli A, Mancinelli R, Fulle S (2017) Dental pulp stem cells grown on dental implant titanium surfaces: An in vitro evaluation of differentiation and microRNAs expression. J Biomed Mater Res B Appl Biomater 105:953–965

230.   Iaquinta MR, Lanzillotti C, Mazziotta C, Bononi I, Frontini F, Mazzoni E, Oton-Gonzalez L, Rotondo JC, Torreggiani E, Tognon M, Martini F (2021) The role of microRNAs in the osteogenic and chondrogenic differentiation of mesenchymal stem cells and bone pathologies. Theranostics 11:6573–6591

231.   Ibarra A, Schwob E, Méndez J (2008) Excess MCM proteins protect human cells from replicative stress by licensing backup origins of replication. Proc Natl Acad Sci U S A 105:8956–8961

232.   Ikeda R, Tsukaara S, Yoshida K, Inoue I (2007) Gene expression changes during the chondrogenic differentiation of human mesenchymal stem cells. J Biol Sci 7:729–736

233.   Ikeda R, . ST, . KY, . II (2007) Gene Expression Changes During the Chondrogenic Differentiation of Human Mesenchymal Stem Cells. J Biol Sci 7:729–736

234.   Iqbal A, Ping J, Ali S, Zhen G, Juan L, Kang JZ, Ziyi P, Huixian L, Zhihui Z (2020) Role of microRNAs in myogenesis and their effects on meat quality in pig — A review. Asian-Australas J Anim Sci 33:1873–1884

235.   Ito E, Miyagawa S, Takeda M, Kawamura A, Harada A, Iseoka H, Yajima S, Sougawa N, Mochizuki-Oda N, Yasuda S, Sato Y, Sawa Y (2019) Tumorigenicity assay essential for facilitating safety studies of hiPSC-derived cardiomyocytes for clinical application. Sci Rep 9:1881

236.   Itzhaki JE, Gilbert CS, Porter AC (1997) Construction by gene targeting in human cells of a "conditional' CDC2 mutant that rereplicates its DNA. Nat Genet 15:258–265

237.   Iwasaki H, Ichihara Y, Morino K, Lemecha M, Sugawara L, Sawano T, Miake J, Sakurai H, Nishi E, Maegawa H, Imamura T (2021) MicroRNA-494-3p inhibits formation of fast oxidative muscle fibres by targeting E1A-binding protein p300 in human-induced pluripotent stem cells. Sci Rep 11:1161

238.   Iwasaki S, Kobayashi M, Yoda M, Sakaguchi Y, Katsuma S, Suzuki T, Tomari Y (2010) Hsc70/Hsp90 chaperone machinery mediates ATP-dependent RISC loading of small RNA duplexes. Mol Cell 39:292–299

239.   Iyer DR, Rhind N (2017) The Intra-S Checkpoint Responses to DNA Damage. Genes 8:E74

240. Jääger K, Islam S, Zajac P, Linnarsson S, Neuman T (2012) RNA-seq analysis reveals different dynamics of differentiation of human dermis- and adipose-derived stromal stem cells. PloS One 7:e38833

241. Jackson DA, Pombo A (1998) Replicon clusters are stable units of chromosome structure: evidence that nuclear organization contributes to the efficient activation and propagation of S phase in human cells. J Cell Biol 140:1285–1295

242. Jacob F, Brenner S, Cuzin F (1963) On the Regulation of DNA Replication in Bacteria. Cold Spring Harb Symp Quant Biol 28:329–348

243. James AW, Leucht P, Levi B, Carre AL, Xu Y, Helms JA, Longaker MT (2010) Sonic Hedgehog influences the balance of osteogenesis and adipogenesis in mouse adipose-derived stromal cells. Tissue Eng Part A 16:2605–2616

244. James AW, Pan A, Chiang M, Zara JN, Zhang X, Ting K, Soo C (2011) A new function of Nell-1 protein in repressing adipogenic differentiation. Biochem Biophys Res Commun 411:126–131

245. James AW (2013) Review of Signaling Pathways Governing MSC Osteogenic and Adipogenic Differentiation. Scientifica 2013:684736

246. Jeng S-F, Rau C-S, Liliang P-C, Wu C-J, Lu T-H, Chen Y-C, Lin C-J, Hsieh C-H (2009) Profiling muscle-specific microRNA expression after peripheral denervation and reinnervation in a rat model. J Neurotrauma 26:2345–2353

247. Jeong JA, Hong SH, Gang EJ, Ahn C, Hwang SH, Yang IH, Han H, Kim H (2005) Differential gene expression profiling of human umbilical cord blood-derived mesenchymal stem cells by DNA microarray. Stem Cells Dayt Ohio 23:584–593

248. Ji J, Zhang J, Huang G, Qian J, Wang X, Mei S (2009) Over-expressed microRNA-27a and 27b influence fat accumulation and cell proliferation during rat hepatic stellate cell activation. FEBS Lett 583:759–766

249. Jiang H, Hong T, Wang T, Wang X, Cao L, Xu X, Zheng M (2019) Gene expression profiling of human bone marrow mesenchymal stem cells during osteogenic differentiation. J Cell Physiol 234:7070–7077

250. Jiang X, Zhang Z, Peng T, Wang G, Xu Q, Li G (2020) miR-204 inhibits the osteogenic differentiation of mesenchymal stem cells by targeting bone morphogenetic protein 2. Mol Med Rep 21:43–50

251. Jin J, Arias EE, Chen J, Harper JW, Walter JC (2006) A family of diverse Cul4-Ddb1-interacting proteins includes Cdt2, which is required for S phase destruction of the replication factor Cdt1. Mol Cell 23:709–721

252. Jin W, Takagi T, Kanesashi S, Kurahashi T, Nomura T, Harada J, Ishii S (2006) Schnurri-2 controls BMP-dependent adipogenesis via interaction with Smad proteins. Dev Cell 10:461–471

253. Jinesh GG, Flores ER, Brohl AS (2018) Chromosome 19 miRNA cluster and CEBPB expression specifically mark and potentially drive triple negative breast cancers. PloS One 13:e0206008

254. Jo H, Shim K, Jeoung D (2022) Potential of the miR-200 Family as a Target for Developing Anti-Cancer Therapeutics. Int J Mol Sci 23:5881

255. Jonas S, Izaurralde E (2015) Towards a molecular understanding of microRNA-mediated gene silencing. Nat Rev Genet 16:421–433

256. Jouravleva K, Vega-Badillo J, Zamore PD (2022) Principles and pitfalls of high-throughput analysis of microRNA-binding thermodynamics and kinetics by RNA Bind-n-Seq. Cell Rep Methods 2:100185

257. Kajimoto K, Naraba H, Iwai N (2006) MicroRNA and 3T3-L1 pre-adipocyte differentiation. RNA N Y N 12:1626–1632

258. Kang M, Yan LM, Li YM, Zhang WY, Wang H, Tang AZ, Ou HS (2013) Inhibitory effect of microRNA-24 on fatty acid-binding protein expression on 3T3-L1 adipocyte differentiation. Genet Mol Res GMR 12:5267–5277

259. Kang Q, Song W-X, Luo Q, Tang N, Luo J, Luo X, Chen J, Bi Y, He B-C, Park JK, Jiang W, Tang Y, Huang J, Su Y, Zhu G-H, He Y, Yin H, Hu Z, Wang Y, Chen L, Zuo G-W, Pan X, Shen J, Vokes T, Reid RR, Haydon RC, Luu HH, He T-C (2009) A comprehensive analysis of the dual roles of BMPs in regulating adipogenic and osteogenic differentiation of mesenchymal progenitor cells. Stem Cells Dev 18:545–559

260. Karakaidos P, Taraviras S, Vassiliou LV, Zacharatos P, Kastrinakis NG, Kougiou D, Kouloukoussa M, Nishitani H, Papavassiliou AG, Lygerou Z, Gorgoulis VG (2004) Overexpression of the replication licensing regulators hCdt1 and hCdc6 characterizes a subset of non-small-cell lung carcinomas: synergistic effect with mutant p53 on tumor growth and chromosomal instability--evidence of E2F-1 transcriptional control over hCdt1. Am J Pathol 165:1351–1365

261. Karbiener M, Fischer C, Nowitsch S, Opriessnig P, Papak C, Ailhaud G, Dani C, Amri E-Z, Scheideler M (2009) microRNA miR-27b impairs human adipocyte differentiation and targets PPARgamma. Biochem Biophys Res Commun 390:247–251

262. Karczewska-Kupczewska M, Stefanowicz M, Matulewicz N, Nikołajuk A, Strączkowski M (2016) Wnt Signaling Genes in Adipose Tissue and Skeletal Muscle of Humans With Different Degrees of Insulin Sensitivity. J Clin Endocrinol Metab 101:3079–3087

263. Kaufman RJ, Brown PC, Schimke RT (1979) Amplified dihydrofolate reductase genes in unstably methotrexate-resistant cells are associated with double minute chromosomes. Proc Natl Acad Sci U S A 76:5669–5673

264. Kawai M, Mushiake S, Bessho K, Murakami M, Namba N, Kokubu C, Michigami T, Ozono K (2007) Wnt/Lrp/beta-catenin signaling suppresses adipogenesis by inhibiting mutual activation of PPARgamma and C/EBPalpha. Biochem Biophys Res Commun 363:276–282

265. Kawai M, Rosen CJ (2009) Insulin-like growth factor-I and bone: lessons from mice and men. Pediatr Nephrol Berl Ger 24:1277–1285

266. Kawakami Y, Rodriguez-León J, Izpisúa Belmonte JC (2006) The role of TGFbetas and Sox9 during limb chondrogenesis. Curr Opin Cell Biol 18:723–729

267.   Kawamata T, Tomari Y (2010) Making RISC. Trends Biochem Sci 35:368–376

268.   Kaykov A, Taillefumier T, Bensimon A, Nurse P (2016) Molecular Combing of Single DNA Molecules on the 10 Megabase Scale. Sci Rep 6:19636

269.   Kean TJ, Lin P, Caplan AI, Dennis JE (2013) MSCs: Delivery Routes and Engraftment, Cell-Targeting Strategies, and Immune Modulation. Stem Cells Int 2013:732742

270.   Kelich JM, Papaioannou H, Skordalakes E (2021) Pol α-primase dependent nuclear localization of the mammalian CST complex. Commun Biol 4:349

271.   Kelman LM, Kelman Z (2014) Archaeal DNA replication. Annu Rev Genet 48:71–97

272.   Kern F, Fehlmann T, Solomon J, Schwed L, Grammes N, Backes C, Van Keuren-Jensen K, Craig DW, Meese E, Keller A (2020) miEAA 2.0: integrating multi-species microRNA enrichment analysis and workflow management systems. Nucleic Acids Res 48:W521–W528

273.   Kern F, Krammes L, Danz K, Diener C, Kehl T, Küchler O, Fehlmann T, Kahraman M, Rheinheimer S, Aparicio-Puerta E, Wagner S, Ludwig N, Backes C, Lenhof H-P, von Briesen H, Hart M, Keller A, Meese E (2021) Validation of human microRNA target pathways enables evaluation of target prediction tools. Nucleic Acids Res 49:127–144

274.   Kern F, Kuhn T, Ludwig N, Simon M, Gröger L, Fabis N, Aparicio-Puerta E, Salhab A, Fehlmann T, Hahn O, Engel A, Wagner V, Koch M, Winek K, Soreq H, Nazarenko I, Fuhrmann G, Wyss-Coray T, Meese E, Keller V, Laschke MW, Keller A (2023) Ageing-associated small RNA cargo of extracellular vesicles. RNA Biol 20:482–494

275.   Kiani M, Movahedin M, Halvaei I, Soleimani M (2023) In vitro differentiation of primed human induced pluripotent stem cells into primordial germ cell-like cells. Mol Biol Rep 50:1971–1979

276.   Kicinski M (2014) How does under-reporting of negative and inconclusive results affect the false-positive rate in meta-analysis? A simulation study. BMJ Open 4:e004831

277.   Kim SY, Kim AY, Lee HW, Son YH, Lee GY, Lee J-W, Lee YS, Kim JB (2010) miR-27a is a negative regulator of adipocyte differentiation via suppressing PPARgamma expression. Biochem Biophys Res Commun 392:323–328

278.   Kim YJ, Hwang SJ, Bae YC, Jung JS (2009) MiR-21 regulates adipogenic differentiation through the modulation of TGF-beta signaling in mesenchymal stem cells derived from human adipose tissue. Stem Cells Dayt Ohio 27:3093–3102

279.   Kintner C (2002) Neurogenesis in embryos and in adult neural stem cells. J Neurosci Off J Soc Neurosci 22:639–643

280.   Klotz-Noack K, McIntosh D, Schurch N, Pratt N, Blow JJ (2012) Re-replication induced by geminin depletion occurs from G2 and is enhanced by checkpoint activation. J Cell Sci 125:2436–2445

281. Ko J-Y, Lee MS, Lian W-S, Weng W-T, Sun Y-C, Chen Y-S, Wang F-S (2017) MicroRNA-29a Counteracts Synovitis in Knee Osteoarthritis Pathogenesis by Targeting VEGF. Sci Rep 7:3584

282. Kole AJ, Swahari V, Hammond SM, Deshmukh M (2011) miR-29b is activated during neuronal maturation and targets BH3-only genes to restrict apoptosis. Genes Dev 25:125–130

283. Komori T (2010) Regulation of osteoblast differentiation by Runx2. Adv Exp Med Biol 658:43–49

284. Koo D-H, Molin WT, Saski CA, Jiang J, Putta K, Jugulam M, Friebe B, Gill BS (2018) Extrachromosomal circular DNA-based amplification and transmission of herbicide resistance in crop weed Amaranthus palmeri. Proc Natl Acad Sci U S A 115:3332–3337

285. Koutsoulidou A, Mastroyiannopoulos NP, Furling D, Uney JB, Phylactou LA (2011) Expression of miR-1, miR-133a, miR-133b and miR-206 increases during development of human skeletal muscle. BMC Dev Biol 11:34

286. Kozomara A, Birgaoanu M, Griffiths-Jones S (2019) miRBase: from microRNA sequences to function. Nucleic Acids Res 47:D155–D162

287. Kozovska Z, Gabrisova V, Kucerova L (2016) Malignant melanoma: diagnosis, treatment and cancer stem cells. Neoplasma 63:510–517

288. Krasinska L, Besnard E, Cot E, Dohet C, Méchali M, Lemaitre J-M, Fisher D (2008) Cdk1 and Cdk2 activity levels determine the efficiency of replication origin firing in Xenopus. EMBO J 27:758–769

289. Krichevsky AM, King KS, Donahue CP, Khrapko K, Kosik KS (2003) A microRNA array reveals extensive regulation of microRNAs during brain development. RNA N Y N 9:1274–1281

290. Kulartz M, Knippers R (2004) The replicative regulator protein geminin on chromatin in the HeLa cell cycle. J Biol Chem 279:41686–41694

291. Kulcenty K, Wroblewska JP, Rucinski M, Kozlowska E, Jopek K, Suchorska WM (2019) MicroRNA Profiling During Neural Differentiation of Induced Pluripotent Stem Cells. Int J Mol Sci 20:E3651

292. Kumar L, E Futschik M (2007) Mfuzz: a software package for soft clustering of microarray data. Bioinformation 2:5–7

293. Kunkel TA, Bebenek K (2000) DNA replication fidelity. Annu Rev Biochem 69:497–529

294. Kuo MT, Sen S, Hittelman WN, Hsu TC (1998) Chromosomal fragile sites and DNA amplification in drug-resistant cells. Biochem Pharmacol 56:7–13

295. Kuriyan AE, Albini TA, Townsend JH, Rodriguez M, Pandya HK, Leonard RE, Parrott MB, Rosenfeld PJ, Flynn HW, Goldberg JL (2017) Vision Loss after Intravitreal Injection of Autologous "Stem Cells" for AMD. N Engl J Med 376:1047–1053

296.   Labib K, De Piccoli G (2011) Surviving chromosome replication: the many roles of the S-phase checkpoint pathway. Philos Trans R Soc Lond B Biol Sci 366:3554–3561

297.   Labit H, Perewoska I, Germe T, Hyrien O, Marheineke K (2008) DNA replication timing is deterministic at the level of chromosomal domains but stochastic at the level of replicons in Xenopus egg extracts. Nucleic Acids Res 36:5623–5634

298.   Lagos-Quintana M, Rauhut R, Yalcin A, Meyer J, Lendeckel W, Tuschl T (2002) Identification of tissue-specific microRNAs from mouse. Curr Biol CB 12:735–739

299.   Laser-Azogui A, Kornreich M, Malka-Gibor E, Beck R (2015) Neurofilament assembly and function during neuronal development. Curr Opin Cell Biol 32:92–101

300.   Laudes M (2011) Role of WNT pathway in the determination of human mesenchymal stem cells into preadipocytes. J Mol Endocrinol JME-10-0169

301.   Lazarenko OP, Rzonca SO, Suva LJ, Lecka-Czernik B (2006) Netoglitazone is a PPAR-gamma ligand with selective effects on bone and fat. Bone 38:74–84

302.   Lee C, Hong B, Choi JM, Kim Y, Watanabe S, Ishimi Y, Enomoto T, Tada S, Kim Y, Cho Y (2004) Structural basis for inhibition of the replication licensing factor Cdt1 by geminin. Nature 430:913–917

303.   Lee EK, Lee MJ, Abdelmohsen K, Kim W, Kim MM, Srikantan S, Martindale JL, Hutchison ER, Kim HH, Marasa BS, Selimyan R, Egan JM, Smith SR, Fried SK, Gorospe M (2011) miR-130 suppresses adipogenesis by inhibiting peroxisome proliferator-activated receptor gamma expression. Mol Cell Biol 31:626–638

304.   Lee JA, Carvalho CMB, Lupski JR (2007) A DNA replication mechanism for generating nonrecurrent rearrangements associated with genomic disorders. Cell 131:1235–1247

305.   Lee J-S, Park J-C, Kim T-W, Jung B-J, Lee Y, Shim E-K, Park S, Choi E-Y, Cho K-S, Kim C-S (2015) Human bone marrow stem cells cultured under hypoxic conditions present altered characteristics and enhanced in vivo tissue regeneration. Bone 78:34–45

306.   Lee K-P, Shin YJ, Panda AC, Abdelmohsen K, Kim JY, Lee S-M, Bahn YJ, Choi JY, Kwon E-S, Baek S-J, Kim S-Y, Gorospe M, Kwon K-S (2015) miR-431 promotes differentiation and regeneration of old skeletal muscle by targeting Smad4. Genes Dev 29:1605–1617

307.   Lee KS, Kim HJ, Li QL, Chi XZ, Ueta C, Komori T, Wozney JM, Kim EG, Choi JY, Ryoo HM, Bae SC (2000) Runx2 is a common target of transforming growth factor beta1 and bone morphogenetic protein 2, and cooperation between Runx2 and Smad5 induces osteoblast-specific gene expression in the pluripotent mesenchymal precursor cell line C2C12. Mol Cell Biol 20:8783–8792

308.   Lee M, Jeong SY, Ha J, Kim M, Jin HJ, Kwon S-J, Chang JW, Choi SJ, Oh W, Yang YS, Kim J-S, Jeon HB (2014) Low immunogenicity of allogeneic human umbilical cord blood-derived mesenchymal stem cells in vitro and in vivo. Biochem Biophys Res Commun 446:983–989

309.   Lee RH, Kim B, Choi I, Kim H, Choi HS, Suh K, Bae YC, Jung JS (2004) Characterization and expression analysis of mesenchymal stem cells from human

bone marrow and adipose tissue. Cell Physiol Biochem Int J Exp Cell Physiol Biochem Pharmacol 14:311–324

310.   Lee S, Yoon DS, Paik S, Lee K-M, Jang Y, Lee JW (2014) microRNA-495 inhibits chondrogenic differentiation in human mesenchymal stem cells by targeting Sox9. Stem Cells Dev 23:1798–1808

311.   Lee Y, Jeon K, Lee J-T, Kim S, Kim VN (2002) MicroRNA maturation: stepwise processing and subcellular localization. EMBO J 21:4663–4670

312.   Lefterova MI, Zhang Y, Steger DJ, Schupp M, Schug J, Cristancho A, Feng D, Zhuo D, Stoeckert CJ, Liu XS, Lazar MA (2008) PPARgamma and C/EBP factors orchestrate adipocyte biology via adjacent binding on a genome-wide scale. Genes Dev 22:2941–2952

313.   Lei L, Huang Z, Feng J, Huang Z, Tao Y, Hu X, Zhang X (2020) Loss of receptor tyrosine kinase-like orphan receptor 2 impairs the osteogenesis of mBMSCs by inhibiting signal transducer and activator of transcription 3. Stem Cell Res Ther 11:137

314.   Leidinger P, Backes C, Blatt M, Keller A, Huwer H, Lepper P, Bals R, Meese E (2014) The blood-borne miRNA signature of lung cancer patients is independent of histology but influenced by metastases. Mol Cancer 13:202

315.   Lerner MR, Boyle JA, Hardin JA, Steitz JA (1981) Two novel classes of small ribonucleoproteins detected by antibodies associated with lupus erythematosus. Science 211:400–402

316.   Lesly S, Bandura JL, Calvi BR (2017) Rapid DNA Synthesis During Early Drosophila Embryogenesis Is Sensitive to Maternal Humpty Dumpty Protein Function. Genetics 207:935–947

317.   Leucht C, Stigloher C, Wizenmann A, Klafke R, Folchert A, Bally-Cuif L (2008) MicroRNA-9 directs late organizer activity of the midbrain-hindbrain boundary. Nat Neurosci 11:641–648

318.   Lewis BP, Shih I -hung, Jones-Rhoades MW, Bartel DP, Burge CB (2003) Prediction of mammalian microRNA targets. Cell 115:787–798

319.   Lewis BP, Burge CB, Bartel DP (2005) Conserved seed pairing, often flanked by adenosines, indicates that thousands of human genes are microRNA targets. Cell 120:15–20

320.   Li A, Blow JJ (2005) Cdt1 downregulation by proteolysis and geminin inhibition prevents DNA re-replication in Xenopus. EMBO J 24:395–404

321.   Li C, Vassilev A, DePamphilis ML (2004) Role for Cdk1 (Cdc2)/cyclin A in preventing the mammalian origin recognition complex's largest subunit (Orc1) from binding to chromatin during mitosis. Mol Cell Biol 24:5875–5886

322.   Li C-J, DePamphilis ML (2002) Mammalian Orc1 protein is selectively released from chromatin and ubiquitinated during the S-to-M transition in the cell division cycle. Mol Cell Biol 22:105–116

323.   Li H, Mao S, Wang H, Zen K, Zhang C, Li L (2014) MicroRNA-29a modulates axon branching by targeting doublecortin in primary neurons. Protein Cell 5:160–169

324.   Li H, Cui Q, Dong Z, Zhang J, Li H, Zhao L (2016) Downregulation of miR-27b is Involved in Loss of Type II Collagen by Directly Targeting Matrix Metalloproteinase 13 (MMP13) in Human Intervertebral Disc Degeneration. Spine 41:E116-123

325.   Li H, Xue M, Xu J, Qin X (2016) MiR-301a is involved in adipocyte dysfunction during obesity-related inflammation via suppression of PPARγ. Pharm 71:84–88

326.   Li X, Guo L, Liu Y, Su Y, Xie Y, Du J, Zhou J, Ding G, Wang H, Bai Y, Liu Y (2017) MicroRNA-21 promotes osteogenesis of bone marrow mesenchymal stem cells via the Smad7-Smad1/5/8-Runx2 pathway. Biochem Biophys Res Commun 493:928–933

327.   Li Y, Luo J, Zhou H, Liao J-Y, Ma L-M, Chen Y-Q, Qu L-H (2008) Stress-induced tRNA-derived RNAs: a novel class of small RNAs in the primitive eukaryote Giardia lamblia. Nucleic Acids Res 36:6048–6055

328.   Li Y, Fan L, Hu J, Zhang L, Liao L, Liu S, Wu D, Yang P, Shen L, Chen J, Jin Y (2015) MiR-26a Rescues Bone Regeneration Deficiency of Mesenchymal Stem Cells Derived From Osteoporotic Mice. Mol Ther J Am Soc Gene Ther 23:1349–1357

329.   Li Y, Roberts ND, Wala JA, Shapira O, Schumacher SE, Kumar K, Khurana E, Waszak S, Korbel JO, Haber JE, Imielinski M, PCAWG Structural Variation Working Group, Weischenfeldt J, Beroukhim R, Campbell PJ, PCAWG Consortium (2020) Patterns of somatic structural variation in human cancer genomes. Nature 578:112–121

330.   Li Y, Wang J (2022) Time series clustering analysis of genes during osteogenic differentiation of human mesenchymal stem cells. Genes Genet Syst 97:209–218

331.   Li YP, Wei XC, Li PC, Chen CW, Wang XH, Jiao Q, Wang DM, Wei FY, Zhang JZ, Wei L (2015) The Role of miRNAs in Cartilage Homeostasis. Curr Genomics 16:393–404

332.   Li Z, Hassan MQ, Jafferji M, Aqeilan RI, Garzon R, Croce CM, van Wijnen AJ, Stein JL, Stein GS, Lian JB (2019) Correction: Biological functions of miR-29b contribute to positive regulation of osteoblast differentiation. J Biol Chem 294:10018

333.   Liao C, Zhou Y, Li M, Xia Y, Peng W (2020) LINC00968 promotes osteogenic differentiation in vitro and bone formation in vivo via regulation of miR-3658/RUNX2. Differ Res Biol Divers 116:1–8

334.   Lin H-P, Oksuz I, Svaren J, Awatramani R (2018) Egr2-dependent microRNA-138 is dispensable for peripheral nerve myelination. Sci Rep 8:3817

335.   Lin Q, Gao Z, Alarcon RM, Ye J, Yun Z (2009) A role of miR-27 in the regulation of adipogenesis. FEBS J 276:2348–2358

336.   Lin S-L, Chang DC, Lin C-H, Ying S-Y, Leu D, Wu DTS (2011) Regulation of somatic cell reprogramming through inducible mir-302 expression. Nucleic Acids Res 39:1054–1065

337.   Lin S-L, Chen JS, Ying S-Y (2020) MiR-302-Mediated Somatic Cell Reprogramming and Method for Generating Tumor-Free iPS Cells Using miR-302. Methods Mol Biol Clifton NJ 2115:199–219

338.   Lin X, Wu L, Zhang Z, Yang R, Guan Q, Hou X, Wu Q (2014) MiR-335-5p promotes chondrogenesis in mouse mesenchymal stem cells and is regulated through two positive feedback loops. J Bone Miner Res Off J Am Soc Bone Miner Res 29:1575–1585

339.   Liontos M, Koutsami M, Sideridou M, Evangelou K, Kletsas D, Levy B, Kotsinas A, Nahum O, Zoumpourlis V, Kouloukoussa M, Lygerou Z, Taraviras S, Kittas C, Bartkova J, Papavassiliou AG, Bartek J, Halazonetis TD, Gorgoulis VG (2007) Deregulated overexpression of hCdt1 and hCdc6 promotes malignant behavior. Cancer Res 67:10899–10909

340.   Liu H, Zhong L, Yuan T, Chen S, Zhou Y, An L, Guo Y, Fan M, Li Y, Sun Y, Li W, Shi Q, Weng Y (2018) MicroRNA-155 inhibits the osteogenic differentiation of mesenchymal stem cells induced by BMP9 via downregulation of BMP signaling pathway. Int J Mol Med 41:3379–3393

341.   Liu S, Yang Y, Wu J (2011) TNFα-induced up-regulation of miR-155 inhibits adipogenesis by down-regulating early adipogenic transcription factors. Biochem Biophys Res Commun 414:618–624

342.   Liu X, Sun Y, Constantinescu SN, Karam E, Weinberg RA, Lodish HF (1997) Transforming growth factor beta-induced phosphorylation of Smad3 is required for growth inhibition and transcriptional induction in epithelial cells. Proc Natl Acad Sci U S A 94:10669–10674

343.   Liu X, Xu H, Kou J, Wang Q, Zheng X, Yu T (2016) MiR-9 promotes osteoblast differentiation of mesenchymal stem cells by inhibiting DKK1 gene expression. Mol Biol Rep 43:939–946

344.   Löb D, Lengert N, Chagin VO, Reinhart M, Casas-Delucchi CS, Cardoso MC, Drossel B (2016) 3D replicon distributions arise from stochastic initiation and domino-like DNA replication progression. Nat Commun 7:11207

345.   Lolli A, Lambertini E, Penolazzi L, Angelozzi M, Morganti C, Franceschetti T, Pelucchi S, Gambari R, Piva R (2014) Pro-chondrogenic effect of miR-221 and slug depletion in human MSCs. Stem Cell Rev Rep 10:841–855

346.   Lovejoy CA, Lock K, Yenamandra A, Cortez D (2006) DDB1 maintains genome integrity through regulation of Cdt1. Mol Cell Biol 26:7977–7990

347.   Lu W, Han L, Su L, Zhao J, Zhang Y, Zhang S, Zhao B, Miao J (2015) A 3'UTR-associated RNA, FLJ11812 maintains stemness of human embryonic stem cells by targeting miR-4459. Stem Cells Dev 24:1133–1140

348.   Lucas I, Feng W (2003) The essence of replication timing: determinants and significance. Cell Cycle Georget Tex 2:560–563

349.   Lujan SA, Williams JS, Kunkel TA (2016) DNA Polymerases Divide the Labor of Genome Replication. Trends Cell Biol 26:640–654

350.   Luo H, Lv W, Tong Q, Jin J, Xu Z, Zuo B (2021) Functional Non-coding RNA During Embryonic Myogenesis and Postnatal Muscle Development and Disease. Front Cell Dev Biol 9:628339

351.   Luo W, Wu H, Ye Y, Li Z, Hao S, Kong L, Zheng X, Lin S, Nie Q, Zhang X (2014) The transient expression of miR-203 and its inhibiting effects on skeletal muscle cell proliferation and differentiation. Cell Death Dis 5:e1347

352.   Lutzmann M, Maiorano D, Méchali M (2006) A Cdt1-geminin complex licenses chromatin for DNA replication and prevents rereplication during S phase in Xenopus. EMBO J 25:5764–5774

353.   Macgregor HC (1965) The role of lampbrush chromosomes in the formation of nucleoli in amphibian oocytes. Q J Microsc Sci 106:215–228

354.   Machida YJ, Dutta A (2007) The APC/C inhibitor, Emi1, is essential for prevention of rereplication. Genes Dev 21:184–194

355.   Maga G, Hubscher U (2003) Proliferating cell nuclear antigen (PCNA): a dancer with many partners. J Cell Sci 116:3051–3060

356.   Magill ST, Cambronne XA, Luikart BW, Lioy DT, Leighton BH, Westbrook GL, Mandel G, Goodman RH (2010) microRNA-132 regulates dendritic growth and arborization of newborn neurons in the adult hippocampus. Proc Natl Acad Sci U S A 107:20382–20387

357.   Mahadevappa R, Neves H, Yuen SM, Bai Y, McCrudden CM, Yuen HF, Wen Q, Zhang SD, Kwok HF (2017) The prognostic significance of Cdc6 and Cdt1 in breast cancer. Sci Rep 7:985

358.   Mailand N, Diffley JFX (2005) CDKs promote DNA replication origin licensing in human cells by protecting Cdc6 from APC/C-dependent proteolysis. Cell 122:915–926

359.   Makeyev EV, Zhang J, Carrasco MA, Maniatis T (2007) The MicroRNA miR-124 promotes neuronal differentiation by triggering brain-specific alternative pre-mRNA splicing. Mol Cell 27:435–448

360.   Mantiero D, Mackenzie A, Donaldson A, Zegerman P (2011) Limiting replication initiation factors execute the temporal programme of origin firing in budding yeast. EMBO J 30:4805–4814

361.   Mao G, Xu Y, Long D, Sun H, Li H, Xin R, Zhang Z, Li Z, Yang Z, Kang Y (2021) Exosome-transported circRNA_0001236 enhances chondrogenesis and suppress cartilage degradation via the miR-3677-3p/Sox9 axis. Stem Cell Res Ther 12:389

362.   Mao Y, Chen W, Wu H, Liu C, Zhang J, Chen S (2020) Mechanisms and Functions of MiR-200 Family in Hepatocellular Carcinoma. OncoTargets Ther 13:13479–13490

363.   Marcon BH, Holetz FB, Eastman G, Origa-Alves AC, Amorós MA, de Aguiar AM, Rebelatto CK, Brofman PRS, Sotelo-Silveira J, Dallagiovanna B (2017) Downregulation of the protein synthesis machinery is a major regulatory event during early adipogenic differentiation of human adipose-derived stromal cells. Stem Cell Res 25:191–201

364.   Marcon BH, Shigunov P, Spangenberg L, Pereira IT, de Aguiar AM, Amorín R, Rebelatto CK, Correa A, Dallagiovanna B (2019) Cell cycle genes are downregulated after adipogenic triggering in human adipose tissue-derived stem cells by regulation of mRNA abundance. Sci Rep 9:5611

365.   Maréchal A, Zou L (2013) DNA damage sensing by the ATM and ATR kinases. Cold Spring Harb Perspect Biol 5:a012716

366.   Marquez MP, Alencastro F, Madrigal A, Jimenez JL, Blanco G, Gureghian A, Keagy L, Lee C, Liu R, Tan L, Deignan K, Armstrong B, Zhao Y (2017) The Role of Cellular Proliferation in Adipogenic Differentiation of Human Adipose Tissue-Derived Mesenchymal Stem Cells. Stem Cells Dev 26:1578–1595

367.   Martinez-Sanchez A, Dudek KA, Murphy CL (2012) Regulation of human chondrocyte function through direct inhibition of cartilage master regulator SOX9 by microRNA-145 (miRNA-145). J Biol Chem 287:916–924

368.   Martinez-Sanchez A, Murphy CL (2013) miR-1247 functions by targeting cartilage transcription factor SOX9. J Biol Chem 288:30802–30814

369.   Mathieu J, Ruohola-Baker H (2013) Regulation of stem cell populations by microRNAs. Adv Exp Med Biol 786:329–351

370.   Mathieu M, Iampietro M, Chuchana P, Guérit D, Djouad F, Noël D, Jorgensen C (2014) Involvement of angiopoietin-like 4 in matrix remodeling during chondrogenic differentiation of mesenchymal stem cells. J Biol Chem 289:8402–8412

371.   Matsui A, Ihara T, Suda H, Mikami H, Semba K (2013) Gene amplification: mechanisms and involvement in cancer. Biomol Concepts 4:567–582

372.   Mazurczyk M, Rybaczek D (2015) Replication and re-replication: Different implications of the same mechanism. Biochimie 108:25–32

373.   McAlinden A, Varghese N, Wirthlin L, Chang L-W (2013) Differentially expressed microRNAs in chondrocytes from distinct regions of developing human cartilage. PloS One 8:e75012

374.   McCarthy JJ, Esser KA (2007) MicroRNA-1 and microRNA-133a expression are decreased during skeletal muscle hypertrophy. J Appl Physiol Bethesda Md 1985 102:306–313

375.   McCarthy JJ, Esser KA, Andrade FH (2007) MicroRNA-206 is overexpressed in the diaphragm but not the hindlimb muscle of mdx mouse. Am J Physiol Cell Physiol 293:C451-457

376.   McClintock B (1941) The Stability of Broken Ends of Chromosomes in Zea Mays. Genetics 26:234–282

377.   McClintock B (1942) The Fusion of Broken Ends of Chromosomes Following Nuclear Fusion. Proc Natl Acad Sci U S A 28:458–463

378.   McCLINTOCK B (1951) Chromosome organization and genic expression. Cold Spring Harb Symp Quant Biol 16:13–47

379.   McGarry TJ, Kirschner MW (1998) Geminin, an inhibitor of DNA replication, is degraded during mitosis. Cell 93:1043–1053

380.   Medina-Gomez G, Gray SL, Yetukuri L, Shimomura K, Virtue S, Campbell M, Curtis RK, Jimenez-Linan M, Blount M, Yeo GSH, Lopez M, Seppänen-Laakso T, Ashcroft

FM, Oresic M, Vidal-Puig A (2007) PPAR gamma 2 prevents lipotoxicity by controlling adipose tissue expandability and peripheral lipid metabolism. PLoS Genet 3:e64

381. Meijer HA, Smith EM, Bushell M (2014) Regulation of miRNA strand selection: follow the leader? Biochem Soc Trans 42:1135–1140

382. Meinhardt G, Kaltenberger S, Fiala C, Knöfler M, Pollheimer J (2015) ERBB2 gene amplification increases during the transition of proximal EGFR(+) to distal HLA-G(+) first trimester cell column trophoblasts. Placenta 36:803–808

383. Melton C, Judson RL, Blelloch R (2010) Opposing microRNA families regulate self-renewal in mouse embryonic stem cells. Nature 463:621–626

384. Méndez J, Zou-Yang XH, Kim S-Y, Hidaka M, Tansey WP, Stillman B (2002) Human origin recognition complex large subunit is degraded by ubiquitin-mediated proteolysis after initiation of DNA replication. Mol Cell 9:481–491

385. Meng F, Li Z, Zhang Z, Yang Z, Kang Y, Zhao X, Long D, Hu S, Gu M, He S, Wu P, Chang Z, He A, Liao W (2018) MicroRNA-193b-3p regulates chondrogenesis and chondrocyte metabolism by targeting HDAC3. Theranostics 8:2862–2883

386. Mens MMJ, Ghanbari M (2018) Cell Cycle Regulation of Stem Cells by MicroRNAs. Stem Cell Rev Rep 14:309–322

387. Menzel J, Tatman P, Black JC (2020) Isolation and analysis of rereplicated DNA by Rerep-Seq. Nucleic Acids Res 48:e58

388. Miller OL, Beatty BR (1969) Extrachromosomal nucleolar genes in amphibian oocytes. Genetics 61:Suppl:133-143

389. Minet M, Abu-Halima M, Du Y, Doerr J, Isted C, Ludwig N, Keller A, Meese E, Fischer U (2022) A Temporary Pause in the Replication Licensing Restriction Leads to Rereplication during Early Human Cell Differentiation. Cells 11:1060

390. Miotto B, Struhl K (2010) HBO1 histone acetylase activity is essential for DNA replication licensing and inhibited by Geminin. Mol Cell 37:57–66

391. Miotto B, Ji Z, Struhl K (2016) Selectivity of ORC binding sites and the relation to replication timing, fragile sites, and deletions in cancers. Proc Natl Acad Sci U S A 113:E4810-4819

392. Miyoshi N, Ishii H, Nagano H, Haraguchi N, Dewi DL, Kano Y, Nishikawa S, Tanemura M, Mimori K, Tanaka F, Saito T, Nishimura J, Takemasa I, Mizushima T, Ikeda M, Yamamoto H, Sekimoto M, Doki Y, Mori M (2011) Reprogramming of mouse and human cells to pluripotency using mature microRNAs. Cell Stem Cell 8:633–638

393. Moiseeva TN, Bakkenist CJ (2019) Dormant origin signaling during unperturbed replication. DNA Repair 81:102655

394. Mok GF, Lozano-Velasco E, Münsterberg A (2017) microRNAs in skeletal muscle development. Semin Cell Dev Biol 72:67–76

395. Møller HD, Parsons L, Jørgensen TS, Botstein D, Regenberg B (2015) Extrachromosomal circular DNA is common in yeast. Proc Natl Acad Sci U S A 112:E3114-3122

396.   Mong EF, Yang Y, Akat KM, Canfield J, VanWye J, Lockhart J, Tsibris JCM, Schatz F, Lockwood CJ, Tuschl T, Kayisli UA, Totary-Jain H (2020) Chromosome 19 microRNA cluster enhances cell reprogramming by inhibiting epithelial-to-mesenchymal transition. Sci Rep 10:3029

397.   Morin RD, O'Connor MD, Griffith M, Kuchenbauer F, Delaney A, Prabhu A-L, Zhao Y, McDonald H, Zeng T, Hirst M, Eaves CJ, Marra MA (2008) Application of massively parallel sequencing to microRNA profiling and discovery in human embryonic stem cells. Genome Res 18:610–621

398.   Mrugala D, Dossat N, Ringe J, Delorme B, Coffy A, Bony C, Charbord P, Häupl T, Daures J-P, Noël D, Jorgensen C (2009) Gene expression profile of multipotent mesenchymal stromal cells: Identification of pathways common to TGFbeta3/BMP2-induced chondrogenesis. Cloning Stem Cells 11:61–76

399.   Muleris M, Almeida A, Dutrillaux AM, Pruchon E, Vega F, Delattre JY, Poisson M, Malfoy B, Dutrillaux B (1994) Oncogene amplification in human gliomas: a molecular cytogenetic analysis. Oncogene 9:2717–2722

400.   Muñoz S, Búa S, Rodríguez-Acebes S, Megías D, Ortega S, de Martino A, Méndez J (2017) In Vivo DNA Re-replication Elicits Lethal Tissue Dysplasias. Cell Rep 19:928–938

401.   Murry CE, Keller G (2008) Differentiation of embryonic stem cells to clinically relevant populations: lessons from embryonic development. Cell 132:661–680

402.   Muruganandan S, Roman AA, Sinal CJ (2009) Adipocyte differentiation of bone marrow-derived mesenchymal stem cells: cross talk with the osteoblastogenic program. Cell Mol Life Sci CMLS 66:236–253

403.   Mushahary D, Spittler A, Kasper C, Weber V, Charwat V (2018) Isolation, cultivation, and characterization of human mesenchymal stem cells. Cytom Part J Int Soc Anal Cytol 93:19–31

404.   Nakanishi N, Nakagawa Y, Tokushige N, Aoki N, Matsuzaka T, Ishii K, Yahagi N, Kobayashi K, Yatoh S, Takahashi A, Suzuki H, Urayama O, Yamada N, Shimano H (2009) The up-regulation of microRNA-335 is associated with lipid metabolism in liver and white adipose tissue of genetically obese mice. Biochem Biophys Res Commun 385:492–496

405.   Nasheri N, Singaravelu R, Goodmurphy M, Lyn RK, Pezacki JP (2011) Competing roles of microRNA-122 recognition elements in hepatitis C virus RNA. Virology 410:336–344

406.   Neve A, Corrado A, Cantatore FP (2011) Osteoblast physiology in normal and pathological conditions. Cell Tissue Res 343:289–302

407.   Ng TK, Yang Q, Fortino VR, Lai NY-K, Carballosa CM, Greenberg JM, Choy KW, Pelaez D, Pang CP, Cheung HS (2019) MicroRNA-132 directs human periodontal ligament-derived neural crest stem cell neural differentiation. J Tissue Eng Regen Med 13:12–24

408.   Nguyen LH, Ong W, Wang K, Wang M, Nizetic D, Chew SY (2020) Effects of miR-219/miR-338 on microglia and astrocyte behaviors and astrocyte-oligodendrocyte precursor cell interactions. Neural Regen Res 15:739–747

409. Nguyen PNN, Huang C-J, Sugii S, Cheong SK, Choo KB (2017) Selective activation of miRNAs of the primate-specific chromosome 19 miRNA cluster (C19MC) in cancer and stem cells and possible contribution to regulation of apoptosis. J Biomed Sci 24:20

410. Nguyen VQ, Co C, Li JJ (2001) Cyclin-dependent kinases prevent DNA re-replication through multiple mechanisms. Nature 411:1068–1073

411. Nishino J, Kim I, Chada K, Morrison SJ (2008) Hmga2 promotes neural stem cell self-renewal in young but not old mice by reducing p16Ink4a and p19Arf Expression. Cell 135:227–239

412. Nishitani H, Lygerou Z, Nishimoto T (2004) Proteolysis of DNA replication licensing factor Cdt1 in S-phase is performed independently of geminin through its N-terminal region. J Biol Chem 279:30807–30816

413. Nishitani H, Sugimoto N, Roukos V, Nakanishi Y, Saijo M, Obuse C, Tsurimoto T, Nakayama KI, Nakayama K, Fujita M, Lygerou Z, Nishimoto T (2006) Two E3 ubiquitin ligases, SCF-Skp2 and DDB1-Cul4, target human Cdt1 for proteolysis. EMBO J 25:1126–1136

414. Noller HF, Green R, Heilek G, Hoffarth V, Hüttenhofer A, Joseph S, Lee I, Lieberman K, Mankin A, Merryman C (1995) Structure and function of ribosomal RNA. Biochem Cell Biol Biochim Biol Cell 73:997–1009

415. Nussbaum J, Minami E, Laflamme MA, Virag JAI, Ware CB, Masino A, Muskheli V, Pabon L, Reinecke H, Murry CE (2007) Transplantation of undifferentiated murine embryonic stem cells in the heart: teratoma formation and immune response. FASEB J Off Publ Fed Am Soc Exp Biol 21:1345–1357

416. Nuzzolo ER, Capodimonti S, Martini M, Iachininoto MG, Bianchi M, Cocomazzi A, Zini G, Leone G, Larocca LM, Teofili L (2014) Adult and cord blood endothelial progenitor cells have different gene expression profiles and immunogenic potential. Blood Transfus Trasfus Sangue 12 Suppl 1:s367-374

417. Ochi S, Manabe S, Kikkawa T, Osumi N (2022) Thirty Years' History since the Discovery of Pax6: From Central Nervous System Development to Neurodevelopmental Disorders. Int J Mol Sci 23:6115

418. Oldehinkel AJ (Tineke) (2018) Editorial: Sweet nothings – the value of negative findings for scientific progress. J Child Psychol Psychiatry 59:829–830

419. Osheim YN, Miller OL (1983) Novel amplification and transcriptional activity of chorion genes in Drosophila melanogaster follicle cells. Cell 33:543–553

420. Osheim YN, Miller OL, Beyer AL (1988) Visualization of Drosophila melanogaster chorion genes undergoing amplification. Mol Cell Biol 8:2811–2821

421. Otto F, Thornell AP, Crompton T, Denzel A, Gilmour KC, Rosewell IR, Stamp GW, Beddington RS, Mundlos S, Olsen BR, Selby PB, Owen MJ (1997) Cbfa1, a candidate gene for cleidocranial dysplasia syndrome, is essential for osteoblast differentiation and bone development. Cell 89:765–771

422. Pandur P, Maurus D, Kühl M (2002) Increasingly complex: new players enter the Wnt signaling network. BioEssays News Rev Mol Cell Dev Biol 24:881–884

423.   Pardo B, Crabbé L, Pasero P (2017) Signaling pathways of replication stress in yeast. FEMS Yeast Res 17:

424.   Park SJ, Cheon EJ, Lee MH, Kim HA (2013) MicroRNA-127-5p regulates matrix metalloproteinase 13 expression and interleukin-1β-induced catabolic effects in human chondrocytes. Arthritis Rheum 65:3141–3152

425.   Patel PK, Kommajosyula N, Rosebrock A, Bensimon A, Leatherwood J, Bechhoefer J, Rhind N (2008) The Hsk1(Cdc7) replication kinase regulates origin efficiency. Mol Biol Cell 19:5550–5558

426.   Patel YM, Lane MD (2000) Mitotic Clonal Expansion during Preadipocyte Differentiation: Calpain-mediated Turnover of p27 *. J Biol Chem 275:17653–17660

427.   Patmanidi AL, Champeris Tsaniras S, Karamitros D, Kyrousi C, Lygerou Z, Taraviras S (2017) Concise Review: Geminin-A Tale of Two Tails: DNA Replication and Transcriptional/Epigenetic Regulation in Stem Cells. Stem Cells Dayt Ohio 35:299–310

428.   Paulsen T, Kumar P, Koseoglu MM, Dutta A (2018) Discoveries of Extrachromosomal Circles of DNA in Normal and Tumor Cells. Trends Genet TIG 34:270–278

429.   Pellin D, Loperfido M, Baricordi C, Wolock SL, Montepeloso A, Weinberg OK, Biffi A, Klein AM, Biasco L (2019) A comprehensive single cell transcriptional landscape of human hematopoietic progenitors. Nat Commun 10:2395

430.   Peng X-D, Xu P-Z, Chen M-L, Hahn-Windgassen A, Skeen J, Jacobs J, Sundararajan D, Chen WS, Crawford SE, Coleman KG, Hay N (2003) Dwarfism, impaired skin development, skeletal muscle atrophy, delayed bone development, and impeded adipogenesis in mice lacking Akt1 and Akt2. Genes Dev 17:1352–1365

431.   Peric-Hupkes D, Meuleman W, Pagie L, Bruggeman SWM, Solovei I, Brugman W, Gräf S, Flicek P, Kerkhoven RM, van Lohuizen M, Reinders M, Wessels L, van Steensel B (2010) Molecular maps of the reorganization of genome-nuclear lamina interactions during differentiation. Mol Cell 38:603–613

432.   Pfaff N, Fiedler J, Holzmann A, Schambach A, Moritz T, Cantz T, Thum T (2011) miRNA screening reveals a new miRNA family stimulating iPS cell generation via regulation of Meox2. EMBO Rep 12:1153–1159

433.   Piscaglia AC, Shupe T, Gasbarrini A, Petersen BE (2007) Microarray RNA/DNA in different stem cell lines. Curr Pharm Biotechnol 8:167–175

434.   Plaut W (1963) ON THE REPLICATIVE ORGANIZATION OF DNA IN THE POLYTENE CHROMOSOME OF DROSOPHILA MELANOGASTER. J Mol Biol 7:632–635

435.   Plaut W, Nash D, Fanning T (1966) Ordered replication of DNA in polytene chromosomes of Drosophila melanogaster. J Mol Biol 16:85–93

436.   Prioleau M-N, MacAlpine DM (2016) DNA replication origins-where do we begin? Genes Dev 30:1683–1697

437.   Qi J, Yu J-Y, Shcherbata HR, Mathieu J, Wang AJ, Seal S, Zhou W, Stadler BM, Bourgin D, Wang L, Nelson A, Ware C, Raymond C, Lim LP, Magnus J, Ivanovska I, Diaz R, Ball A, Cleary MA, Ruohola-Baker H (2009) microRNAs regulate human embryonic stem cell division. Cell Cycle Georget Tex 8:3729–3741

438.   Qian S-W, Tang Y, Li X, Liu Y, Zhang Y-Y, Huang H-Y, Xue R-D, Yu H-Y, Guo L, Gao H-D, Liu Y, Sun X, Li Y-M, Jia W-P, Tang Q-Q (2013) BMP4-mediated brown fat-like changes in white adipose tissue alter glucose and energy homeostasis. Proc Natl Acad Sci U S A 110:E798-807

439.   Qin L, Chen Y, Niu Y, Chen W, Wang Q, Xiao S, Li A, Xie Y, Li J, Zhao X, He Z, Mo D (2010) A deep investigation into the adipogenesis mechanism: profile of microRNAs regulating adipogenesis by modulating the canonical Wnt/beta-catenin signaling pathway. BMC Genomics 11:320

440.   Rajewska M, Wegrzyn K, Konieczny I (2012) AT-rich region and repeated sequences - the essential elements of replication origins of bacterial replicons. FEMS Microbiol Rev 36:408–434

441.   Ralph E, Boye E, Kearsey SE (2006) DNA damage induces Cdt1 proteolysis in fission yeast through a pathway dependent on Cdt2 and Ddb1. EMBO Rep 7:1134–1139

442.   Rape M, Reddy SK, Kirschner MW (2006) The processivity of multiubiquitination by the APC determines the order of substrate degradation. Cell 124:89–103

443.   Reeves SA, Helman LJ, Allison A, Israel MA (1989) Molecular cloning and primary structure of human glial fibrillary acidic protein. Proc Natl Acad Sci 86:5178–5182

444.   Reifenberger G, Ichimura K, Reifenberger J, Elkahloun AG, Meltzer PS, Collins VP (1996) Refined mapping of 12q13-q15 amplicons in human malignant gliomas suggests CDK4/SAS and MDM2 as independent amplification targets. Cancer Res 56:5141–5145

445.   Reisman M, Adams KT (2014) Stem cell therapy: a look at current research, regulations, and remaining hurdles. P T Peer-Rev J Formul Manag 39:846–857

446.   Remus D, Beuron F, Tolun G, Griffith JD, Morris EP, Diffley JFX (2009) Concerted loading of Mcm2-7 double hexamers around DNA during DNA replication origin licensing. Cell 139:719–730

447.   Reynolds JJ, Bicknell LS, Carroll P, Higgs MR, Shaheen R, Murray JE, Papadopoulos DK, Leitch A, Murina O, Tarnauskaitė Ž, Wessel SR, Zlatanou A, Vernet A, von Kriegsheim A, Mottram RMA, Logan CV, Bye H, Li Y, Brean A, Maddirevula S, Challis RC, Skouloudaki K, Almoisheer A, Alsaif HS, Amar A, Prescott NJ, Bober MB, Duker A, Faqeih E, Seidahmed MZ, Al Tala S, Alswaid A, Ahmed S, Al-Aama JY, Altmüller J, Al Balwi M, Brady AF, Chessa L, Cox H, Fischetto R, Heller R, Henderson BD, Hobson E, Nürnberg P, Percin EF, Peron A, Spaccini L, Quigley AJ, Thakur S, Wise CA, Yoon G, Alnemer M, Tomancak P, Yigit G, Taylor AMR, Reijns MAM, Simpson MA, Cortez D, Alkuraya FS, Mathew CG, Jackson AP, Stewart GS (2017) Mutations in DONSON disrupt replication fork stability and cause microcephalic dwarfism. Nat Genet 49:537–549

448.   Rhim C, Cheng CS, Kraus WE, Truskey GA (2010) Effect of microRNA modulation on bioartificial muscle function. Tissue Eng Part A 16:3589–3597

449.   Rice C, Skordalakes E (2016) Structure and function of the telomeric CST complex. Comput Struct Biotechnol J 14:161–167

450.   Riddle RD, Johnson RL, Laufer E, Tabin C (1993) Sonic hedgehog mediates the polarizing activity of the ZPA. Cell 75:1401–1416

451.   Riveiro AR, Brickman JM (2020) From pluripotency to totipotency: an experimentalist's guide to cellular potency. Dev Camb Engl 147:dev189845

452.   Robert AW, Angulski ABB, Spangenberg L, Shigunov P, Pereira IT, Bettes PSL, Naya H, Correa A, Dallagiovanna B, Stimamiglio MA (2018) Gene expression analysis of human adipose tissue-derived stem cells during the initial steps of in vitro osteogenesis. Sci Rep 8:4739

453.   Robert AW, Marcon BH, Dallagiovanna B, Shigunov P (2020) Adipogenesis, Osteogenesis, and Chondrogenesis of Human Mesenchymal Stem/Stromal Cells: A Comparative Transcriptome Approach. Front Cell Dev Biol 8:561

454.   Rodriguez A, Griffiths-Jones S, Ashurst JL, Bradley A (2004) Identification of mammalian microRNA host genes and transcription units. Genome Res 14:1902–1910

455.   Ross SE, Hemati N, Longo KA, Bennett CN, Lucas PC, Erickson RL, MacDougald OA (2000) Inhibition of adipogenesis by Wnt signaling. Science 289:950–953

456.   Roush S, Slack FJ (2008) The let-7 family of microRNAs. Trends Cell Biol 18:505–516

457.   Ruby JG, Jan CH, Bartel DP (2007) Intronic microRNA precursors that bypass Drosha processing. Nature 448:83–86

458.   Rudkin GT, Corlette SL (1957) DISPROPORTIONATE SYNTHESIS OF DNA IN A POLYTENE CHROMOSOME REGION. Proc Natl Acad Sci U S A 43:964–968

459.   Ryba T, Hiratani I, Lu J, Itoh M, Kulik M, Zhang J, Schulz TC, Robins AJ, Dalton S, Gilbert DM (2010) Evolutionarily conserved replication timing profiles predict long-range chromatin interactions and distinguish closely related cell types. Genome Res 20:761–770

460.   Saatchi F, Kirchmaier AL (2019) Tolerance of DNA Replication Stress Is Promoted by Fumarate Through Modulation of Histone Demethylation and Enhancement of Replicative Intermediate Processing in Saccharomyces cerevisiae. Genetics 212:631–654

461.   Sakabe K, Okazaki R (1966) A unique property of the replicating region of chromosomal DNA. Biochim Biophys Acta 129:651–654

462.   Santarius T, Shipley J, Brewer D, Stratton MR, Cooper CS (2010) A census of amplified and overexpressed human cancer genes. Nat Rev Cancer 10:59–64

463.   Savelyeva L, Schwab M (2001) Amplification of oncogenes revisited: from expression profiling to clinical application. Cancer Lett 167:115–123

464. Schaarschmidt D, Ladenburger E-M, Keller C, Knippers R (2002) Human Mcm proteins at a replication origin during the G1 to S phase transition. Nucleic Acids Res 30:4176–4185

465. Scheideler M, Elabd C, Zaragosi L-E, Chiellini C, Hackl H, Sanchez-Cabo F, Yadav S, Duszka K, Friedl G, Papak C, Prokesch A, Windhager R, Ailhaud G, Dani C, Amri E-Z, Trajanoski Z (2008) Comparative transcriptomics of human multipotent stem cells during adipogenesis and osteoblastogenesis. BMC Genomics 9:340

466. Schimke RT, Kaufman RJ, Alt FW, Kellems RF (1978) Gene amplification and drug resistance in cultured murine cells. Science 202:1051–1055

467. Schimke RT (1984) Gene amplification in cultured animal cells. Cell 37:705–713

468. Schimke RT, Sherwood SW, Hill AB, Johnston RN (1986) Overreplication and recombination of DNA in higher eukaryotes: potential consequences and biological implications. Proc Natl Acad Sci U S A 83:2157–2161

469. Schnall-Levin M, Zhao Y, Perrimon N, Berger B (2010) Conserved microRNA targeting in Drosophila is as widespread in coding regions as in 3'UTRs. Proc Natl Acad Sci U S A 107:15751–15756

470. Schröck E, Thiel G, Lozanova T, du Manoir S, Meffert MC, Jauch A, Speicher MR, Nürnberg P, Vogel S, Jänisch W (1994) Comparative genomic hybridization of human malignant gliomas reveals multiple amplification sites and nonrandom chromosomal gains and losses. Am J Pathol 144:1203–1218

471. Schwab M, Amler LC (1990) Amplification of cellular oncogenes: a predictor of clinical outcome in human cancer. Genes Chromosomes Cancer 1:181–193

472. Schwamborn JC, Berezikov E, Knoblich JA (2009) The TRIM-NHL protein TRIM32 activates microRNAs and prevents self-renewal in mouse neural progenitors. Cell 136:913–925

473. Schwämmle V, Jensen ON (2010) A simple and fast method to determine the parameters for fuzzy c-means cluster analysis. Bioinforma Oxf Engl 26:2841–2848

474. Seenprachawong K, Nuchnoi P, Nantasenamat C, Prachayasittikul V, Supokawej A (2016) Computational identification of miRNAs that modulate the differentiation of mesenchymal stem cells to osteoblasts. PeerJ 4:e1976

475. Selvarajah S, Yoshimoto M, Park PC, Maire G, Paderova J, Bayani J, Lim G, Al-Romaih K, Squire JA, Zielenska M (2006) The breakage-fusion-bridge (BFB) cycle as a mechanism for generating genetic heterogeneity in osteosarcoma. Chromosoma 115:459–467

476. Sempere LF, Freemantle S, Pitha-Rowe I, Moss E, Dmitrovsky E, Ambros V (2004) Expression profiling of mammalian microRNAs uncovers a subset of brain-expressed microRNAs with possible roles in murine and human neuronal differentiation. Genome Biol 5:R13

477. Shah JA, Khattak S, Rauf MA, Cai Y, Jin J (2021) Potential Biomarkers of miR-371-373 Gene Cluster in Tumorigenesis. Life Basel Switz 11:984

478. Shen J, James AW, Chung J, Lee K, Zhang JB, Ho S, Lee KS, Kim TM, Niimi T, Kuroda S, Ting K, Soo C (2012) NELL-1 promotes cell adhesion and differentiation via Integrinβ1. J Cell Biochem 113:3620–3628

479. Shi C, Zhang M, Tong M, Yang L, Pang L, Chen L, Xu G, Chi X, Hong Q, Ni Y, Ji C, Guo X (2015) miR-148a is Associated with Obesity and Modulates Adipocyte Differentiation of Mesenchymal Stem Cells through Wnt Signaling. Sci Rep 5:9930

480. Shi Y, Long F (2017) Hedgehog signaling via Gli2 prevents obesity induced by high-fat diet in adult mice. eLife 6:e31649

481. Shibata M, Kurokawa D, Nakao H, Ohmura T, Aizawa S (2008) MicroRNA-9 modulates Cajal-Retzius cell differentiation by suppressing Foxg1 expression in mouse medial pallium. J Neurosci Off J Soc Neurosci 28:10415–10421

482. Shimada K, Pasero P, Gasser SM (2002) ORC and the intra-S-phase checkpoint: a threshold regulates Rad53p activation in S phase. Genes Dev 16:3236–3252

483. Siefert JC, Clowdus EA, Goins D, Koren A, Sansam CL (2018) Profiling DNA Replication Timing Using Zebrafish as an In Vivo Model System. J Vis Exp JoVE

484. Silber J, Lim DA, Petritsch C, Persson AI, Maunakea AK, Yu M, Vandenberg SR, Ginzinger DG, James CD, Costello JF, Bergers G, Weiss WA, Alvarez-Buylla A, Hodgson JG (2008) miR-124 and miR-137 inhibit proliferation of glioblastoma multiforme cells and induce differentiation of brain tumor stem cells. BMC Med 6:14

485. Sinha S, Chen JK (2006) Purmorphamine activates the Hedgehog pathway by targeting Smoothened. Nat Chem Biol 2:29–30

486. Slack A, Thornton PC, Magner DB, Rosenberg SM, Hastings PJ (2006) On the mechanism of gene amplification induced under stress in Escherichia coli. PLoS Genet 2:e48

487. Small EM, O'Rourke JR, Moresi V, Sutherland LB, McAnally J, Gerard RD, Richardson JA, Olson EN (2010) Regulation of PI3-kinase/Akt signaling by muscle-enriched microRNA-486. Proc Natl Acad Sci 107:4218–4223

488. Smieszek A, Marcinkowska K, Pielok A, Sikora M, Valihrach L, Marycz K (2020) The Role of miR-21 in Osteoblasts-Osteoclasts Coupling In Vitro. Cells 9:E479

489. Smirnova L, Gräfe A, Seiler A, Schumacher S, Nitsch R, Wulczyn FG (2005) Regulation of miRNA expression during neural cell specification. Eur J Neurosci 21:1469–1477

490. Smith CA, Vinograd J (1972) Small polydisperse circular DNA of HeLa cells. J Mol Biol 69:163–178

491. Smith OK, Kim R, Fu H, Martin MM, Lin CM, Utani K, Zhang Y, Marks AB, Lalande M, Chamberlain S, Libbrecht MW, Bouhassira EE, Ryan MC, Noble WS, Aladjem MI (2016) Distinct epigenetic features of differentiation-regulated replication origins. Epigenetics Chromatin 9:18

492. Smrt RD, Szulwach KE, Pfeiffer RL, Li X, Guo W, Pathania M, Teng Z-Q, Luo Y, Peng J, Bordey A, Jin P, Zhao X (2010) MicroRNA miR-137 regulates neuronal

maturation by targeting ubiquitin ligase mind bomb-1. Stem Cells Dayt Ohio 28:1060–1070

493.   Somoza RA, Welter JF, Correa D, Caplan AI (2014) Chondrogenic differentiation of mesenchymal stem cells: challenges and unfulfilled expectations. Tissue Eng Part B Rev 20:596–608

494.   Somoza RA, Correa D, Labat I, Sternberg H, Forrest ME, Khalil AM, West MD, Tesar P, Caplan AI (2018) Transcriptome-Wide Analyses of Human Neonatal Articular Cartilage and Human Mesenchymal Stem Cell-Derived Cartilage Provide a New Molecular Target for Evaluating Engineered Cartilage. Tissue Eng Part A 24:335–350

495.   Song G, Xu G, Ji C, Shi C, Shen Y, Chen L, Zhu L, Yang L, Zhao Y, Guo X (2014) The role of microRNA-26b in human adipocyte differentiation and proliferation. Gene 533:481–487

496.   Song H, Stevens CF, Gage FH (2002) Astroglia induce neurogenesis from adult neural stem cells. Nature 417:39–44

497.   Song W, Zhang X, Xia X (2015) Atoh7 promotes the differentiation of Müller cells-derived retinal stem cells into retinal ganglion cells in a rat model of glaucoma. Exp Biol Med Maywood NJ 240:682–690

498.   Song WQ, Gu WQ, Qian YB, Ma X, Mao YJ, Liu WJ (2015) Identification of long non-coding RNA involved in osteogenic differentiation from mesenchymal stem cells using RNA-Seq data. Genet Mol Res GMR 14:18268–18279

499.   Sosunov AA, Wu X, Tsankova NM, Guilfoyle E, McKhann GM, Goldman JE (2014) Phenotypic Heterogeneity and Plasticity of Isocortical and Hippocampal Astrocytes in the Human Brain. J Neurosci 34:2285–2298

500.   Sottile V, Seuwen K (2000) Bone morphogenetic protein-2 stimulates adipogenic differentiation of mesenchymal precursor cells in synergy with BRL 49653 (rosiglitazone). FEBS Lett 475:201–204

501.   Spangenberg L, Shigunov P, Abud APR, Cofré AR, Stimamiglio MA, Kuligovski C, Zych J, Schittini AV, Costa ADT, Rebelatto CK, Brofman PRS, Goldenberg S, Correa A, Naya H, Dallagiovanna B (2013) Polysome profiling shows extensive posttranscriptional regulation during human adipocyte stem cell differentiation into adipocytes. Stem Cell Res 11:902–912

502.   Spradling AC, Mahowald AP (1980) Amplification of genes for chorion proteins during oogenesis in Drosophila melanogaster. Proc Natl Acad Sci U S A 77:1096–1100

503.   Spradling AC (1981) The organization and amplification of two chromosomal domains containing Drosophila chorion genes. Cell 27:193–201

504.   Stadler B, Ivanovska I, Mehta K, Song S, Nelson A, Tan Y, Mathieu J, Darby C, Blau CA, Ware C, Peters G, Miller DG, Shen L, Cleary MA, Ruohola-Baker H (2010) Characterization of microRNAs involved in embryonic stem cell states. Stem Cells Dev 19:935–950

505.   Stark A, Lin MF, Kheradpour P, Pedersen JS, Parts L, Carlson JW, Crosby MA, Rasmussen MD, Roy S, Deoras AN, Ruby JG, Brennecke J, Harvard FlyBase

curators, Berkeley Drosophila Genome Project, Hodges E, Hinrichs AS, Caspi A, Paten B, Park S-W, Han MV, Maeder ML, Polansky BJ, Robson BE, Aerts S, van Helden J, Hassan B, Gilbert DG, Eastman DA, Rice M, Weir M, Hahn MW, Park Y, Dewey CN, Pachter L, Kent WJ, Haussler D, Lai EC, Bartel DP, Hannon GJ, Kaufman TC, Eisen MB, Clark AG, Smith D, Celniker SE, Gelbart WM, Kellis M (2007) Discovery of functional elements in 12 Drosophila genomes using evolutionary signatures. Nature 450:219–232

506.   Stark GR, Debatisse M, Giulotto E, Wahl GM (1989) Recent progress in understanding mechanisms of mammalian DNA amplification. Cell 57:901–908

507.   Stewart JA, Wang F, Chaiken MF, Kasbek C, Chastain PD, Wright WE, Price CM (2012) Human CST promotes telomere duplex replication and general replication restart after fork stalling. EMBO J 31:3537–3549

508.   Stratmann SA, van Oijen AM (2014) DNA replication at the single-molecule level. Chem Soc Rev 43:1201–1220

509.   Strazisar M, Cammaerts S, van der Ven K, Forero DA, Lenaerts A-S, Nordin A, Almeida-Souza L, Genovese G, Timmerman V, Liekens A, De Rijk P, Adolfsson R, Callaerts P, Del-Favero J (2015) MIR137 variants identified in psychiatric patients affect synaptogenesis and neuronal transmission gene sets. Mol Psychiatry 20:472–481

510.   Su X, Liao L, Shuai Y, Jing H, Liu S, Zhou H, Liu Y, Jin Y (2015) MiR-26a functions oppositely in osteogenic differentiation of BMSCs and ADSCs depending on distinct activation and roles of Wnt and BMP signaling pathway. Cell Death Dis 6:e1851

511.   Sugimoto I, Murakami H, Tonami Y, Moriyama A, Nakanishi M (2004) DNA replication checkpoint control mediated by the spindle checkpoint protein Mad2p in fission yeast. J Biol Chem 279:47372–47378

512.   Sumiyoshi K, Kubota S, Ohgawara T, Kawata K, Nishida T, Shimo T, Yamashiro T, Takigawa M (2010) Identification of miR-1 as a micro RNA that supports late-stage differentiation of growth cartilage cells. Biochem Biophys Res Commun 402:286–290

513.   Sun G, Ye P, Murai K, Lang M-F, Li S, Zhang H, Li W, Fu C, Yin J, Wang A, Ma X, Shi Y (2011) miR-137 forms a regulatory loop with nuclear receptor TLX and LSD1 in neural stem cells. Nat Commun 2:529

514.   Sun J, Kong D (2010) DNA replication origins, ORC/DNA interaction, and assembly of pre-replication complex in eukaryotes. Acta Biochim Biophys Sin 42:433–439

515.   Sun T, Fu M, Bookout AL, Kliewer SA, Mangelsdorf DJ (2009) MicroRNA let-7 regulates 3T3-L1 adipogenesis. Mol Endocrinol Baltim Md 23:925–931

516.   Sun Y, Ge Y, Drnevich J, Zhao Y, Band M, Chen J (2010) Mammalian target of rapamycin regulates miRNA-1 and follistatin in skeletal myogenesis. J Cell Biol 189:1157–1169

517.   Sunnerhagen P, SjÖberg R-M, Karlsson A-L, Lundh L, Bjursell G (1986) Molecular cloning and characterization of small polydisperse circular DNA from mouse 3T6 cells. Nucleic Acids Res 14:7823–7838

518. Swarts DC, Makarova K, Wang Y, Nakanishi K, Ketting RF, Koonin EV, Patel DJ, van der Oost J (2014) The evolutionary journey of Argonaute proteins. Nat Struct Mol Biol 21:743–753

519. Szulwach KE, Li X, Smrt RD, Li Y, Luo Y, Lin L, Santistevan NJ, Li W, Zhao X, Jin P (2010) Cross talk between microRNA and epigenetic regulation in adult neurogenesis. J Cell Biol 189:127–141

520. Taipaleenmäki H, Abdallah BM, AlDahmash A, Säämänen A-M, Kassem M (2011) Wnt signalling mediates the cross-talk between bone marrow derived pre-adipocytic and pre-osteoblastic cell populations. Exp Cell Res 317:745–756

521. Tajbakhsh S (2009) Skeletal muscle stem cells in developmental versus regenerative myogenesis. J Intern Med 266:372–389

522. Takahashi K, Yamanaka S (2006) Induction of pluripotent stem cells from mouse embryonic and adult fibroblast cultures by defined factors. Cell 126:663–676

523. Takahashi K, Tanabe K, Ohnuki M, Narita M, Ichisaka T, Tomoda K, Yamanaka S (2007) Induction of pluripotent stem cells from adult human fibroblasts by defined factors. Cell 131:861–872

524. Takahashi S, Miura H, Shibata T, Nagao K, Okumura K, Ogata M, Obuse C, Takebayashi S-I, Hiratani I (2019) Genome-wide stability of the DNA replication program in single mammalian cells. Nat Genet 51:529–540

525. Takanabe R, Ono K, Abe Y, Takaya T, Horie T, Wada H, Kita T, Satoh N, Shimatsu A, Hasegawa K (2008) Up-regulated expression of microRNA-143 in association with obesity in adipose tissue of mice fed high-fat diet. Biochem Biophys Res Commun 376:728–732

526. Takaya T, Ono K, Kawamura T, Takanabe R, Kaichi S, Morimoto T, Wada H, Kita T, Shimatsu A, Hasegawa K (2009) MicroRNA-1 and MicroRNA-133 in spontaneous myocardial differentiation of mouse embryonic stem cells. Circ J Off J Jpn Circ Soc 73:1492–1497

527. Tan K, Peng Y-T, Guo P (2018) MiR-29a promotes osteogenic differentiation of mesenchymal stem cells via targeting HDAC4. Eur Rev Med Pharmacol Sci 22:3318–3326

528. Tanaka S, Nakato R, Katou Y, Shirahige K, Araki H (2011) Origin association of Sld3, Sld7, and Cdc45 proteins is a key step for determination of origin-firing timing. Curr Biol CB 21:2055–2063

529. Tang X, Lin J, Wang G, Lu J (2017) MicroRNA-433-3p promotes osteoblast differentiation through targeting DKK1 expression. PloS One 12:e0179860

530. Tang Y-F, Zhang Y, Li X-Y, Li C, Tian W, Liu L (2009) Expression of miR-31, miR-125b-5p, and miR-326 in the adipogenic differentiation process of adipose-derived stem cells. Omics J Integr Biol 13:331–336

531. Tanny RE, MacAlpine DM, Blitzblau HG, Bell SP (2006) Genome-wide analysis of re-replication reveals inhibitory controls that target multiple stages of replication initiation. Mol Biol Cell 17:2415–2423

532.   Tay Y, Zhang J, Thomson AM, Lim B, Rigoutsos I (2008) MicroRNAs to Nanog, Oct4 and Sox2 coding regions modulate embryonic stem cell differentiation. Nature 455:1124–1128

533.   Tayebi B, Babaahmadi M, Pakzad M, Hajinasrollah M, Mostafaei F, Jahangiri S, Kamali A, Baharvand H, Baghaban Eslaminejad M, Hassani S-N, Hajizadeh-Saffar E (2022) Standard toxicity study of clinical-grade allogeneic human bone marrow-derived clonal mesenchymal stromal cells. Stem Cell Res Ther 13:213

534.   Thomson JA, Itskovitz-Eldor J, Shapiro SS, Waknitz MA, Swiergiel JJ, Marshall VS, Jones JM (1998) Embryonic Stem Cell Lines Derived from Human Blastocysts. Science 282:1145–1147

535.   Tiane A, Schepers M, Rombaut B, Hupperts R, Prickaerts J, Hellings N, van den Hove D, Vanmierlo T (2019) From OPC to Oligodendrocyte: An Epigenetic Journey. Cells 8:E1236

536.   Tiscornia G, Izpisúa Belmonte JC (2010) MicroRNAs in embryonic stem cell function and fate. Genes Dev 24:2732–2741

537.   Tomé M, López-Romero P, Albo C, Sepúlveda JC, Fernández-Gutiérrez B, Dopazo A, Bernad A, González MA (2011) miR-335 orchestrates cell proliferation, migration and differentiation in human mesenchymal stem cells. Cell Death Differ 18:985–995

538.   Tourrière H, Pasero P (2007) Maintenance of fork integrity at damaged DNA and natural pause sites. DNA Repair 6:900–913

539.   Townley-Tilson WHD, Callis TE, Wang D (2010) MicroRNAs 1, 133, and 206: critical factors of skeletal and cardiac muscle development, function, and disease. Int J Biochem Cell Biol 42:1252–1255

540.   Tracy ET, Zhang CY, Gentry T, Shoulars KW, Kurtzberg J (2011) Isolation and expansion of oligodendrocyte progenitor cells from cryopreserved human umbilical cord blood. Cytotherapy 13:722–729

541.   Truong LN, Wu X (2011) Prevention of DNA re-replication in eukaryotic cells. J Mol Cell Biol 3:13–22

542.   Tsunematsu T, Takihara Y, Ishimaru N, Pagano M, Takata T, Kudo Y (2013) Aurora-A controls pre-replicative complex assembly and DNA replication by stabilizing geminin in mitosis. Nat Commun 4:1885

543.   Tuduri S, Crabbé L, Conti C, Tourrière H, Holtgreve-Grez H, Jauch A, Pantesco V, De Vos J, Thomas A, Theillet C, Pommier Y, Tazi J, Coquelle A, Pasero P (2009) Topoisomerase I suppresses genomic instability by preventing interference between replication and transcription. Nat Cell Biol 11:1315–1324

544.   Tuduri S, Tourrière H, Pasero P (2010) Defining replication origin efficiency using DNA fiber assays. Chromosome Res Int J Mol Supramol Evol Asp Chromosome Biol 18:91–102

545.   Urbán N, Guillemot F (2014) Neurogenesis in the embryonic and adult brain: same regulators, different roles. Front Cell Neurosci 8:396

546. van Gastel N, Stegen S, Eelen G, Schoors S, Carlier A, Daniëls VW, Baryawno N, Przybylski D, Depypere M, Stiers P-J, Lambrechts D, Van Looveren R, Torrekens S, Sharda A, Agostinis P, Lambrechts D, Maes F, Swinnen JV, Geris L, Van Oosterwyck H, Thienpont B, Carmeliet P, Scadden DT, Carmeliet G (2020) Lipid availability determines fate of skeletal progenitor cells via SOX9. Nature 579:111–117

547. van Rooij E, Quiat D, Johnson BA, Sutherland LB, Qi X, Richardson JA, Kelm RJ, Olson EN (2009) A family of microRNAs encoded by myosin genes governs myosin expression and muscle performance. Dev Cell 17:662–673

548. Vassilev A, DePamphilis ML (2017) Links between DNA Replication, Stem Cells and Cancer. Genes 8:E45

549. Vaziri C, Saxena S, Jeon Y, Lee C, Murata K, Machida Y, Wagle N, Hwang DS, Dutta A (2003) A p53-dependent checkpoint pathway prevents rereplication. Mol Cell 11:997–1008

550. Velicky P, Meinhardt G, Plessl K, Vondra S, Weiss T, Haslinger P, Lendl T, Aumayr K, Mairhofer M, Zhu X, Schütz B, Hannibal RL, Lindau R, Weil B, Ernerudh J, Neesen J, Egger G, Mikula M, Röhrl C, Urban AE, Baker J, Knöfler M, Pollheimer J (2018) Genome amplification and cellular senescence are hallmarks of human placenta development. PLoS Genet 14:e1007698

551. Venkatesh K, Kumari A, Sen D (2019) MicroRNA signature changes during induction of neural stem cells from human mesenchymal stem cells. Nanomedicine Nanotechnol Biol Med 17:94–105

552. Visvanathan J, Lee S, Lee B, Lee JW, Lee S-K (2007) The microRNA miR-124 antagonizes the anti-neural REST/SCP1 pathway during embryonic CNS development. Genes Dev 21:744–749

553. Vo N, Klein ME, Varlamova O, Keller DM, Yamamoto T, Goodman RH, Impey S (2005) A cAMP-response element binding protein-induced microRNA regulates neuronal morphogenesis. Proc Natl Acad Sci U S A 102:16426–16431

554. Vogelstein B, Pardoll DM, Coffey DS (1980) Supercoiled loops and eucaryotic DNA replicaton. Cell 22:79–85

555. Voinnet O (2009) Origin, biogenesis, and activity of plant microRNAs. Cell 136:669–687

556. Volarevic V, Markovic BS, Gazdic M, Volarevic A, Jovicic N, Arsenijevic N, Armstrong L, Djonov V, Lako M, Stojkovic M (2018) Ethical and Safety Issues of Stem Cell-Based Therapy. Int J Med Sci 15:36–45

557. Volkert FC, Broach JR (1986) Site-specific recombination promotes plasmid amplification in yeast. Cell 46:541–550

558. Vroegrijk IOCM, van Klinken JB, van Diepen JA, van den Berg SAA, Febbraio M, Steinbusch LKM, Glatz JFC, Havekes LM, Voshol PJ, Rensen PCN, van Dijk KW, van Harmelen V (2013) CD36 is important for adipocyte recruitment and affects lipolysis. Obes Silver Spring Md 21:2037–2045

559.   Wa Q, He P, Huang S, Zuo J, Li X, Zhu J, Hong S, Lv G, Cai D, Xu D, Zou X, Liu Y (2017) miR-30b regulates chondrogenic differentiation of mouse embryo-derived stem cells by targeting SOX9. Exp Ther Med 14:6131–6137

560.   Wabitsch M, Hauner H, Heinze E, Teller WM (1995) The role of growth hormone/insulin-like growth factors in adipocyte differentiation. Metabolism 44:45–49

561.   Wagner V, Kern F, Hahn O, Schaum N, Ludwig N, Fehlmann T, Engel A, Henn D, Rishik S, Isakova A, Tan M, Sit R, Neff N, Hart M, Meese E, Quake S, Wyss-Coray T, Keller A (2023) Characterizing expression changes in noncoding RNAs during aging and heterochronic parabiosis across mouse tissues. Nat Biotechnol 1–10

562.   Wahl GM, Padgett RA, Stark GR (1979) Gene amplification causes overproduction of the first three enzymes of UMP synthesis in N-(phosphonacetyl)-L-aspartate-resistant hamster cells. J Biol Chem 254:8679–8689

563.   Wang B, Majumder S, Nuovo G, Kutay H, Volinia S, Patel T, Schmittgen TD, Croce C, Ghoshal K, Jacob ST (2009) Role of microRNA-155 at early stages of hepatocarcinogenesis induced by choline-deficient and amino acid-defined diet in C57BL/6 mice. Hepatol Baltim Md 50:1152–1161

564.   Wang H, Ma D, Zhang X, Xu S, Ning T, Wu B (2018) Comparative proteomic profiling of human dental pulp stem cells and periodontal ligament stem cells under in vitro osteogenic induction. Arch Oral Biol 89:9–19

565.   Wang J, Guan X, Guo F, Zhou J, Chang A, Sun B, Cai Y, Ma Z, Dai C, Li X, Wang B (2013) miR-30e reciprocally regulates the differentiation of adipocytes and osteoblasts by directly targeting low-density lipoprotein receptor-related protein 6. Cell Death Dis 4:e845

566.   Wang J, Zhao L, Peng X, Liu K, Zhang C, Chen X, Han Y, Lai Y (2020) Evaluation of miR-130 family members as circulating biomarkers for the diagnosis of bladder cancer. J Clin Lab Anal 34:e23517

567.   Wang N, Zheng J, Chen Z, Liu Y, Dura B, Kwak M, Xavier-Ferrucio J, Lu Y-C, Zhang M, Roden C, Cheng J, Krause DS, Ding Y, Fan R, Lu J (2019) Single-cell microRNA-mRNA co-sequencing reveals non-genetic heterogeneity and mechanisms of microRNA regulation. Nat Commun 10:95

568.   Wang S, Liu Z, Wang J, Ji X, Yao Z, Wang X (2020) miR-21 promotes osteoclastogenesis through activation of PI3K/Akt signaling by targeting Pten in RAW264.7 cells. Mol Med Rep 21:1125–1132

569.   Wang YM, Ding XB, Dai Y, Liu XF, Guo H, Zhang Y (2015) Identification and bioinformatics analysis of miRNAs involved in bovine skeletal muscle satellite cell myogenic differentiation. Mol Cell Biochem 404:113–122

570.   Watanabe T, Horiuchi T (2005) A novel gene amplification system in yeast based on double rolling-circle replication. EMBO J 24:190–198

571.   Watanabe T, Tanabe H, Horiuchi T (2011) Gene amplification system based on double rolling-circle replication as a model for oncogene-type amplification. Nucleic Acids Res 39:e106

572. Wayman GA, Davare M, Ando H, Fortin D, Varlamova O, Cheng H-YM, Marks D, Obrietan K, Soderling TR, Goodman RH, Impey S (2008) An activity-regulated microRNA controls dendritic plasticity by down-regulating p250GAP. Proc Natl Acad Sci U S A 105:9093–9098

573. Weier HU, Wang M, Mullikin JC, Zhu Y, Cheng JF, Greulich KM, Bensimon A, Gray JW (1995) Quantitative DNA fiber mapping. Hum Mol Genet 4:1903–1910

574. Weinert T (1998) DNA damage checkpoints update: getting molecular. Curr Opin Genet Dev 8:185–193

575. Wellner U, Schubert J, Burk UC, Schmalhofer O, Zhu F, Sonntag A, Waldvogel B, Vannier C, Darling D, zur Hausen A, Brunton VG, Morton J, Sansom O, Schüler J, Stemmler MP, Herzberger C, Hopt U, Keck T, Brabletz S, Brabletz T (2009) The EMT-activator ZEB1 promotes tumorigenicity by repressing stemness-inhibiting microRNAs. Nat Cell Biol 11:1487–1495

576. Williams JS, Tumbale PP, Arana ME, Rana JA, Williams RS, Kunkel TA (2021) High-fidelity DNA ligation enforces accurate Okazaki fragment maturation during DNA replication. Nat Commun 12:482

577. Wohlschlegel JA, Dwyer BT, Dhar SK, Cvetic C, Walter JC, Dutta A (2000) Inhibition of eukaryotic DNA replication by geminin binding to Cdt1. Science 290:2309–2312

578. Woodward AM, Göhler T, Luciani MG, Oehlmann M, Ge X, Gartner A, Jackson DA, Blow JJ (2006) Excess Mcm2-7 license dormant origins of replication that can be used under conditions of replicative stress. J Cell Biol 173:673–683

579. Wu C, Tian B, Qu X, Liu F, Tang T, Qin A, Zhu Z, Dai K (2014) MicroRNAs play a role in chondrogenesis and osteoarthritis (review). Int J Mol Med 34:13–23

580. Wu P-YJ, Nurse P (2009) Establishing the program of origin firing during S phase in fission Yeast. Cell 136:852–864

581. Wu T, Zhou H, Hong Y, Li J, Jiang X, Huang H (2012) miR-30 family members negatively regulate osteoblast differentiation. J Biol Chem 287:7503–7511

582. Xavier CP, Melikova M, Chuman Y, Üren A, Baljinnyam B, Rubin JS (2014) Secreted Frizzled-related protein potentiation versus inhibition of Wnt3a/β-catenin signaling. Cell Signal 26:94–101

583. Xian L, Wu X, Pang L, Lou M, Rosen CJ, Qiu T, Crane J, Frassica F, Zhang L, Rodriguez JP, Xiaofeng Jia null, Shoshana Yakar null, Shouhong Xuan null, Argiris Efstratiadis null, Mei Wan null, Xu Cao null (2012) Matrix IGF-1 maintains bone mass by activation of mTOR in mesenchymal stem cells. Nat Med 18:1095–1101

584. Xiao H, Wen Y, Pan Z, Shangguan Y, Qin J, Tan Y, Jiang H, Li B, Zhang Q, Chen L, Wang H (2018) Increased H3K27ac level of ACE mediates the intergenerational effect of low peak bone mass induced by prenatal dexamethasone exposure in male offspring rats. Cell Death Dis 9:638

585. Xie H, Sun L, Lodish HF (2009) Targeting microRNAs in obesity. Expert Opin Ther Targets 13:1227–1238

586.   Xie H, Lim B, Lodish HF (2009) MicroRNAs induced during adipogenesis that accelerate fat cell development are downregulated in obesity. Diabetes 58:1050–1057

587.   Xie Q, Wei W, Ruan J, Ding Y, Zhuang A, Bi X, Sun H, Gu P, Wang Z, Fan X (2017) Effects of miR-146a on the osteogenesis of adipose-derived mesenchymal stem cells and bone regeneration. Sci Rep 7:42840

588.   Xouri G, Lygerou Z, Nishitani H, Pachnis V, Nurse P, Taraviras S (2004) Cdt1 and geminin are down-regulated upon cell cycle exit and are over-expressed in cancer-derived cell lines. Eur J Biochem 271:3368–3378

589.   Xu J, Kang Y, Liao W, Yu L (2012) MiR-194 regulates chondrogenic differentiation of human adipose-derived stem cells by targeting Sox5. PloS One 7:e31861

590.   Xu N, Papagiannakopoulos T, Pan G, Thomson JA, Kosik KS (2009) MicroRNA-145 regulates OCT4, SOX2, and KLF4 and represses pluripotency in human embryonic stem cells. Cell 137:647–658

591.   Xu N, You Y, Liu C, Balasov M, Lun LT, Geng Y, Fung CP, Miao H, Tian H, Choy TT, Shi X, Fan Z, Zhou B, Akhmetova K, Din RU, Yang H, Hao Q, Qian P, Chesnokov I, Zhu G (2020) Structural basis of DNA replication origin recognition by human Orc6 protein binding with DNA. Nucleic Acids Res 48:11146–11161

592.   Yaffe E, Farkash-Amar S, Polten A, Yakhini Z, Tanay A, Simon I (2010) Comparative analysis of DNA replication timing reveals conserved large-scale chromosomal architecture. PLoS Genet 6:e1001011

593.   Yamamoto T, Sato Y, Yasuda S, Shikamura M, Tamura T, Takenaka C, Takasu N, Nomura M, Dohi H, Takahashi M, Mandai M, Kanemura Y, Nakamura M, Okano H, Kawamata S (2022) Correlation Between Genetic Abnormalities in Induced Pluripotent Stem Cell-Derivatives and Abnormal Tissue Formation in Tumorigenicity Tests. Stem Cells Transl Med 11:527–538

594.   Yan C, Wang Y, Shen X-Y, Yang G, Jian J, Wang H-S, Chen G-Q, Wu Q (2011) MicroRNA regulation associated chondrogenesis of mouse MSCs grown on polyhydroxyalkanoates. Biomaterials 32:6435–6444

595.   Yang B, Guo H, Zhang Y, Chen L, Ying D, Dong S (2011) MicroRNA-145 regulates chondrogenic differentiation of mesenchymal stem cells by targeting Sox9. PloS One 6:e21679

596.   Yang S-H, Kalkan T, Morrisroe C, Smith A, Sharrocks AD (2012) A genome-wide RNAi screen reveals MAP kinase phosphatases as key ERK pathway regulators during embryonic stem cell differentiation. PLoS Genet 8:e1003112

597.   Yang S-J, Chen C-Y, Chang G-D, Wen H-C, Chen C-Y, Chang S-C, Liao J-F, Chang C-H (2013) Activation of Akt by advanced glycation end products (AGEs): involvement of IGF-1 receptor and caveolin-1. PloS One 8:e58100

598.   Yang Z, Bian C, Zhou H, Huang S, Wang S, Liao L, Zhao RC (2011) MicroRNA hsa-miR-138 inhibits adipogenic differentiation of human adipose tissue-derived mesenchymal stem cells through adenovirus EID-1. Stem Cells Dev 20:259–267

599.   Yang Z, Hao J, Hu Z-M (2015) MicroRNA expression profiles in human adipose-derived stem cells during chondrogenic differentiation. Int J Mol Med 35:579–586

600. Yasunaga S, Ohno Y, Shirasu N, Zhang B, Suzuki-Takedachi K, Ohtsubo M, Takihara Y (2016) Role of Geminin in cell fate determination of hematopoietic stem cells (HSCs). Int J Hematol 104:324–329

601. Yeh C-H, Jin L, Shen F, Balian G, Li XJ (2016) miR-221 attenuates the osteogenic differentiation of human annulus fibrosus cells. Spine J Off J North Am Spine Soc 16:896–904

602. Yekezare M, Gómez-González B, Diffley JFX (2013) Controlling DNA replication origins in response to DNA damage - inhibit globally, activate locally. J Cell Sci 126:1297–1306

603. Yi R, Qin Y, Macara IG, Cullen BR (2003) Exportin-5 mediates the nuclear export of pre-microRNAs and short hairpin RNAs. Genes Dev 17:3011–3016

604. Yi R, Fuchs E (2011) MicroRNAs and their roles in mammalian stem cells. J Cell Sci 124:1775–1783

605. Yoo AS, Staahl BT, Chen L, Crabtree GR (2009) MicroRNA-mediated switching of chromatin-remodelling complexes in neural development. Nature 460:642–646

606. Yoo JK, Jung HY, Kim C-H, Son WS, Kim JK (2013) miR-7641 modulates the expression of CXCL1 during endothelial differentiation derived from human embryonic stem cells. Arch Pharm Res 36:353–358

607. Yoshida CA, Yamamoto H, Fujita T, Furuichi T, Ito K, Inoue K, Yamana K, Zanma A, Takada K, Ito Y, Komori T (2004) Runx2 and Runx3 are essential for chondrocyte maturation, and Runx2 regulates limb growth through induction of Indian hedgehog. Genes Dev 18:952–963

608. Yu J, Vodyanik MA, Smuga-Otto K, Antosiewicz-Bourget J, Frane JL, Tian S, Nie J, Jonsdottir GA, Ruotti V, Stewart R, Slukvin II, Thomson JA (2007) Induced pluripotent stem cell lines derived from human somatic cells. Science 318:1917–1920

609. Yuasa K, Hagiwara Y, Ando M, Nakamura A, Takeda S, Hijikata T (2008) MicroRNA-206 is highly expressed in newly formed muscle fibers: implications regarding potential for muscle regeneration and maturation in muscular dystrophy. Cell Struct Funct 33:163–169

610. Zakrzewski W, Dobrzyński M, Szymonowicz M, Rybak Z (2019) Stem cells: past, present, and future. Stem Cell Res Ther 10:68

611. Zaragosi L-E, Wdziekonski B, Brigand KL, Villageois P, Mari B, Waldmann R, Dani C, Barbry P (2011) Small RNA sequencing reveals miR-642a-3p as a novel adipocyte-specific microRNA and miR-30 as a key regulator of human adipogenesis. Genome Biol 12:R64

612. Zhan X, Cai P, Lei D, Yang Y, Wang Z, Lu Z, Zheng L, Zhao J (2019) Comparative profiling of chondrogenic differentiation of mesenchymal stem cells (MSCs) driven by two different growth factors. Cell Biochem Funct 37:359–367

613. Zhang F, Khajavi M, Connolly AM, Towne CF, Batish SD, Lupski JR (2009) The DNA replication FoSTeS/MMBIR mechanism can generate genomic, genic and exonic complex rearrangements in humans. Nat Genet 41:849–853

614.   Zhang H, Jiang L-H, Sun D-W, Li J, Ji Z-L (2017) The role of miR-130a in cancer. Breast Cancer Tokyo Jpn 24:521–527

615.   Zhang H, Wang Y, Yang G, Yu H, Zhou Z, Tang M (2019) MicroRNA-30a regulates chondrogenic differentiation of human bone marrow-derived mesenchymal stem cells through targeting Sox9. Exp Ther Med 18:4689–4697

616.   Zhang J, Fu M, Cui T, Xiong C, Xu K, Zhong W, Xiao Y, Floyd D, Liang J, Li E, Song Q, Chen YE (2004) Selective disruption of PPARgamma 2 impairs the development of adipose tissue and insulin sensitivity. Proc Natl Acad Sci U S A 101:10703–10708

617.   Zhang J, Tu Q, Bonewald LF, He X, Stein G, Lian J, Chen J (2011) Effects of miR-335-5p in modulating osteogenic differentiation by specifically downregulating Wnt antagonist DKK1. J Bone Miner Res Off J Am Soc Bone Miner Res 26:1953–1963

618.   Zhang L, Su P, Xu C, Chen C, Liang A, Du K, Peng Y, Huang D (2010) Melatonin inhibits adipogenesis and enhances osteogenesis of human mesenchymal stem cells by suppressing PPARγ expression and enhancing Runx2 expression. J Pineal Res 49:364–372

619.   Zhang W, Wu Y, Shiozaki Y, Sugimoto Y, Takigawa T, Tanaka M, Matsukawa A, Ozaki T (2018) miRNA-133a-5p Inhibits the Expression of Osteoblast Differentiation-Associated Markers by Targeting the 3' UTR of RUNX2. DNA Cell Biol 37:199–209

620.   Zhang W-B, Zhong W-J, Wang L (2014) A signal-amplification circuit between miR-218 and Wnt/β-catenin signal promotes human adipose tissue-derived stem cells osteogenic differentiation. Bone 58:59–66

621.   Zhang X, Ting K, Bessette CM, Culiat CT, Sung SJ, Lee H, Chen F, Shen J, Wang JJ, Kuroda S, Soo C (2011) Nell-1, a key functional mediator of Runx2, partially rescues calvarial defects in Runx2(+/-) mice. J Bone Miner Res Off J Am Soc Bone Miner Res 26:777–791

622.   Zhang Y, Xie R-L, Croce CM, Stein JL, Lian JB, van Wijnen AJ, Stein GS (2011) A program of microRNAs controls osteogenic lineage progression by targeting transcription factor Runx2. Proc Natl Acad Sci U S A 108:9863–9868

623.   Zhang Y, Li Z, Hao Q, Tan W, Sun J, Li J, Chen C-W, Li Z, Meng Y, Zhou Y, Han Z, Pei H, DePamphilis ML, Zhu W (2019) The Cdk2-c-Myc-miR-571 Axis Regulates DNA Replication and Genomic Stability by Targeting Geminin. Cancer Res 79:4896–4910

624.   Zhang Y, Zhao Q, Chen Q, Xu L, Yi S (2023) Transcriptional Control of Peripheral Nerve Regeneration. Mol Neurobiol 60:329–341

625.   Zhang Z, Hou C, Meng F, Zhao X, Zhang Z, Huang G, Chen W, Fu M, Liao W (2015) MiR-455-3p regulates early chondrogenic differentiation via inhibiting Runx2. FEBS Lett 589:3671–3678

626.   Zhao C, Sun G, Li S, Shi Y (2009) A feedback regulatory loop involving microRNA-9 and nuclear receptor TLX in neural stem cell fate determination. Nat Struct Mol Biol 16:365–371

627.   Zhao C, Sun G, Li S, Lang M-F, Yang S, Li W, Shi Y (2010) MicroRNA let-7b regulates neural stem cell proliferation and differentiation by targeting nuclear receptor TLX signaling. Proc Natl Acad Sci U S A 107:1876–1881

628.   Zhao H, Halicka HD, Li J, Biela E, Berniak K, Dobrucki J, Darzynkiewicz Z (2013) DNA damage signaling, impairment of cell cycle progression, and apoptosis triggered by 5-ethynyl-2'-deoxyuridine incorporated into DNA. Cytom Part J Int Soc Anal Cytol 83:979–988

629.   Zhao M, Qiao M, Harris SE, Chen D, Oyajobi BO, Mundy GR (2006) The zinc finger transcription factor Gli2 mediates bone morphogenetic protein 2 expression in osteoblasts in response to hedgehog signaling. Mol Cell Biol 26:6197–6208

630.   Zhao W, Tang Y, Yang Y, Wang M, Yu H (2019) Low-Magnitude, High-Frequency Vibration Promotes Osteogenic Differentiation via Intensifying miRNA-335-5p Expression. J Environ Pathol Toxicol Oncol Off Organ Int Soc Environ Toxicol Cancer 38:271–283

631.   Zhao X, Zhao Y, Sun X, Xing Y, Wang X, Yang Q (2020) Immunomodulation of MSCs and MSC-Derived Extracellular Vesicles in Osteoarthritis. Front Bioeng Biotechnol 8:575057

632.   Zheng L, Meng Y, Campbell JL, Shen B (2020) Multiple roles of DNA2 nuclease/helicase in DNA metabolism, genome stability and human diseases. Nucleic Acids Res 48:16–35

633.   Zheng Q, Zhang S, Guo W-Z, Li X-K (2021) The Unique Immunomodulatory Properties of MSC-Derived Exosomes in Organ Transplantation. Front Immunol 12:659621

634.   Zhong N, Sun J, Min Z, Zhao W, Zhang R, Wang W, Tian J, Tian L, Ma J, Li D, Han Y, Lu S (2012) MicroRNA-337 is associated with chondrogenesis through regulating TGFBR2 expression. Osteoarthritis Cartilage 20:593–602

635.   Zhou BB, Elledge SJ (2000) The DNA damage response: putting checkpoints in perspective. Nature 408:433–439

636.   Zhou C, Yang B, Tian Y, Jiao H, Zheng W, Wang J, Guan F (2011) Immunomodulatory effect of human umbilical cord Wharton's jelly-derived mesenchymal stem cells on lymphocytes. Cell Immunol 272:33–38

637.   Zhou H, Rigoutsos I (2014) MiR-103a-3p targets the 5' UTR of GPRC5A in pancreatic cells. RNA N Y N 20:1431–1439

638.   Zhou J, Guo F, Wang G, Wang J, Zheng F, Guan X, Chang A, Zhang X, Dai C, Li S, Li X, Wang B (2015) miR-20a regulates adipocyte differentiation by targeting lysine-specific demethylase 6b and transforming growth factor-β signaling. Int J Obes 2005 39:1282–1291

639.   Zhou Q, Anderson DJ (2002) The bHLH transcription factors OLIG2 and OLIG1 couple neuronal and glial subtype specification. Cell 109:61–73

640.   Zhou X, Zhang Z, Feng JQ, Dusevich VM, Sinha K, Zhang H, Darnay BG, de Crombrugghe B (2010) Multiple functions of Osterix are required for bone growth and homeostasis in postnatal mice. Proc Natl Acad Sci U S A 107:12919–12924

641. Zhu D, Shi S, Wang H, Liao K (2009) Growth arrest induces primary-cilium formation and sensitizes IGF-1-receptor signaling during differentiation induction of 3T3-L1 preadipocytes. J Cell Sci 122:2760–2768

642. Zhu N, Wang D, Xie F, Qin M, Wang Y (2022) MiR-335-3p/miR-155-5p Involved in IGFBP7-AS1-Enhanced Odontogenic Differentiation. Int Dent J S0020-6539(22)00180–0

643. Zhu W, Chen Y, Dutta A (2004) Rereplication by depletion of geminin is seen regardless of p53 status and activates a G2/M checkpoint. Mol Cell Biol 24:7140–7150

644. Zhu W, Dutta A (2006) Activation of fanconi anemia pathway in cells with re-replicated DNA. Cell Cycle Georget Tex 5:2306–2309

645. Zinovkina LA (2019) DNA Replication in Human Mitochondria. Biochem Biokhimiia 84:884–895

646. Zou J, Du J, Tu H, Chen H, Cong K, Bi Z, Sun J (2021) Resveratrol benefits the lineage commitment of bone marrow mesenchymal stem cells into osteoblasts via miR-320c by targeting Runx2. J Tissue Eng Regen Med 15:347–360

647. zur Nieden NI, Kempka G, Rancourt DE, Ahr H-J (2005) Induction of chondro-, osteo- and adipogenesis in embryonic stem cells by bone morphogenetic protein-2: effect of cofactors on differentiating lineages. BMC Dev Biol 5:1

7. Appendices

Table 7.1: Cluster pairs considered for the overlap analysis.

Pair/Trio number	RNA type	First cluster		Second cluster		Third cluster	
		Assay	Cluster	Assay	Cluster	Assay	Cluster
Similar 1	miRNA	hMSC adipogenesis	3	hNSC	3		
Similar 2	miRNA	hNSC	4	hMSC chondrogenesis	2		
Similar 3	miRNA	hMSC osteogenesis	5	HSkM	5		
Similar 4	miRNA	hMSC osteogenesis	1	HSkM	3		
Similar 5	mRNA	hMSC osteogenesis	6	HSkM	4		
Similar 6	mRNA	hMSC adipogenesis	6	hMSC osteogenesis	4		
Similar 7	mRNA	hNSC	2	hMSC chondrogenesis	1		
Similar 8	mRNA	hNSC	9	hMSC adipogenesis	1		
Similar 9	mRNA	hNSC	7	hMSC chondrogenesis	3		
Similar 10	mRNA	HSkM	8	hMSC osteogenesis	7		
Similar 11	miRNA	hMSC osteogenesis	4	hMSC adipogenesis	5	hMSC chondrogenesis	1
Similar 12	miRNA	hNSC	2	hMSC chondrogenesis	4	HSkM	1
Similar 13	mRNA	hNSC	1	hMSC adipogenesis	4	hMSC osteogenesis	3
Similar 14	mRNA	hNSC	4	HSkM	2	hMSC osteogenesis	5
Similar 15	mRNA	hNSC	3	hMSC osteogenesis	2	hMSC chondrogenesis	8
Control 1	miRNA	hNSC	5	hMSC osteogenesis	3		
Control 2	miRNA	hMSC chondrogenesis	5	hMSC adipogenesis	4		
Control 3	mRNA	hMSC chondrogenesis	7	hNSC	6		
Control 4	mRNA	hMSC adipogenesis	4	HSkM	5		
Control 5	mRNA	hNSC	6	hMSC adipogenesis	5		
Control 6	mRNA	hMSC adipogenesis	5	hMSC chondrogenesis	5		
Control 7	mRNA	hMSC adipogenesis	3	hMSC osteogenesis	2		
Control 8	mRNA	hMSC adipogenesis	7	hMSC chondrogenesis	8		
Control 9	mRNA	hMSC adipogenesis	2	HSkM	2		
Control 10	mRNA	hMSC adipogenesis	4	hMSC osteogenesis	7		
Control 11	mRNA	hMSC adipogenesis	8	hMSC osteogenesis	7	hNSC	2
Control 12	mRNA	hMSC adipogenesis	5	hMSC chondrogenesis	3	hMSC osteogenesis	7

Control 13	miRNA	hNSC		1	hMSC adipogenesis	5	HSkM	5
Control 14	mRNA	HSkM		2	hMSC chondrogenesis	7	hNSC	4
Control 15	miRNA	hMSC chondrogenesis		3	hMSC osteogenesis	4	hNSC	5

Table 7.2: miRNA and gene cluster pairs considered for the pathway enrichment analysis.

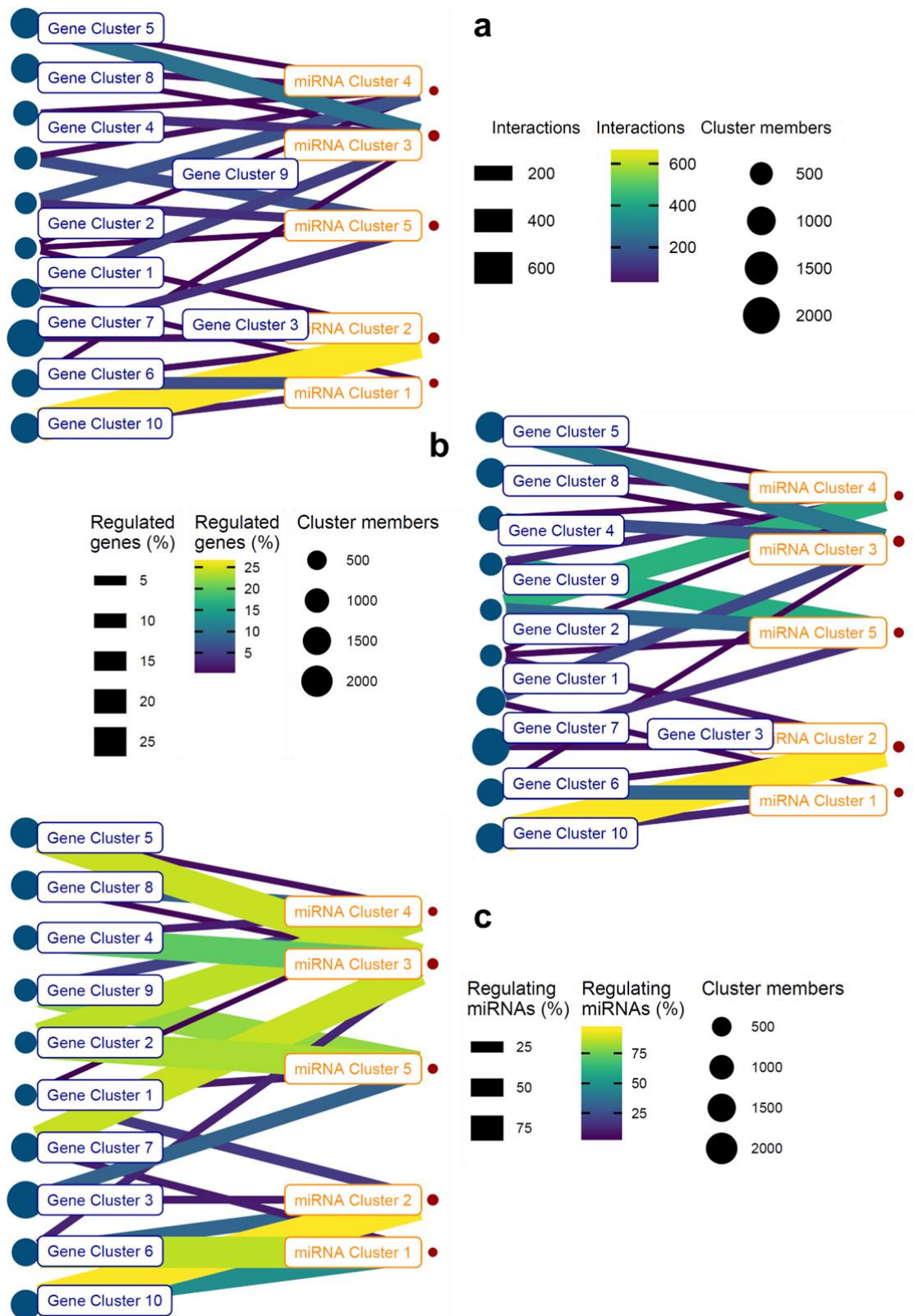| Differentiation assay	miRNA cluster	gene cluster
hMSC adipogenesis	2	10
hMSC adipogenesis	3	5
hMSC adipogenesis	4	2
hMSC chondrogenesis	1	8
hMSC chondrogenesis	2	7
hMSC chondrogenesis	2	8
hMSC chondrogenesis	4	3
hMSC chondrogenesis	5	4
hMSC osteogenesis	1	1
hMSC osteogenesis	1	5
hMSC osteogenesis	4	3
hMSC osteogenesis	6	2
hNSC	1	2
hNSC	1	7
hNSC	2	2
hNSC	2	7
hNSC	3	6
hNSC	4	3
HSkM	1	8
HSkM	2	9
HSkM	3	2
HSkM	3	5
HSkM	4	1
HSkM	4	9
HSkM	5	4
HSkM	5	9
HSkM	6	8

Figure 7.1: Networks of interactions between gene clusters (left) and miRNA clusters (right) of the hMSC adipogenesis assay. **a**: Non-normalized interaction network. **b**: Interaction network normalized by the percentage of genes regulated in each cluster. **c**: Interaction network normalized by the percentage of miRNAs participating in the regulation in each cluster.
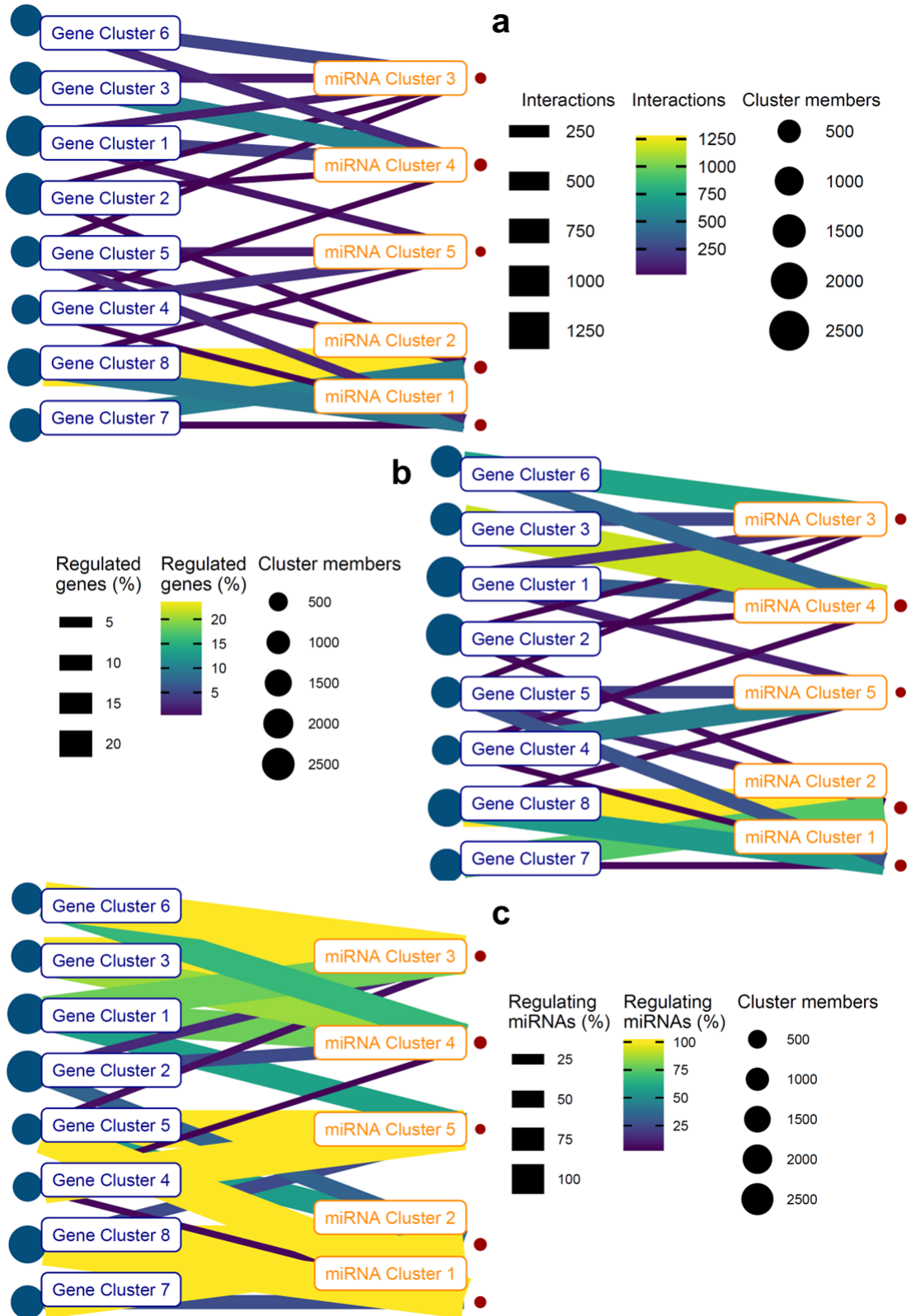
Figure 7.2: Networks of interactions between gene clusters (left) and miRNA clusters (right) of the hMSC chondrogenesis assay. **a**: Non-normalized interaction network. **b**: Interaction network normalized by the percentage of genes regulated in each cluster. **c**: Interaction network normalized by the percentage of miRNAs participating in the regulation in each cluster.
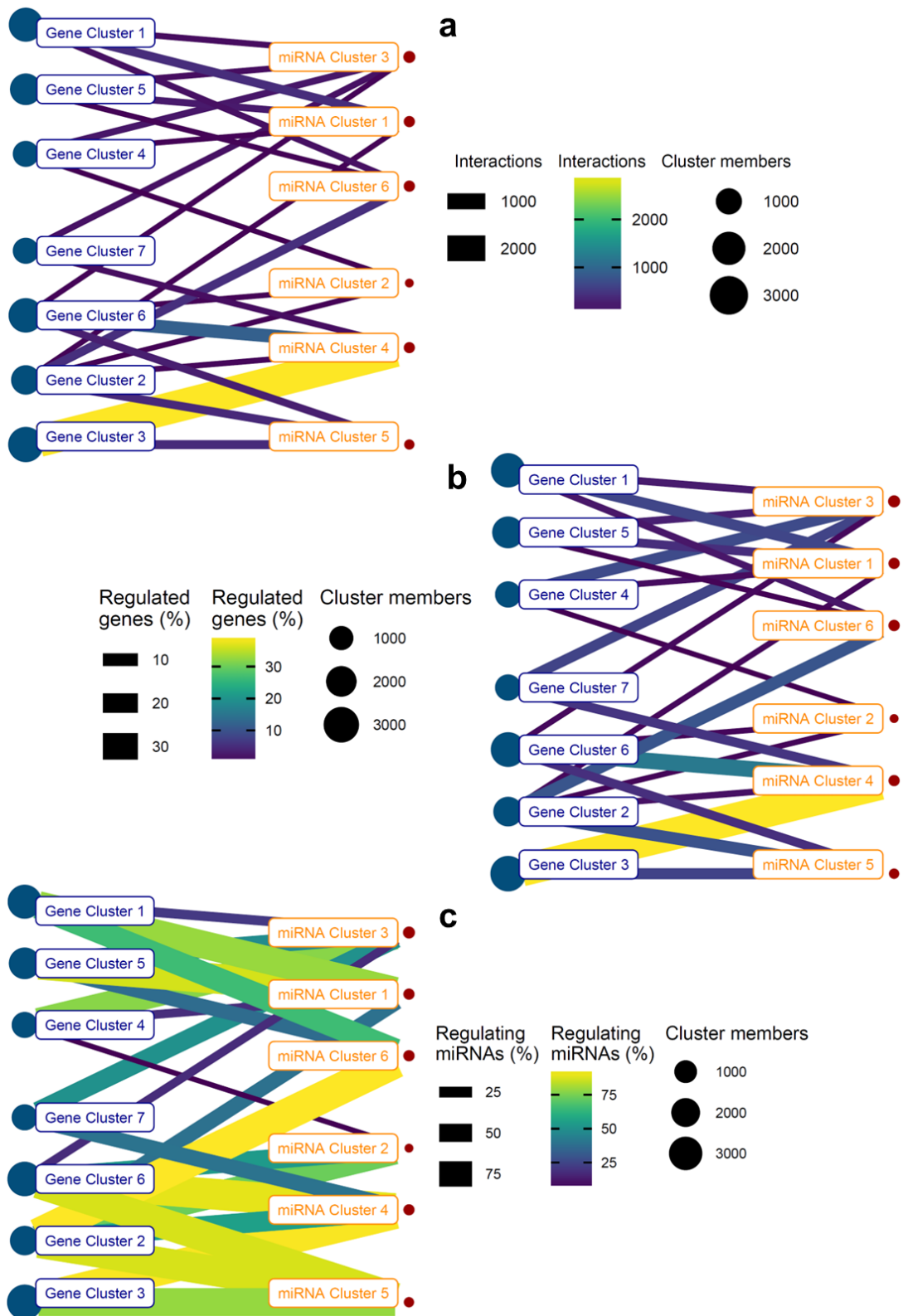
Figure 7.3: Networks of interactions between gene clusters (left) and miRNA clusters (right) of the hMSC osteogenesis assay. **a**: Non-normalized interaction network. **b**: Interaction network normalized by the percentage of genes regulated in each cluster. **c**: Interaction network normalized by the percentage of miRNAs participating in the regulation in each cluster.
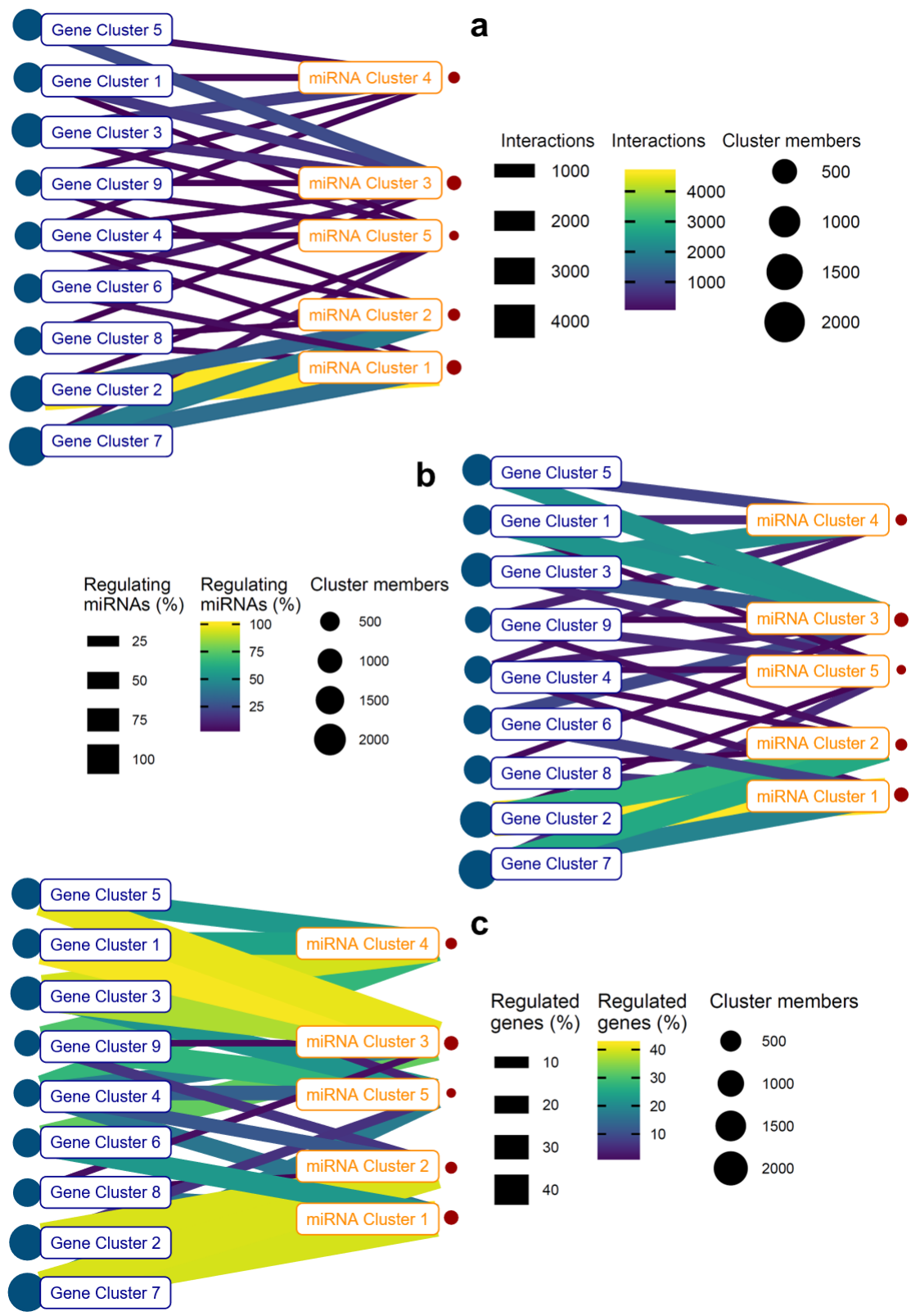
Figure 7.4: Networks of interactions between gene clusters (left) and miRNA clusters (right) of the hNSC differentiation assay. **a**: Non-normalized interaction network. **b**: Interaction network normalized by the percentage of genes regulated in each cluster. **c**: Interaction network normalized by the percentage of miRNAs participating in the regulation in each cluster.
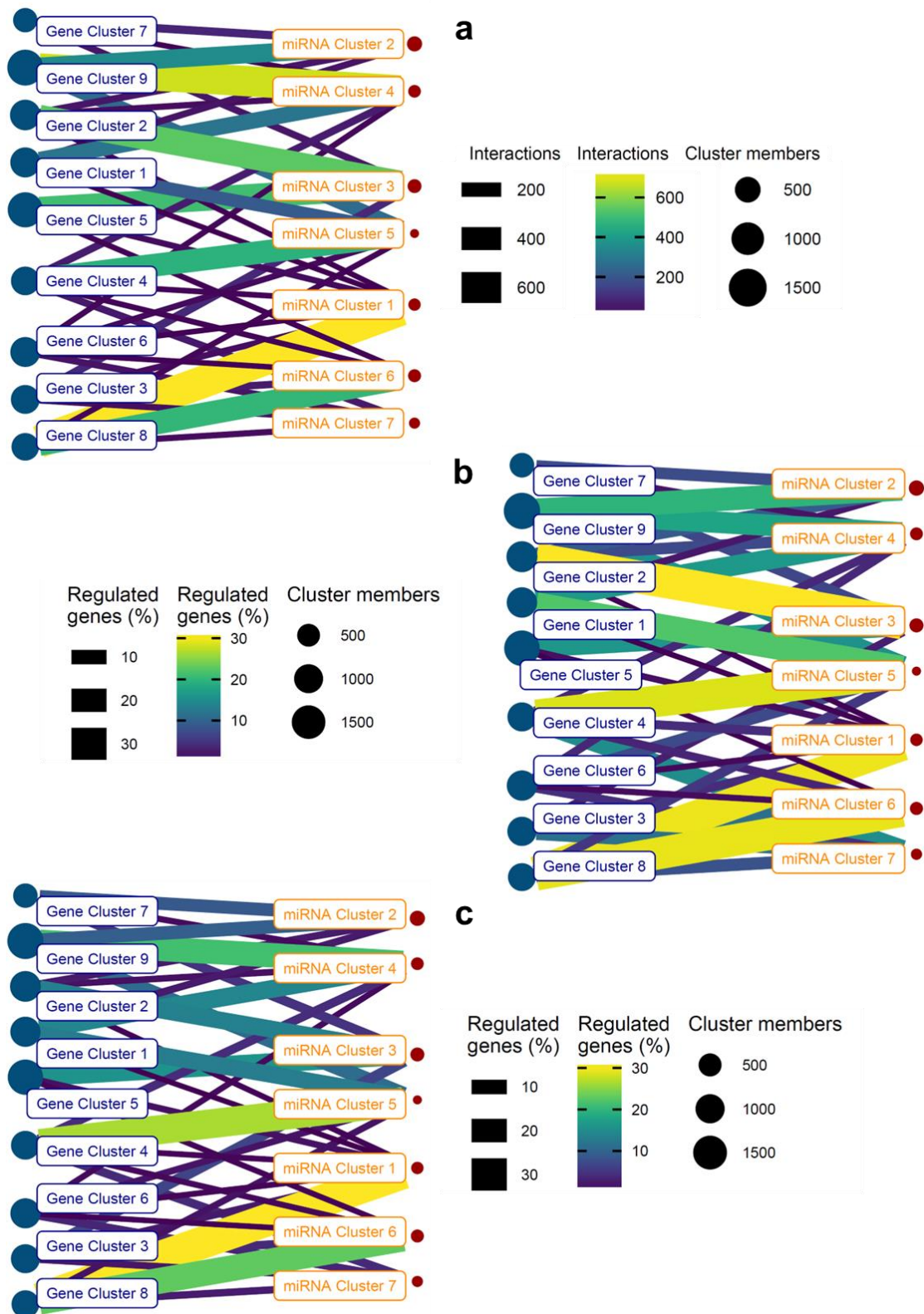
Figure 7.5: Networks of interactions between gene clusters (left) and miRNA clusters (right) of the HSkM differentiation assay. **a**: Non-normalized interaction network. **b**: Interaction network normalized by the percentage of genes regulated in each cluster. **c**: Interaction network normalized by the percentage of miRNAs participating in the regulation in each cluster.

Table 7.3: List of genes involved in adipogenesis or osteogenesis according to the literature.

Process	Direction	Gene	Reference
Adipogenesis	Inhibiting	CTNNB1	[262]
Adipogenesis	Inhibiting	GLI1	[480]
Adipogenesis	Inhibiting	GLI2	[480]
Adipogenesis	Inhibiting	GLI3	[480]
Adipogenesis	Inhibiting	PTCH1	[480]
Adipogenesis	Inhibiting	RUNX2	[618]
Adipogenesis	Inhibiting	SMAD6	[201]
Adipogenesis	Inhibiting	TAZ	[55]
Adipogenesis	Inhibiting	WNT1	[479]
Adipogenesis	Inhibiting	WNT10B	[455]
Adipogenesis	Inhibiting	WNT3A	[264]
Adipogenesis	Promoting	AKT1	[641]
Adipogenesis	Promoting	AKT2	[430]
Adipogenesis	Promoting	BMP2	[500]
Adipogenesis	Promoting	BMP4	[46]
Adipogenesis	Promoting	BMPR1A	[220]
Adipogenesis	Promoting	CEBPA	[95]
Adipogenesis	Promoting	DKK1	[183]
Adipogenesis	Promoting	DKK2	[300]
Adipogenesis	Promoting	DKK3	[300]
Adipogenesis	Promoting	DKK4	[300]
Adipogenesis	Promoting	HIVEP2	[252]
Adipogenesis	Promoting	IGF1	[560]
Adipogenesis	Promoting	IGF1R	[560]
Adipogenesis	Promoting	MAPK1	[201]
Adipogenesis	Promoting	NOX1	[597]
Adipogenesis	Promoting	PPARA	[65]
Adipogenesis	Promoting	PPARD	[65]
Adipogenesis	Promoting	PPARG	[312]
Adipogenesis	Promoting	RXRA	[179]
Adipogenesis	Promoting	SMAD1	[220]
Adipogenesis	Promoting	SMAD5	[220]
Adipogenesis	Promoting	SMAD9	[220]
Adipogenesis	Promoting	SRC	[597]
Osteogenesis	Inhibiting	ADIPOQ	[485]

Process	Direction	Gene	Reference
Osteogenesis	Inhibiting	CD36	[485]
Osteogenesis	Inhibiting	CEBPA	[584]
Osteogenesis	Inhibiting	CFD	[485]
Osteogenesis	Inhibiting	DKK1	[167]
Osteogenesis	Inhibiting	GREM1	[438]
Osteogenesis	Inhibiting	LEP	[485]
Osteogenesis	Inhibiting	NOG	[66]
Osteogenesis	Inhibiting	PPARG	[301]
Osteogenesis	Promoting	ADAR	[422]
Osteogenesis	Promoting	AKT1	[430]
Osteogenesis	Promoting	APC	[422]
Osteogenesis	Promoting	AXIN1	[422]
Osteogenesis	Promoting	BMP2	[647]
Osteogenesis	Promoting	BMP4	[75]
Osteogenesis	Promoting	BMP6	[75]
Osteogenesis	Promoting	BMP7	[75]
Osteogenesis	Promoting	BMPR1B	[75]
Osteogenesis	Promoting	BRAF	[265]
Osteogenesis	Promoting	CBFB	[20]
Osteogenesis	Promoting	CTNNB1	[62]
Osteogenesis	Promoting	DISP1	[629]
Osteogenesis	Promoting	FZD1	[582]
Osteogenesis	Promoting	GDF2	[75]
Osteogenesis	Promoting	GLI1	[629]
Osteogenesis	Promoting	GLI2	[629]
Osteogenesis	Promoting	GLI3	[629]
Osteogenesis	Promoting	GRB2	[265]
Osteogenesis	Promoting	GSK3A	[422]
Osteogenesis	Promoting	GSK3B	[422]
Osteogenesis	Promoting	HNF1A	[422]
Osteogenesis	Promoting	IGF1	[583]
Osteogenesis	Promoting	IGF1R	[583]
Osteogenesis	Promoting	IGFBP1	[265]
Osteogenesis	Promoting	IGFBP2	[265]
Osteogenesis	Promoting	IGFBP3	[265]
Osteogenesis	Promoting	IGFBP4	[265]
Osteogenesis	Promoting	IGFBP5	[265]
Osteogenesis	Promoting	IGFBP6	[265]

| Process	Direction	Gene	Reference
Osteogenesis	Promoting	IHH	[38]
Osteogenesis	Promoting	IRS1	[265]
Osteogenesis	Promoting	ITGA3	[13]
Osteogenesis	Promoting	ITGB1	[478]
Osteogenesis	Promoting	JUN	[67]
Osteogenesis	Promoting	LRP5	[422]
Osteogenesis	Promoting	LRP6	[422]
Osteogenesis	Promoting	MAPK1	[265]
Osteogenesis	Promoting	MAPK8	[265]
Osteogenesis	Promoting	MTOR	[583]
Osteogenesis	Promoting	NELL1	[621]
Osteogenesis	Promoting	NRAS	[265]
Osteogenesis	Promoting	PDK1	[182]
Osteogenesis	Promoting	PIK3CA	[182]
Osteogenesis	Promoting	PTCH1	[629]
Osteogenesis	Promoting	PTCH2	[629]
Osteogenesis	Promoting	ROR2	[313]
Osteogenesis	Promoting	RUNX2	[607]
Osteogenesis	Promoting	SHC1	[265]
Osteogenesis	Promoting	SHH	[450]
Osteogenesis	Promoting	SMO	[629]
Osteogenesis	Promoting	SOCS1	[265]
Osteogenesis	Promoting	SP7	[640]
Osteogenesis	Promoting	TAZ	[55]
Osteogenesis	Promoting	WNT1	[62]
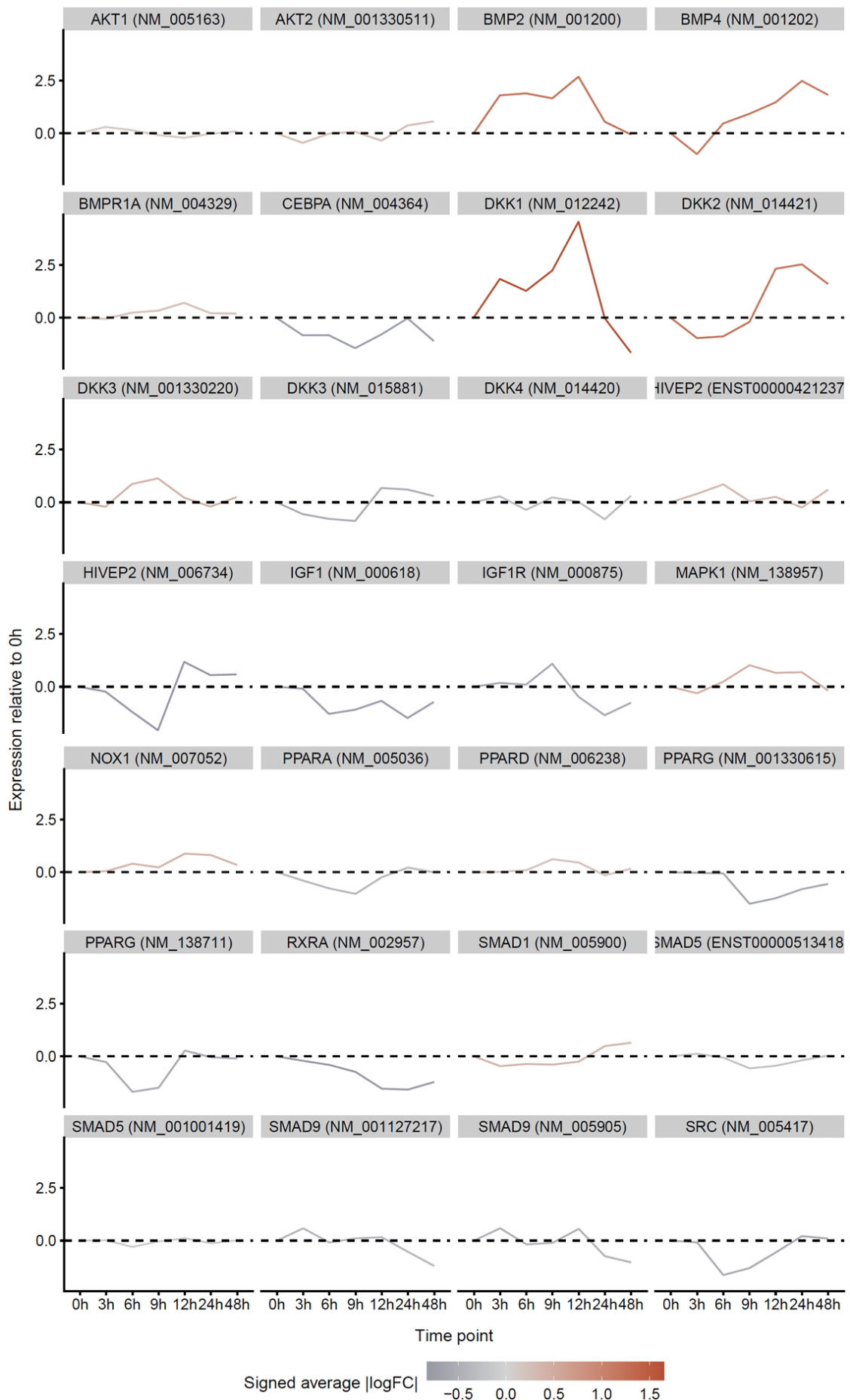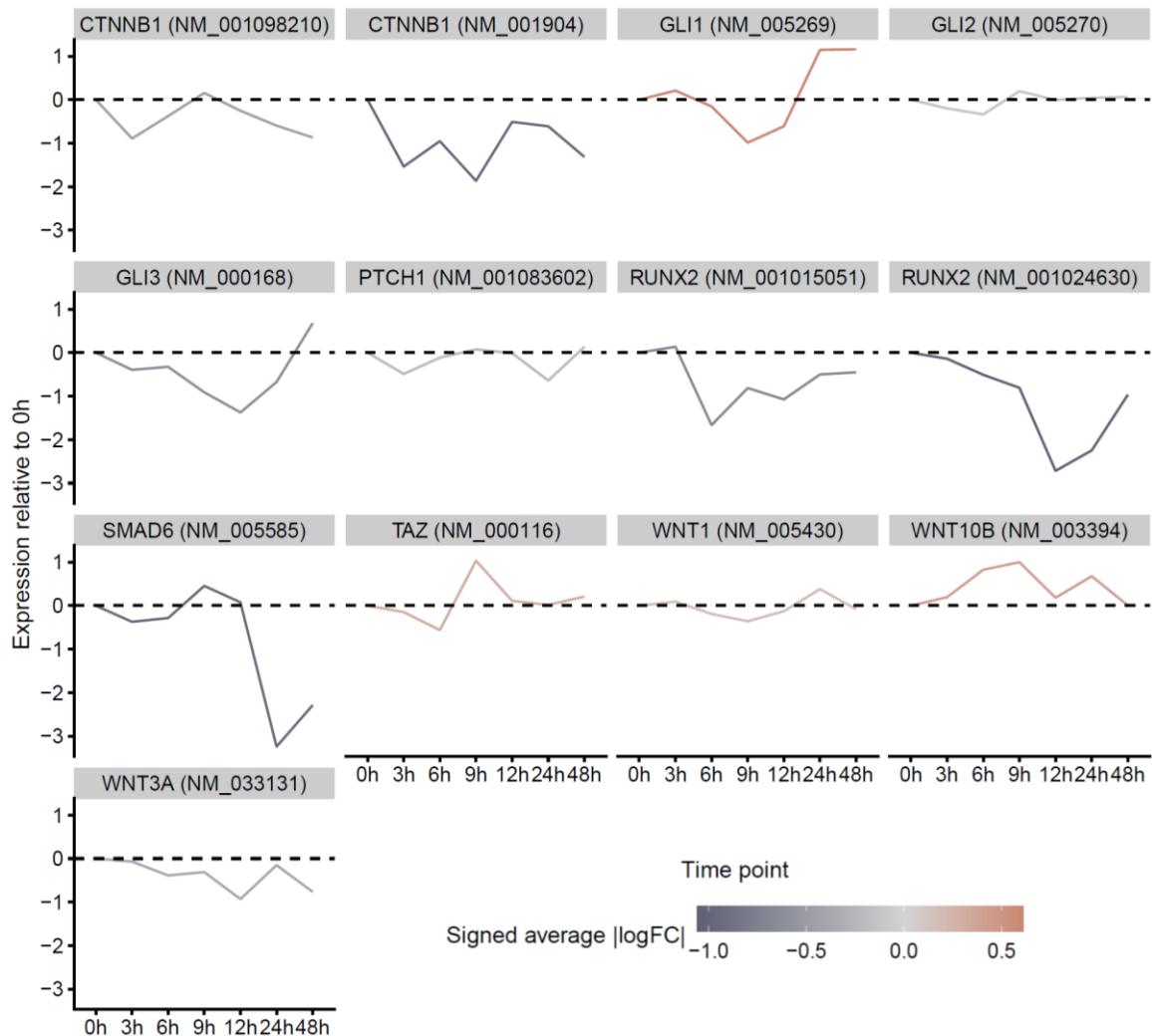
Figure 7.7: Time-resolved gene expression relative to 0 h for genes known to inhibit adipogenesis, in the hMSC adipogenesis assay. The color scale indicates the maximum fold change in gene expression between two time points.
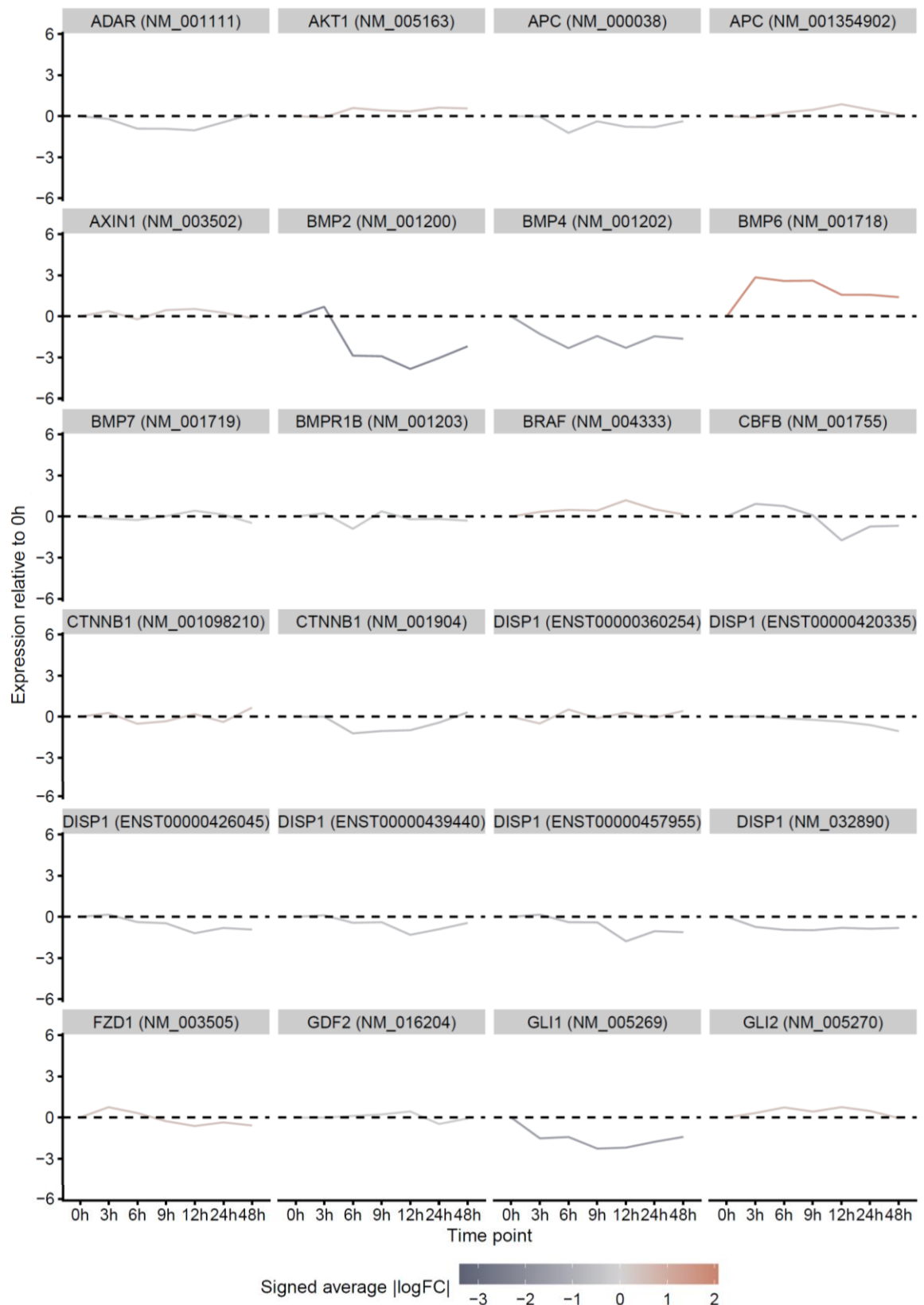
Figure 7.8: Time-resolved gene expression relative to 0 h for genes known to promote osteogenesis, in the hMSC osteogenesis assay. The color scale indicates the maximum fold change in gene expression between two time points.
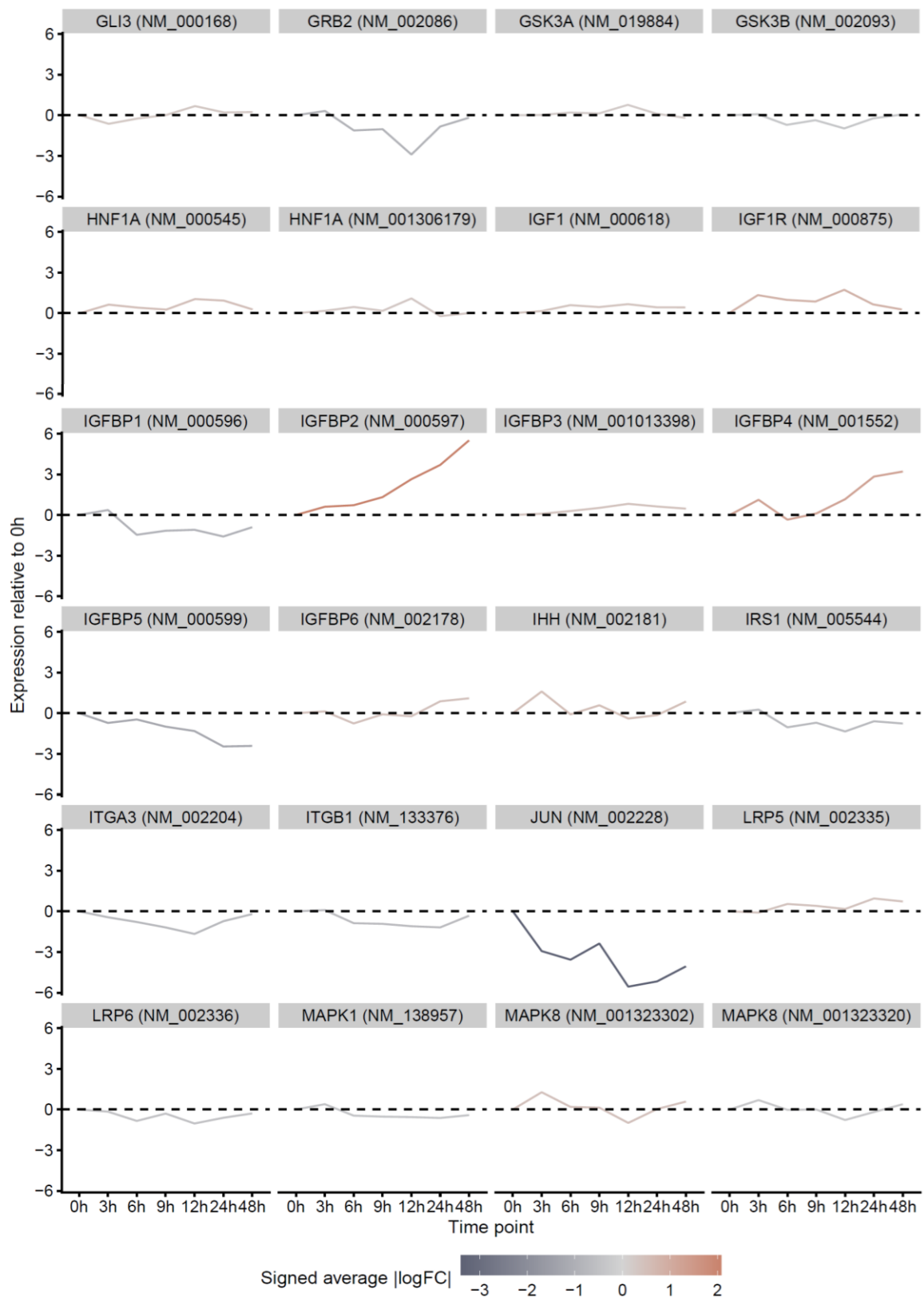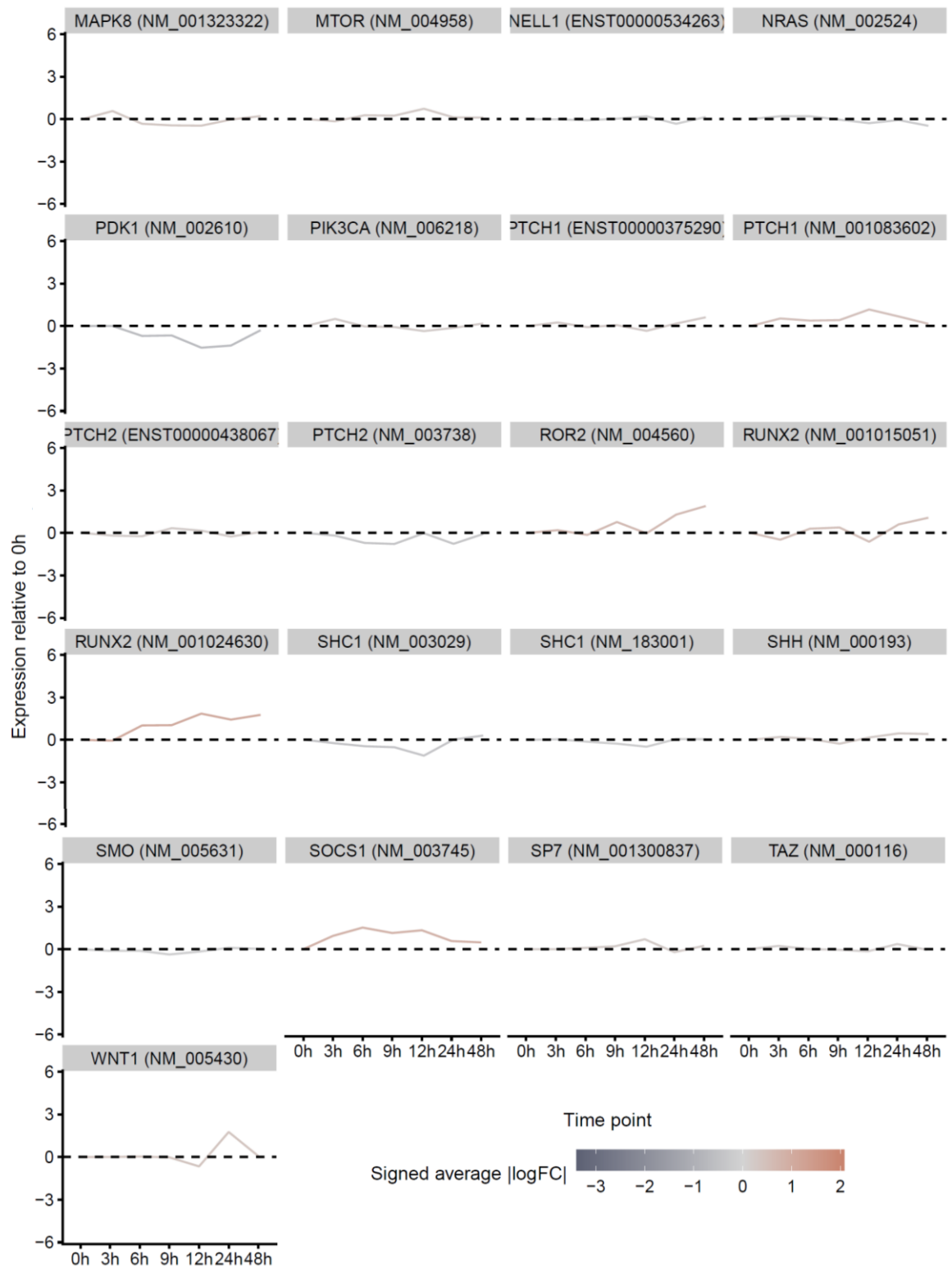
Figure 7.8 continued

Figure 7.8 continued

Figure 7.9: Time-resolved gene expression relative to 0 h for genes known to inhibit osteogenesis, in the hMSC osteogenesis assay. The color scale indicates the maximum fold change in gene expression between two time points.

Table 7.4: List of miRNAs enriched in embryonic stem cells or involved in the regulation of their transcriptome according to the literature.

miRNA gene	Mature miRNA	Cluster/family	Reference
hsa-mir-1283-1	hsa-miR-1283	chromosome 19 miRNA cluster	[504]
hsa-mir-1283-2	hsa-miR-1283	chromosome 19 miRNA cluster	[504]
hsa-mir-1323	hsa-miR-1323	chromosome 19 miRNA cluster	[504]
hsa-mir-498	hsa-miR-498-5p	chromosome 19 miRNA cluster	[504]
hsa-mir-498	hsa-miR-498-3p	chromosome 19 miRNA cluster	[504]
hsa-mir-512-1	hsa-miR-512-5p	chromosome 19 miRNA cluster	[504]
hsa-mir-512-1	hsa-miR-512-3p	chromosome 19 miRNA cluster	[504]
hsa-mir-512-2	hsa-miR-512-5p	chromosome 19 miRNA cluster	[504]
hsa-mir-512-2	hsa-miR-512-3p	chromosome 19 miRNA cluster	[504]
hsa-mir-515-1	hsa-miR-515-5p	chromosome 19 miRNA cluster	[504]
hsa-mir-515-1	hsa-miR-515-3p	chromosome 19 miRNA cluster	[504]
hsa-mir-515-2	hsa-miR-515-5p	chromosome 19 miRNA cluster	[504]
hsa-mir-515-2	hsa-miR-515-3p	chromosome 19 miRNA cluster	[504]
hsa-mir-516a-1	hsa-miR-516a-5p	chromosome 19 miRNA cluster	[504]
hsa-mir-516a-1	hsa-miR-516a-3p	chromosome 19 miRNA cluster	[504]
hsa-mir-516a-2	hsa-miR-516a-5p	chromosome 19 miRNA cluster	[504]
hsa-mir-516a-2	hsa-miR-516a-3p	chromosome 19 miRNA cluster	[504]
hsa-mir-516b-1	hsa-miR-516b-5p	chromosome 19 miRNA cluster	[504]
hsa-mir-516b-1	hsa-miR-516b-3p	chromosome 19 miRNA cluster	[504]
hsa-mir-516b-2	hsa-miR-516b-5p	chromosome 19 miRNA cluster	[504]
hsa-mir-516b-2	hsa-miR-516b-3p	chromosome 19 miRNA cluster	[504]
hsa-mir-517a	hsa-miR-517a-3p	chromosome 19 miRNA cluster	[504]
hsa-mir-517a	hsa-miR-517-5p	chromosome 19 miRNA cluster	[504]
hsa-mir-517b	hsa-miR-517b-3p	chromosome 19 miRNA cluster	[504]
hsa-mir-517b	hsa-miR-517-5p	chromosome 19 miRNA cluster	[504]
hsa-mir-517c	hsa-miR-517c-3p	chromosome 19 miRNA cluster	[504]
hsa-mir-517c	hsa-miR-517-5p	chromosome 19 miRNA cluster	[504]
hsa-mir-518a-1	hsa-miR-518a-5p	chromosome 19 miRNA cluster	[504]
hsa-mir-518a-1	hsa-miR-518a-3p	chromosome 19 miRNA cluster	[504]
hsa-mir-518a-2	hsa-miR-518a-5p	chromosome 19 miRNA cluster	[504]
hsa-mir-518a-2	hsa-miR-518a-3p	chromosome 19 miRNA cluster	[504]
hsa-mir-518b	hsa-miR-518b	chromosome 19 miRNA cluster	[504]
hsa-mir-518c	hsa-miR-518c-5p	chromosome 19 miRNA cluster	[504]
hsa-mir-518c	hsa-miR-518c-3p	chromosome 19 miRNA cluster	[504]
hsa-mir-518d	hsa-miR-518d-5p	chromosome 19 miRNA cluster	[504]
hsa-mir-518d	hsa-miR-518d-3p	chromosome 19 miRNA cluster	[504]
hsa-mir-518e	hsa-miR-518e-5p	chromosome 19 miRNA cluster	[504]
hsa-mir-518e	hsa-miR-518e-3p	chromosome 19 miRNA cluster	[504]
hsa-mir-518f	hsa-miR-518f-5p	chromosome 19 miRNA cluster	[504]
hsa-mir-518f	hsa-miR-518f-3p	chromosome 19 miRNA cluster	[504]

hsa-mir-519a-1	hsa-miR-519a-5p	chromosome 19 miRNA cluster	[504]
hsa-mir-519a-1	hsa-miR-519a-3p	chromosome 19 miRNA cluster	[504]
hsa-mir-519a-2	hsa-miR-519a-3p	chromosome 19 miRNA cluster	[504]
hsa-mir-519a-2	hsa-miR-519a-2-5p	chromosome 19 miRNA cluster	[504]
hsa-mir-519b	hsa-miR-519b-5p	chromosome 19 miRNA cluster	[504]
hsa-mir-519b	hsa-miR-519b-3p	chromosome 19 miRNA cluster	[504]
hsa-mir-519c	hsa-miR-519c-5p	chromosome 19 miRNA cluster	[504]
hsa-mir-519c	hsa-miR-519c-3p	chromosome 19 miRNA cluster	[504]
hsa-mir-519d	hsa-miR-519d-5p	chromosome 19 miRNA cluster	[504]
hsa-mir-519d	hsa-miR-519d-3p	chromosome 19 miRNA cluster	[504]
hsa-mir-519e	hsa-miR-519e-5p	chromosome 19 miRNA cluster	[504]
hsa-mir-519e	hsa-miR-519e-3p	chromosome 19 miRNA cluster	[504]
hsa-mir-520a	hsa-miR-520a-5p	chromosome 19 miRNA cluster	[504]
hsa-mir-520a	hsa-miR-520a-3p	chromosome 19 miRNA cluster	[504]
hsa-mir-520b	hsa-miR-520b-5p	chromosome 19 miRNA cluster	[504]
hsa-mir-520b	hsa-miR-520b-3p	chromosome 19 miRNA cluster	[504]
hsa-mir-520c	hsa-miR-520c-5p	chromosome 19 miRNA cluster	[504]
hsa-mir-520c	hsa-miR-520c-3p	chromosome 19 miRNA cluster	[504]
hsa-mir-520d	hsa-miR-520d-5p	chromosome 19 miRNA cluster	[504]
hsa-mir-520d	hsa-miR-520d-3p	chromosome 19 miRNA cluster	[504]
hsa-mir-520e	hsa-miR-520e-5p	chromosome 19 miRNA cluster	[504]
hsa-mir-520e	hsa-miR-520e-3p	chromosome 19 miRNA cluster	[504]
hsa-mir-520f	hsa-miR-520f-5p	chromosome 19 miRNA cluster	[504]
hsa-mir-520f	hsa-miR-520f-3p	chromosome 19 miRNA cluster	[504]
hsa-mir-520g	hsa-miR-520g-5p	chromosome 19 miRNA cluster	[504]
hsa-mir-520g	hsa-miR-520g-3p	chromosome 19 miRNA cluster	[504]
hsa-mir-520g	hsa-miR-520h	chromosome 19 miRNA cluster	[504]
hsa-mir-521-1	hsa-miR-521	chromosome 19 miRNA cluster	[504]
hsa-mir-521-2	hsa-miR-521	chromosome 19 miRNA cluster	[504]
hsa-mir-522	hsa-miR-522-5p	chromosome 19 miRNA cluster	[504]
hsa-mir-522	hsa-miR-522-3p	chromosome 19 miRNA cluster	[504]
hsa-mir-523	hsa-miR-523-5p	chromosome 19 miRNA cluster	[504]
hsa-mir-523	hsa-miR-523-3p	chromosome 19 miRNA cluster	[504]
hsa-mir-524	hsa-miR-524-5p	chromosome 19 miRNA cluster	[504]
hsa-mir-524	hsa-miR-524-3p	chromosome 19 miRNA cluster	[504]
hsa-mir-525	hsa-miR-525-5p	chromosome 19 miRNA cluster	[504]
hsa-mir-525	hsa-miR-525-3p	chromosome 19 miRNA cluster	[504]
hsa-mir-526a-1	hsa-miR-526a-5p	chromosome 19 miRNA cluster	[504]
hsa-mir-526a-1	hsa-miR-526a-3p	chromosome 19 miRNA cluster	[504]
hsa-mir-526a-2	hsa-miR-526a-5p	chromosome 19 miRNA cluster	[504]
hsa-mir-526b	hsa-miR-526b-5p	chromosome 19 miRNA cluster	[504]
hsa-mir-526b	hsa-miR-526b-3p	chromosome 19 miRNA cluster	[504]
hsa-mir-527	hsa-miR-527	chromosome 19 miRNA cluster	[504]
hsa-let-7a-1	hsa-let-7a-5p	let-7 family	[386]
hsa-let-7a-1	hsa-let-7a-3p	let-7 family	[386]

hsa-let-7a-2	hsa-let-7a-5p	let-7 family	[386]
hsa-let-7a-2	hsa-let-7a-2-3p	let-7 family	[386]
hsa-let-7a-3	hsa-let-7a-5p	let-7 family	[386]
hsa-let-7a-3	hsa-let-7a-3p	let-7 family	[386]
hsa-let-7b	hsa-let-7b-5p	let-7 family	[386]
hsa-let-7b	hsa-let-7b-3p	let-7 family	[386]
hsa-let-7c	hsa-let-7c-5p	let-7 family	[386]
hsa-let-7c	hsa-let-7c-3p	let-7 family	[386]
hsa-let-7d	hsa-let-7d-5p	let-7 family	[386]
hsa-let-7d	hsa-let-7d-3p	let-7 family	[386]
hsa-let-7e	hsa-let-7e-5p	let-7 family	[386]
hsa-let-7e	hsa-let-7e-3p	let-7 family	[386]
hsa-let-7f-1	hsa-let-7f-5p	let-7 family	[386]
hsa-let-7f-1	hsa-let-7f-1-3p	let-7 family	[386]
hsa-let-7f-2	hsa-let-7f-5p	let-7 family	[386]
hsa-let-7f-2	hsa-let-7f-2-3p	let-7 family	[386]
hsa-let-7g	hsa-let-7g-5p	let-7 family	[386]
hsa-let-7g	hsa-let-7g-3p	let-7 family	[386]
hsa-let-7i	hsa-let-7i-5p	let-7 family	[386]
hsa-let-7i	hsa-let-7i-3p	let-7 family	[386]
hsa-mir-98	hsa-miR-98-5p	let-7 family	[386]
hsa-mir-98	hsa-miR-98-3p	let-7 family	[386]
hsa-mir-130a	hsa-miR-130a-5p	miR-130 family	[504]
hsa-mir-130a	hsa-miR-130a-3p	miR-130 family	[504]
hsa-mir-130b	hsa-miR-130b-5p	miR-130 family	[504]
hsa-mir-130b	hsa-miR-130b-3p	miR-130 family	[504]
hsa-mir-106a	hsa-miR-106a-5p	miR-17 family	[386]
hsa-mir-106a	hsa-miR-106a-3p	miR-17 family	[386]
hsa-mir-106b	hsa-miR-106b-5p	miR-17 family	[386]
hsa-mir-106b	hsa-miR-106b-3p	miR-17 family	[386]
hsa-mir-17	hsa-miR-17-5p	miR-17 family	[386]
hsa-mir-17	hsa-miR-17-3p	miR-17 family	[386]
hsa-mir-18a	hsa-miR-18a-5p	miR-17 family	[386]
hsa-mir-18a	hsa-miR-18a-3p	miR-17 family	[386]
hsa-mir-18b	hsa-miR-18b-5p	miR-17 family	[386]
hsa-mir-18b	hsa-miR-18b-3p	miR-17 family	[386]
hsa-mir-20a	hsa-miR-20a-5p	miR-17 family	[386]
hsa-mir-20a	hsa-miR-20a-3p	miR-17 family	[386]
hsa-mir-20b	hsa-miR-20b-5p	miR-17 family	[386]

| hsa-mir-20b	hsa-miR-20b-3p	miR-17 family	[386]
hsa-mir-93	hsa-miR-93-5p	miR-17 family	[386]
hsa-mir-93	hsa-miR-93-3p	miR-17 family	[386]
hsa-mir-141	hsa-miR-141-5p	miR-200 family	[504]
hsa-mir-141	hsa-miR-141-3p	miR-200 family	[504]
hsa-mir-200a	hsa-miR-200a-5p	miR-200 family	[504]
hsa-mir-200a	hsa-miR-200a-3p	miR-200 family	[504]
hsa-mir-200b	hsa-miR-200b-5p	miR-200 family	[504]
hsa-mir-200b	hsa-miR-200b-3p	miR-200 family	[504]
hsa-mir-200c	hsa-miR-200c-5p	miR-200 family	[504]
hsa-mir-200c	hsa-miR-200c-3p	miR-200 family	[504]
hsa-mir-429	hsa-miR-429	miR-200 family	[504]
hsa-mir-302a	hsa-miR-302a-5p	miR-302 cluster	[386]
hsa-mir-302a	hsa-miR-302a-3p	miR-302 cluster	[386]
hsa-mir-302b	hsa-miR-302b-5p	miR-302 cluster	[386]
hsa-mir-302b	hsa-miR-302b-3p	miR-302 cluster	[386]
hsa-mir-302c	hsa-miR-302c-5p	miR-302 cluster	[386]
hsa-mir-302c	hsa-miR-302c-3p	miR-302 cluster	[386]
hsa-mir-302d	hsa-miR-302d-5p	miR-302 cluster	[386]
hsa-mir-302d	hsa-miR-302d-3p	miR-302 cluster	[386]
hsa-mir-367	hsa-miR-367-5p	miR-302 cluster	[386]
hsa-mir-367	hsa-miR-367-3p	miR-302 cluster	[386]
hsa-mir-371a	hsa-miR-371a-5p	miR-371/373 cluster	[504]
hsa-mir-371a	hsa-miR-371a-3p	miR-371/373 cluster	[504]
hsa-mir-371b	hsa-miR-371b-5p	miR-371/373 cluster	[504]
hsa-mir-371b	hsa-miR-371b-3p	miR-371/373 cluster	[504]
hsa-mir-372	hsa-miR-372-5p	miR-371/373 cluster	[437,504]
hsa-mir-372	hsa-miR-372-3p	miR-371/373 cluster	[437,504]
hsa-mir-373	hsa-miR-373-5p	miR-371/373 cluster	[504]
hsa-mir-373	hsa-miR-373-3p	miR-371/373 cluster	[504]
hsa-mir-134	hsa-miR-134-5p	-	[532]
hsa-mir-134	hsa-miR-134-3p	-	[532]
hsa-mir-145	hsa-miR-145-5p	-	[504,590]
hsa-mir-145	hsa-miR-145-3p	-	[504,590]
hsa-mir-183	hsa-miR-183-5p	-	[383]
hsa-mir-183	hsa-miR-183-3p	-	[383]
hsa-mir-195	hsa-miR-195-5p	-	[437]
hsa-mir-195	hsa-miR-195-3p	-	[437]
hsa-mir-203a	hsa-miR-203a-5p	-	[383]
hsa-mir-203a	hsa-miR-203a-3p	-	[383]
hsa-mir-203b	hsa-miR-203b-5p	-	[383]
hsa-mir-203b	hsa-miR-203b-3p	-	[383]
hsa-mir-296	hsa-miR-296-5p	-	[532]
hsa-mir-296	hsa-miR-296-3p	-	[532]
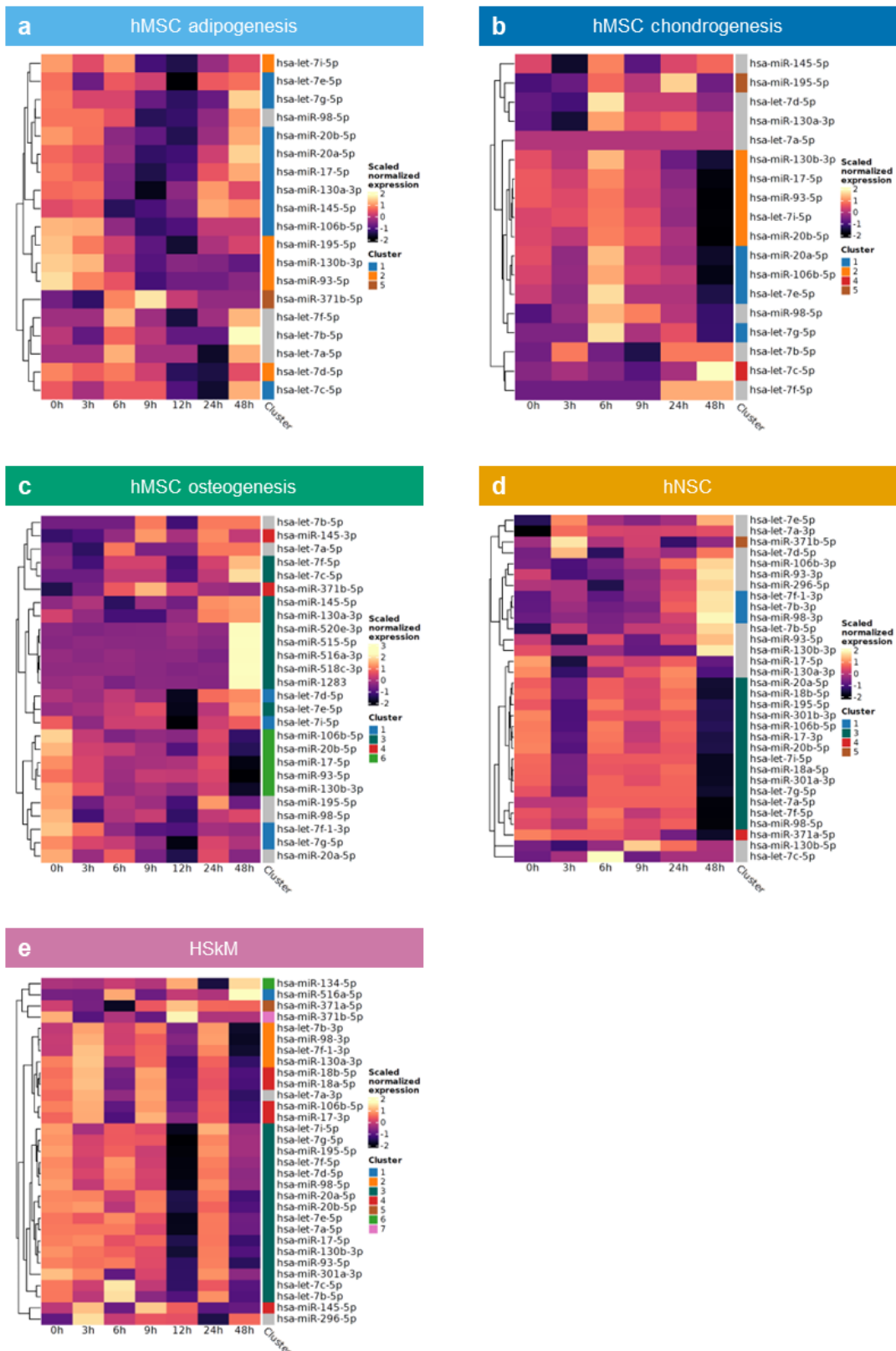
Figure 7.10: Heatmaps of the scaled and normalized expression levels of miRNAs known to be important in embryonic stem cells (ESCs) in the hMSC adipogenesis (a), chondrogenesis (b), osteogenesis (c), hNSC (d), and HSkM (e) differentiation assays. The cluster memberships of the miRNAs are shown at the right of each heatmap. A grey square in the cluster column indicates that the miRNA did not present a fold change over 1.5 between two time points.
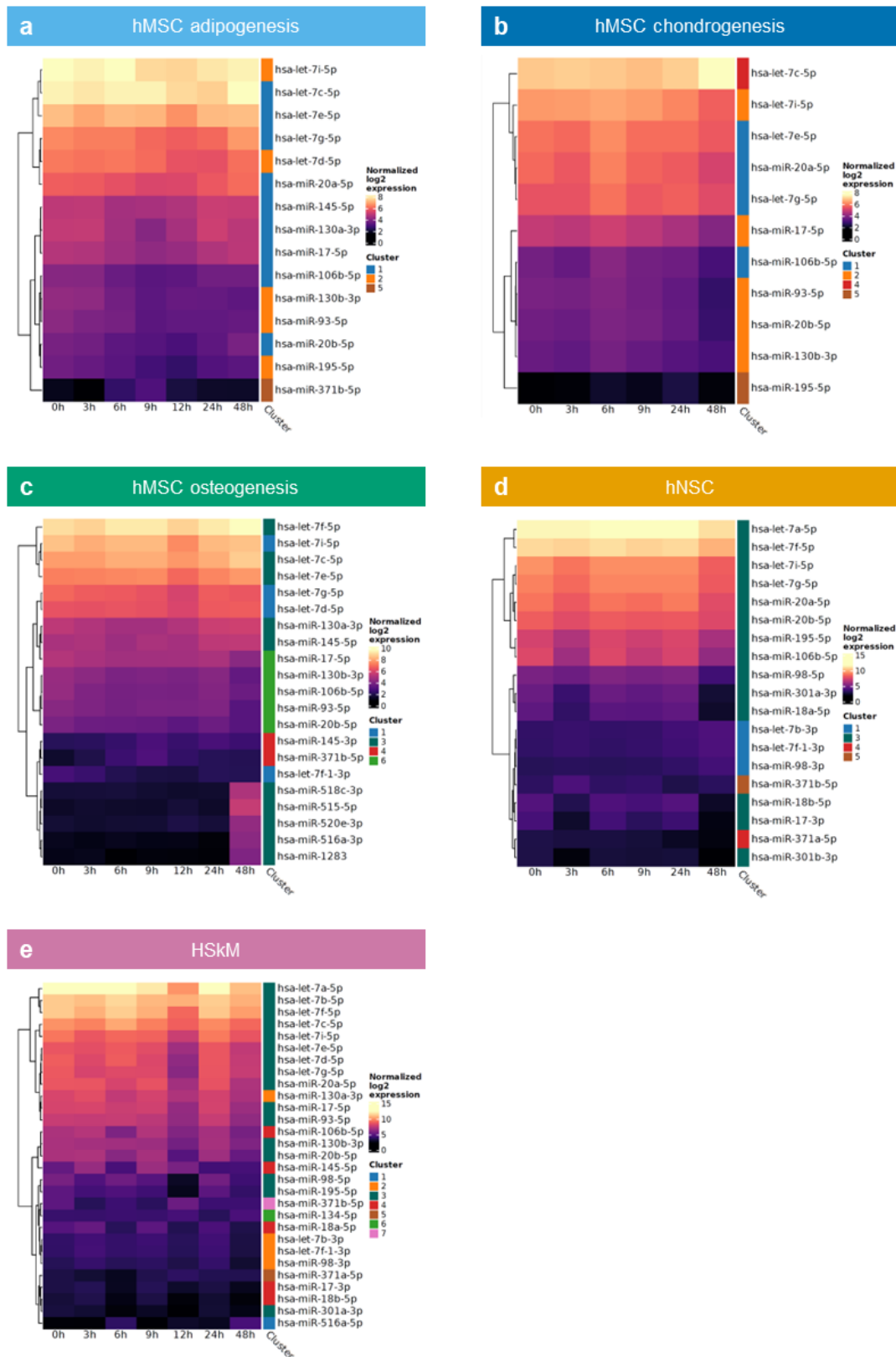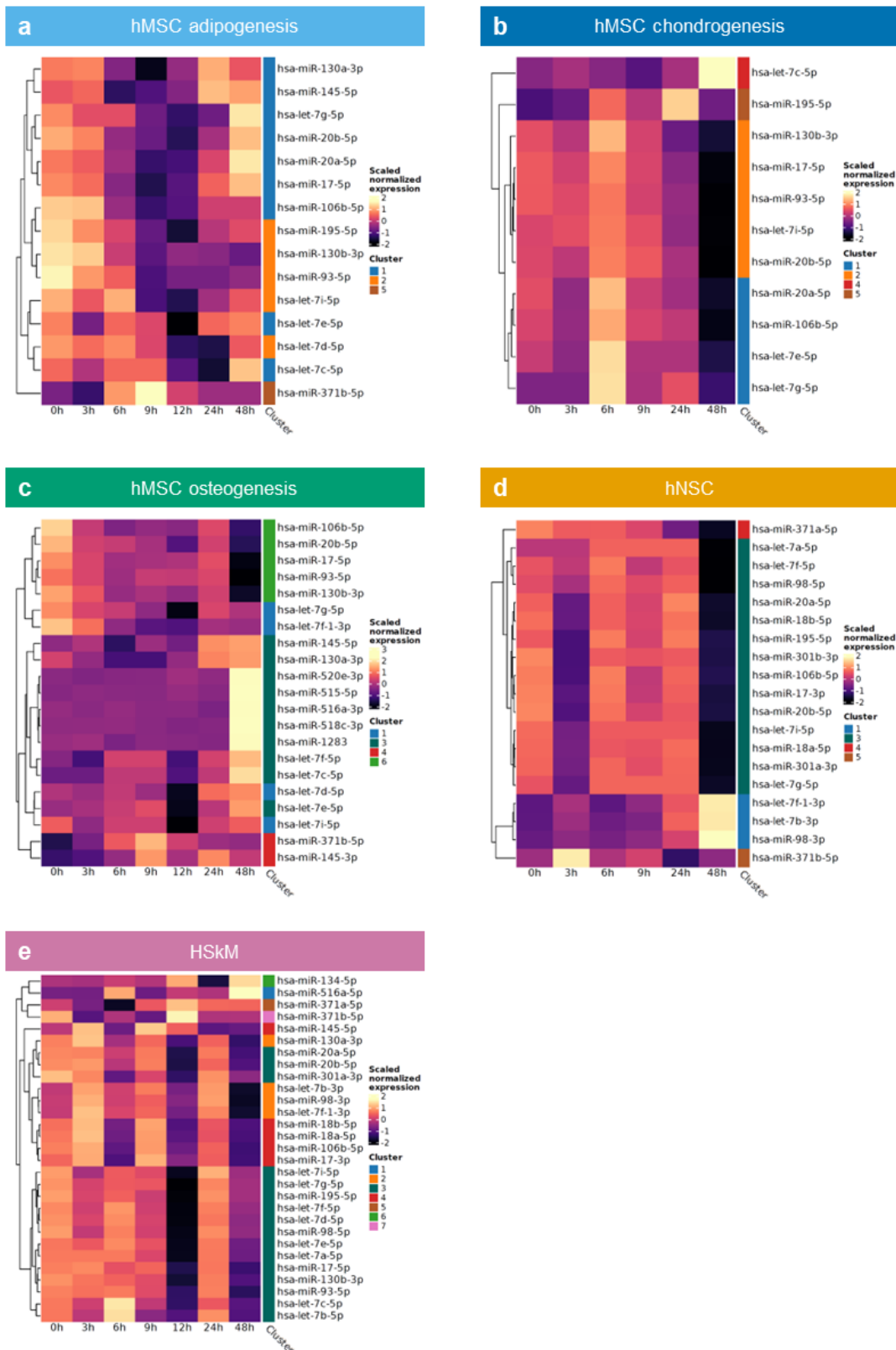
Figure 7.11: Heatmaps of the normalized expression levels of miRNAs known to be important in embryonic stem cells (ESCs) and found to be deregulated in the hMSC adipogenesis (a), chondrogenesis (b), osteogenesis (c), hNSC (d), and HSkM (e) differentiation assays. The cluster memberships of the miRNAs are shown at the right of each heatmap.

Figure 7.12: Heatmaps of the scaled and normalized expression levels of miRNAs known to be important in embryonic stem cells (ESCs) and found to be deregulated in the hMSC adipogenesis (a), chondrogenesis (b), osteogenesis (c), hNSC (d), and HSkM (e) differentiation assays. The cluster memberships of the miRNAs are shown at the right of each heatmap.
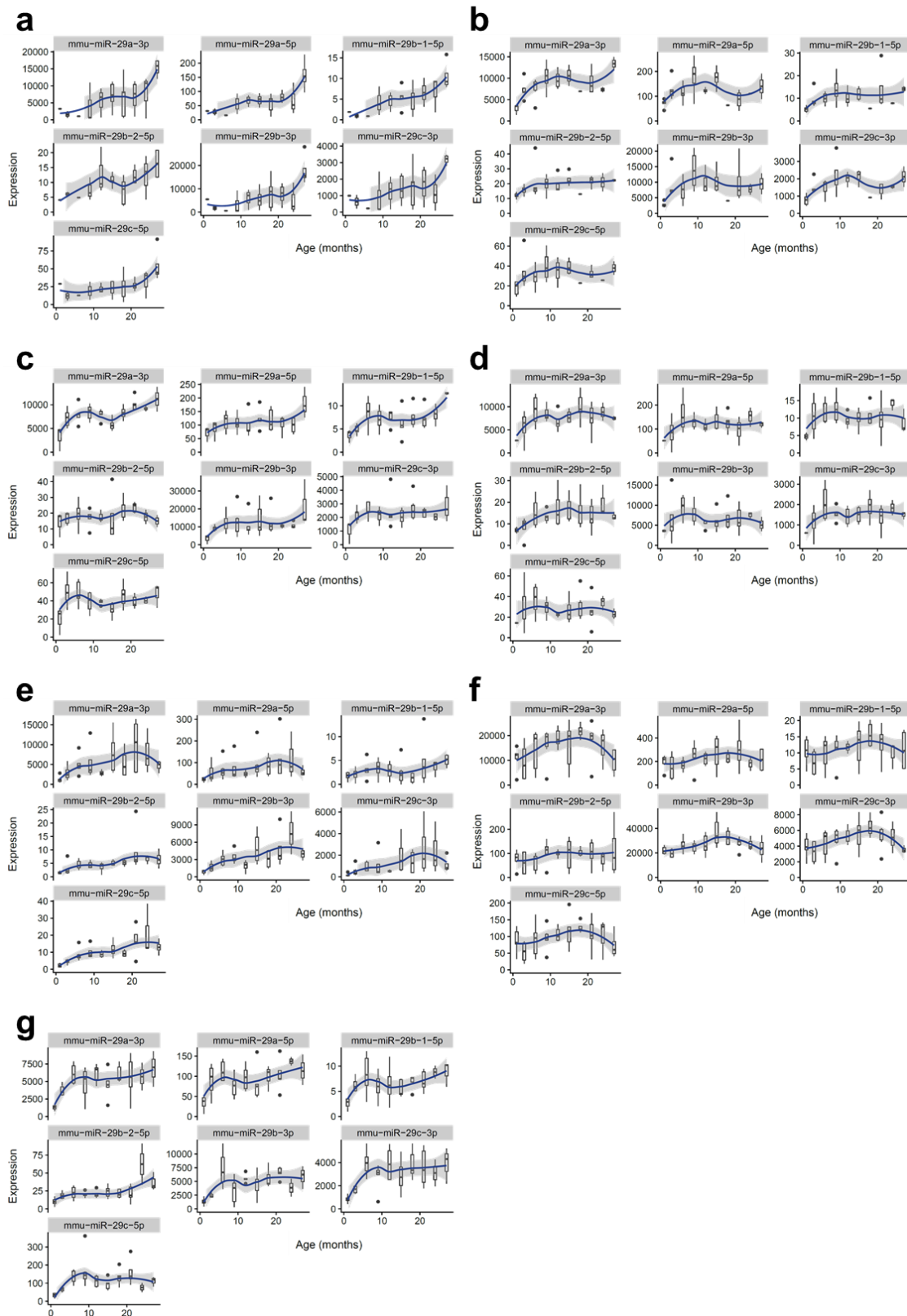
Figure 7.13: Time-resolved boxplots of the expression levels of members of the mmu-miR-29 family in the brown adipose tissue (BAT; **a**), gonadal adipose tissue (GAT; **b**), marrow adipose tissue (MAT; **c**), subcutaneous adipose tissue (SCAT; **d**), bone (**e**), brain (**f**), and skeletal muscle (**g**). The expression data were obtained from the Tabula Muris Senis dataset. The line was fitted with a loess formula (s.e. 95%).

8. Publication list

During my doctoral studies at the Institute of Human Genetics (Medical Faculty of the Saarland University) under the supervision of Univ.-Prof. Dr. rer. nat. Eckart Meese, the following publications were written (in chronological order):

Fehlmann T, Laufer T, Backes C, Kahramann M, Alles J, Fischer U, **Minet M**, Ludwig N, Kern F, Kehl T, Galata V, Düsterloh A, Schrörs H, Kohlhaas J, Bals R, Huwer H, Geffers L, Krüger R, Balling R, Lenhof H-P, Meese E, Keller A (2019) Large-scale validation of miRNAs by disease association, evolutionary conservation and pathway activity. *RNA Biology* **16**:93–103.

Alles J, Fehlmann T, Fischer U, Backes C, Galata V, **Minet M**, Hart M, Abu-Halima M, Grässer FA, Lenhof H-P, Keller A, Meese E (2019) An estimate of the total number of true human miRNAs. *Nucleic Acids Research* **47**:3353–3364.

Minet M, Abu-Halima M, Du Y, Doerr J, Isted C, Ludwig N, Keller A, Meese E, Fischer U (2022) A Temporary Pause in the Replication Licensing Restriction Leads to Rereplication during Early Human Cell Differentiation. *Cells* **11**:1060.

Poster:

Michaeli E, Schmartz GP, **Minet M**, Beganovic A, Ludwig N, Keller A, Meese E and Fischer U (2023) Evidence of re-replication in human stem cells in time windows during early differentiation. *Eukaryotic DNA Replication & Genome Maintenance*, CSHL, NY, USA. 05.-9.09.2023.

9. Acknowledgments

10. Curriculum vitae

The curriculum vitae was removed from the electronic version of the doctoral thesis for reasons of data protection.